Sediment management for catchments with hydropower dams under uncertainty in future projections

Bikesh Shrestha

Department of Civil and Natural Resources Engineering

University of Canterbury

Christchurch, New Zealand

2020

Acknowledgement

I would like to acknowledge my mentors Professor Thomas A. Cochrane, Dr. Mauricio A. Arias and Dr. Brian S. Caruso for the immense support and guidance. Thank you, University of Canterbury (UC), for providing UC Doctoral Scholarship for pursuing my Ph.D. I appreciate the John D. and Catherine T. MacArthur Foundation for travel and data collection funds. I gratefully acknowledge the Mekong River Commission (MRC) for providing all necessary data required for the study. Special thanks to Dr. Dat Nguyen Dinh and Dr. Ornanorg Vonnarart of Information and Knowledge Management Programme, MRC for putting together all the database for the 3S SWAT model. I also acknowldege support from Dr. Thanapon Piman. Special thanks to Dr. Thomas B. Wild for support with the *PySedSim* model.

Finally, I am very grateful to my parents, family members and friends for their constant support and encouragement. Special thanks to my wife Mona and son Arohan for standing by my side throughout the Ph.D. process.

Summary

The sustainability of hydropower reservoirs in catchments undergoing rapid development in the Mekong River Basin depends on the projected level of sedimentation. Excess sedimentation of reservoirs can be mitigated by using appropriate sediment management, but uncertainties in sediment predictions need to be addressed to better inform the selection of sediment management options. It is necessary to understand the magnitude of uncertainty in future sediment in response to land use/ land cover (LULC) change, climate change and sediment model parameterization. It is also necessary to evaluate the implication of catchment and reservoir-level sediment management options and costs under uncertainty in sediment projections.

Hence, this study aims to evaluate the uncertainty in sediment projections due to LULC, climate and model parameterization, and the implication of sediment management options and costs for catchments with hydropower dams. The following specific questions were investigated:

a. How do future climate scenarios and model parameterization affect the uncertainty in flow and sediment projections?
b. How do LULC change scenarios affect the uncertainty in flow and sediment projections?
c. How do combined future climate scenarios, model parameterization and LULC change scenarios affect the uncertainty in flow and sediment projections? What is the major source of uncertainty in flow and sediment projections?
d. What is the implication of sediment management options and associated cost under the greatest source of uncertainty in sediment projections?

The Sekong, Sesan and Srepok (3S) sub-basin of the greater Mekong River Basin was used as a case study.

The Soil and Water Assessment Tool (SWAT) was used to simulate flow and sediment. Uncertainty in future climate scenarios was addressed using three Global Climate Models (GCMs) and three Representative Concentration Pathways (RCPs). Model parameter uncertainty was analyzed by calibrating SWAT model using three different optimal objective functions. For evaluation of LULC change uncertainty, twelve LULC change scenarios were generated applying Land Change Modeler (LCM), and combining three LULC demands, two transition potential models and retaining or not protected areas. The catchment-level sediment management options of terracing, vegetative filter strips and no tillage were evaluated using SWAT. The reservoir-level sediment management option of flushing was assessed using the

Sediment Simulation Screening Python Model (*PySedSim*). Costs of sediment management options were assessed via the economic value of loss in hydropower production and the avoided cost of dredging.

The evaluation of uncertainty in flow and sediment projections associated with future climate scenarios and model parameterization suggests that the dominating source of uncertainty in flow and sediment can vary spatially and temporally for large basins. In short-term period projections (2030s), model parameterization dominates the uncertainty in flow and sediment, while in long-term projections (2060s) selection of climate scenarios dominate. Model parametrization uncertainty needs to be incorporate in climate change impact studies and efforts should be made to reduce the uncertainty due to model parametrization through a careful calibration and validation.

The assessment of uncertainty in flow and sediment in response to LULC change alone suggest uncertainty is primarily driven by LULC demand, resulting in large variability of flow and sediment projections.

The evaluation of uncertainty in flow and sediment in response to future climate scenarios, model parametrization and LULC change suggest that for a basin undergoing rapid LULC change uncertainty in future flow and sediment is dominated by the choice of LULC change scenarios. Hence, LULC change uncertainty should not be neglected in evaluation of climate change impact on basin hydrology.

Uncertainty in future sediment loads in response to LULC change can result in high variability in loss of reservoir capacity and cost of sediment management. Terracing performed best among the catchment-level management options in reducing the magnitude and variability in loss of reservoir capacity, but it is the most expensive option to implement. Flushing, although effective in increasing the life span of reservoir, was found less cost effective compared to catchment-level management options. The research outcome suggests that the best catchment-management option for reservoir sustainability may not be the best in terms of cost. Further, catchment-level management options do not address the issue to sediment starvation downstream, hence integrated sediment management approaches (i.e, combining both catchment-level and reservoir-level) may be required to reduce the adverse effect on reservoir storage and permit sediment flux downstream of the reservoir.

Deputy Vice-Chancellor's Office
Postgraduate Research Office

UNIVERSITY OF CANTERBURY
Te Whare Wānanga o Waitaha
CHRISTCHURCH NEW ZEALAND

Co-Authorship Form

This form is to accompany the submission of any thesis that contains research reported in co-authored work that has been published, accepted for publication, or submitted for publication. A copy of this form should be included for each co-authored work that is included in the thesis. Completed forms should be included at the front (after the thesis abstract) of each copy of the thesis submitted for examination and library deposit.

Please indicate the chapter/section/pages of this thesis that are extracted from co-authored work and provide details of the publication or submission from the extract comes:

Chapter 2:

Shrestha, B, Cochrane, TA, Caruso, BS, Arias, ME, Piman, T, 2016. Uncertainty in flow and sediment projections due to future climate scenarios for the 3S Rivers in the Mekong Basin. Journal of Hydrology, 540: 1088-1104. DOI:10.1016/j.jhydrol.2016.07.019

Chapter 3:

Shrestha, B, Cochrane, TA, Caruso, BS, Arias, ME, 2018. Land use change uncertainty impacts on streamflow and sediment projections in areas undergoing rapid development: A case study in the Mekong Basin. Land Degradation and Development, 29(3): 835-848. DOI:10.1002/ldr.2831

Chapter 5:

Shrestha, B, Cochrane, TA, Caruso, BS, Arias, ME, Wild, TB, 2020. Sediment management for reservoir sustainability and cost implications under land use/land cover change uncertainty, Water Resources Research (Under Review).

Please detail the nature and extent (%) of contribution by the candidate:

Methodology development – 80%, modelling and data analysis – 100%, and writing manuscripts – 80%. Over all contribution of candidate ~ 90%. Co-authors involvement mainly in development of methodologies, reviewing, editing and proof reading of manuscript.

Certification by Co-authors:

If there is more than one co-author then a single co-author can sign on behalf of all
The undersigned certifies that:

- The above statement correctly reflects the nature and extent of the Doctoral candidate's contribution to this co-authored work
- In cases where the candidate was the lead author of the co-authored work he or she wrote the text

Name: *Thomas A. Cochrane* Signature:  Date: *20/08/2020*

List of Acronyms

AGRI	Agriculture- intensive
C_d	Unit cost of dredging
C_{hp}	Cost of loss in hydropower production
C_{sr}	Cost of reservoir sediment removal
CCAI	Climate Change and Adaptation Initiative
CDF	Cumulative Distribution Functions
CMIP	Coupled Model Intercomparison Project
CN	Curve Number
DECD	Deciduous
FCRP	Field Crop
GCM	Global Climate Model
GFDL-CM3	Geophysical Fluid Dynamics Laboratory Climate model version 3
GISS-E2-R-CC	Goddard Institute for Space Studies Model E2, coupled with the Russell ocean model, with carbon cycle
GWh	Giga Watt hour
HPG	Hydropower generated
HRU	Hydrological Response Unit
IKMP	Information and Knowledge Management Programme
IPCC	International Panel on Climate Change
IPSL-CM5A-MR	Institute Pierre-Simon Laplace Coupled Model, version 5A, coupled with NEMO, mid resolution
km	Kilometers
kWh	Kilo Watt hour
LCM	Land Change Modeller
LR	Logistics Regression
LMB	Lower Mekong Basin

LULC	Land use/ land cover
LULCC	Land use/ land cover change
m	Meters
MP	Model parameters
MRC	Mekong River Commission
MSE	Mean Square Error
Mt	Million tons
MUSLE	Modified Universal Soil Loss Equation
MW	Mega Watt
NOTILL	No tillage
NPV	Net Present Value
NS	Nash-Sutcliffe Efficiency
OBS	Observed
PBIAS	Percent Bias
PDR	People's Democratic Republic
PySedSim	Sediment Simulation Screening Python Model
R^2	Coefficient of Determination
RCP	Representative Concentration Pathway
RESCON	REServoir CONservation
RSR	Ratio of Standard Deviation of Observations to Root Mean Square Error
3S	Sekong, Sesan and Srepok
SIM	Simulated
SUFI	Sequential Uncertainty Fitting
SW	Similarity-Weighted instance-based machine learning tool
SWAT	Soil and Water Assessment Tool

TERR	Terracing
TSS	Total Suspended Solids
VFS	Vegetative Filter Strips

Table of Contents

List of Figures

List of Tables

Chapter 1 Introduction

Background and Statement of Problem

Dams and reservoirs store and divert water for human needs. Irrigation, drinking and industrial water supply, hydropower, flood control, commercial fishing, inland navigation and recreation are crucial services provided by dams and reservoirs. The majority of dams around the world are built for irrigation purposes (24 – 50%), followed by hydropower (16 – 20%), water supply (11 – 17%) and flood control (9 – 19%) (ICOLD, 2018). Recent data suggest that dams generates 16% of global electricity (IEA, 2018) and irrigate 40% of global irrigable land (FAO, 2016). On the other hand, dams are often linked to negative ecological (Winemiller et al., 2016) and social implications (Huang et al., 2018). Trade-offs between pros and cons of dam are often controversial and complex (Intralawan et al., 2018), but it can be argued that in order to meet the future water, food and energy demands of growing populations dam are necessary (Shi et al., 2019) and thus sustainability of reservoir storage is crucial (Palmieri et al., 2001).

Dams and reservoir, in general, trap sediment due to the reduced riverine carrying capacity. Intercepted sediment loads can threaten the sustainability of reservoir storage, affect the operation and reduce the useful life of dams and reservoirs (Kondolf et al., 2014a). McCartney et al. (2000) estimated that approximately 1% of global reservoir storage is lost annually as a result of sediment trapping. Trapping of sediment by reservoirs not only changes the natural sediment fluxes, but also influence the overall river morphology and ecosystem (Kummu et al., 2010). Hence, trapping of sediment by reservoir is an important global issue (Kondolf et al., 2014a).

Catchment erosion is generally the main source of sediment of receiving surface water bodies. Anthropogenic activities, such as landscape alteration, can accelerate erosion and sediment flux to lakes and rivers, which can exacerbate sedimentation, water quality degradation, and subsequent impacts (Yang et al., 2019; Walter and Merritts, 2008; Moehansyah et al., 2002). For instance, accelerate rates of erosion in a catchment can significantly reduce hydropower generation due to excess sedimentation (Arias et al., 2011). Changes in temperature and rainfall associated with a changing climate could also affect soil erosion rates (Pruski and Nearing, 2002; Michael et al., 2005; O'Neal et al., 2005; Li and Fang, 2016) and sediment fluxes (Xu, 2003; Syvitski et al., 2005; Zhu et al., 2008; Samaras and Koutitas, 2014; Dahl et al., 2018). Changes in climate could alter future sediment loads posing challenges to sediment

management in planned reservoirs (Shrestha et al., 2013). Hence, reservoir sedimentation in response to climate change and land use/ land cover (LULC) change can be significant.

Loss of reservoir capacity can be mitigated by implementing three sediment management strategies: sediment yield reduction, sediment routing, and sediment removal (Sumi and Kantoush, 2011). Catchment erosion control and upstream sediment trapping (check dams and sediment traps) are the main strategies implemented to reduce catchment sediment yields (Morris and Fan, 1998). Catchment erosion control can be achieved by using different land conservation approaches such as maintaining forest and vegetation cover, tillage management, sediment traps and best management practices (Tiˇgrek and Aras, 2012). It is important to note that sediment yield reduction addresses the reservoir capacity issue only. It does not address the issue of sediment starvation downstream, while the remaining methods maintain reservoir capacity as well as release sediment to downstream reaches (Kondolf et al., 2014a) which is essential for healthy riverine morphology and ecology. Sediment routing strategies minimizes the amount of sediment deposition in reservoirs. This is done by manipulating reservoir hydraulics, geometry, or both, to pass sediment through or around the reservoir (Morris and Fan, 1998). Sediment routing is the most river environment friendly option as compared to other sediment management strategies because it partially preserves the natural sediment dynamism of the river (Kondolf et al., 2014a). Sluicing and turbid density currents venting are two main sediment pass through methods and flood by pass channels and off-channel reservoirs are the two main techniques practiced to route sediment around the reservoir. Hydraulic flushing, hydraulic dredging and dry excavation are strategies to remove deposited sediment from reservoirs. The technical and economic feasibility of each option is a function of location, amount of deposited sediment (Morris and Fan, 1998), and physical, hydrological and financial parameters (Palmieri et al., 2001). Better result may be achieved through combination of sediment management options (Palmieri et al., 2001). However, management of sediment in a catchment with series of hydropower dams can be challenging and complex.

Addressing uncertainty in future sediment in response to climate change and LULC change can better inform selection of sediment management plans for catchments with hydropower dams. Lack of understanding of sediment predictions uncertainty can mislead policy makers and resources manager in selecting effective sediment management strategies and can have cost implications. Understanding of uncertainty in hydrologic predictions is also essential for proper resource management (Brown et al., 2012; Milly et al., 2008). Uncertainty in future sediment prediction comes from uncertainty in climate change predictions, uncertainty

associated with models used to simulate sediment changes and uncertainty in LULC changes. Selection of Global Climate Models (GCMs), emission scenarios and downscaling methods are the major uncertainty sources linked to future climate predictions (Maurer, 2007; Minville et al., 2008; Surfleet and Tullos, 2013; Gao et al., 2019). Uncertainty in model, in general, comes from input errors, model calibration, model structure and model parameters (Refsgaard and Storm, 1996). Land use/ land cover (LULC) change uncertainty is largely portrayed by high uncertainty in quantity and location of change (Dalla-Nora et al., 2014). Cascading of uncertainty sources is commonly carried out to portray the relative implication of various uncertainty sources on hydrological response of catchments to future climate (Vetter et al., 2015; Bosshard et al., 2013; Wilby and Dessai, 2010). There are numerous studies carried out to evaluate the uncertainty of flow predictions. In most studies, GCMs are found to dominate the sources of uncertainty (Prudhomme and Davies, 2009; Chen et al., 2011b; Di Baldassarre et al., 2011; Elshamy et al., 2013; Thompson et al., 2013; Addor et al., 2014; Joseph et al., 2018; Gao et al., 2019). Other studies have highlighted that the emissions scenarios (Maurer, 2007), downscaling method (Chen et al., 2011a; Teutschbein et al., 2011), hydrologic model structures (Troin et al., 2018; Mockler et al., 2016; Poulin et al., 2011) and parameter uncertainty (Mendoza et al., 2015) are dominant sources of uncertainty.

Mathematical modelling is often used to simulate future sediment in response to LULC and climate changes; nevertheless traditionally, inclusion of the uncertainty in modelling when interpreting results has been given less importance. However, in recent years, efforts have been made by the scientific community to better understand the influence of model uncertainty in climate impact studies (Mendoza et al., 2015). Several studies have suggested that parameter uncertainty dominates other sources of uncertainty linked to model (Chen et al., 2013; Mendoza et al., 2015). Quantifying uncertainty linked to model is important to highlight the robustness of model results and identify which input(s) and parameter(s) is dominant uncertainty source (Smith and Heath, 2001). Land use/land cover change uncertainty, which can have significant influence on the characterization of uncertainty in hydrological prediction due to climate change (Feddema et al., 2005; Karlsson et al., 2016; Rodriguez-Lloveras et al., 2016) is often overlooked and not included in climate change impact studies (Bennett et al., 2012; Surfleet and Tullos, 2013). Overall, while there has been consistent progress in the literature on hydrological uncertainty with regards to climate, the interplay of this major driver with land surface processes is still understudied. The understanding of uncertainty in future sediment due to climate change is still limited and needs more exploration. The catchment erosion and

sediment flux response to future climate can vary from place to place because of high sensitivity of erosion and sediment movement process to variability in catchment physical characteristics and human intervention (Zhang and Nearing, 2005; Berc et al., 2003). There is also a need to understand the entangled and disentangled implication of major uncertainty sources for flow and sediment prediction for better characterization of the dominant uncertainty source.

In general, hydropower reservoirs with rapidly developing watersheds, such as the Mekong River Basin, are under threat of excess sedimentation, leading to potential detrimental energy production losses over time. Extensive dam development (over 200 dams) are planned in the Mekong River (Xue et al., 2011). A more rapid dam development is happening in tributaries of the Mekong River. The Sesan, Srepok and Sekong (3S) sub-basins is one such tributary where multiple hydropower dams are planned (Piman et al., 2013). Dam development in the Mekong region are particularly driven by changes in human demographics, energy and food security, development needs, economic cooperation, and climate change (Grumbine et al., 2012). Uncertainty in sediment prediction, however, can make the selection of sediment management options difficult. Sediment management options need to be evaluated from a feasibility and cost perspective considering uncertainties in sediment prediction. Several studies have analysed the cost of sediment management options (for example, Smith et al., 2013; Palmieri et al., 2001), but evaluation of the implication of sediment management options and cost under uncertainty in sediment projections are limited.

Research is thus needed to understand the magnitude of uncertainties related to LULC change, climate change and sediment modelling, and it will be of particular importance to regions such as the Mekong where there is ongoing rapid development.

Objectives

The main aim of this research is to evaluate the uncertainty in sediment predictions and the implication of sediment management options and cost under uncertainty in sediment projections for catchments with hydropower dams. In order to address the main research objective, the following questions formed the focus of the research:

a. How do future climate scenarios and model parameterization affect the uncertainty in flow and sediment projections?
b. How do LULC change scenarios affect the uncertainty in flow and sediment projections?

c. How do combined future climate scenarios, model parameterization and LULC change scenarios affect the uncertainty in flow and sediment projections? What is the major source of uncertainty in flow and sediment projections?
d. What is the implication of sediment management options and associated cost under the greatest source of uncertainty in sediment projections?

To address these research objectives, the Sekong, Sesan and Srepok (3S) sub-basins of the greater Mekong River Basin was used as a case study for the following reasons: (a) the 3S basins are trans boundary with hydrological significance (Adamson et al., 2009) (i.e major contribution to the Mekong flows and sediment) and ecological significance to downstream water bodies and the Mekong Delta (Piman et al., 2013), (b) the 3S basins are experiencing a dynamic LULC transition (Takamatsu et al., 2014), (c) rapid hydropower dam developed is happening in the 3S basins (17 dams operating, 6 dams ongoing and future development of 19 dams; (WLE–Mekong, 2017)), (d) change in sediment due to future LULC and climates can have significant implications for reservoir sedimentation and power production in the 3S basins, and (e) there are significant amount of data (for example spatial, hydro-meteorological) available for these river systems and hydrological (SWAT), reservoir sedimentation (SedSim) and hydropower (HECResSim) models have already been developed for these basins.

Thesis Outline

This is a paper-based thesis and comprises six chapters. Chapter 1 presents background of the study, statement of problem and objectives of the study. Chapter 2 presents the finding on investigation of the uncertainty in flow and sediment projections associated with future climate scenarios and model parameterization (Published as Shrestha et al. (2016)). Chapter 3 describes the implication of uncertainty in LULC change on future streamflow and sediment (Published as Shrestha et al. (2018a)). Chapter 4 evaluates the effect of combined future climate scenarios, model parameterization and LULC change scenarios uncertainty in flow and sediment projections and identifies the major source of uncertainty in flow and sediment projections (Unpublished paper). Chapter 5 describes the implication of sediment management options and associated cost under the greatest source of uncertainty in sediment projections (Submitted paper). Chapter 6 presents conclusion, recommendation and future area of research. A separate chapter for literature review is not provided because relevant literature review is included within Chapters 1 to Chapter 5.

Chapter 2

Uncertainty in flow and sediment projections due to future climate scenarios for the 3S Rivers in the Mekong Basin

Published as: Shrestha, B, Cochrane, TA, Caruso, BS, Arias, ME, Piman, T, 2016. Uncertainty in flow and sediment projections due to future climate scenarios for the 3S Rivers in the Mekong Basin. Journal of Hydrology, 540: 1088-1104. DOI:10.1016/j.jhydrol.2016.07.019

Abstract

Reliable projections of discharge and sediment are essential for future water and sediment management plans under climate change, but these are subject to numerous uncertainties. This study assessed the uncertainty in flow and sediment projections using the Soil and Water Assessment Tool (SWAT) associated with three Global Climate Models (GCMs), three Representative Concentration Pathways (RCPs) and three model parameter (MP) sets for the 3S Rivers in the Mekong River Basin. The uncertainty was analyzed for the short term future (2021-2040 or 2030s) and long term future (2051-2070 or 2060s) time horizons. Results show that dominant sources of uncertainty in flow and sediment constituents vary spatially across the 3S basin. For peak flow, peak sediment, and wet seasonal flows projection, the greatest uncertainty sources also vary with time horizon. For 95% low flows and for seasonal and annual flow projections, GCM and MP were the major sources of uncertainty, whereas RCPs had less of an effect. The uncertainty due to RCPs is large for annual sediment load projections. While model parameterization is the major source of uncertainty in the short term (2030s), GCMs and RCPs are the major contributors to uncertainty in flow and sediment projections in the longer term (2060s). Overall, the uncertainty in sediment load projections is larger than the uncertainty in flow projections. In general, the study results suggest the need to investigate the major contributing sources of uncertainty in large basins temporally and at different scales, as this can have major consequences for water and sediment management decisions. Further, since model parameterization uncertainty can play a significant role for flow and sediment projections, there is a need to incorporate hydrological model parameter uncertainty in climate change studies and efforts to reduce the parameter uncertainty as much as possible should be considered through a careful calibration and validation process.

Introduction

Reliable projections of discharge and sediment are essential for successful and efficient water and sediment management plans. Implementation of such plans considering the changing climate requires an understanding of uncertainty in model projections. Estimating the uncertainty and presenting the range of hydrologic projections is thus critical to managing resources under a non-stationary hydrologic regime (Cameron et al., 2000; Maurer, 2007; Milly et al., 2008 as cited by Surfleet and Tullos, 2013). There are various sources of uncertainty related to climate change predictions: (a) the use of Global Climate Models (GCMs) which includes several levels of uncertainty, from lack of knowledge regarding future emissions of greenhouse gases and differing responses of GCMs to greenhouse gases, to uncertainty added by the downscaling used to translate large-scale GCMs to local scales or finer resolution (Maurer, 2007); (b) uncertainty in land use/ land cover (LULC) change, which is often overlooked and could play a major role in the overall uncertainty of climate change impacts on hydrology (Bennett et al., 2012); and (c) uncertainty due to hydrological and sediment modeling (Surfleet and Tullos, 2013). Several studies have characterized the uncertainties in flow projection under climate change. For instance, Kay et al. (2009) and Chen et al. (2011b) investigated the uncertainties originating from greenhouse gas emission scenarios (GHGES), GCMs, GCM initial conditions, downscaling techniques, hydrological model structures and hydrological model parameters, suggesting that GCM structure is the largest source of uncertainty. For the Mekong River specifically, Thompson et al. (2013) assessed the uncertainty in river flow projections using seven GCMs and three hydrological models, finding that the choice of GCM is the major uncertainty contributor. In California, Maurer (2007) analyzed uncertainty in hydrologic impacts of climate change and concluded that future emissions scenarios play a significant role in the degree of impacts to water resources. Najafi et al. (2011) assessed the uncertainties associated with statistically downscaled outputs from eight GCMs, two emission scenarios, and four hydrologic models. Their results show that the hydrologic model uncertainty is considerably smaller than GCM uncertainty, except during the dry season, suggesting that the selection of hydrologic model is critical when assessing the hydrologic climate change impact. Others have investigated the uncertainty in downscaling techniques. For instance, Khan et al. (2006) compared three downscaling methods (SDSM, LarsWG and ANN) and showed the significant uncertainties in the downscaled daily precipitation, and daily maximum and minimum temperatures. Although different conclusions were drawn about the contribution of downscaling techniques and hydrologic models to

uncertainty, GCMs and emission scenarios are generally considered to be the two major dominant sources of uncertainty in quantifying the climate change impacts on flows (Chen et al., 2011b).

The assessment of hydrological model uncertainty is of major importance in hydrologic and sediment modeling (Jiang et al., 2007). It is also essential to advance the understanding of catchment processes (Clark et al., 2011). Traditionally, uncertainties associated with hydrologic models have been considered less important than other sources of uncertainties in climate change impact studies. However, in recent years, the hydrologic community has redirected efforts to better understand the effects of hydrologic modeling approaches to the assessment of climate change impacts (Mendoza et al., 2015). Generally, there are three principal sources of model uncertainty: errors with input and calibration, imperfection in model structures, and uncertainty in model parameters (Refsgaard and Storm, 1996). Model parameters that require calibration have an embedded degree of uncertainty (Kay et al., 2009). Parameter uncertainty has been demonstrated to be more important than model structure uncertainty or other model-based uncertainties (Chen et al., 2013; Mendoza et al., 2015). The uncertainty associated with model parameters should be taken into account for climate change impact analysis as they might have significant impacts on river flows in different hydrological years (Zhang et al., 2013). One way to study model parameter uncertainty is by calibrating a model using different optimal objective functions (e.g Gädeke et al., 2014; Najafi et al., 2011). Using a different measure of fit (objective function), will likely result in different calibrated parameter values, which is particularly true where there is any sort of interdependence between parameters (Kay et al., 2009). Models perform differently according to each distinct objective function, hence each model calibrated by different objective functions is treated separately (Najafi et al., 2011).

Previous contributions have clearly shown that quantifying the uncertainty at every step in the modelling process (cascading uncertainty) can address the challenge in quantitative assessment of climate change impacts on catchment hydrology considering the full range of uncertainties involved. However, most studies have generally focused on flow. There is still limited knowledge about the uncertainty in sediment projection due to future climate scenarios. The actual response of sediment flux to future climate scenarios in a particular place can vary extensively because it is highly affected by the physical characteristics of the catchment and human activities in it (Zhang and Nearing, 2005; Berc et al., 2003). Further, assessing the uncertainty in flow and sediment projections is of particular importance to regions such as the

Mekong in Southeast Asia where there is ongoing rapid development. A number of large, flow-regulating dams have been built in recent decades, and over 135 dams are planned in the Mekong River (Cochrane et al., 2014). Development of dams along the main stem of the Mekong River is ongoing, but tributary dam development is proceeding at a faster pace. Of main concern are the Sesan, Srepok, and Sekong (3S) subbasins, where an extensive network of hydropower projects, consisting of individual dams and cascade dams, are planned (Piman et al., 2013). Annual discharge from the 3S basin represents approximately 17-20% of the total annual flows of the Mekong main stream (91,000 x 10^6 m^3 or an average of 2,886 m^3/s), making it the largest tributary contribution to the Mekong River Basin and therefore of great hydrological importance (Adamson et al., 2009). The 3S basin is also a major contributing source of sediment in the Lower Mekong Basin (LMB). Annual sediment load from the 3S is estimated at 10 – 25 Mt (Kondolf et al., 2014b), but proposed dams are expected to trap 40 – 80% (Kummu et al., 2010; Wild and Loucks, 2014). In addition, the 3S basin is critical for maintaining flooding regime, aquatic biodiversity and ecosystem services (fish habitats and migration routes) to the downstream Mekong floodplains (Arias et al., 2014b; Ziv et al., 2012). Given the hydrological and ecological significance of the 3S basin, all dams (constructed, ongoing and future) need to be located, operated and managed in a way that minimizes disruptions to the natural flow regime and sediment fluxes. Changes to water flow and sediment may also alter future power production and reservoir sediment trapping efficiency. Thus, it is imperative that planners and decision-makers have access to information on uncertainty in flows and sediment loads so these can be accounted for in the design of new dams and the operation of current and future reservoirs.

This study aims to investigate the uncertainty in flow and sediment projections associated with future climate scenarios and model parameterization for the 3S basin. Specifically, three sources of uncertainty were evaluated: uncertainty derived from use of (1) three different GCMs, (2) three emission scenarios and (3) three sets of fitted/calibrated model parameters based on three different objective functions. Uncertainty in LULC change is not included in this study as it is the scope for further work. Flow and sediment projections for two future time horizons: short term future (2021-2040 or 2030s) and long term future (2051-2070 or 2060s) are compared to the baseline period (1986-2005) using mean annual, seasonal (dry and wet), annual peak and 95% low-flow metrics.

Methods

Study area

The 3S basin, a conglomerate of the three transboundary basins of the Sekong, Sesan and Srepok Rivers, is located in the Lower Mekong region in Southeast Asia (Figure 2-1). The 3S basin covers a total area of 78,645 km^2 of which 33% is in Cambodia, 29% is in Lao People's Democratic Republic, and 38% is in Vietnam. The elevation of the basin ranges from 49 to 2360 m above the mean sea level. The monsoon-driven climate is characterized by a wet season (May to October) and a dry season (November to April). The average annual temperature ranges from 23 to 27 °C. The basin receives about 2600 mm of average annual rainfall, 88% of which comes during the wet season. Acrisols (68%) and Ferralsols (12%) with sandy clay loam and clay texture are the dominant soils in the basin. Based on the 2003 LULC map the basin was dominated by forest (77%), while agriculture covered nearly 11% of the total area. Table 2-1 provides details on basin characteristics, meteorology, and major soil and LULC type for all three subbasins. Readers are referred to the Appendix 2-1 for details on soil distribution and properties, and LULC of the study area (Figures S2-1 and S2-2 and Table S2-1).

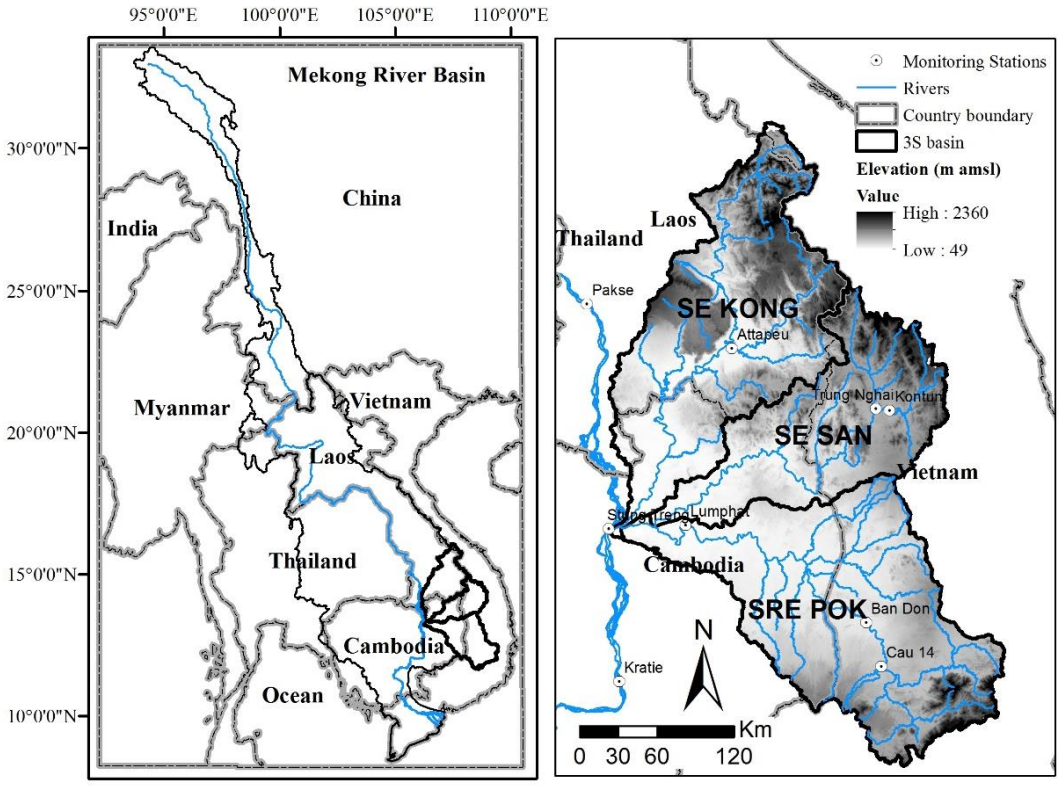

Figure 2-1. Location of the study area and river monitoring stations (Source: MRC, 2010). Note that Strung Treng monitoring station is on main stream of Mekong (below the confluence with 3S) and, Trung Nghia station is downstream of Kontum station but in different tributary.

Table 2-1. Details on basin characteristics, meteorology, and major soil and LULC type for each subbasin. m amsl = meters above mean sea level

	Sekong	Sesan	Srepok
Basin characteristics			
Area (km^2)	28,815	18,888	30,942
Elevation range (m amsl)	49 – 2165	50 – 2360	49 – 2358
Average elevation (m amsl)	543	576	392
Meteorology			
Average annual temperature range (°C)	26 – 28	22 – 27	22 – 27
Total average annual precipitation (mm)	2774	2605	2510
Total wet season precipitation (mm) and percentage (%) of total	2451 (88)	2342 (90)	2142 (85)
Total dry season precipitation (mm) and percentage (%) of total	323 (12)	263 (10)	368 (15)
Soil and landuse			
Major soil type and percentage (%) of total basin area	Acrisol (70) Cambisol (14)	Acrisol (79) Ferralsol (14)	Acrisol (60) Ferralsol (20)
Major LULC type and percentage (%) of total basin area	Forest (90) Agriculture (5)	Forest (60) Agriculture (13)	Forest (66) Agriculture (17)

Hydrological and sediment modeling

The Soil and Water Assessment Tool, SWAT (Arnold et al., 1998; Srinivasan et al., 1998), was used for simulating flows and sediment in the 3S basin because it is one of the most widely used watershed modeling tools, applied extensively for a broad range of water quantity and quality problems worldwide (Gassman et al., 2014). It is also capable of assessing catchment management scenarios. SWAT model has been extensively used in Mekong region and found to simulate the region's hydrology with high accuracy (Rossi et al., 2009). Apart from its proven ability to simulate flows and sediment, SWAT is already used by the Mekong River Commission (MRC) as part of the MRC's modeling Toolbox (MRC, 2010). Between 2010 and 2011, a preliminary SWAT model was calibrated for the 3S basins using actual river flow and rainfall measurements from 1985 to 2006 (MRC, 2011). The main strengths of SWAT are its semi-distributed structure which is capable of modelling water quantity and quality, and its flexible framework which allows to assess various catchment management options. Intensive input data requirements, requirement of large parameter calibration and non-spatial portrayal of hydraulic response unit (HRU) are some of the main drawbacks of the SWAT model. For details on strength and weakness of SWAT model readers are referred to Glavan and Pintar (2012), Gassman et al. (2014) and Cambien et al. (2020). Theoretical details on the SWAT model are provided in the Appendix 2-1.

The main input data for the SWAT model consists of daily precipitation, maximum and minimum air temperatures, wind speed, humidity, solar radiation, and spatial data on DEM, LULC and soil layers. All model input data were provided by the Information and Knowledge Management Programme (IKMP) of the MRC. Meteorological data (temperatures, wind speed, humidity and solar radiation) were acquired for six stations in the 3S basin. The observed precipitation data provided by MRC are at the subbasin level. MRC uses the MQUAD program (Hardy, 1971) to interpolate and aggregate the observed precipitation data from stations to the subbasins. The network of precipitation gauge stations in Mekong River Basin is sporadic and MQUAD is a practical and efficient interpolation method to determine spatial precipitation (Shaw and Lynn, 1972). MQUAD estimates areal rainfall by calculating a multiquadratic surface from available point rain gauge data, such that the surface passes through all gauge points. For details on MQUAD and its benefits over other interpolation techniques readers are referred to Shaw and Lynn (1972). MRC vectorised contours and spot heights from scanned topographical map to create a 250 m resolution DEM for the lower Mekong. MRC used FAO/UNESCO 1988 soil classification to create the soil map with 78 soil types. The LULC map was developed processing satellite information for 2003 and contains 33 various classes.

Model calibration, validation and performance evaluation

The 3S SWAT model was calibrated (1985-2000) and validated (2001-2007) for daily streamflow at seven sites with observed data: Attapeu, Trung Nghai, Kontum, Cau 14, Ban Don, Lumphat and Stung Treng (See locations in Figure 2-1). The model was only calibrated (2005-2008) for monthly sediment at three sites: Ban Don, Lumphat and the 3S basin outlet. For this study, the sediment load was calibrated, but not validated, because of the scarcity of data in the basin. There is a tradeoff between improving estimates using a longer data set for only calibration, versus using a shorter data set for calibration with additional validation. A study by Muleta and Nicklow (2005) suggests that relatively short calibration and validation periods can adversely affect hydrological model predictions. The model should perform well in the range of conditions for the calibration, but because of the lack of validation estimates may possibly not be as good outside that range or time period, or for more extreme conditions. Hence, instead of splitting the short period of observed sediment data into calibration and validation periods, the whole set of observed data was used for calibration to improve model performance. There are several studies (for example Hanratty and Stefan, 1998; Shrestha et al., 2013) where calibration only was performed for improving sediment load estimates when short periods of observed data were available. Total suspended solids (TSS) measurements were

available for the Lumphat and Bandon stations in the 3S basin, and for Pakse, Stung Treng and Kratie in the Mekong River (near the vicinity of the 3S basin outlet). Monthly sediment estimates were used to calibrate the model at Ban Don, Lumphat and 3S outlet. As no direct sediment measurements were made at the 3S outlet for the calibration/validation period, sediment loads at the 3S basin outlets (SED_{3S}) were approximated as follows:

$$SED_{3s} = TSS_{Stung\ Treng} * (Q_{Stung\ Treng} - Q_{pakse}) \quad (2.1)$$

where $TSS_{Stung\ Treng}$ is the TSS concentrations in the Mekong River at Stung Treng, and $Q_{Stung\ Treng}$ and Q_{Pakse} are the river flows along the Mekong at Stung Treng and Pakse, respectively.

Equation 2.1 was used to overcome two major difficulties: (a) lack of long–term TSS monitoring at the 3S outlet, and (b) monthly TSS concentrations and computed sediment loads at the farthest upstream station in the study area (Pakse) are often larger than at the downstream stations Stung Treng and Kratie. TSS at Pakse was not used in above equation. The consideration of the sediment concentration and load at Pakse and assumption that this represents the contribution of the main river to the load measured at Stung Treng would mean that there is no contribution of sediment from 3S to the Stung Treng because of the above-mentioned reason (i.e., TSS at Pakse larger than TSS at Stung Treng). This counter intuitive decrease in sediment loads downstream in the Lower Mekong has been risen as an issue before (Koehnken, 2012), and others have explained this phenomenon as a result of the overall deposition-dominated nature of the river channels in the lower Mekong (Lu et al., 2014b). Mean monthly sediment loads for the three stations were estimated using the program LOADEST (Runkel et al., 2004). LOADEST estimates mean monthly sediment loads using rating curves developed from the best-fitted polynomial model and coefficients based on an Adjusted Maximum Likelihood Estimation Method. Due to unavailability of SSC data, TSS data were used for this study. TSS stands for Total Suspended Solids, an indicator primarily used for water pollution characterization and it is derived from filtering a small water subsample (100-250 mL) from a single grab sample collected at arm reach below the water surface in the middle of the river channel. SSC stands for Suspended Sediment Concentration, an indicator specifically scoped for natural waters, in which the full content of relatively large samples (1-L normally) are obtained in order to represent the entire depth of the water body. The difference between TSS and SSC decrease when the fraction of small particles is large (Gray et al., 2000). The suspended sediments in the Lower Mekong River are mainly composed

of silt- and clay-sized particles (Walling, 2005). Koehnken (2012) indicated that the suspended sediments are mostly comprised of silt and clay downstream of Pakse and typically all of the suspended sediments are less than 63 μm in the Mekong at Kratie. In general suspended particles that are finer than 60 μm are uniformly vertically concentrated in rivers (Guy and Norman, 1970; Partheniades, 1977). Thus, the difference between loads estimated with TSS and SC measurements in this part of the lower Mekong should not be expected to be as large as what others have found in the basin's upper reaches upstream of Pakse (Walling, 2008).

For the SWAT model, parameters are spatially designated at watershed, subbasin and Hydrological Response Unit (HRU: the lumped land area within the subbasin that comprise unique land cover, soil, slope and management combinations) levels; hence a two-stage calibration procedure was adopted in this study. First, the model was calibrated from upstream to downstream for parameters specified at subbasin and HRU levels. Second, once the parameters for subbasin and HRU levels were calibrated, they were kept unchanged and parameters specified at the watershed level were calibrated.

The SWAT-CUP software (Abbaspour, 2008) was used for the automatic calibration of the 3S SWAT model. The user interaction or manual component of the SWAT-CUP calibration forces the user to obtain a better understanding of the overall hydrologic processes (e.g., baseflow ratios, evapotranspiration, sediment sources and sinks, crop yields, and nutrient balances) and of parameter sensitivity (Arnold et al., 2012). The Sequential Uncertainty Fitting (SUFI-2) algorithm (Abbaspour et al., 2004; Abbaspour et al., 2007) was used for the parameter optimization. SUFI-2 enables sensitivity analysis, calibration, validation, and uncertainty analysis of SWAT models. This algorithm is known to produce comparable results with widely used other auto-calibration methods (Yang et al., 2008). In order to run the automatic calibration in SUFI-2, the parameters to be calibrated (most sensitive ones) and their initial ranges (Table 2-2) were specified based on a literature review (Neitsch et al., 2011; Shrestha et al., 2013). In SUFI-2 there are two ways to change parameter values during calibration: directly changing the absolute value of a parameter, and changing the absolute value relative to the initial value specified for the parameter. Readers are referred to Abbaspour et al. (2007) for details of SUFI-2 approach.

The calibrated models were evaluated by comparing the simulated with the observed constituents using the Nash-Sutcliffe efficiency (NS), Coefficient of Determination (R^2) and percent bias (PBIAS). NS and R^2 are the most widely applied and well recommended

performance measures (Masih et al., 2011), and PBIAS is also recommended as one of the measures that should be included in model performance reports (Moriasi et al., 2007).

Table 2-2. Calibrated parameters and their initial range for the 3S SWAT model.

Parameter name	Description and units	Initial range	
		Minimum	Maximum
Flow variables			
v__GW_DELAY.gw[a]	Groundwater delay time (days)	0	100
v__ALPHA_BF.gw	Baseflow alpha factor (1/days)	0	1
v__GWQMN.gw[b]	Threshold depth of water in the shallow aquifer required to return flow to occur (mm)	0	1000
v__GW_REVAP.gw	Groundwater "revap" coefficient (-)	0.02	0.2
v__REVAPMN.gw	Threshold depth of water in the shallow aquifer for "revap" or percolation to the deep aquifer to occur (mm)	0	2000
v__RCHRG_DP.gw	Deep aquifer percolation fraction (-)	0	0.5
v__LAT_TTIME.hru	Lateral flow travel time (days)	0	180
v__SLSOIL.hru[b]	Slope length for lateral subsurface flow (m)	0	100
v__CANMX.hru	Maximum canopy storage (mm)	0	20
v__ESCO.hru	Soil evaporation compensation factor (-)	0	1
v__CH_N2.rte	Mannings "n" value for the main channel	0.014	0.15
v__CH_K2.rte	Effective hydraulic conductivity in main channel alluvium (mm/hr)	0	25
v__ALPHA_BNK.rte	Baseflow alpha factor for bank storage (days)	0	1
v__CH_N1.sub	Manning's "n" value for the tributary channels	0.014	0.15
v__CH_K1.sub	Effective hydraulic conductivity in tributary channel alluvium (mm/hr)	0	25
r__SOL_AWC(1).sol	Available water capacity in the soil layer (mm/mm soil)	-0.3	0.3
r__CN2.mgt[c]	Initial SCS runoff curve number for moisture condition II (-)	-0.15	0.15
Sediment variables			
v_SPCON.bsn	Linear parameter for calculating the maximum amount of sediment that can be re-entrained during channel sediment routing (-)	0.001	0.01
v_SPEXP.bsn	Exponent parameter for calculating sediment re-entrained in channel sediment routing (-)	1	1.5
v_PRF_BSN.bsn	Peak rate adjustment factor for sediment routing in the main channel (-)	0	2
v_USLE_C (Forest).dat	Minimum value for the cover and management factor for the land cover (-)	0.001	0.02
v_USLE_C (Agriculture).dat		0.01	0.4
v_USLE_C (Grass land).dat		0.01	0.15
v_USLE_C (Barren land).dat		0.5	1
v_CH_COV1.rte	Channel erodibility factor (-)	0	1
v_CH_COV2.rte	Channel cover factor (-)	0	1
v_CH_ERODMO.rte	Channel erodability factor (-)	0	1
v_USLE_K .sol	USLE equation soil erodibility (K) factor (0.013 metric ton m^2 hr / (m^3-metric ton cm))	0	0.65

Note: [a] The extension (e.g., .gw) refers to the SWAT input file where the parameter occurs; [b] The qualifier (v) refers to the substitution of a parameter by a value from the given range; [c] The qualifier (r) refers to relative change in the parameter where the value from the SWAT database is multiplied by 1 plus a factor in the given range.

Model uncertainty: uncertainty in parameter estimation

The final model parameter ranges are always conditioned on the form of the objective function (Abbaspour et al., 2004). The objective function used in the generation of the response surface (objective criteria) is crucial in the automatic calibration process (Gan et al., 1997). To address the uncertainty in parameter estimation, three different objective functions were used to calibrate the 3S SWAT model. The three different objective functions were selected based on recommendations in the literature and options available in SWAT-CUP. During the automatic calibration process in the SWAT-CUP software using the SUFI-2 optimizing algorithm, the objective function and meaningful absolute minimum and maximum ranges for the parameters being optimized were defined initially. Parameters were then calibrated using a Latin Hypercube sampling procedure three times for each objective function; the first was derived from 1000 simulations and the subsequent two were derived from 500 simulations. Out of the best three resulting parameter sets, the parameter set that performed well for all performance indicators considered (NS, R^2 and PBIAS) was chosen. As a result, three different model configurations were used in this study in order to assess the uncertainty in parameter estimation (Figure 2-2).

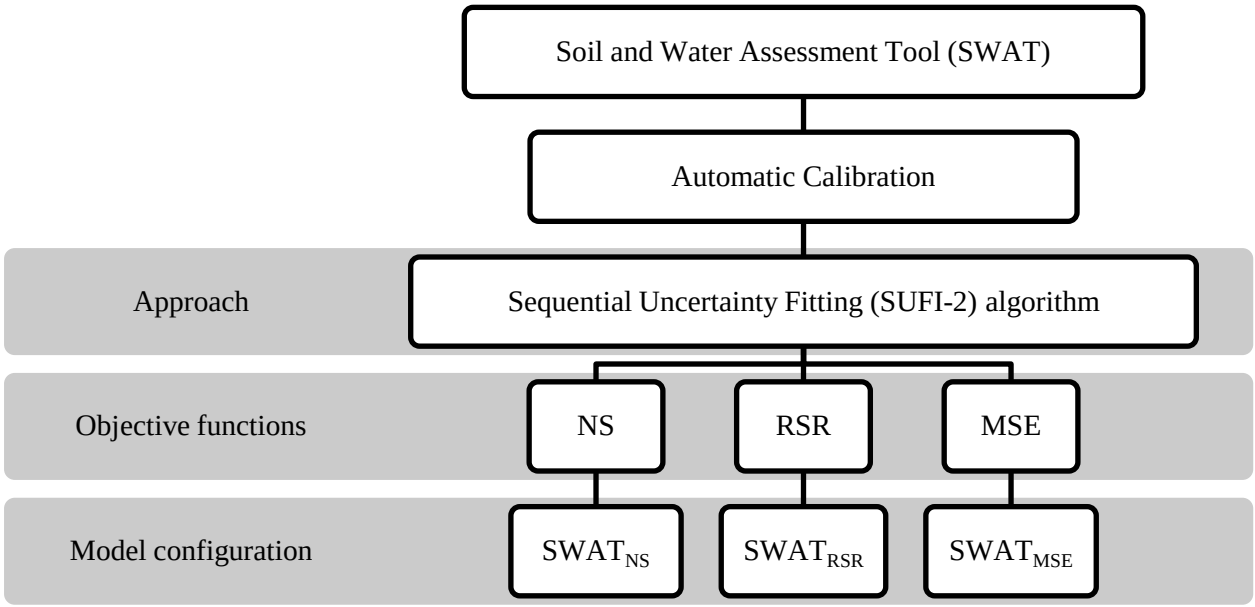

Figure 2-2. Approach for assessing the uncertainty in SWAT parameter estimation.

Nash-Sutcliffe efficiency (NS)

NS is a normalized statistic that determines the relative magnitude of the residual variance compared to the measured data variance (Nash and Sutcliffe, 1970). It indicates how well the plot of observed versus simulated data fits the 1:1 line. NS is computed as:

$$NS = 1 - \frac{\sum_i (Q_m - Q_s)_i^2}{\sum_i (Q_{m,i} - \bar{Q}_m)^2} \quad (2.2)$$

where $Q_{m,i}$ is the observed value (sediment load or flow) at time-step *i*, Q_s is the simulated value at time-step *i*, $\bar{Q}_m$ is the mean observed value.

NS is widely used (Gupta et al., 2009; Moriasi et al., 2007) and is the best objective function for reflecting the overall fit of a hydrograph (Servat and Dezetter, 1991). NS ranges between negative infinity to 1, where 1 shows a perfect model. Values between 0 and 1 are generally viewed as acceptable levels of performance.

Ratio of Standard Deviation of Observations to Root Mean Square Error (RSR)

RSR standardizes the Root Mean Square Error using the observations' standard deviation. RSR incorporates the benefits of error index statistics and includes a scaling/normalization factor, so that the resulting statistics and reported values can apply to various constituents (Moriasi et al., 2007). RSR is calculated as:

$$RSR = \frac{\sqrt{\sum_{i=1}^{n} (Q_m - Q_s)_i^2}}{\sqrt{\sum_{i=1}^{n} (Q_m - \bar{Q}_m)^2}} \quad (2.3)$$

where $Q_{m,i}$ is the observed value at time-step *i*, Q_s is the simulated value at time-step *i*, $\bar{Q}_m$ is the mean observed value, *n* is the total number of time-steps.

RSR varies from 0 to larger positive values. The lower the RSR, the better the model fit.

Mean square error (MSE)

MSE measures the average of the squares of the errors. The equation for MSE is:

$$MSE = \frac{1}{n} \sum_{i=1}^{n} (Q_m - Q_s)_i^2 \quad (2.4)$$

where $Q_{m,i}$ is the observed value at time-step *i*, Q_s is the simulated value at time-step *i*, *n* is the total number of time-steps.

MSE is the most commonly used criteria for calibration and evaluation of hydrological models with observed data (Gupta et al., 2009). MSE varies from 0 to infinity. An MSE value of 0 indicates a perfect fit.

In general, these objective functions tend to better fit the higher portions of the hydrograph at the expense of the lower portions to achieve a higher value of the objective function (Krause

et al., 2005). Most of sediment load is transported by the high flows and sediment is the main focus of the study hence it is more relevant to choose objectives functions which tend to focus on the upper sections of the hydrograph.

Future climate scenarios and downscaling technique

GCMs and emission scenarios

A previous study on selection of climate change scenarios for the Lower Mekong (MRC, 2015) found that in order to maximize the amount of uncertainty captured, climate change scenarios should be developed based on three GCMs (GISS-E2-R-CC, IPSL-CM5-MR and GFDL-CM3) and three emission scenario (referred to as Representative Concentration Pathways (RCPs)): RCP2.6 (low emissions), RCP6.0 (medium) and RCP8.5 (high). The three representative GCMs (GISS-E2-R-CC, IPSL-CM5-MR and GFDL-CM3) were downsized from the 15 shortlisted GCMs, which best captured the spatial and temporal climatic patterns of the region, so that a wide range of uncertainty is still covered with plausible climate projections and the time required to do the hydrological modelling is feasible (MRC, 2015). Further, these three GCMs are selected based on their satisfactory performance in simulating the most influencing climate processes in the Asian monsoon region (MRC, 2015). Hence, for this study the aforementioned three GCMs and three RCPs are used (Table 2-3). Details of three RCPs used are provided in the Appendix 2-1 (Table S2-3).

Table 2-3. Future climate scenarios used for this study.

GCM (Model ID)	Country	Emission scenario	Spatial resolution (longitude x latitude)
Goddard Institute for Space Studies Model E2, coupled with the Russell ocean model, with carbon cycle (GISS-E2-R-CC)	USA	RCP2.6 RCP6.0 RCP8.5	2.5^0 x 2^0
Institute Pierre-Simon Laplace Coupled Model, version 5A, coupled with NEMO, mid resolution (IPSL-CM5A-MR)	France	RCP2.6 RCP6.0 RCP8.5	2.5^0 x 1.27^0
Geophysical Fluid Dynamics Laboratory Climate model version 3 (GFDL-CM3)	USA	RCP2.6 RCP6.0 RCP8.5	2.5^0 x 2^0

The GCMs selected are part of the Coupled Model Intercomparison Project-5 (CMIP5) models, i.e. IPCC 5th Assessment Report GCMs. The CMIP5 models are newer, of higher resolution

and more sophisticated than the older CMIP3, i.e. IPCC 4th Assessment Report GCMs (MRC, 2015). For rainfall of the East Asian monsoon, the CMIP5 models outperformed the CMIP3 models in terms of the interannual variability and intraseasonal variability (Sperber et al., 2013). The CMIP5 models are also superior to the older CMIP3 models in terms of utilizing the most up to date scientific information and computing technology (MRC, 2015).

The two time horizons, short term future (2021-2040) and long term future (2051-2070), were used to produce climate change projections for the 3S basin. These time horizons are critical for planning purposes and have been used in previous MRC work.

Climate model downscaling

The climate change projections dataset used for this study was provided by the MRC Climate Change and Adaptation Initiative (CCAI). This dataset includes SWAT model-ready monthly 'change factors' for precipitation, temperature, solar radiation and relative humidity. MRC CCAI uses SimCLIM software to downscale the climate projections. SimCLIM is an integrated assessment model that was originally developed to enable integrated assessments of the effects of climate change on New Zealand's environment (Kenny et al., 1995). It is designed by CLIM systems, which uses projections of global mean temperature change and combines them with spatial patterns of change from GCM simulations to derive future climate projections for a range of variables at high spatial resolutions. SimCLIM employs pattern scaling plus bilinear interpolation to downscale the GCM outputs. Pattern scaling constructs future climate time series by linearly relating change in any variable (at any region or time in the future) with the change in global mean temperature for the corresponding GHG emission and time period. In pattern scaling for a given climate variable (V), its anomaly ΔV^* for a particular grid cell *i*, month *j* and year or period *y* under an emission scenario is given by:

$$\Delta V^*_{yij} = \Delta T_y \Delta V'_{ij} \quad (2.5)$$

where ΔT is the change in annual global mean temperature and $\Delta V'_{ij}$ is the local change pattern value.

$\Delta V'_{ij}$ is calculated from the GCM simulation anomaly (ΔV_{yij}) using linear least squares regression as:

$$\Delta V'_{ij} = \frac{\sum_{y=1}^{m} \Delta T_y \Delta V_{yij}}{\sum_{y=1}^{m} (\Delta T_y)^2} \quad (2.6)$$

where *m* is the number of future 5-year sample periods used (i.e from 2006-2100, 19 periods in total).

Pattern scaling is a computationally efficient approach and proven to perform well for seasonal and annual means of precipitation and temperature (Tebaldi and Arblaster, 2014). The major weakness of the pattern scaling is its assumption of linearity between temporal or spatial changes in the weather system (e.g monsoon dynamics) to changes in mean temperature and its specification as monthly change factors which does not properly represent the distribution of changes (MRC, 2015). For details on strength and weakness of pattern-scaling readers are referred to Tebaldi and Arblaster (2014).

Pattern scaling is done at the GCM grid scale, hence it does not downscale. Downscaled information is obtained by bilinear interpolation. This method interpolates the pattern scaled data from the original resolution (i.e the resolution of the GCM) to 0.5° x 0.5° grids which ensures consistency and allows comparison across the different GCMs, different time horizons, different emission scenarios, different variables, and with the baseline data.

SimCLIM provides 'change factors' and 'absolute projected values' to quantify the projected alterations to the climate. Change factors are the differences between GCM future and GCM historical climate simulations while absolute projected values are the actual GCM future climate change simulations. MRC CCAI uses change factors to quantify the projected alterations to the climate because the change factor approach represents the simplest and most practical way to produce scenarios based on multiple GCMs, emission scenarios, sensitivities, time horizons and locations (MRC, 2015).

Uncertainty analysis

The uncertainty analysis for this study is based on the methodology suggested by Chen et al. (2011b). Three different 3S SWAT model configurations (use of separate parameter solutions sets) were used for each of three GCMs and three RCPs combinations for a total of 27 simulations for each of two time horizons (Table 2-4). The flow and sediment projections from the same source of uncertainty were first grouped and then averaged for a mean projection and compared with the baseline period (1986-2005). For instance, to investigate the uncertainty linked to GCMs, flow and sediment projections were grouped by GCMs (three GCMs), each group including flow and sediment projections from three emission scenarios and three model configurations.

Table 2-4. Combination and sample size for each group of source of uncertainty.

Source of uncertainty	Group size	Combination of each group	Sample size of each group
GCM	3	3 RCP x 3 MP	9
RCP	3	3 GCM x 3MP	9
Model parameters (MP)	3	3 GCM x 3 RCP	9

The mean flow and sediment loads for the baseline period were represented by the average of the simulations of the three model configurations for the baseline period. The ranges of difference between the future hydrologic projections resulting from the use of different GCM, RCP and MP as compared to the baseline are referred to as uncertainty due to GCM, RCP and MP, respectively. Five major hydrological parameters for flow (annual, dry, wet, peak and 95% low flows) and two parameters for sediment (total annual and peak sediments) were calculated to investigate each source of uncertainty.

Results and discussion

Calibration and Validation of the SWAT model

The comparisons for the observed and model simulated discharge and sediment load show an overall good agreement in seasonal patterns with some discrepancies in peak events and interannual variability (Figure 2-3 and Figure 2-4). None of the model configurations ($SWAT_{NS}$, $SWAT_{RSR}$, $SWAT_{MSE}$) were able to capture peak flows for three stations (Kontum, Cau 14 and Ban Don; Figure 2-3), which might be attributed to precipitation data, potential errors in the observed stream flow data (especially during high flows), and inadequate representation of natural or man-made processes in the model. Several researchers have acknowledged the limitation in observed precipitation data of Mekong Region. The distribution of precipitation gauges is spare and uneven across the Mekong Basin (Wang et al., 2016; Ono et al., 2013). MRC conglomerates data from different riparian countries. The practice of data sharing among the riparian countries is limited (Nguyen et al., 2018). Further, precipitation data gathered during the second half of the 20th century by riparian countries is limited and of poor quality (i.e., many gaps and discontinuities) (Lutz et al., 2014). A study in 3S basin by Trang et al. (2017) reported poor flow calibration results for Kontum gauging station due to lack of observed precipitation data for areas upstream. Nguyen et al. (2018) also acknowledge the poor quality of precipitation data for Sre Pok sub basin. The data gap and uneven distribution of precipitation gauges can result to inaccurate spatial representations of precipitation which impacts model performances significantly (Zabaleta et al., 2014; Watson

and Putz, 2014; Xu et al., 2013). Further in Mekong Basin the errors in stream flow gauging (i.e., recording errors for low flow and gauging errors for high flow) are more evident for tributaries river (Rossi et al., 2009). Similarly, none of the model configurations were able to capture the peak sediment events (Figure 2-4). Since peak value of stream was not captured well this can have some influence on sediment results, nevertheless sediment results can be considerably affected by several other reasons. Although long-term flow observation is available, flow and sediment do not always follow same tendency or 1:1 linear relationship. Inaccuracy in temporal and/or spatial precipitation data can impact sediment yield results (e.g., Zabaleta et al., 2014; Lu et al., 2014a). (Bieger et al., 2014) highlighted that quality (resolution of) DEM (for example slope value calculated from DEM), soil data and LULC data can also influence sediment yield results. This mismatch in peak sediment may also be due to uncertainty in the modified universal soil loss equation (MUSLE) used in SWAT. MUSLE tends to overpredict the sediment yields for small events and underpredict yields for large events (Jackson et al., 1986; Johnson et al., 1986). Further, high sediment yields during the wet season may be caused by effects that cannot be captured by the model; for instance, heavy (local) rainfall-induced landslides, river bank collapses or human activities. Moreover, the model's poor capture of the interannual variability in sediment loads could be related to the uncertainty in sediment sampling itself, which for the dataset used to calibrate this model was done based on grab samples of suspended solids as opposed to detailed suspended sediment concentration data (Walling, 2008), which only began to be monitored very recently in the 3S and for which only one year of data are available at the 3S outlet (Koehnken, 2014).

The performance of the 3S SWAT model for the three model configurations was also verified in terms of three different statistical parameters/indicators (Table 2-5 and Table 2-6). In general, the results indicate that all three model configurations performed satisfactorily with performance indicators within the expected range for SWAT applications in other data-scarce basins (Ndomba et al., 2008b, a; Rostamian et al., 2008; Setegn et al., 2010; Shrestha et al., 2013). To our knowledge, there is only one other SWAT application that has been calibrated for suspended sediments in the Mekong (Shrestha et al., 2013), and a comparison of calibration results (all R^2 and NS values below 0.60) highlights the difficulty of accurately calibrating a sediment model in this basin. Assessment of the sediment flux of a river system is predominantly dependent upon the number and locations of measuring stations, the amount of available data, reliability, accuracy, the temporal resolution of the data, and, finally, the length of the records (Walling, 2008). A number of key SWAT parameters (for example, SPCON,

SPEXP and PRF) can only have single values across the whole watershed; however, in a large watershed these parameters may vary considerably and this restriction could affect modeling performance (Gong et al., 2012). The PBIAS for flow tends to be higher in the validation period as compared to the calibration period, which might be due to over fitting of volume–sensitive parameters (Bennett et al., 2012), assumptions that the calibrated parameters are stationary (and valid for both calibration and validation periods), or not incorporating dynamic land cover.

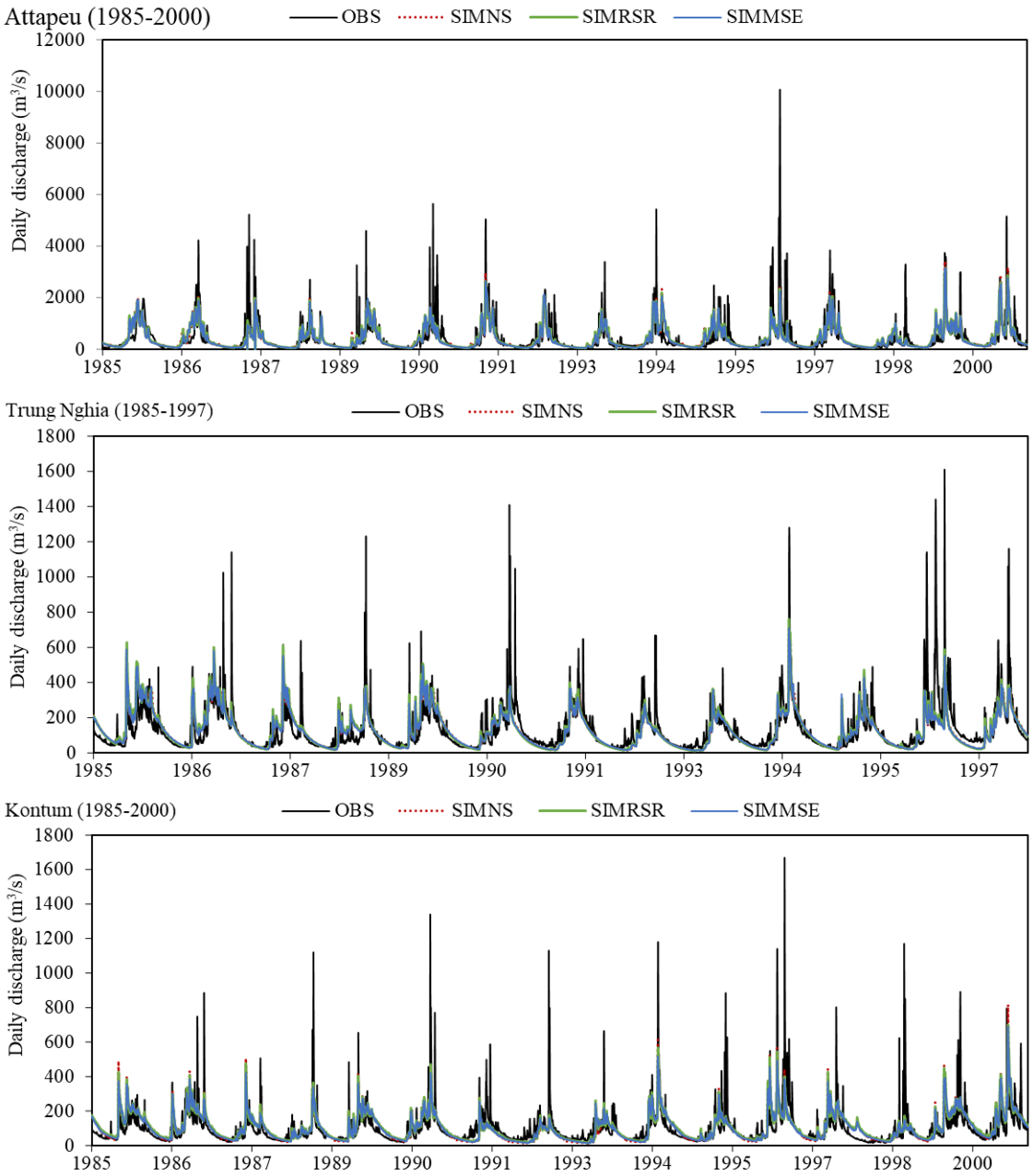

Figure 2-3 (continued)

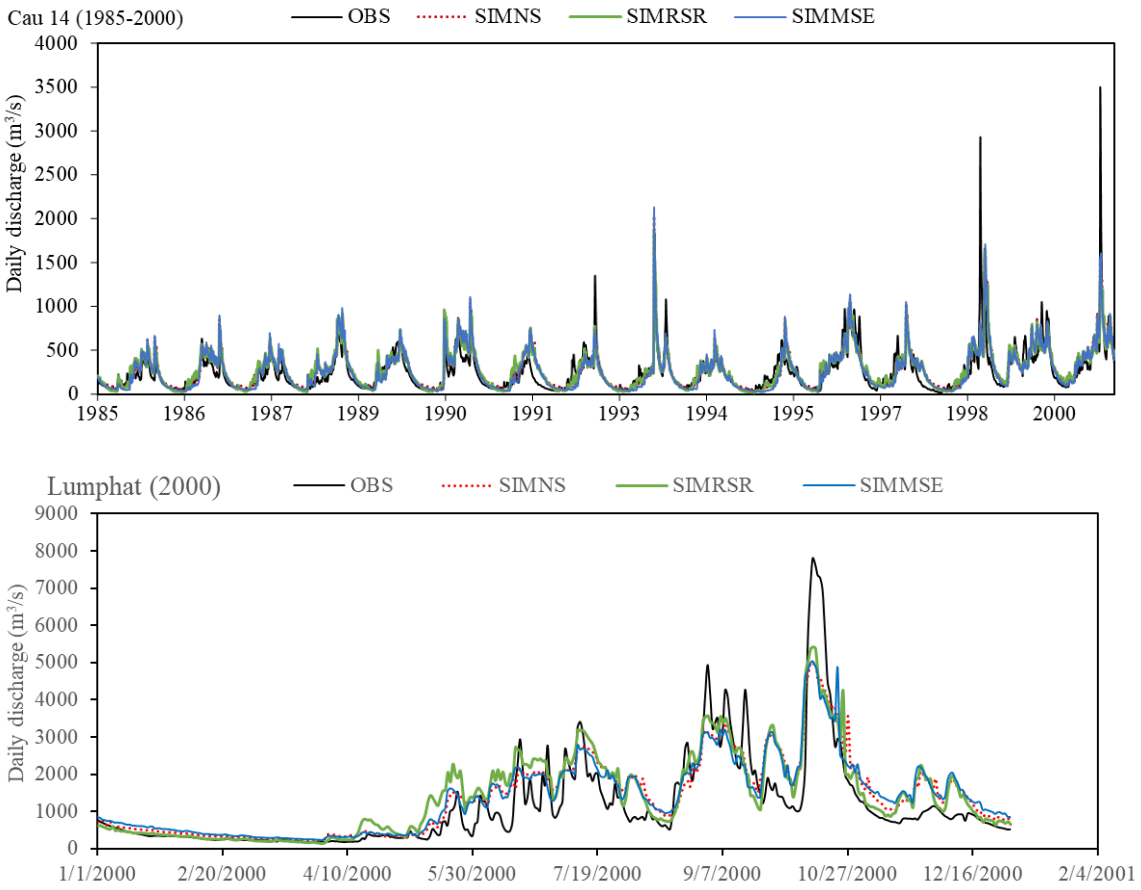

Figure 2-3. Observed (OBS) and simulated (SIM) discharge for six gauging stations within the 3S basin for the calibration period. SIM_{NS}, SIM_{RSR} and SIM_{MSE} refer to simulation using three different model configurations: $SWAT_{NS}$, $SWAT_{RSR}$, and $SWAT_{MSE}$, respectively.

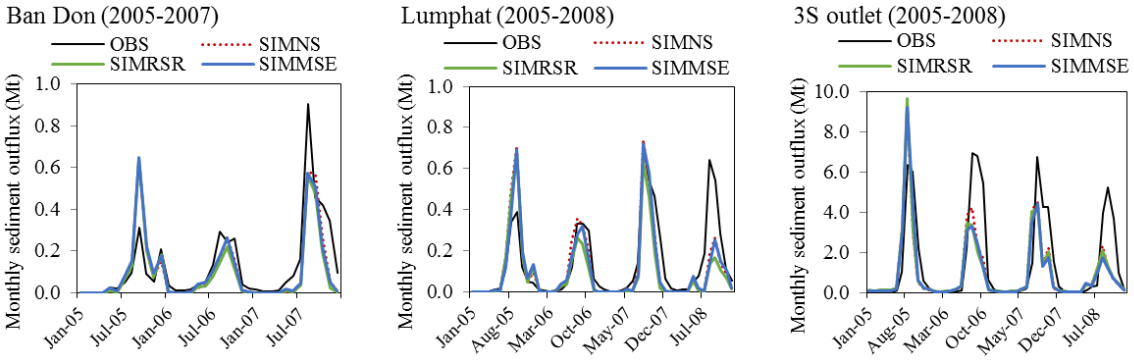

Figure 2-4. Observed (OBS) and simulated (SIM) sediment load for three gauging stations within the 3S basin for the calibration period.

Table 2-5. 3S SWAT model performance for daily discharge in the calibration and validation periods.

Name of Station	Objective function	Calibration				Validation			
		Period	Performance indicators			Period	Performance indicators		
			NS	R^2	PBIAS		NS	R^2	PBIAS
Attapeu	NS	1985-2000	0.57	0.57	3.01%	2001-2005	0.68	0.69	6.32%
	RSR		0.56	0.56	-0.90%		0.67	0.67	2.61%
	MSE		0.57	0.57	3.94%		0.69	0.69	7.44%
Trung Nghai	NS	1985-1997	0.51	0.51	4.93%	-	-	-	-
	RSR		0.51	0.51	2.63%		-	-	-
	MSE		0.5	0.51	5.97%		-	-	-
Kontum	NS	1985-2000	0.42	0.44	-1.96%	2001-2006	0.48	0.54	-20.27%
	RSR		0.43	0.44	-6.12%		0.45	0.53	-25.36%
	MSE		0.43	0.44	-3.36%		0.44	0.52	-22.85%
Cau 14	NS	1985-2000	0.67	0.68	-9.14%	-	-	-	-
	RSR		0.66	0.68	-9.96%		-	-	-
	MSE		0.66	0.68	-5.49%		-	-	-
Ban Don	NS	1985-2000	0.66	0.70	-14.51%	2001-2007	0.53	0.66	-26.28%
	RSR		0.66	0.70	-15.42%		0.55	0.68	-27.60%
	MSE		0.64	0.69	-12.21%		0.52	0.66	-23.35%
Lumphat	NS	2000	0.73	0.76	-19.81%	2001-2007	0.58	0.70	-38.89%
	RSR		0.70	0.74	-22.19%		0.45	0.68	-46.40%
	MSE		0.71	0.74	-19.97%		0.58	0.69	-40.13%
Stung Treng	NS	1985-2000	0.96	0.97	-4.69%	2001-2007	0.97	0.97	-5.33%
	RSR		0.96	0.97	-5.08%		0.97	0.97	-5.69%
	MSE		0.96	0.97	-4.10%		0.97	0.97	-4.80%

Table 2-6. 3S SWAT model performance for monthly sediment load in the calibration period.

Name of Station	Objective function	Calibration			
		Period	Performance indicators		
			NS	R^2	PBIAS
Ban Don	NS	2005-2007	0.65	0.68	21.20%
	RSR		0.61	0.64	28.84%
	MSE		0.64	0.66	20.27%
Lumphat	NS	2005-2008	0.65	0.68	18.09%
	RSR		0.54	0.59	32.76%
	MSE		0.63	0.67	22.57%
3S outlet	NS	2005-2008	0.49	0.53	31.46%
	RSR		0.44	0.48	33.67%
	MSE		0.50	0.54	35.20%

Based on the visual and statistical performance indicators comparison, the overall performance of the models was not affected substantially when different objective functions were used for

calibration. The resulting range of selected parameters used for the model calibration is provided in the Appendix 2-1 (Figure S2-4).

Climate change projections

Projected changes in the seasonal (dry and wet) and annual temperature (differences) and precipitation (ratio) for the 3S basin are presented by GCMs and emission scenarios (RCP) to illustrate each source of uncertainty (Figure 2-5). Climate projections from the same source are first grouped and then averaged for a mean climate projection. Further, the changes were also calculated for the three subbasins (Sekong, Sesan and Srepok) to reflect the variability of projections across the 3S basin. Readers are referred to the Appendix 2-1 (Figure S2-5) for results at the subbasin level.

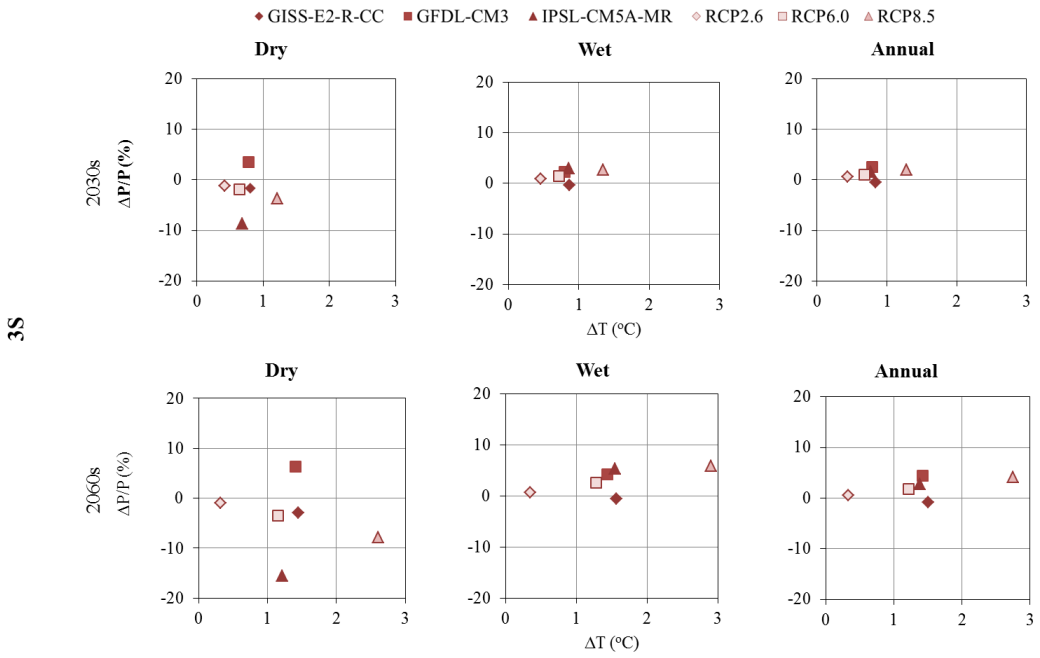

Figure 2-5. Scatterplots of changes in mean temperature (ΔT) and precipitation average (ΔP/P) over the whole 3S basin presented by GCMs (average value of three RCPs for each GCM) and RCPs (average value of three GCMs each RCP) for 2030s (2021 – 2040) and 2060s (2051 – 2070) time horizons as compared to the base line period (1986 – 2005).

All GCMs and RCPs show an increase in seasonal and annual temperature across the 3S basin, with similar variability in shifts for all subbasins, for future horizons. In the case of precipitation for all subbasins, two GCMs (except GFDL-CM3) and RCPs suggest decreases in the mean dry season precipitation. In general, all projections show an increase in the wet season and annual precipitation over the 3S basin. However, for the Srepok subbasin, GISS-E2-R-CC GCM suggests a decrease in wet season and annual precipitation.

In contrast to temperature, the variability in annual and seasonal precipitation differs among subbasins. For instance, the projected changes in wet season precipitation for 2060s (2051 – 2070) range from 1.0 to 8.5% for Sekong, 0.9 to 7.4% for Sesan, and -5.4 to 5.0% for the Srepok subbasin. Projected changes in precipitation are not unidirectional and vary depending on the GCMs, time period, and season. The bidirectional changes in precipitation may be due to the complexity in interpreting precipitation, as different GCMs often do not agree with regard to changes in both magnitude and direction at a specific location (Girvetz et al., 2009).

The uncertainties related to GCMs and RCPs for two variables increase with time as shown by the higher variability in temperature and precipitation changes from the 2030's and 2060's projections (Figure 2-5). The uncertainty linked to the GCMs is higher than for RCPs for seasonal and annual precipitation for the 3S basin. In contrast, basin wide analysis showed that the uncertainty related to the GCMs is smaller than for RCPs for wet season and annual precipitation for the Sekong and Sesan subbasins. The uncertainty related to GCMs arises due to incomplete understanding of the physical processes and the limitations in implementing such understanding in the models (Vetter et al., 2015). For precipitation projections, uncertainty due to GCMs is generally the dominant source of uncertainty for longer time horizons (Hawkins and Sutton, 2011). Uncertainty related to RCPs is larger for temperature than precipitation, and this is even greater for the 2060s period than for the 2030s period, which largely agrees with other studies (Yip et al., 2011).

Uncertainty analysis

Flow

The cumulative distribution functions (CDFs) of peak flow and 95% low flow changes for the two future time periods (or horizons) (2030s and 2060s) were analyzed for the 3S basin (Figure 2-6 and Figure 2-7, respectively). CDFs are plotted to compare the importance of all three uncertainty components. The peak flow is likely to increase for both time horizons. For example, for the 2060s (2051-2070) period using GISS, GFDL and IPSL GCMs, there is a likelihood of nearly 64%, 74% and 69%, respectively, of increased (i.e., positive changes) peak flow (Figure 2-6). Model parameter is the main contributor to uncertainty in peak flow for the 2030s period, while RCP is the main source of uncertainty for the 2060s period which is clearly indicated by the large differences between CDFs of RCP for more extreme peak flow increases. For the 2060s, the likelihood of increased peak flow ranges from 54.1% under RCP 2.6 to 78.9% under RCP 8.5. GCM is the source of uncertainty with the least influence for both time

periods. In contrast, the low flow is likely to decrease for all future horizons except for GFDL GCM, which predicts about 68% and 75% likelihood of increased low flows for the 2030s and 2060s periods, respectively (Figure 2-7). In comparison, the uncertainty due to GCM is large, which is mainly due to the GFDL model. RCPs provide the smallest source of uncertainty for low flow for the 2030s, while model parameter is the least source of uncertainty for the 2060s period.

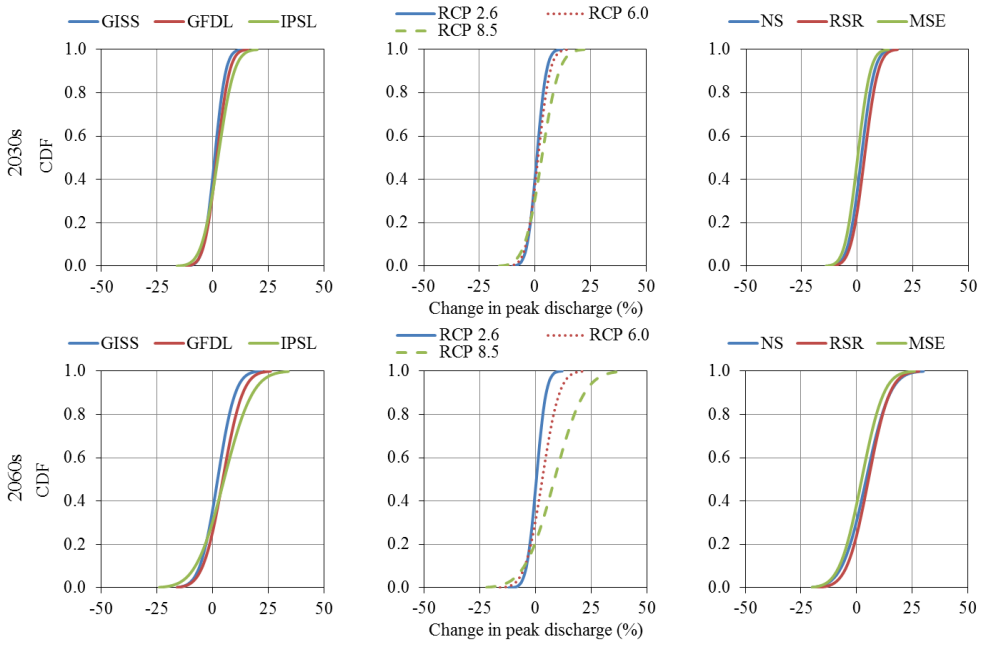

Figure 2-6. Cumulative distribution functions of peak flow changes for 2030s and 2060s periods at the 3S basin outlet reflecting uncertainty in GCMs, RCPs and MPs.

Results at the subbasin level suggest that there is substantial spatial variability in changes in peak and low flows across the 3S basin (Figure 2-8). For the Sekong subbasin, RCP is the main contributor to uncertainty of peak flow for both periods. For instance, the absolute differences (i.e., absolute differences between minimum and maximum values as shown in Figure 2-8) in the peak flow for GCM, RCP and model parameter are 2.9%, 4.1% and 1.2%, respectively. In comparison, the largest absolute difference is for RCP which makes RCP the largest source of uncertainty. Model parameters result in the least uncertainty among sources. For low flows, the uncertainty due to GCM is large and mainly due to the GFDL model. Model parameter is the least source of uncertainty for both periods. With regard to the Sesan subbasin, model parameter is the main source of uncertainty for both periods, while GCM is the least contributor to uncertainty of peak flow. Model parameter is the main source of uncertainty and RCP is the least source of uncertainty for low flow projections for both time horizons. For the Srepok subbasin, model parameter is the main contributor to uncertainty of peak flow for the 2030s

period, while GCM is the main source of uncertainty for the 2060s period. RCP result in the least uncertainty among sources. For low flows, model parameter is the main contributor and RCP is the least contributor to uncertainty for all time horizons.

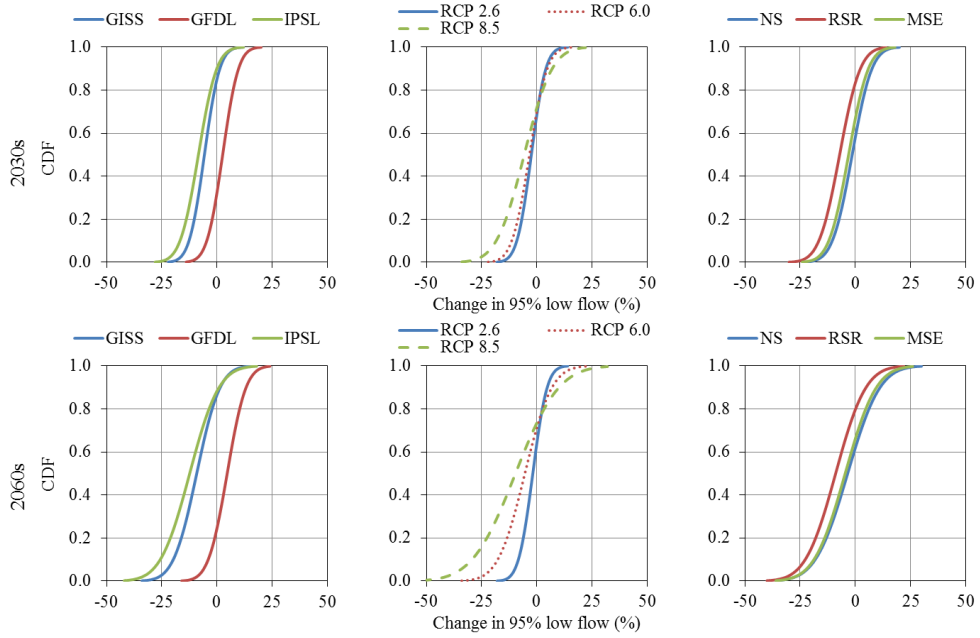

Figure 2-7. Cumulative distribution functions of 95% low flow changes for 2030s and 2060s periods at the 3S basin outlet reflecting uncertainty in GCMs, RCPs and MPs.

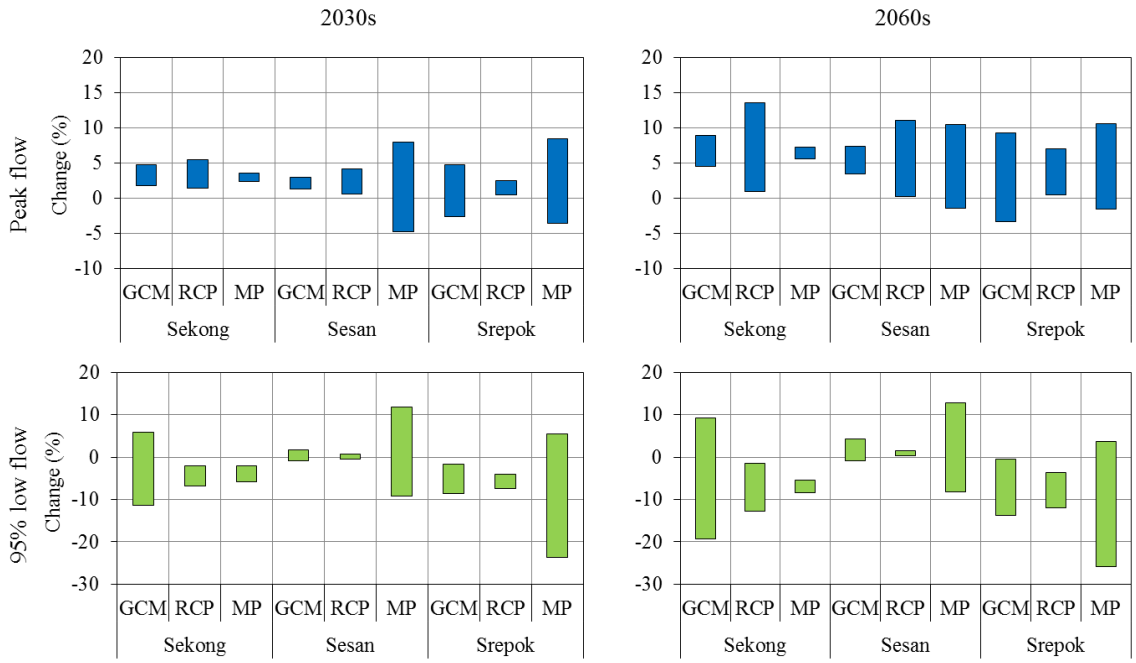

Figure 2-8. Spatial variability in peak and low flows across subbasins. Range of percent changes in peak flows and 95% low flows between baseline (1986 – 2005) and future (2030s and 2060s) periods for three sources of uncertainty. GCM = Global climate model; RCP = Representative concentration pathway; MP = Model parameter.

In general, the greatest source of uncertainty for peak flows projection varies both with time horizon and space, while for low flows the major contributing sources of uncertainty vary spatially primarily. Nevertheless, model parameter and GCM are the two major contributors to uncertainty in low-flow projections, while RCPs have a lesser effect. The uncertainties in peak and low flow projection due to hydrological model parameters can be significant, which was also concluded by Wilby and Harris (2006). Najafi et al. (2011) also found that the hydrologic model uncertainties become important when analyzing dry season flows. Hydrological model parameter uncertainty and careful calibration and validation to reduce parameter uncertainty should be taken into account in practical use of hydrological models for decision making (Zhang et al., 2014). The parameter uncertainty should be properly addressed in climate change studies to avoid an over-confident portrayal of climate change impacts (Mendoza et al., 2015).

The changes in seasonal as well as annual flows are bidirectional (Figure 2-9 and Table 2-7) as the projections of hydrological changes in the basin are highly dependent on the direction of the projected changes in precipitation (Kingston et al., 2011; Shrestha et al., 2013). Similar to peak and low flows, the dominant source of uncertainty for seasonal and annual flow varies spatially across the 3S basin (Table 2-7). For the Sekong subbasin, GCM is the major contributing source of uncertainty for seasonal and annual flow for all future time horizons. In contrast, uncertainty due to model parameter is larger for seasonal and annual flow in the Sesan. For the Srepok subbasin, uncertainty due to model parameter dominates during the 2030s period for seasonal flows and for dry season flow during the 2060s, which is mainly caused by model parameterization in the RSR model configuration. Spatial variability may be due to sensitivity of basin runoff processes to variability in climate, physiographic factors and spread/range of hydrological model parameters used to capture the runoff process in the basin. The spatial variability in LULC is large for Sesan and Srepok subbasins as compared to Sekong subbasin. High spatial variability in physical properties (such as LULC and soil type) can results to high model parameter uncertainty and considerable difference in basin behaviour (Teuling et al., 2009). For instance, RCPs represent an important driving factor for basins where the more certain projected trends in temperature are probably more relevant for projected discharges than the precipitation process (Vetter et al., 2015). Variability in spread/range of the selected hydrological model parameter(s) can have variable influences in the watersheds and the uncertainty because hydrologic parameter uncertainty tends to be larger when GCM and emissions anomalies are larger (Bennett et al., 2012). Parameter sets with similar performance, but located in different regions of the parameter space, can generate a range of projections for

future catchment behavior (Mendoza et al., 2015). The study results support that optimal solutions may lead to a wide range, and spatially variable set of hydrological model parameters (Figure S2-4 in the Appendix 2-1).

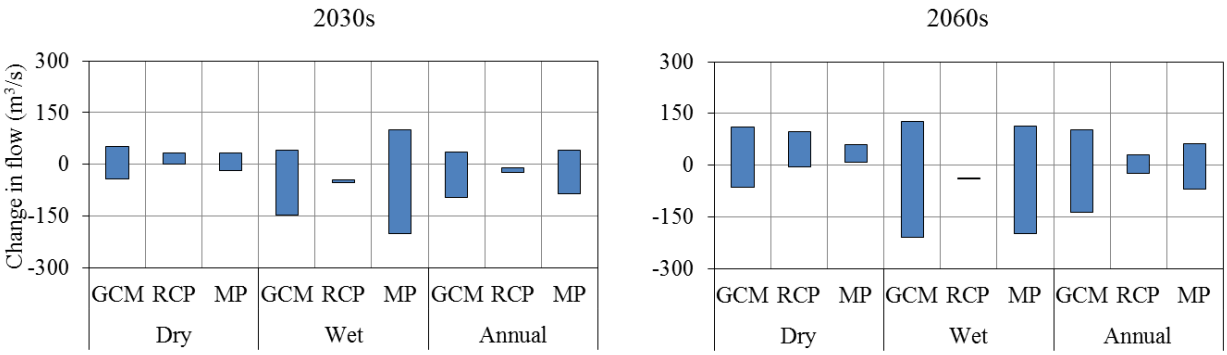

Figure 2-9. Range of changes in seasonal and annual outlet flows from the 3S basin for the future (2030s and 2060s) relative to baseline period (1986-2005) for three sources of uncertainty.

Table 2-7. Minimum and maximum changes in flows (m^3/s) between baseline (1986 – 2005) and future (2030s and 2060s) periods for three sources of uncertainty.

Subbasin	Source of uncertainty	Flow change (m^3/s)					
		2030s			2060s		
		Dry	Wet	Annual	Dry	Wet	Annual
Sekong	GCM	-11.34 , 19.43	-27.26 , 42.01	-7.85 , 30.37	-16.32 , 40.87	-43.55 , 80.86	-8.37 , 58.15
	RCP	2.71 , 16.42	-3.48 , 9.78	-0.39 , 13.1	1.93 , 43.63	-4.22 , 34.99	-1.14 , 39.31
	MP	0.98 , 13.47	-10.7 , 25.04	-1.49 , 19.26	12.69 , 24.72	-2.16 , 34.59	8.57 , 29.65
Sesan	GCM	-2.06 , 14.62	-13.01 , 5.97	-7.54 , 9.61	-3.57 , 28.65	-10.79 , 27.58	-7.18 , 26.5
	RCP	1.98 , 12.22	-10.36 , 7.18	-4.19 , 9.7	1.27 , 28.85	-9.97 , 40.15	-4.35 , 34.5
	MP	-18.51 , 33.43	-71.58 , 66.74	-45.04 , 35.82	-11.7 , 41.52	-57.42 , 81.42	-34.56 , 46.82
Srepok	GCM	-28.2 , 16.53	-125.39 , -6.35	-76.79 , 2.83	-42.48 , 38.58	-190.5 , 21.12	-116.49 , 22.14
	RCP	-4.7 , 3.05	-65.89 , -28.84	-31.42 , -16.77	-8.5 , 23.37	-104.91 , -22.42	-40.77 , -15.46
	MP	-66.36 , 51.38	-121.77 , 76.06	-43.35 , 4.85	-59.35 , 60.09	-138.54 , 67.85	-45.63 , 4.25

Note: Color coding represents the descending ranking of all sources of uncertainty for each variable as follow:

1 (highest) 2 3 (lowest)

In general, the results suggest that in the short term (2030s) uncertainty due to model parameter can be most significant for wet season flows, but in the longer term (2060s) GCM is the major contributing source of uncertainty for seasonal as well as annual flow projections (Figure 2-9). The dominance of uncertainty due to GCM has been reported before (e.g., Chen et al., 2011b), mostly due to the large uncertainty contribution of climate models for precipitation projections (Vetter et al., 2015). The change in the major source of uncertainty with time, however, is a key finding from this research that should be studied in more detail as it could result in important implications for the way climate change scenarios are translated from GCMs to watershed models.

Sediment

The cumulative distribution functions (CDFs) of peak sediment load changes were plotted to compare three uncertainty components in peak sediment load projection for the 2030s and 2060s time horizons (Figure 2-10).

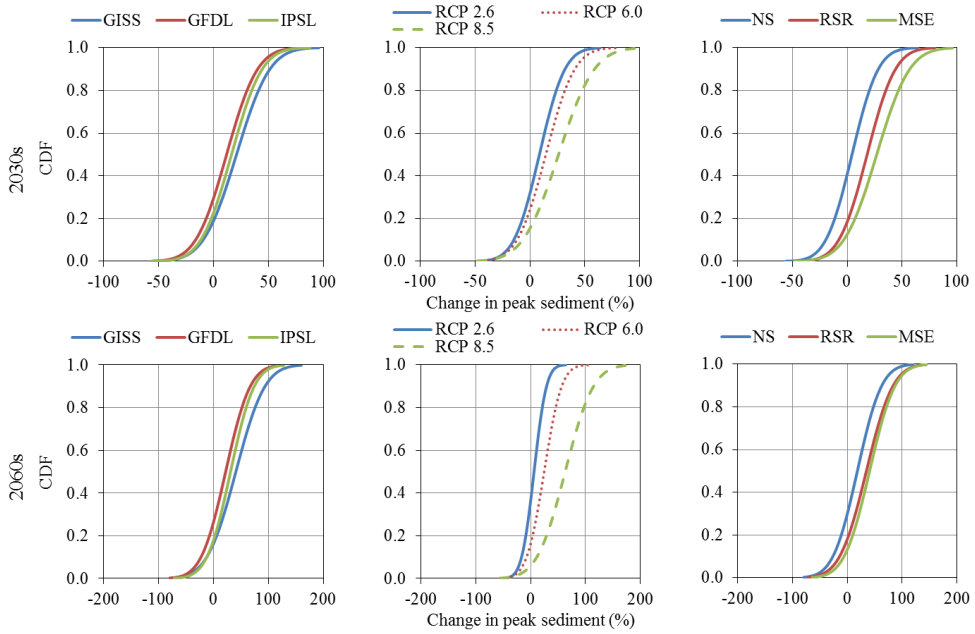

Figure 2-10. Cumulative distribution functions of peak sediment load changes for 2030s and 2060s periods at the 3S basin outlet reflecting uncertainty in GCMs, RCPs and MPs.

Similar to peak flows, the dominant source of uncertainty for peak sediment projection is subbasin dependent (Figure 2-11). In general, all simulations show that the peak sediment load is likely to increase in the future. For instance, under emission scenarios the likelihoods of increased peak sediment load ranges between 63.5 and 94% for the 3S basin as a whole, with subbasin variability of 61.19 – 93.10%, 63.38 – 78.91% and 56.67 – 72.50% for the Sekong, Sesan and Srepok subbasins, respectively. Overall, the results for the 3S basin suggest that

model parameter is the main contributor to uncertainty of peak sediment load in the short term (2030s), while RCP is the main source of uncertainty in the longer term (2060s). The choice of GCM results in the smallest source of uncertainty. In contrast, in the Srepok uncertainty due to GCM dominates the uncertainty in peak sediment load projections. This is mainly due to GISS GCM that predicts decrease in peak sediment load for the Srepok in opposite to other two subbasins. Model parameter is the smallest source of uncertainty for peak sediment load for the 2060s period and the uncertainty due to RCPs is small for 2030s.

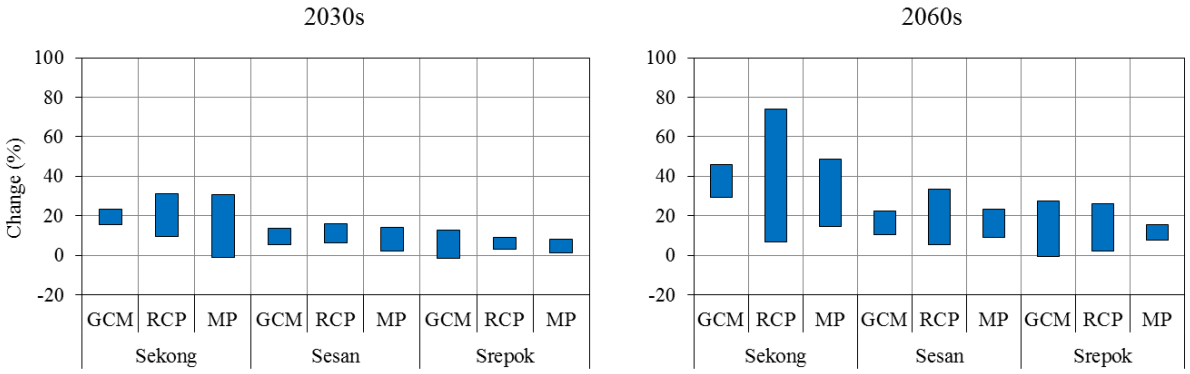

Figure 2-11. Spatial variability in peak sediment load across subbasins. Range of percent changes in peak sediment load between baseline (1986 – 2005) and future (2030s and 2060s) periods for three sources of uncertainty.

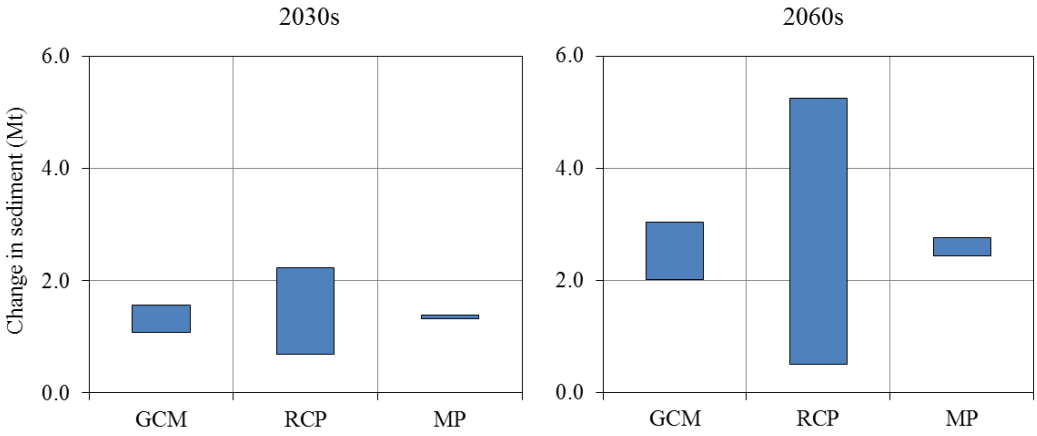

Figure 2-12. Range of changes in annual outlet sediment load from the 3S basin for the future (2030s and 2060s) relative to the baseline period (1986-2005) for three sources of uncertainty.

Basin wide analysis shows that the annual sediment load is likely to increase in the future (Figure 2-12), despite differences in the direction of change among subbasins load (Table 2-8). One of the possible explanations for this spatial variability could be due to differences in hydrologic properties (like precipitation, temperature). For instance, the changes in wet season precipitation for the Srepok appeared to be bidirectional which is opposite from the other two subbasins (where changes are unidirectional). The wet season precipitation change for the

Srepok ranges from -3.0 to 2.8% for the 2030s and -5.4 to 5.0% for 2060s. This larger response to precipitation events may explain why there is bidirectional change in annual sediment yield. Dry season sediment loads are an insignificant fraction compared to wet season sediment loads for the 3S basin. In general, changes in sediment loads follow patterns of flow, however the results indicate bidirectional flow projections can all lead to increasing sediment load for both periods. The changes of sediment yield and discharge in response to climate change do not always happen in the same direction (Shrestha et al., 2013). This also suggests that the sediment yield projection is more sensitive to temperature and rainfall changes than flow. Decrease in rainfall and increase in temperature can lead to water stress, which reduces the growth of plants and hence increases the erosion rate. This change in erosion rate causes change in the sediment flux in a river, which was also outlined by (Zhu et al., 2008). The temporal and spatial variability in the major contributing sources of uncertainty for the annual sediment load projections is also observed across the 3S basin (Table 2-8). Results of the subbasin wide analysis show that model parameter and RCP are the largest sources of uncertainty for the annual sediment load during the 2030s and uncertainty due to RCPs and GCMs dominates for the 2060s.

In general, the uncertainty due to RCPs is larger than other two sources of uncertainty for the annual sediment load projection of the 3S basin Figure 2-12). The uncertainty due to RCP is large mainly due to RCP 8.5, in which change signals are expected to be larger (i.e emissions continue to rise heading to radiative forcing > 8.5 W/m^2 in 2100). This indicates that annual sediment projections for the 3S basin have a much larger response to temperature changes than precipitation changes. Other studies have shown that sediment yield can be influenced by temperature changes. Harrison (2000) found temperature was exponentially related to the erosion rates, and Syvitski et al. (2003) indicated there was a negative relationship between temperature and sediment load in a tropical zone. Increased temperature may increase the soil erosion rate and, consequently, increase sediment flux through its influence on vegetation and weathering (Li et al., 2011; Zhu et al., 2008). SWAT simulates plant growth based on daily accumulated heat units where temperature is a major factor governing the plant growth. Increase in temperature may result in water stress, which reduces plant growth and hence increases the erosion rate. The decrease in sediment flux may be due to significant influence of increased evapotranspiration and crop growth process under warmer climate (Bogaart et al., 2003). Further, it is also interesting to note that the uncertainty in the sediment load projection is larger than the uncertainty in the flow projections, which is most probably due to higher

changes in sediment yields than the corresponding changes in flow. For instance, the annual sediment load change for the 3S basin ranges from 4.8 to 50.1% for 2060s while for the flow the changes range from -0.6 to 3.1%. A study by Shrestha et al. (2013) has also concluded that the impact of climate change on sediment yield can be greater than on flow. Although analysis of uncertainty due to LULC change is not included in this study, it is important to note that the sediment prediction uncertainty due to the climate signal might be smaller than LULC change uncertainty. A comparison of the contributions of climate and LULC change in China by Ma et al. (2014) and Dai et al. (2009) for instance, showed that projected LULC change governed changes in sediment yield. Hence, it is essential to include uncertainty in LULC change as it could help understand the range and major sources of uncertainties for better sediment management planning.

Table 2-8. Minimum and maximum changes in sediment load (Mt/yr) between baseline (1986 – 2005) and future (2030s and 2060s) periods for three sources of uncertainty.

Subbasin	Source of uncertainty	Sediment load change (Mt/yr)	
		2030s	2060s
Sekong	GCM	1.03, 1.52	1.90, 3.02
	RCP	0.63, 2.05	0.46, 4.86
	MP	1.11, 1.38	2.28, 2.57
Sesan	GCM	0.14, 0.33	0.28, 0.61
	RCP	0.13, 0.42	0.10, 0.93
	MP	0.15, 0.46	0.36, 0.66
Srepok	GCM	-0.06, 0.11	-0.09, 0.22
	RCP	0.02, 0.05	0.02, 0.15
	MP	-0.08, 0.11	-0.04, 0.15

Note: Color coding represents the descending ranking of all sources of uncertainty for each variable as follow:

1 (highest) 2 3 (lowest)

Conclusion

This study investigated the uncertainty in flow and sediment projections from climate change for the 3S basin using SWAT. Three sources of uncertainty were evaluated: GCMs, RCPs, and model parameterization. The analysis of climate change projections results showed that all of the GCMs and RCPs suggest an increase in seasonal and annual temperature across the 3S basin, with similar variability in shifts for the Sekong, Sesan and Srepok subbasins for the 2030s and 2060s. In contrast to temperature, projected changes in precipitation are bidirectional and vary depending on the GCM, time horizon, season, and subbasin. GCM is the major contributor to uncertainty in dry season precipitation projections, whereas uncertainty related to RCP is large for wet/annual precipitation and temperature across the 3S basin.

A major finding of this study is that the dominant sources of uncertainty in flow and sediment constituents vary temporally, and that results are scale dependent (basin or subbasin scale). Model parameters and GCMs are the two major contributors to the uncertainty in low flow projections, whereas RCPs had less of an effect. Model parameterization is the major contributing source of uncertainty for wet seasonal flow projections in the short term (2030s), whereas uncertainty due to GCMs dominates for seasonal and annual flow projections in the longer term (2060s). Although the uncertainty due to RCPs is large for the peak and annual sediment load projections, model parameterization uncertainty can play a significant role in uncertainty of the sediment projections for the 2030s period. The results also suggest that there is more uncertainty in sediment loads than flow projections.

In general, the study highlights that it is essential to investigate the major contributing sources of uncertainty in large basins over time and at different scales, as this can have important consequences for decision making on flow and sediment management as part of adaptation to climate change implications. Careful investigation of sources of uncertainty is an important step for decision making as it helps to improve characterization of uncertainties and avoid an over-confident portrayal of climate change impacts (Mendoza et al., 2014). Decision making under climate change should be based on assessments of risk of potential outcomes rather than traditional norm-based probability assessments (Juston et al., 2013). Overall, there are two major practical uses of uncertainty assessments: (1) through uncertainty analysis more reliable and robust predictions are produced (Addor et al., 2014) and (2) risk will be better communicated, which can be essential in gaining and retaining the trust of the public (Juston et al., 2013). This is more important for sediment projections because impact of climate change

on sediment yield is expected to be greater than on flow. Further, since model parameterization uncertainty can be significant for flow and sediment projections, there is a need to incorporate parameter uncertainty in climate change studies and efforts to reduce the parameter uncertainty as much as possible should be considered through a careful calibration and validation. Land use/land cover (LULC) could also be an important influence in model projections, and Chapter 3 evaluate the uncertainty associated with this factor.

Chapter 3

Land use/ land cover change uncertainty impacts on streamflow and sediment projections in areas undergoing rapid development: A case study in the Mekong Basin

Published as: Shrestha, B, Cochrane, TA, Caruso, BS, Arias, ME, 2018. Land use change uncertainty impacts on streamflow and sediment projections in areas undergoing rapid development: A case study in the Mekong Basin. Land Degradation and Development, 29(3): 835-848. DOI:10.1002/ldr.2831

Abstract

Quantitative understanding of potential changes in streamflow and sediment load is complicated by uncertainty related to land use/ land cover (LULC) change projections which is characterized by a high uncertainty in terms of demand (quantity) and location of changes (spatial distribution). The Sesan, Srepok, and Sekong Rivers (3S), the most important tributaries of the lower Mekong River, was simulated with the Soil and Water Assessment Tool (SWAT) to investigate the implications of conversion of forest to agricultural lands. Multiple LULC transitions in the 3S basin are projected using the Land Change Modeler. The uncertainty in LULC projection was addressed using an ensemble forecasting approach for 2060 combining: (1) three land demand scenarios, (2) two transition potential modeling approaches (i.e., approach to create maps of the likelihood for areas to transition from one LULC type to another) and (3) retaining or not protected areas. Land demand leads to the greatest uncertainty in LULC change projections. Transition potential modeling approaches do not make much difference in the total change, but can result in spatial variations of change. Retaining protected areas can contribute significantly to uncertainty in LULC change projections. Decrease in annual streamflow of the 3S basin varied from 3 to 21 % and changes in annual sediment outflux from the basin ranged from -8 to 249% for simulated scenarios. LULC demand uncertainty results in the highest streamflow and sediment load changes and can thus have major consequences for water and sediment management strategies in areas undergoing rapid development.

Introduction

Land use/ land cover (LULC) transition is a major driver of global environmental change with serious implications for greenhouse gas emissions and the hydrological cycle (Turner et al., 2007). At the catchment level, effects of LULC change include variations in vegetation stomatal conductance, surface roughness, hydraulic connectivity, and several soils' properties such as organic content, structure and infiltration rate (Fiener et al., 2011; Wei et al., 2009).

These alterations are important to the hydrologic cycle and have particular implications for water quality, sediment production, transport and delivery to rivers (Braud et al., 2001; Rey, 2003). Land use/ land cover (LULC) change can lead to deterioration in the physical and chemical properties of soils, which may contribute to soil erosion, reduction of soil fertility and land degradation (Khresat et al., 2008).

Numerous projection models have been used to analyse the causes and consequences of LULC change in order to support planning and policy (Verburg et al., 2004). LULC change models can be static or dynamic, spatial or non-spatial (i.e., exploring patterns of change versus rates of change), inductive or deductive (i.e., with model parameters based on statistical correlations versus explicit descriptions of the process), agent-based or pattern based (i.e., emulation of individual decision makers versus inference of underlying behaviours from the observation patterns in the LULC change; (Mas et al., 2014). A detailed review of different types of models were provided by Agarwal et al. (2001), Briassoulis (2000) and Verburg et al. (2004). Despite the diversity of LULC change models, most are based on the partition between the land demand calculation (the magnitude or quantity of change) and the land allocation (the spatial distribution of change, including the transition potential calculation (Dalla-Nora et al., 2014). In both cases, these projections are computed based on a number of driving factors, a portion of which are related to land demand calculations, and others related only to land allocation. Certain driving factors (for example the remaining or not of existing protected areas) can be important for both the demand calculation and the allocation process.

Quantifying the impact of LULC change over time on streamflow and sediment is challenging and often not well understood; however, model-based projections of future LULC change are often used in evaluating the impacts over time. Despite significant improvement in LULC change models, projections of LULC change remain rather uncertain. The limited availability of historical information reduces the potential to calibrate LULC change models. Even in the case when successful calibration is achieved, using it both for diagnostic and prognostic studies, the reliability of future simulations is not guaranteed. Hence, rather than relying on a single or case-specific simulation, using the same model with different assumptions (i.e., different inputs/parameterisations) will provide multiple results (Santini and Valentini, 2011) and allow consideration of a wide array of possible changes and their implied uncertainties (Araújo and New, 2007). Uncertainty in LULC change model projections is a function of their structure and formulation, and quantifying this uncertainty not only indicates the robustness of

the model's ability to predict changes, but also provides information about which inputs/parameterisations lead to the greatest uncertainty (Smith and Heath, 2001). Without assessing uncertainty, it will be difficult for policy makers and resource managers to use model results for developing more effective LULC policies and management programs (Ogle et al., 2003). Although uncertainty in LULC change could play a major role in hydrological alterations variability, it is often overlooked. A few studies have analysed the uncertainty in LULC change by multiple initial conditions, boundary conditions, parameters, input data and models (e.g. Santini and Valentini, 2011; Prestele et al., 2016). However, these studies excluded implications on hydrology. There is a clear need for improved understanding of the implication of LULC change uncertainty on the estimation of streamflow and sediment loads. This chapter aims to investigate the implication of uncertainty in LULC change projections on streamflow and sediment projections. This chapter only considers uncertainty in LULC change out of four important uncertainty sources (i.e., model parameters, global climate models, representative concentration pathways and LULC change) considered for the study because there is a need to disentangle and evaluate in detail the implication of uncertainty in LULC change for flow and sediment prediction for better characterization of the dominant uncertainty source. Further the disentangled assessment also facilities identification of major source of uncertainty in LULC change projections and selection of LULC change scenarios that captures maximum range of uncertainty. We use the Sesan, Srepok, and Sekong Rivers (3S) – the most important tributaries of the lower Mekong River – as the case study, but lessons learnt from this research can be useful globally.

Methodology

Site Description

The 3S basin, which contains the Sekong, Sesan and Srepok subbasins, is located in the Lower Mekong region in Southeast Asia (Figure 3-1). The region that includes the 3S basin (the Lower Mekong Basin) is experiencing accelerated LULC transition because of rapid changes in its economy, society, and environment. Based on the 2003 LULC map, the basin was dominated by forest (77%). Readers are referred to the Appendix 3-1 for details on LULC with original LULC class and corresponding simplified category of the study area (Figure S3-1 and Table S3-1).

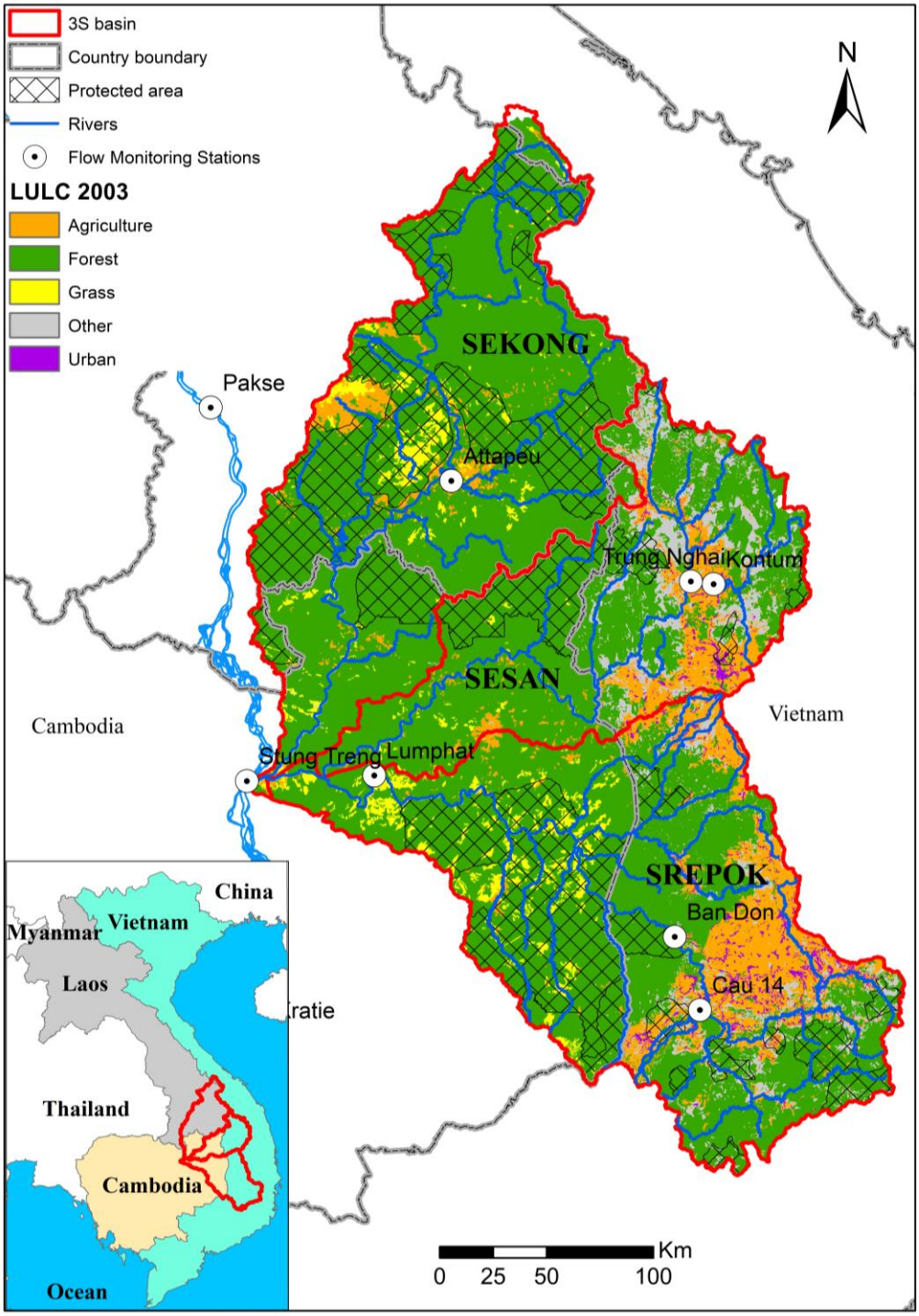

Figure 3-1. Location of the study area with 2003 LULC (simplified class) and river monitoring sites (Source: MRC, 2010).

Major LULC transitions include deforestation of native rainforest, expansion of agricultural and urban areas, and expansion of commercial plantation such as rubber trees and oil palms (Takamatsu et al., 2014). Apart from LULC change, hydropower development is progressing rapidly in the 3S basin, particularly in Vietnam and Lao PDR as a result of economic growth and a need for security in electricity production. Development of dams and reservoirs is also

tied to agro-industrial expansion because reservoirs provide opportunities for large scale irrigation and mining as lower-cost electricity becomes available. Hydropower construction typically provides road access as well. As a result, forested catchments and reserved natural areas in the 3S basin are threatened. The details on basin characteristics, meteorology and major soil are presented in methods section of Chapter 2.

Land use/ land cover data

SWAT, and most other watershed-scale hydrological models, does not incorporate interannual dynamism in LULC. That is, a fixed LULC map is maintained throughout the simulation, which is a limitation of the model (and most other catchment models). Often this limitation is dealt with parameter calibration. SWAT model study by Wang et al. (2018) found inconsiderable effect of non-stationary LULC inputs on model performance for flow simulation. However, for sediment the stationarity of LULC dynamism could affect the model performance, which should be studied in more detail. Although the 3S SWAT model was calibrated using 2003 information, LULC maps for the years 1993, 1997 and 2010, developed by the Mekong River Commission (MRC), were used as the baseline map in three other simulations to analyze historic changes and to create future LULC change scenarios. Since the 2010 map used different categories from the 1993 and 1997 maps, the original categories were simplified into five major categories to make best use of all three LULC data sets: Agriculture, Forest, Grass, Urban, and Others (Table 3-1). The maps for 1993 and 1997 were interpreted and delineated manually from complete coverage of Landsat Thematic Mapper (TM) images (Stibig, 1997), and the 2010 data were classified from these same satellite images by National line agencies (MRC in Cambodia, Lao and Vietnam).

Land use/ land cover change modelling

The Land Change Modeler (LCM;(Eastman, 2009) was used to project multiple LULC transitions for the 3S basin (Figure 3-2). LCM has been used and validated in multiple case studies and has proven to be capable of simulating LULC dynamics in tropical regions (Sangermano et al., 2012), mountainous regions (Rodríguez Eraso et al., 2013), and Southeast Asia (Fuller et al., 2011). Further, the model offers multiple approaches to transition potential modeling and has a user friendly platform (Mas et al., 2014). Theoretical description of the LCM is provided in the Appendix 3-1.

Table 3-1. Simplified LULC classes.

MRC Original Category			Simplified category
1993 and 1997		2010	
Plantations forest; Cropping mosaic, cropping area >30%; Agricultural land		Shifting cultivation; paddy field; annual crop; industrial plantation; orchard; forest plantation	Agriculture
Evergreen, high cover density forest; evergreen, medium-low cover forest density; evergreen mosaic forest; mixed, high cover density forest; mixed medium-low cover density forest; mixed mosaic forest; deciduous forest; deciduous mosaic forest; regrowth forest; woo-and shrub land, evergreen; bamboo; cropping mosaic, cropping area<30%		Deciduous forest; evergreen forest; bamboo forest; flooded forest; coniferous forest	Forest
Grassland; wood-and shrub land, dry		Grassland; shrub land	Grass
Urban or built-over area		Urban area	Urban
Barren land; water; other	Barren land; water; clouds; wetland; other	Bare land; water body; marshes/swamp area	Others

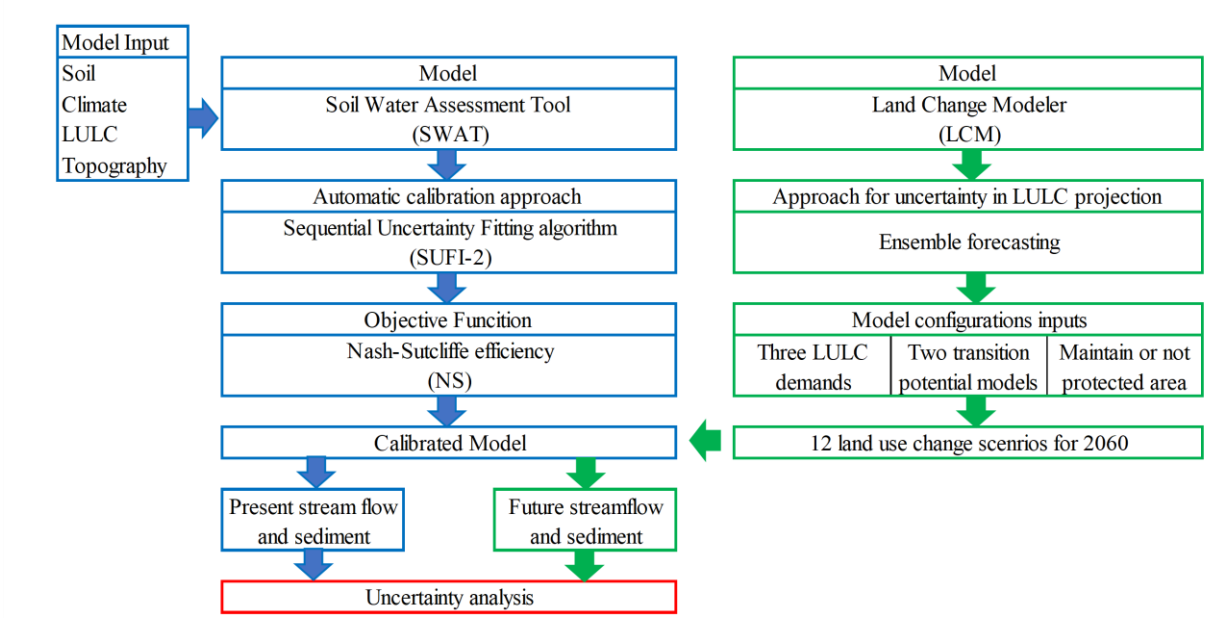

Figure 3-2. Methodological framework for evaluating the impact of LULC change uncertainty on streamflow and sediment.

Uncertainty in land use/ land cover change

The uncertainty in LULC change was addressed in this study using an *ensemble forecasting approach* as suggested by Santini and Valentini (2011). This approach is commonly used in meteorology and climatology to quantify the predictive uncertainty of weather forecasts and climate change simulations (Murphy et al., 2004) and impact studies (Bormann et al., 2009; Breuer et al., 2009; Huisman et al., 2009) by using different initial conditions, boundary conditions, parameterizations, input data and models (Santini and Valentini, 2011). Simulating

several alternative views of the future in an ensemble study will not necessarily contain the most likely prospects, but offers the range of possible changes (Koomen et al., 2008). For this study, an *ensemble forecasting* of likely future LULC change was conducted combining three different model configurations/inputs:

a) Three LULC demand scenarios based on the historic trends during the (1) 1993–1997, (2) 1993–2010 and (3) 1997–2010 periods: The future land demands were estimated through simple extrapolations of past trends of the three different historic periods. Each historic period gave a different projected quantity of change. Based on past historical trend analysis the annual rate of change for major LULC class (i.e., forest and agriculture) is lowest for the period 1993–1997(-0.2% for forest and 2.6% for agriculture), followed by 1993–2010 (-0.9% for forest and 5.8% for agriculture) and the period 1997–2010 (-1.1% for forest and 6.2% for agriculture). Hence, these three scenarios were defined as low, medium and high LULC demand, respectively.
b) Two transition potential modeling approaches: (1) logistic regression (LR), and (2) a similarity-weighted instance-based machine learning tool (SimWeight; SW). LR uses logistic regression to calculate relationships between LULC change and drivers. SimWeight models transitions without the necessity of understanding the relationship between drivers and change. It models transitions through a modified machine learning procedure (See Appendix 3-1 for details).
c) Constraints on and off: Using (or not) protected areas to constrain the LULC allocation. The data for protected areas in the study basin were obtained from MRC.

These combinations lead to 12 different LULC change simulations starting from the baseline LULC distribution (Table 3-2). LULC change up to 2060 was simulated to observe a non-trivial change in land cover, with measurable effects added to uncertainty in water and sediment flow projections. Future LULC change data were generated using nine transitions, namely: forest to agriculture, forest to grass, forest to others, agriculture to forest, agriculture to grass, agriculture to others, grass to forest, grass to agriculture and grass to others (See Appendix 3-1 for details on these transitions [Table S3-3], driving factors, and LCM model calibration).

Table 3-2. LULC change scenarios.

Scenario	Description		
	Transition potential model	**LULC demand based on period**	**Constraints (maintain protected areas)**
LR_A1	Logistic Regression (LR)	1993–1997	No
LR_B1		1993–2010	
LR_C1		1997–2010	
LR_A2		1993–1997	Yes
LR_B2		1993–2010	
LR_C2		1997–2010	
SW_A1	SimWeight (SW)	1993–1997	No
SW_B1		1993–2010	
SW_C1		1997–2010	
SW_A2		1993–1997	Yes
SW_B2		1993–2010	
SW_C2		1997–2010	

The LCM generated future LULC maps with simplified class (as presented in Table 3-1) was transformed to original LULC class for hydrological and sediment modelling as presented in Figure 3-3. The LULC for 2003 with original LULC class was simplified into five classes. The simplified LULC for 2003 was then compared with future LULC for 2060 forecasted using LCM. The cell where change happened was reclassified back to the original LULC class. For example, if a cell with class 1 changed to class 2, then it was reclassified back to its corresponding original class i.e., 91.

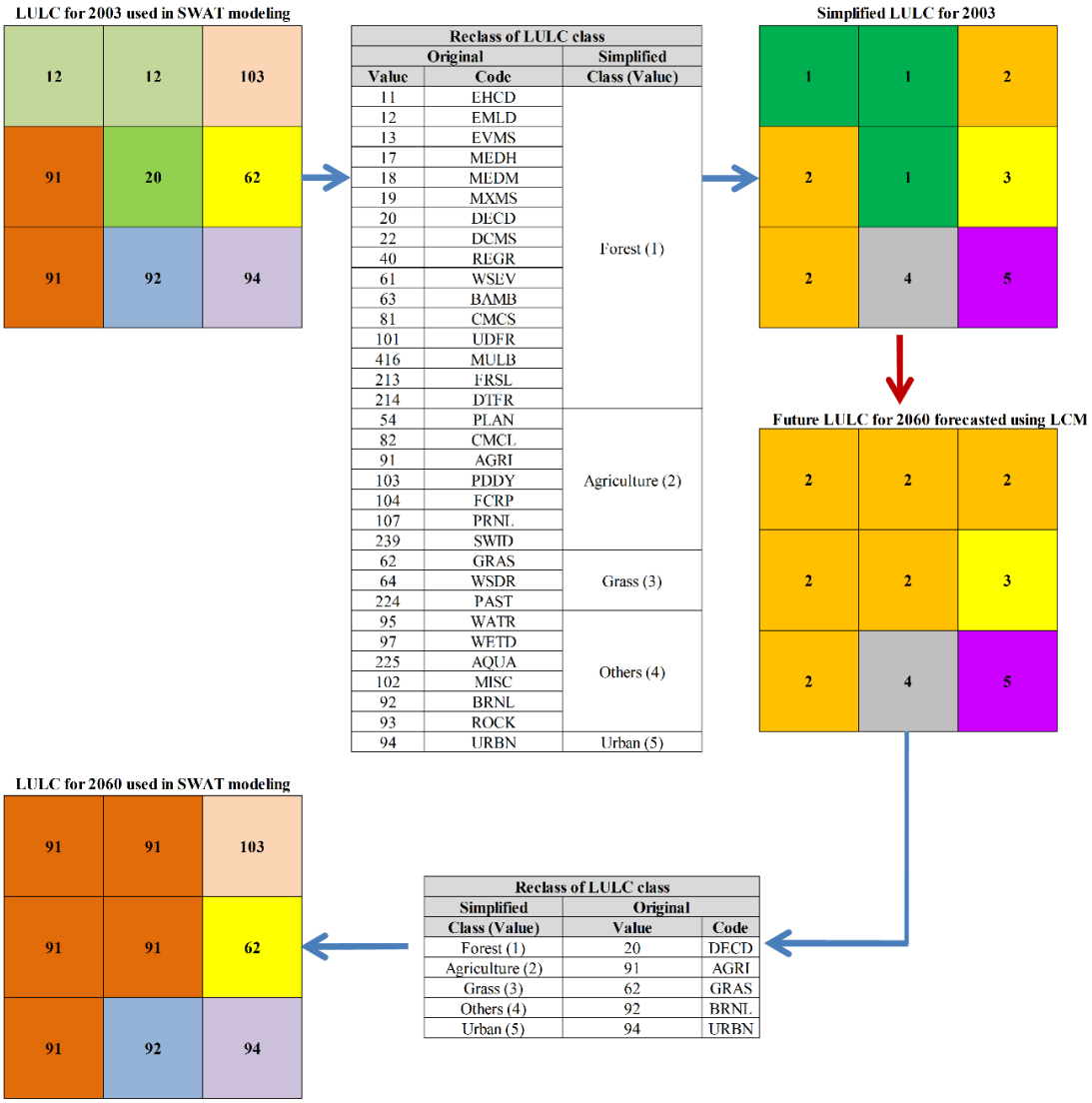

Figure 3-3. Process flow used to transform future LULC with simplified class to original LULC class.

Hydrological and sediment modeling

The Soil and Water Assessment Tool (SWAT;(Arnold et al., 1998; Srinivasan et al., 1998), was used for simulating streamflows and sediment in the 3S basin because SWAT is used by MRC as part of their modeling Toolbox (MRC, 2010), and the performance of the 3S-specific application has been well investigated (e.g.Shrestha et al., 2016; Oeurng et al., 2016). The theoretical description of SWAT is provided in the Appendix 2-1. All model input data (for example meteorological, spatial) were provided by MRC. The management data for various LULC classes used in this study were also provided by MRC (including local forests). MRC has actual values for some agricultural classes (for example, field crop and paddy field) while

for some classes (for instance, agricultural intensive land) SWAT default values were used. Readers are referred to the Appendix 3-1 (Table S3-5) for details on the management data used.

Model calibration, validation and performance evaluation

The 3S SWAT model was calibrated for daily flow and monthly sediment load at various locations with observed data. The validation was only carried out for daily flow. The details on model calibration and validation process are presented in methodology section of Chapter 2. It is to be noted that for this chapter the 3S SWAT model which was calibrated for Nash-Sutcliffe efficiency (NS) objective function is used because of its wider use (Gupta et al., 2009; Moriasi et al., 2007) and its better performance in reflecting the overall fit of a hydrograph (Servat and Dezetter, 1991). Details of the parameters calibrated and their fitted ranges are provided in Appendix 3-1 (Table S3-6). The calibrated parameter values given in this study may not necessarily represent the uniquely best parameter combination because a good model simulation can be achieved using various combinations of the model parameters. This issue is well known in hydrology and often termed as equifinality or non-uniqueness of the parameters (Beven, 2001). The calibrated models were evaluated by comparing the simulated with the observed constituents using the NS, Coefficient of Determination (R^2) and percent bias (PBIAS) (refer to Table 2-5 and Table 2-6 in Chapter 2). The prediction efficiency of a calibrated model can often be judged as satisfactory if NS and R2 values are > 0.6 for mean behavior (Santhi et al., 2001; Benaman et al., 2005; Setegn et al., 2010); however, this threshold, is rather subjective and should be used with caution and with consideration of the model's objective variable (Oeurng et al., 2016). A PBIAS value <15% has been considered a satisfactory performance rating of a calibrated model (Santhi et al., 2001; Van Liew et al., 2007). Comparisons between observed and simulated streamflows and sediment load show an overall good agreement in seasonal patterns, with some discrepancies in peak events and interannual variability (Figure 3-4 and Figure 3-5). Further details on model performance are provided in results and discussion section of Chapter 2.

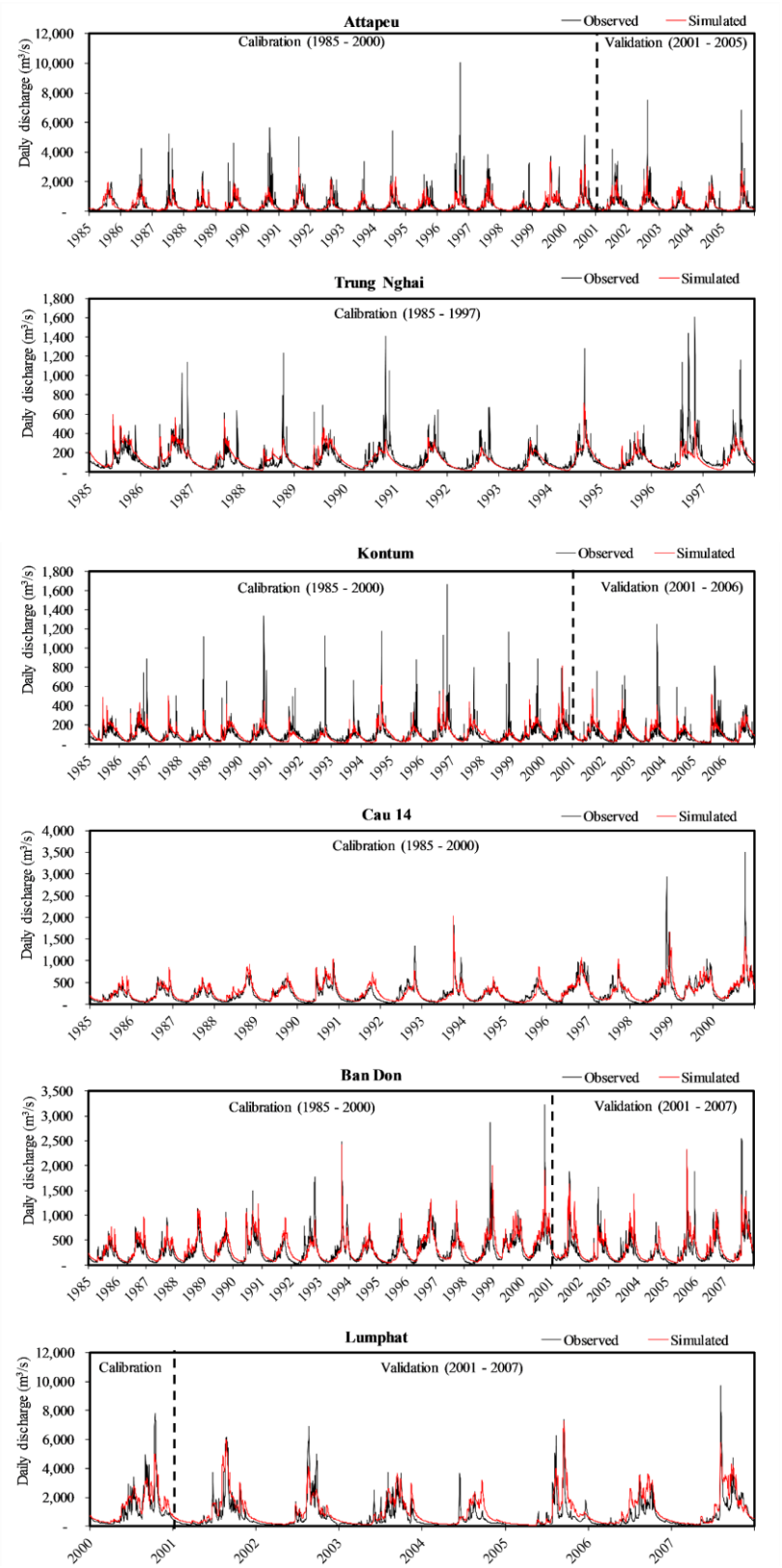

Figure 3-4. Observed (OBS) and simulated (SIM) discharge for six gauging stations within the 3S basin for the calibration and validation periods.

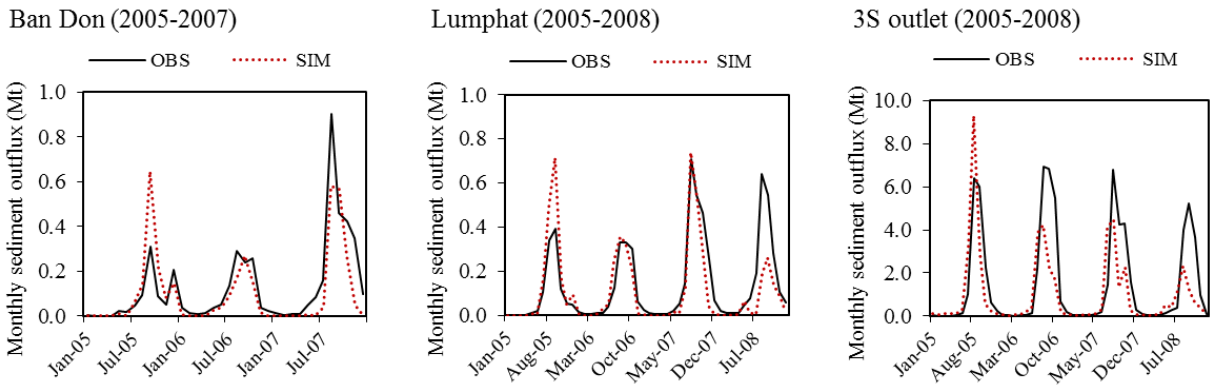

Figure 3-5. Observed (OBS) and simulated (SIM) sediment load for three gauging stations within the 3S basin for the calibration period.

Uncertainty analysis

The calibrated 3S SWAT model was run with projected future LULC maps to evaluate the impact of uncertainty in LULC change on streamflows and sediment. The 3S SWAT model was calibrated using LULC for 2003 with the original classes; hence, before the model simulation, the future LULC with simplified categories were transformed back to representative 2003 LULC classes (see details in Appendix 3-1). Although the analysis of LULC change between 1993 and 2010 shows that the LULC in the catchment was not stable, 2003 LULC was used for the baseline hydrological simulations, as if no LULC change occurred throughout a single given simulation. The mean streamflow and sediment projections under different LULC change scenarios for the 2060s period (2051–2070) were compared with the baseline period (1986–2005). The ranges of difference between the future hydrologic projections resulting from different scenarios as compared to the baseline is referred to as uncertainty due to LULC change.

Results and Discussion

Uncertainty in land use/ land cover projection

The magnitude of projected change in LULC varies drastically, depending on the configuration of the different scenarios (Figure 3-6 and Figure 3-7). For instance, based on the simulated future LULC maps, by 2060 the area covered by forest is expected to decrease 9–53% while the agricultural area (which is characterized as intensive by MRC) is projected to increase 12–44% (Figure 3-7). The largest change in area as well as the largest variation in transition was from forest to agriculture, with area change ranging from 11,400 to 35,000 km^2 (Figure 3-8). Previous studies on projection of future LULC in the 3S basin also suggest significant growth

of agricultural areas by replacing forests and grasslands (Ty et al., 2012; Takamatsu et al., 2014).

The analysis of LULC change showed that land demand is the major source of uncertainty. For example, under the LR modelling approach the highest range of change in forest was observed between LR_A1 (a non-constraint scenario based on low LULC demand) and LR_C1 (a non-constraint scenario based on high LULC demand) (Figure 3-7). The decrease in forest area varied from almost 9 to 53%. The land demand calculation is one of the most critical and uncertain aspects of LULC modelling (Dalla-Nora et al., 2014). Further, the results suggest that modelling approaches do not make much difference in the total area covered by each LULC category, but can result in spatial variations of change. For instance, the LR_C1 scenario forecasted the forest coverage to decrease to 36% and 29% for the Sekong and Sesan subbasins respectively, while the SW model approach forecasted the forest coverage to decrease to 33% for both subbasins (Table 3-3).

The difference in range of transition area between the baseline (2003) and future (2060) LULC information for all nine transitions between modellings approaches (LR and SW) was not large (Figure 3-8). The location (spatial distribution) of change was different between modelling approaches (LR and SW) because it was based on the change/transition potential or suitability maps (see details on spatial variability of changes in the Appendix 3-1 Table S3-7). A similar situation was observed by Mas et al. (2014) in a study where various LULC change models were compared for a virtual case study. The LR and SW very different approaches to produce the change/transition potential. One of the major differences between these two methods is that in LR an empirical formulation for the relationship between land change and drivers is needed in order to generate change/transition potential, while SW produces change/transition potential maps through a modified machine learning procedure without an empirical formulation. It is also interesting to note that retaining (or not) protected areas to constrain the LULC allocation can also contribute significantly to uncertainty in LULC change projections. For instance, under SW_C1 (non-constraint scenario) the forest cover decreased to 29%, while for SW_C2 (constraint scenario) the forest cover decreased to 52% only (Figure 3-7). Constraints are crucial as they influence both the future LULC demands and location of change.

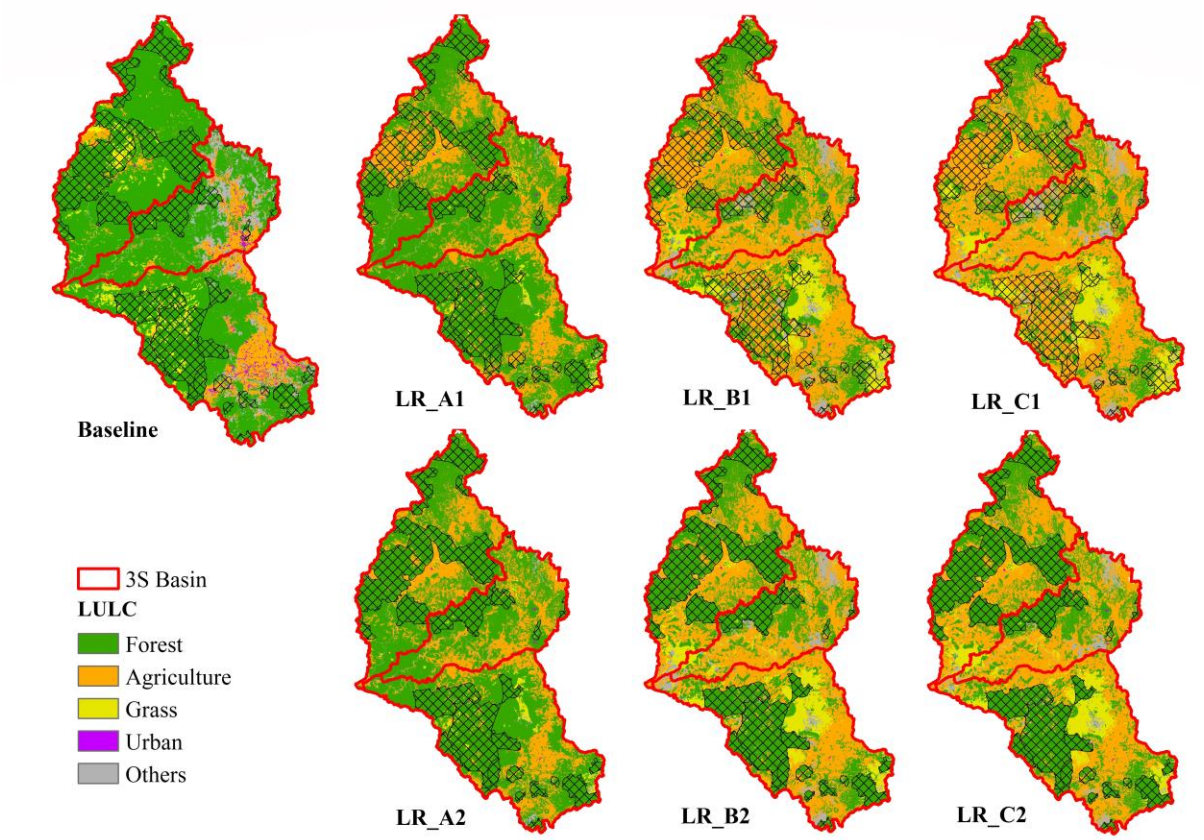

Figure 3-6. LULC change projections for 2060 based on different scenarios outlined in Table 3-2. The gridded areas are protected areas within the basin.

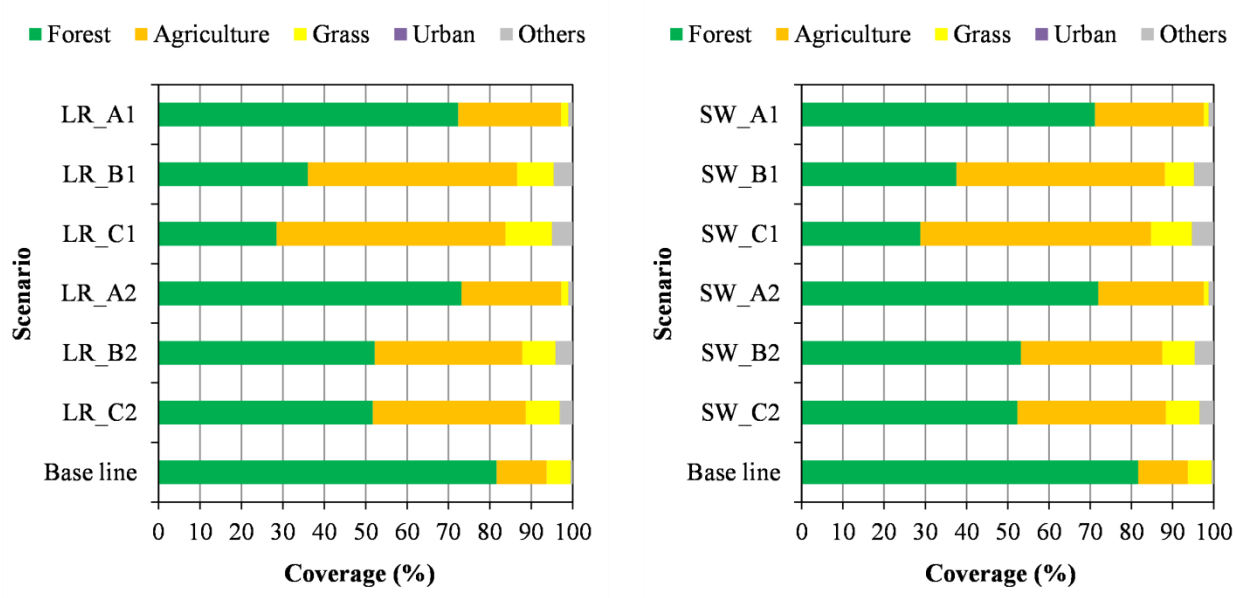

Figure 3-7. Percent cover for LULC classes in the baseline year of 2003 and projections for 2060.

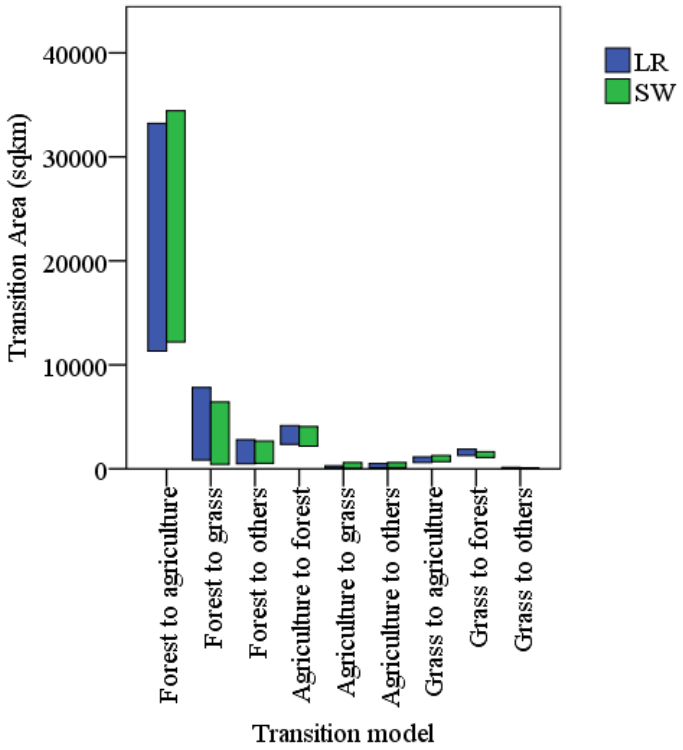

Figure 3-8. Range of transition area between the baseline LULC (2003) and future LULC (2060) for nine different transitions and two transition potential models.

Hydrological implications of uncertainty in land use/ land cover projection

Streamflow

All scenarios showed a decrease in annual and peak 3S basin outlet streamflow varying from 3–22 % and 3–9% respectively (Table 3-3). The monthly streamflow decrease ranges from less than 1 to almost 1450 m^3/s (Figure 3-9). The result suggests that the decrease in streamflow will be more significant for the wet season (May to October) than the dry season. Streamflow reduction can be attributed to the factors that result in increased evapotranspiration due to conversion of forest to intensive agriculture. The results suggest an increase in annual evapotranspiration rate of 6–59% compared to the current baseline (Table 3-3). Streamflow is the net result of the difference between effective rainfall and evapotranspiration; thus, an increase in evapotranspiration could lead to significant reductions on surface runoff and groundwater recharge (Calder, 1993). SWAT uses the Soil Conservation Service (SCS) curve number method, which relates the amount of net surface runoff volume to the degree of surface permeability, LULC and antecedent soil water conditions (USDA-SCS, 1972); hence, changes in curve number cause a direct change in streamflow. As per the MRC database for crops used in SWAT modeling, the curve number (CN) assigned to intensive agriculture is lower than that of major forest LULC class. The forest cover in the 3S basin is comprised mainly of deciduous and evergreen trees with medium- to low- density cover. The default CN for intensive

agriculture ranged from 31 to 79 based on hydrologic soil group. For deciduous forest CN ranged from 45 to 83. For details on CN values readers are referred to Table S3-1 of the Appendix 3-1. Hence, conversion of forest to intensive agriculture with lower CN decreased the surface runoff and increased the amount of water lost to infiltration. The result suggests that the fraction of runoff from forest is 17% of the total water yield, while under agriculture it is 14%. Baseflow is higher under forest, than under agriculture while evapotranspiration is higher under agriculture than under forest. A study by Ty et al. (2012) of the Srepok subbasin also indicated that doubling the current area of intensive agriculture may lead to increased water stress in the subbasin by more than 100% by 2050. Small-scale (<1 km^2) studies have generally indicated that clearing forest for agriculture leads to an increase in water yield in temperate, humid and dry tropical areas. However, studies that evaluated the effects of changes in land cover in larger river basins (>1000km^2) generally have not found similar relationships (e.g. Wilk et al., 2001; Bruijnzeel, 1990) because larger river basins tend to include a diversity of land-uses and practices, geology, topography, soils and climate which will moderate the hydrological response of the basin. The modelling results showed that replacing forest by intensive agriculture could reduce streamflow, which suggest that different crops and management methods can play a big role in flow discharge differences between regions. Recent studies have shown that the influence of deforestation on runoff is strongly dependent on the crop type (Yu et al., 2015), and the way the vegetation cover is managed controls streamflow more than land cover (i.e. theoretical evapotranspiration characteristics of the vegetation) (Lacombe et al., 2016). In the Lower Mekong Basin, commercial crop agriculture is expanding and replacing subsistence rice-based systems in upland and low elevation zones (ICEM, 2013). Maize, cassava, sugarcane and soya are the main commercial crops cultivated, in addition to rice. In this study, it is assumed that maize and cassava will be the main crop farmed intensively in the 3S basin. Research on impacts of various cropping systems and soil types on runoff and shallow groundwater in the U.S. Midwest showed that water use by row crops like maize can reduce runoff and percolation resulting in decreases in baseflow and streamflow (USACE, 2007).

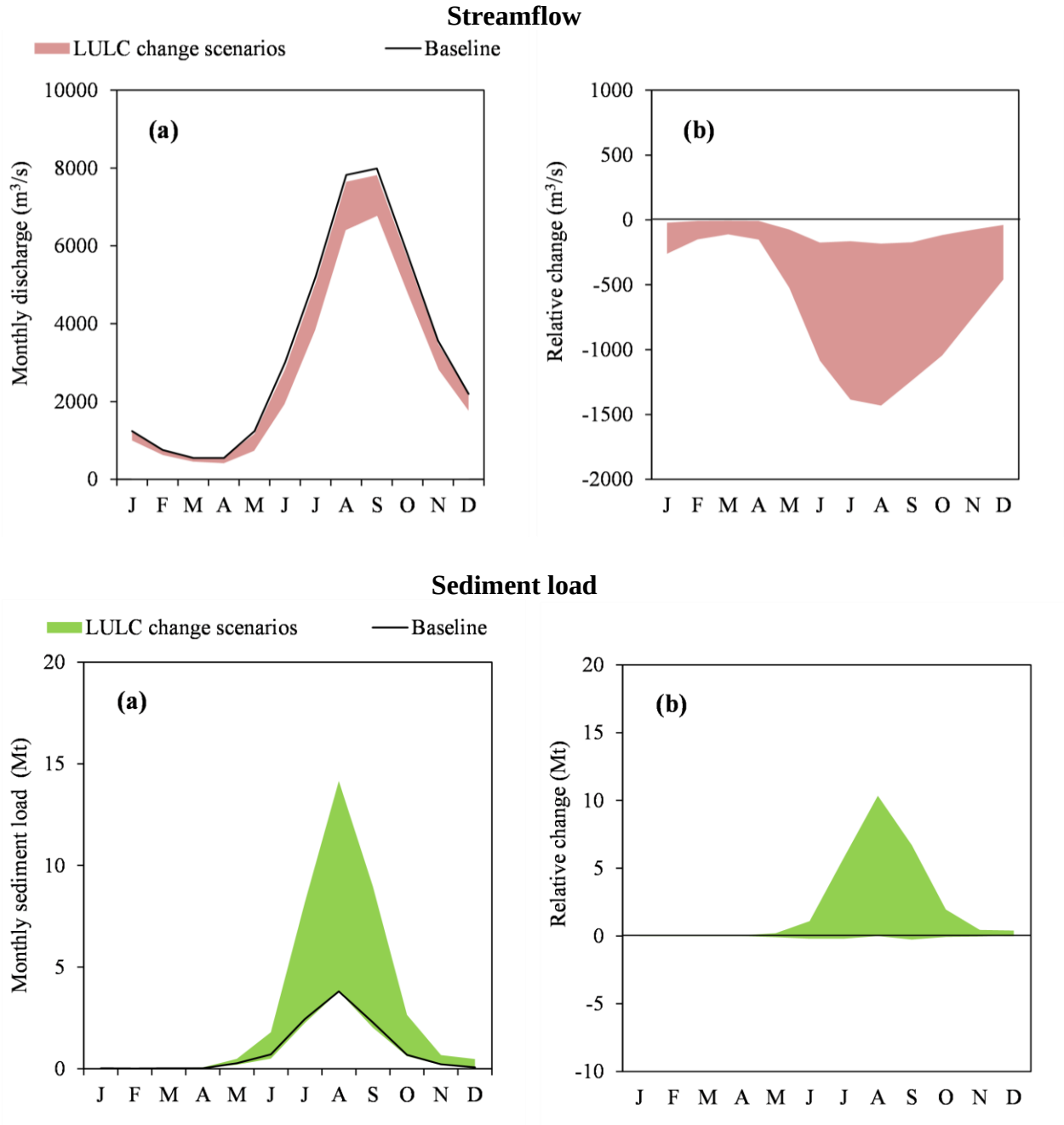

Figure 3-9. (a) Annual streamflow and sediment load cycle for the baseline period (1986 – 2005) and the range of all LULC change scenarios and (b) range of relative changes in future (2060s period) monthly outlet streamflows and sediment loads from the 3S basin for all LULC change scenarios relative to 1986 – 2005.

Table 3-3. LULC change scenarios and resulting changes in annual evapotranspiration (ET), outlet streamflows and sediment loads relative to baseline (1986–2005).

LULC Scenario	Major LULC class coverage (%)								Change (%)				
	Forest				Agriculture				ET	Stream flow		Sediment load	
	Sekong	Sesan	Srepok	3S	Sekong	Sesan	Srepok	3S		Annual	Peak	Annual	Peak
LR_A1	69	73	75	72	30	24	21	25	9	-4	-7	26	41
LR_B1	42	38	29	36	53	51	48	51	52	-19	-8	154	169
LR_C1	36	29	22	29	58	55	53	55	59	-22	-9	207	212
LR_A2	76	67	74	73	23	30	22	24	7	-3	-7	-8	16
LR_B2	62	43	49	52	32	45	33	36	35	-12	-6	48	75
LR_C2	61	43	49	52	34	46	34	37	36	-12	-6	50	89
SW_A1	76	68	69	71	23	30	28	27	7	-4	-4	69	102
SW_B1	39	41	34	38	54	41	54	51	47	-18	-8	218	310
SW_C1	33	33	22	29	58	44	62	56	58	-21	-7	249	339
SW_A2	79	66	69	72	19	32	28	26	6	-3	-3	18	62
SW_B2	61	46	51	53	33	33	37	34	34	-11	-7	71	165
SW_C2	60	46	49	52	33	35	39	36	36	-12	-8	75	170

The variation in simulated streamflow between various LULC change scenarios used in this study is significant, which indicates a high degree of uncertainty in the magnitude of streamflow changes due to LULC change (Table 3-3 and Figure 3-9). The high variability in streamflow changes was mainly due to larger uncertainties that exist in future LULC forecast mainly due to LULC demand. The scenario with the lowest land demand (1993–1997) or forest to agriculture transition (e.g. LR_A2) resulted to lower rate of streamflow changes while the scenario with the highest land demand (1997–2010) or forest to agriculture transition (e.g. LR_C1) resulted to higher rate of streamflow changes. There was not much difference in streamflow changes between two transitions modeling approaches (LR and SW). Overall, what it most clear about the implications of LULC change uncertainty on streamflows is that even the direction of change is highly variable, and that LULC derived parameters in hydrological models also play a major role.

Sediment load

The annual sediment load change ranges from an 8% decrease to a 249% increase, depending upon LULC change scenarios (Table 3-3). All scenarios showed an increase in peak sediment load varying from 16–339 %. The monthly changes in sediment load range from -0.3 to 10.4 Mt (Figure 3-9). Most simulations show that the sediment load is likely to increase in the future due to conversion of forest to intensive agriculture. Deforestation and an increase in agricultural land typically leads to higher soil erosion and subsequent increase in river sediment transport (Walling, 1999). LULC transitions towards agriculture increase sediment loads usually due to lower vegetation cover, either permanently or during critical soil mobilization periods (tillage). LULC change led to higher sediment loads than the corresponding changes in streamflows. Increased sediment load can have great implications for water resources management, including reservoir siltation and related loss of water storage and hydropower capacity (Arias et al., 2011), as well as loss of conveyance capacity and increased turbidity of rivers (Walling, 2008). Increased sediment load can also affect water quality due to sediment-bound nutrients. The variation in simulated sediment load among LULC change scenarios is significant which indicates high uncertainty in the magnitude of sediment load change due to LULC change. Although the high variability in sediment load changes can be mainly attributed to large uncertainties in future LULC forecast due to simulated demands, uncertainties in transition modeling approaches also contribute significantly to this variability. The range of sediment load changes between the scenario with the lowest land demand or forest to agriculture transition and the scenario with the highest land demand or forest to agriculture

transition was -8 to 207% and 18 to 249% for LR and SW, respectively (Table 3-3). This difference in range of change between transition modeling approaches is mainly due to the spatial variability of LULC changes as discussed earlier. This is also clearly indicated by the variation in the spatial distribution of annual average sediment yield from the studied basin among the LULC changes scenarios (Figure 3-10).

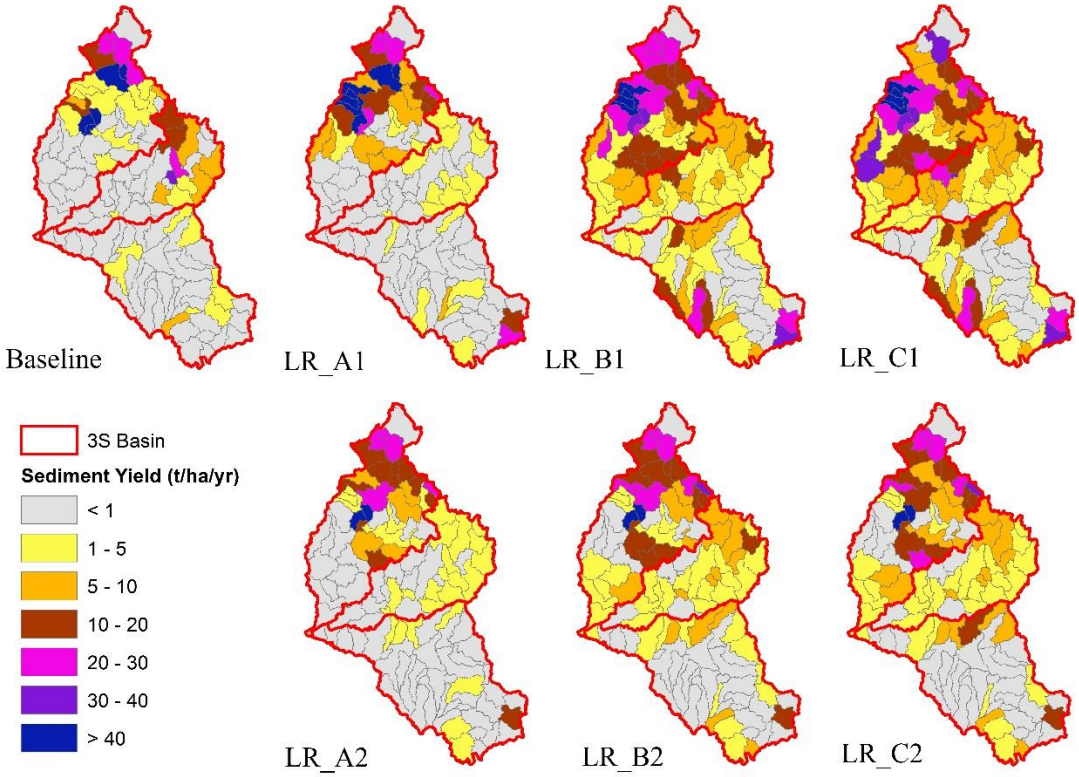

Figure 3-10. Average annual sediment yields (t/ha/yr) from various 3S subbasins for baseline (1986-2005) and future (2060s period) for various LULC change scenarios.

It is interesting to note that the Sekong river sediment yields increase although large areas of forest remain in all scenarios. On the other hand, large LULC conversions in the Srepok and Sesan result in small increased yields. This variability in sediment yields is due to sensitivity of basin sediment yield to variability in climate, topography, catchment morphology, soil type, and drainage/hydrological model parameters used to capture the erosion and deposition of eroded soil particles in the basin. Soil erosion is not only sensitive to LULC but also other factors such as slope. Basins with higher elevations and steeper terrain slopes contribute greater sediment yields than basins in lowlands. In the 3S, subbasins with agriculture LULC class, acrisols soil and higher elevation produced the highest sediment yields. The Sekong has a number of highland subbasins where the combination of steep terrain and large rainfall precipitation (some of the largest in the Mekong Basin) results in large increased yields. The

uncertainty in the sediment load projection is larger than the uncertainty in the streamflow projections, which is due to higher sensitivity of sediment prediction parameters to LULC change.

Despite the considerable variability in streamflow and sediment load due to uncertainty in LULC change projections, the results show that future LULC could have significant effects on streamflow and sediment load of the 3S basin. Hence, there is a need for soil and water management for the 3S Rivers. Moreover, some of the results show very large increase in erosion yields (up to 250 %), which should raise the concern of hydropower developers as the design, operation and reservoir sedimentation of future dams would need to be reassessed. There is thus a need to investigate appropriate reservoir sediment management strategies to reduce the adverse effects of LULC change. Further, it is imperative that planners and decision-makers take the uncertainty in LULC change into account in the design of reservoir dams that have been planned.

Analysis of uncertainty due to model parametrization, climate models, emission scenarios and agricultural management was not included in this study. It is important to note that uncertainty in parameters characterizing different LULC might lead to uncertainty in model predictions of LULC change effects (Eckhardt et al., 2003). A recent study by Prestele et al. (2016) suggested that both initial data and model parameters can contribute substantially to the uncertainty in LULC change projections. There are several studies which suggests that the sediment prediction uncertainty due to the climate signal might be smaller than LULC change uncertainty. For instance, a study by Rodriguez-Lloveras et al. (2016) concluded that LULC change are the most critical factor affecting the erosion and sediment production, even more so than climate change emission scenarios or peak flow interval. Similarly, a comparison of the contributions of climate and LULC change in China by Ma et al. (2014) and Dai et al. (2009), showed that projected LULC change governed changes in sediment yield. However, changes in temperature and precipitation can alter the pattern of the system response to LULC change (Bussi et al., 2016). Furthermore, agricultural management can significantly impact streamflow and more specifically sediment losses. Hence, it is essential to include uncertainty due to model parameterization, climate models, emission scenarios and agricultural management in addition to uncertainty in LULC change as it could help understand the range and major sources of uncertainties for better sediment management planning. Johnston and Smakhtin (2014) have also outlined that more focus is needed on reporting uncertainty, to allow

more realistic assessment of the degree of confidence in using results for policy and management.

Conclusions

In this study, the implication of uncertainty in LULC change on streamflow and sediment projections of the 3S basin was evaluated. The uncertainty in LULC change was addressed using an *ensemble forecasting* approach where three model approaches/inputs were combined consisting of land demand scenarios, transition potential modeling approaches, and constraints (or not) on protected areas. LULC demand induces large uncertainties in future LULC forecasting, hence, care should be taken when choosing LULC demand scenarios for projecting future LULC. Modeling approaches do not make much difference in the total change, but can result in spatial variations of change. Constraining the LULC allocation can also contribute significantly to uncertainty in LULC change projections as it influences both the future LULC demands and location of change. The considerable variability in streamflow and sediment load changes was attributed to large uncertainty in LULC projections, driven primarily by LULC demand. In general, the range of outcomes in sediment load projections was larger than in streamflow projections. This emphasizes a need to incorporate uncertainty in LULC change for decision making on water and sediment management strategies in areas undergoing rapid development. The 3S basin modelling results showed that deforestation by expansion of intensive agriculture could result in reduced streamflow, suggesting that appropriate parametrization of LULC characteristics in hydrological models needs to be carefully considered when using this approach in other tropical regions/areas undergoing rapid development. The results were limited to uncertainty in LULC change projections because it is the key driver of uncertainty, but combining uncertainty due to climate models, emission scenarios and hydrological model parameters could add additional value to understanding the range and major source of uncertainty for better water and sediment management planning, which is evaluated in Chapter 4

Chapter 4

Flow and sediment projection uncertainty in basins dominated by land use/land cover conversions under climate change

Abstract

Climate change impact studies on future flow and sediment often do not take into account uncertainty in land use/land cover (LULC) change. In this chapter flow and sediment projection uncertainty was evaluated combining three LULC change scenarios along with three Global Climate Models (GCM), three Representative Concentration Pathways (RCP) and three Model Parameters (MP) for the rapidly developing 3S (Sekong, Sesan and Srepok) basin, in Southeast Asia. The Soil and Water Assessment Tool model was used for flow and sediment modelling, and uncertainty was analyzed for the 2060s (2051-2070) time horizon. Overall, study results show that choice of LULC change scenarios is the primary uncertainty source for flow and sediment projection. However, for flow peak and 95% low flows the major uncertainty (LULC, GCM, RCP, or MP) source varies with space, but overall, the choice of GCM and RCP was found to yield more uncertainty for flow extremes. Results from this study highlight that for a basin undergoing LULC conversion, hydrological response of the basin can be even more receptive to LULC changes than climate. Hence, it is necessary to combine LULC uncertainty with other important sources of uncertainty as it can change the portrayal of climate change implications on basin hydrology. Further, it can also help improve the understanding of combined effects for improving flow and sediment management plans.

Introduction

Human induced global warming can have a significant implication on the climate (IPCC, 2013). The changes in climate could significantly affect streamflow (Chen et al., 2019; Dierauer et al., 2018), soil erosion (Li and Fang, 2016) and sediment flux (Dahl et al., 2018; Samaras and Koutitas, 2014). However, quantifying changes in hydrology under probable climate change scenarios is a complex issue because of uncertainty in projection of future climate (Minville et al., 2008). The uncertainty in future climate can be due to differences in choice of General Circulation Models (GCM), representative concentration pathway (RCP) and downscaling methods (Gao et al., 2019). The uncertainty in hydrological model used (Jiang et al., 2007) and land use/land cover (LULC) change further complicates the quantitative assessment of potential hydrologic changes due to climate change.

There are numerous studies investigating uncertainty of climate change impacts on flows. Some of these have found that GCMs are primary sources of uncertainty (Gao et al., 2019; Joseph et al., 2018; Addor et al., 2014; Thompson et al., 2013). Vetter et al. (2015), for instance, assessed multi-modal climate impact on future discharge of three river basins combining five GCMs, four RCPs and three hydrological models. This study found GCM to be the largest uncertainty source for the Niger River (Africa), but results were not as clear for the Upper Yellow Basin (China) and the Rhine Basin (Europe). Others have demonstrated that the emissions scenarios (Maurer, 2007), downscaling method (Chen et al., 2011a; Teutschbein et al., 2011), hydrologic model structures (Troin et al., 2018; Mockler et al., 2016; Poulin et al., 2011) and parameter uncertainty (Mendoza et al., 2015) are dominant sources of uncertainty. Overall, while there has been consistent progress in the literature on hydrological uncertainty with regards to climate, the interplay of this major driver with land surface processes is still understudied.

LULC change uncertainty is usually not considered and rarely investigated in the hydrological implication of climate change (Bennett et al., 2012; Surfleet and Tullos, 2013). Only a few climate change studies have also included uncertainties associated with LULC change. For example, Feddema et al. (2005) and Karlsson et al. (2016) evaluated the hydrological implication of climate signals using various sources of uncertainties (i.e. hydrological models, climate models, and LULC change) and demonstrated that uncertainty in LULC change can play a major role in predicting uncertainty for the future. The quantification of uncertainty in flow combining LULC change, GCMs, RCPs and model parameters has been previously carried out by Jung et al. (2011) and Chawla and Mujumdar (2018). However, little attention was given to understanding uncertainty in sediment predictions. For basins undergoing rapid development, evaluation of the uncertainty in LULC change along with other important sources of uncertainties (i.e. GCMs, RCPs and model parameters) could provide critical understanding about the range and dominant source of uncertainty in prediction of flows and sediment which is essential for better water and sediment management planning (Shrestha et al., 2018a).

This chapter is an expansion of the previous studies (chapters), in which the flow and sediment projection uncertainty combining GCMs, RCPs and model parametrization were assessed (Chapter 2) (Shrestha et al., 2016) and LULC change alone was assessed (Chapter 3) (Shrestha et al., 2018a). In this chapter, four important sources of uncertainties: GCMS, RCPs, model

parameterization, and LULC change scenarios were combined and evaluated their implication in flow and sediment projection uncertainty of the 3S basin.

Methodology

Flow and sediment modeling

The flow and sediment modeling of the 3S basin was carried out with the Soil and Water Assessment Tool (SWAT) model (Arnold et al., 1993a). SWAT is watershed-scale hydrological model (Gassman et al., 2014) capable of simulating flow, sediment, nutrient and pesticides loadings from watershed. There has been widespread use of the SWAT model globally by the scientific community, including numerous applications in the Mekong region (Mohammed et al., 2018). Readers are referred to Neitsch et al. (2011) for details on physical process modelled by SWAT. Meteorological data, elevation, soil distribution and LULC distribution are the main inputs to the SWAT model. All the input data for the 3S basin SWAT model were obtained from the Mekong River Commission (MRC).

Model calibration, validation and performance evaluation

The 3S SWAT model was calibrated in automatic mode, using SWAT-CUP software (Abbaspour, 2008), for daily streamflow (1985 – 2000) and monthly sediment (2005 – 2008) and validated for daily flow (2001 – 2007) at various river monitoring sites. The calibration of parameters was done within an acceptable and realistic range of values for each parameter. Model performance was evaluated using three commonly used statistical parameters, Coefficient of Determination (R^2), Nash-Sutcliffe efficiency (NS) and percent bias (PBIAS). Detail results and discussion on model calibration and validation are presented in Chapter 2 (Shrestha et al., 2016).

Uncertainty analysis

The approach used to assess the uncertainty in GCMs, RCPs and model parameters is presented in detail in Chapter 2 (Shrestha et al., 2016), but a brief description of the method is presented here. Figure 4-1 presents the methodological framework for assessing uncertainty. Three GCMs (GISS-E2-R-CC, IPSL-CM5-MR and GFDL-CM3) and three RCPs (RCP 2.6, RCP 6.0 and RCP 8.5), were selected to investigate the uncertainty due to future climate. These were selected to capture the maximum possible range of uncertainty in future climate (MRC, 2015). The 3S SWAT model was calibrated for three different objective functions: Nash-Sutcliffe efficiency (NS), Ratio of Standard Deviation of Observations to Root Mean Square Error

(RSR) and Mean Square Error (MSE) to generate three different model parameter sets (model configurations) for assessing model parameter uncertainty.

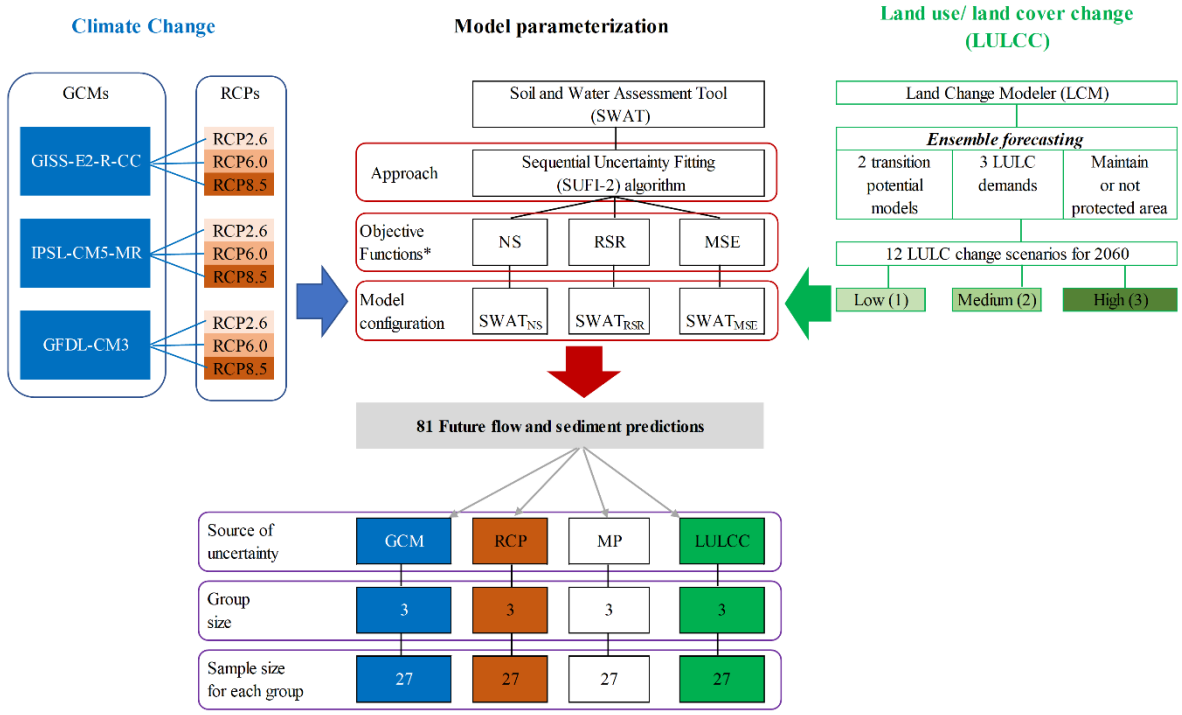

Figure 4-1. Methodological framework for assessing uncertainty. * Note, NS = Nash-Sutcliffe efficiency, RSR = Ratio of Standard Deviation of Observations to Root Mean Square Error and MSE = Mean Square Error, MP = Model Parameters

Following an *ensemble forecasting approach* as suggested by Santini and Valentini (2011), twelve likely LULC change scenarios were generated using Land Change Modeler (LCM) (Eastman, 2009) by combining two transition potential models (SimWeight (SR) and Logistic Regression (LR)), three LULC demands (high, medium and low), and two constrains to LULC allocation (the remaining or not protected areas). Further details on the generation of 12 LULC scenarios are presented in Chapter 3 (Shrestha et al., 2018a). Out of 12 scenarios, the three scenarios which represented the highest (SW_C1), medium (SW_C2) and lowest (LR_A2) changes in LULC class were used to evaluate uncertainty due to LULC projections. These scenarios represent a large spread in LULC changes. Details on three LULC projections used in this study are presented in Figure 4-2.

The three SWAT model configurations were simulated for each GCMs, RCPs and LULC change projections (LULCCs) which generated a total of 81 timeseries of flow and sediment load for 2060s (2051 – 2070) time horizon (Figure 4-1). Following the approach suggested by Chen et al. (2011b), the SWAT generated flows and sediment loads were first grouped into

four sources of uncertainty and then means for each group were estimated and compared with the mean flow and sediment estimates for the 1986-2005 period (base period), respectively. For example, to evaluate the uncertainty due to LULC change scenarios, for each LULC change scenario the mean estimate of 27 hydrographs is compared with the mean estimate of the base period.

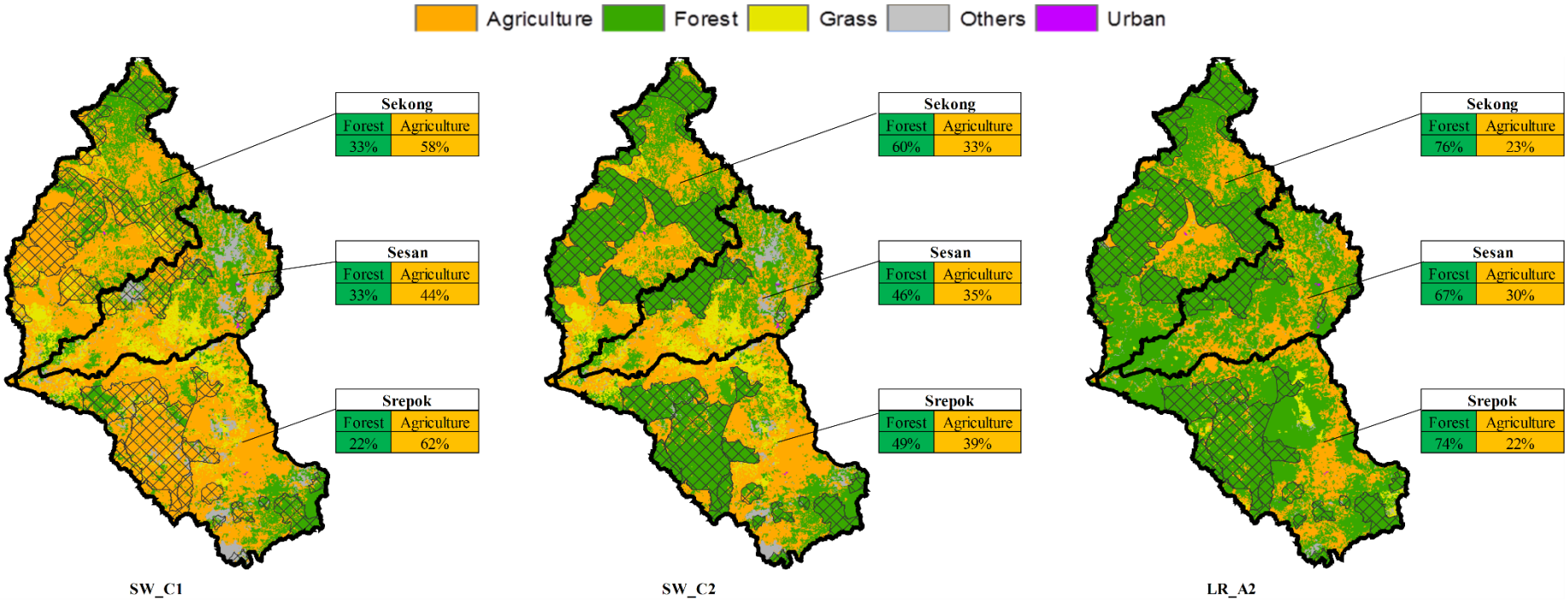

Figure 4-2. Land use/ land cover (LULC) change projections for the selected scenarios and coverage of major LULC classes by 2060 for the 3S Basin (in percent of basin area). SW_C1: scenario generated considering LULC demand based on period 1997 – 2010, SimWeight as transition potential model, constraints off; SW_C2: scenario generated considering LULC demand based on period 1997 – 2010, SimWeight as transition potential model, constraints on; and LR_A2: scenario generated considering LULC demand based on period 1993 – 1997, Logistic Regression as transition potential model, constraints on.

Results and discussion

Uncertainties in flow projection

For the 3S basin as a whole, the projected changes showed a general decrease in peak and low flows for the 2051 – 2070 period. The estimated decrease in peak flow (i.e, negative changes) ranges from 42 to 90%, and between 78 to 100% for low flow depending on various GCMs, RCPs, MPs and LUC scenarios (Figure 4-3). For both peak and low flows, the difference between the cumulative distribution functions (CDFs) of LULC change scenarios is the largest among sources of uncertainty, which suggest that uncertainty in future peak and low flow is dominated by LULC change. Uncertainty in model parameters is least important for peak and low flows projections.

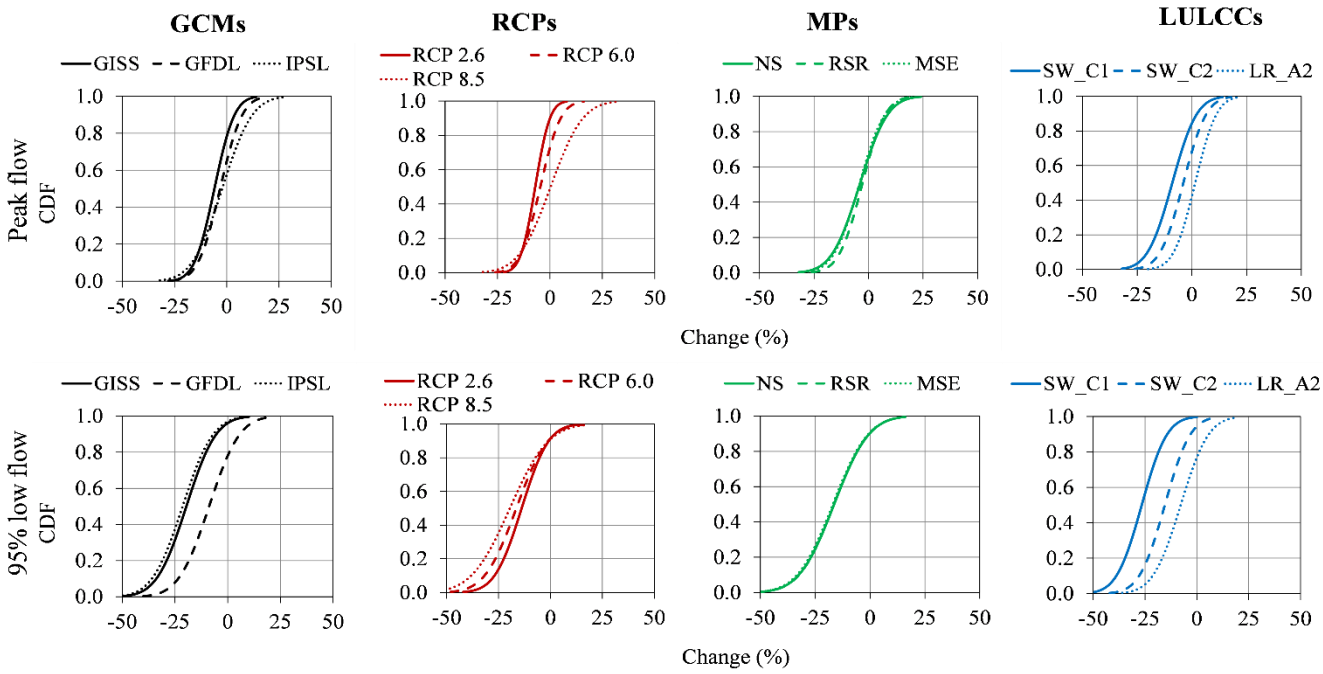

Figure 4-3. Plots of cumulative distribution function (CDF) to show the variability in annual peak flow and 95% low-flow changes at the outlet of 3S basin for 2060s period due to uncertainty in global climate models (GCMs), representative concentration pathways (RCPs), model parameters (MPs) and land use/land cover changes (LULCCs).

Interestingly, results at the subbasin scale show that the changes in peak flows are bidirectional and the primary uncertainty source can vary spatially for both peak and low flows (Table 4-1). In general, the results suggest that at the subbasin level the peak and low flow projection uncertainty as a result of climate signals (GCMs and RCPs) can be larger than the one caused by LULC change for some scenarios, which is in agreement with Karlsson et al. (2016). This was also suggested by Bussi et al. (2016), who found changes in precipitation and temperature altered the basin response to changes in LULC.

For the Sesan subbasin, the contribution of choice of LULC change scenario is high for uncertainty in peak and low flow projection. In contrast, for the Sekong subbasin, RCP dominates the uncertainty in peak flow and GCM dominates the uncertainty in low flow, which is clearly indicated by the largest absolute difference in peak flow and low flow changes for RCP and GCM, respectively. This spatial variability can be attributed to variability in subbasin characteristics (for instances, soil), their hydrological response to climate and LULC changes, and variability in model parameter set use to simulate those responses. For basins where hydrological processes are more sensitive to temperature changes the choice of RCP can dominate the uncertainty in future projections, while GCM dominates the uncertainty for basins with hydrology more responsive to precipitation projections (Vetter et al., 2015). LULC change can influence watershed hydrology by regulating runoff generation, routing, and evapotranspiration (Arias et al., 2018; Wohl et al., 2012; DeFries and Eshleman, 2004). LULC change can be a significant driver for basins where LULC-related processes such as evapotranspiration and infiltration are more sensitive to hydrological processes than precipitation. In hydrological models, simulation of land cover changes is executed with parameter modifications (Eckhardt et al., 2003). SWAT has the option of using the Natural Resources Conservation Service (NRCS) curve number (CN) method to calculate the direct runoff generation. The magnitude of change in direct runoff due to LULC changes is estimated by changing the CN parameter. Surface runoff is particularly sensitive to CN, which also influences infiltration, baseflow and recharge significantly (Du et al., 2013). Spatial variability and uncertainty in land cover related hydrological model parameter(s) such as CN can result in uncertainty in hydrological prediction under LULC change (Eckhardt et al., 2003). Further, spatial variability in LULC changes can influence the LULC contribution towards uncertainty (Chawla and Mujumdar, 2018).

In general, the results suggest that at the subbasin level the peak and low flow projection uncertainty as a result of climate signals (GCMs and RCPs) can be larger than the one caused by LULC change for some scenarios, which is in agreement with Karlsson et al. (2016). This was also suggested by Bussi et al. (2016), who found changes in precipitation and temperature altered the basin response to changes in LULC.

Table 4-1. Spatial variability in changes in projected extreme flow variables across subbasins for 2060s period for four sources of uncertainty namely global climate model (GCM), representative concentration pathway (RCP), model parameter (MP) and land use/ land cover change (LULCC).

Subbasin	Sources of uncertainty	Peak flow				95% low flow			
		Maximum change in % (a)	Minimum change in % (b)	Absolute difference in % |a - b|	Rank	Maximum change in % (a)	Minimum change in % (b)	Absolute difference in % |a - b|	Rank
Sekong	GCM	-0.1	-3.9	3.8	3	**-6.9**	**-29.5**	**22.6**	**1**
	RCP	**4.5**	**-7.5**	**12.0**	**1**	-15.6	-24.0	8.4	3
	MP	-1.1	-2.8	1.7	4	-19.1	-20.8	1.7	4
	LULCC	2.6	-7.1	9.7	2	-10.9	-33.3	22.4	2
Sesan	GCM	-1.1	-4.9	3.7	3	-7.8	-10.4	2.7	2
	RCP	2.0	-7.8	9.8	2	-8.8	-10.2	1.4	4
	MP	-2.1	-5.1	3.0	4	-8.5	-10.6	2.1	3
	LULCC	**2.4**	**-7.8**	**10.2**	**1**	**-1.4**	**-15.6**	**14.2**	**1**
Srepok	GCM	**5.9**	**-7.8**	**13.8**	**1**	-8.8	-21.6	12.8	2
	RCP	2.4	-3.1	5.5	3	-11.7	-19.1	7.4	3
	MP	1.1	-1.7	2.7	4	-14.5	-15.6	1.1	4
	LULCC	3.4	-4.9	8.3	2	**-5.5**	**-23.2**	**17.7**	**1**

Note: Rank 1 represents the highest source of uncertainty and rank 4 represents the lowest source of uncertainty.

In contrast to peak flow, the changes in seasonal and annual flows are unidirectional (i.e, likely to decrease). The uncertainty analysis of flow in the 3S basin without considering LULC change uncertainty (Chapter 2) (Shrestha et al., 2016) displayed bidirectional changes in seasonal and annual flows, which clearly reflected the high dependence of the projected flow changes on the direction of change in future rainfall. The unidirectional changes in seasonal and annual flow observed in this study are probably mostly due to processes related to LULC change. This suggests that for the 3S basin, the overall impact of LULC change is likely to be larger than climate effects on river flow. Under all LULC change scenarios, agricultural land (which is intensive) is projected to expand (ranging from 24 to 56%) at the expense of the forested areas (refer to Figure 4-2). The forest cover in the 3S basin is comprised mainly of deciduous and evergreen trees with medium- to low- density cover (refer to Table 4-2 and chapter 3 for details on description of forest cover). Farmers are replacing rice-based agriculture with commercial crops such as cassava, maize, soy and sugarcane in high and low land of the Lower Mekong Basin (ICEM, 2013). Hence, cassava and maize are more likely to be the main type of intensive agricultural crop for the 3S basin.

In general, replacing forest by agriculture is likely to increase streamflow in most basins due to decreased evapotranspiration. The study results in terms of changes in streamflow due to replacing (local) forest by intensive agriculture is opposite to most other studies, but a few exceptions do exist (for example USACE, 2007). The uncertainty in this outcome can be both due to model calibration issues and due to type/amount of LULC differences.

The contrasting outcome can be the result of calibration/parameterization issues, more specifically hard calibration. Hard calibration refers to the process where the model is calibrated against hard data i.e, long term, measured time series, typically at a point in the outlet and typically used for visual comparison of hydrographs and model evaluation statistics (Bieger et al., 2019). The problem with the hard calibration is that a model can show excellent statistical agreement with in measured stream gauge data, while misrepresenting processes (water balance, nutrient balance, sediment source/sinks) within a field or watershed. This will cause errors when running management, LULC and climate scenarios. The 3S model was calibrated against long term, measured time series stream flow data (hard data), but was not calibrated for soft data. Soft data refers to information on individual process within a budget such as evapotranspiration, which may not be directly measured within a study area but cause considerable uncertainty (Bieger et al., 2019).

Table 4-2 presents the SWAT default CN values for the 3S basin (by MRC) and Table 4-3 presents the calibrated CN values used for the 3S basin. During the calibration, the default CN values are optimized by multiplying them by a relative fraction to match modelled and observed flows. It is also to be noted that in 3S basin there is no soil type with hydrological group A characteristics. The range in CN number in Table 4-3 for each hydrological soil group for each LULC type is due to different relative change fractions assigned to different subbasin during the calibration process. It is worthwhile to note that the curve number of a LULC type for a similar hydrologic soil group can vary spatially because other hydrological parameter/characteristics such as slope which can have impact to runoff is not considered under the choice of CN number. SWAT does not adjust CN for slope. The curve number (CN) assigned to intensive agriculture is lower than that of major forest land-use class (Table 4-2 and (Table 4-3). Hence, conversion of forest to intensive agriculture with lower CN is likely to decrease the surface runoff and increase the amount of water lost to infiltration. This gives the impression that the CN assigned for intensive agriculture by MRC may not have been representative of intensive agriculture. Hence, the 3S SWAT model was re-run for a sample case where all the agriculture-intensive crop was replaced by LMB field crop (FCRP), which

has higher CN value as compared to forest land cover types. The results showed that replacing the parameters of agriculture-intensive LULC by LMB field crop did not change the outcome (Figure 4-4).

Table 4-2. SWAT default CN values (proposed by MRC).

Land use/land cover description	Code	Simplified Category	Percent area in 3S Basin *	SWAT Default Curve Number			
				A	B	C	D
Evergreen,medium-low cover den	EMLD	Forest	21.01	28	61	77	85
Deciduous	DECD		27.45	45	66	77	83
LMB Disturbed forest land	DTFR		16.04	36	60	73	79
LMB Field crop	FCRP	Agriculture	1.91	67	78	85	89
Agricultural land - intensive	AGRI		2.7	31	59	72	79

Note * The percent area in 3S Basin for major LULC type presented in the table is for 2003, which was used to calibrate 3S SWAT model.

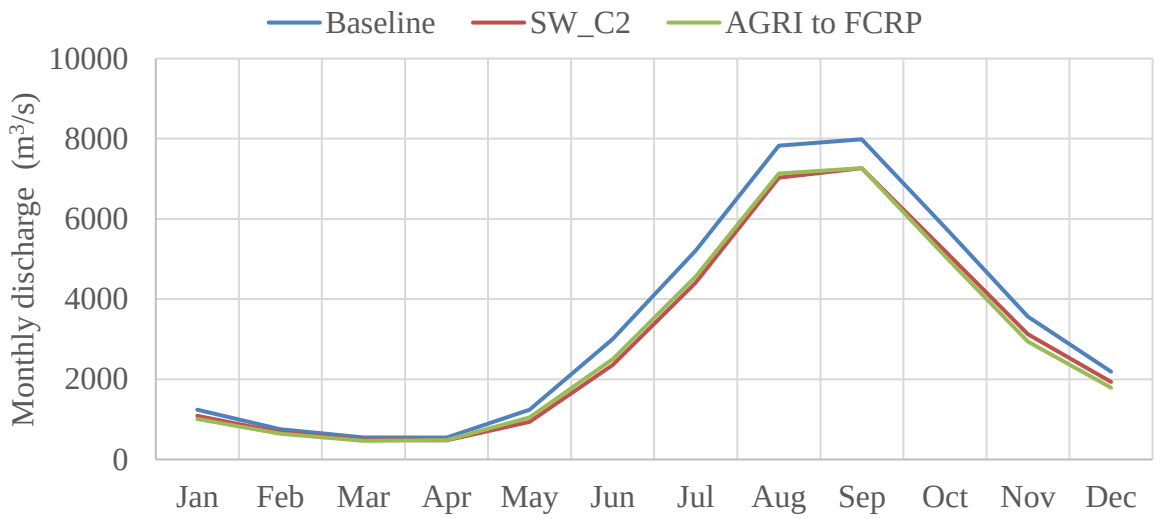

Figure 4-4. Mean annual discharge at 3S outlet under baseline, SW_C2 scenario where the agriculture-intensive LULC is used and AGRI to FCRP case where all agriculture-intensive LULC is converted to LMB field crop.

Table 4-3. Calibrated CN values to match flow observation sites for model configuration with NS as objective function.

`	Calibrated Curve Number		
	Max	**Min**	**Average**
EMLD			
B	68.6	60.5	62.6
C	83.1	77.0	79.7
D	96.1	84.7	89.4
DECD			
B	74.8	60.8	67.6
C	83.1	71.0	76.8
D	94.1	81.0	86.4
DTFR			
B	64.8	55.3	60.2
D	81.1	81.1	81.1
FCRP			
B	88.5	71.9	79.0
C	91.7	84.1	87.3
D	100.9	86.8	91.1
AGRI			
B	66.9	54.4	60.4
C	77.7	72.0	74.6
D	89.6	77.1	81.7

Further analysis was carried out at the hydrological response unit (HRU) level where all the major components of water balance were assessed (Figure 4-5). The results clearly show that total runoff for both AGRI and FCRP is less than deciduous forest type (DECD). It is interesting to note that evapotranspiration for DECD was quite low compared to agricultural crops. It seems baseflow is contributing significantly to the flow for both DECD and AGRI and not so for FCRP. FCRP produced more surface runoff than AGRI and DECD. This gives us an indication that while CN may be sensitive for surface runoff generation only, parametrization of crop-growth sub-models and evapotranspiration sub-model may have a significant influence on both surface runoff and baseflow generation and hence total runoff generation (i.e. Total runoff = surface runoff + baseflow) from the catchment. The modelling results highlights that model calibration process and parametrization needs to be carefully considered as this can have implications on the direction of streamflow changes.

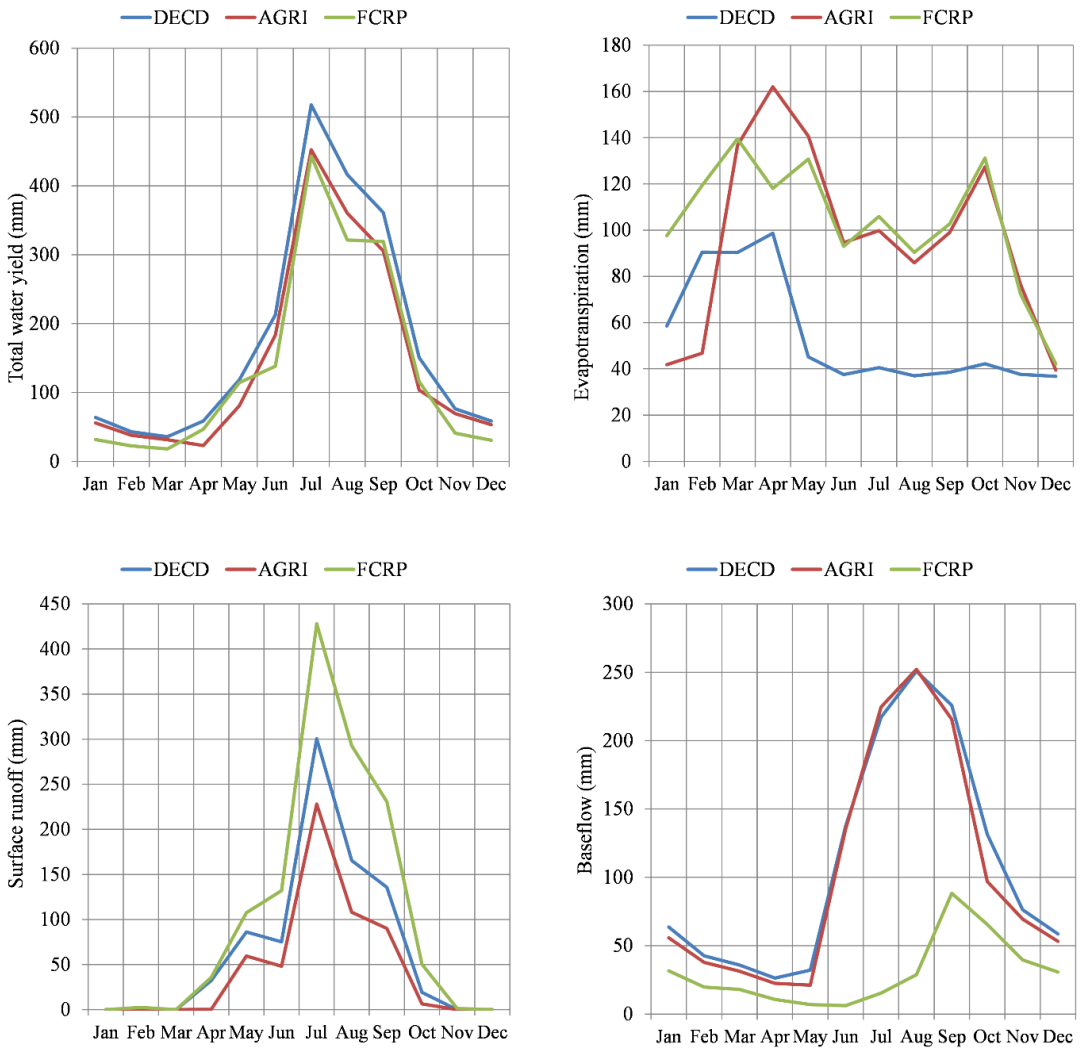

Figure 4-5. Comparison of monthly water balance component at the hydrological response unit (HRU) level for three major LULC type: Decidious (DECD), Agriculture-intensive (AGRI) and LMB field crop (FCRP). Note Total water yield = surface runoff + baseflow.

On the other hand, although there is a preconceived notion that in general deforestation leads to increase in runoff, it can be argued that it is not always the case and it would depend on the original forest type and what it was being substituted for and other factors such as topography, soil type, and conservation practices used. It is also important to acknowledge that all forests are not equal and that local dry land bush type forest in the 3S basin may have lower water use potential than intensive agriculture. The crop type and management practice used can play key roles in governing flow (Lacombe et al., 2016; Yu et al., 2015). The parameters chosen for the forest (for example CN number) in the region (mostly dryland bush type forest) does not evapotranspiration as much as the agriculture that would substitute it. LUC uncertainty can have implications on the direction of streamflow changes, and the influence of hydrological model parameters related to LULC can be significant (Shrestha et al., 2018a). The modelling

results highlights that in this particular basin/ecosystem, calibration of parameters influencing LULC change may need revision or flow changes as a result of deforestation may not be as generally expected, and it is thus an important issue to address for future research. Recent study by Ellison et al. (2017) outlines lack of sound evidence on the influence of tree cover on water balance components (such as infiltration) which further complicates modelling of the effect of forest cover on hydrology.

Overall the variability in seasonal (dry and wet) and annual flow projections across the subbasins as well as the whole 3S basin (Figure 4-6) is large under the LULC change scenarios. Details on the variability of future seasonal and annual flows for the subbasins are presented in Figure 4-7 . This clearly depicts that the choice of LULC change scenarios is the greatest source of uncertainty as compared to GCMs, RCPs and MPs for the dry, wet and annual flow projections for the 3S basin. Uncertainty due to MPs and RCPs is found to be the least source of uncertainty in general, however, for the Srepok subbasin model parameters has the largest uncertainty among sources for dry seasonal flow. The choice of GCMs has been generally portrayed as the largest and primary sources of uncertainty for flow projections. In contrast, the results suggest that this portrayal of climate signals (GCMs and RCPs) as major sources of uncertainty cannot be generalized and flow prediction uncertainty due to LULC, which is projected to undergo rapid modification, can dwarf the uncertainty due to future climate.

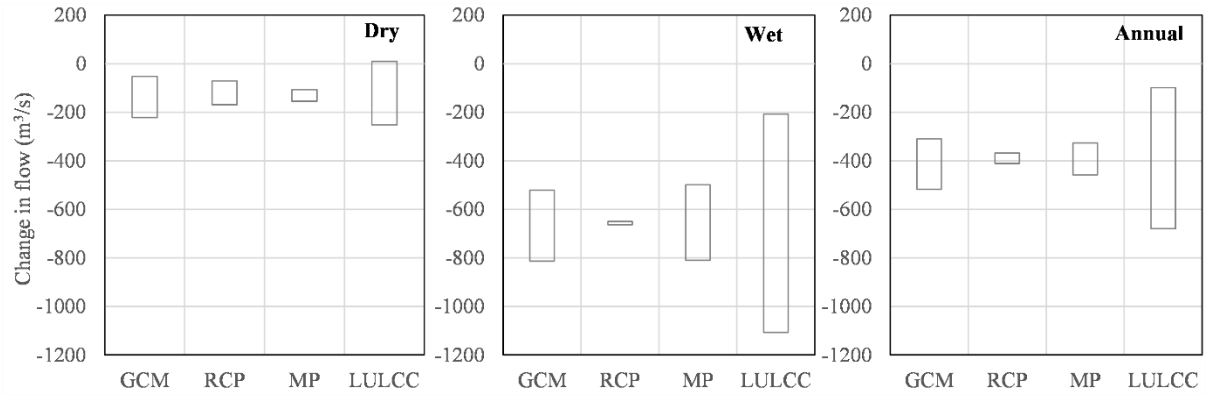

Figure 4-6. Plots of range of seasonal (dry and wet) and annual flow changes at the outlet of the 3S basin for 2060s period for four sources of uncertainty namely global climate model (GCM), representative concentration pathway (RCP), model parameter (MP) and land use/ land cover change (LULCC).

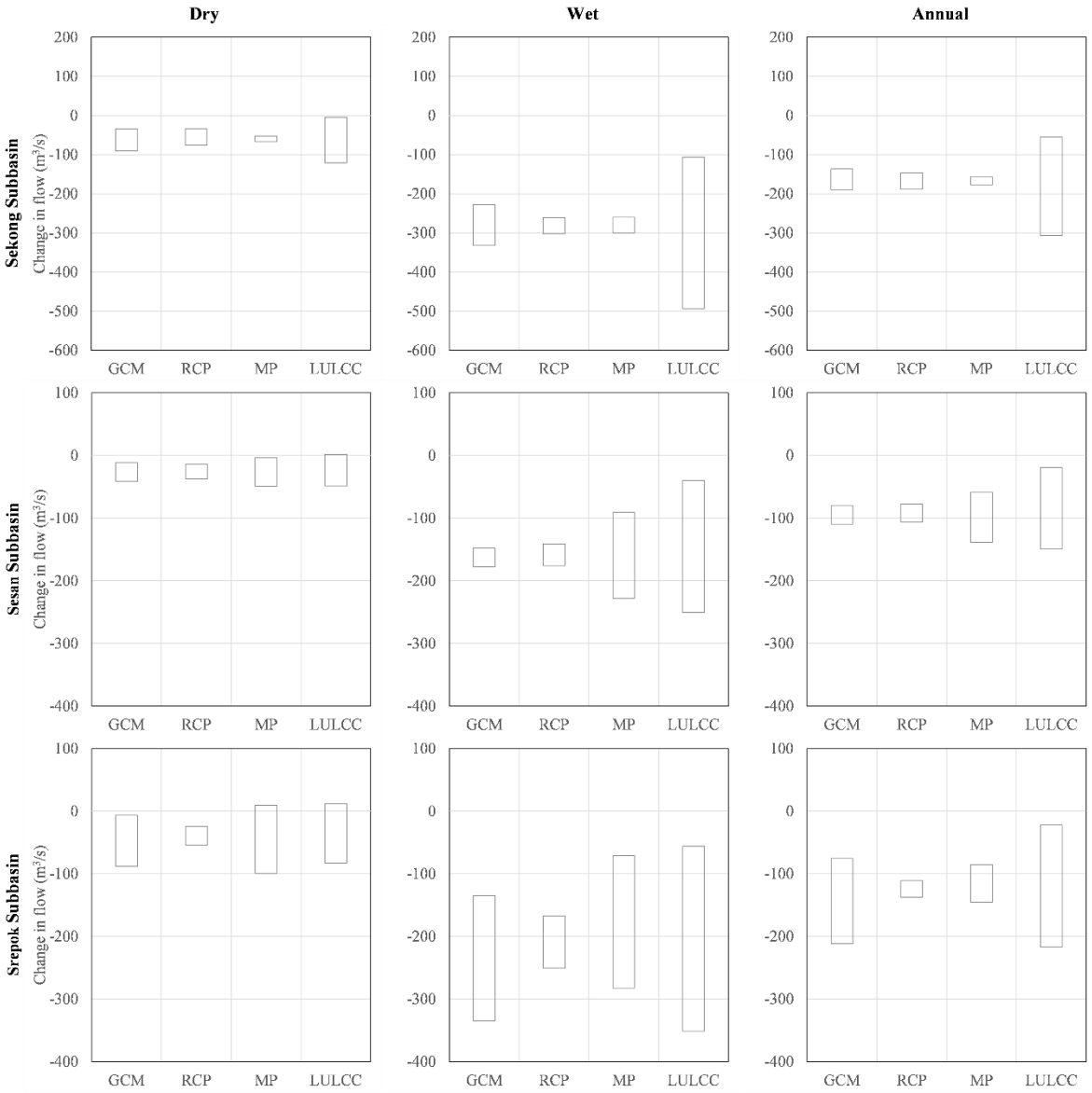

Figure 4-7. Plots of range of changes in seasonal (dry and wet) and annual flow across subbasins for 2060s relative to baseline (1986 – 2005) for four sources of uncertainty namely global climate model (GCM), representative concentration pathway (RCP), model parameter (MP) and land use/ land cover change (LULCC).

It should be noted that the analysis was done for the 2060s period, which is considered a medium-term period for climate change impact studies. Studies by Rodriguez-Lloveras et al. (2016) and Karlsson et al. (2016) indicated that, in the short to medium term, LULC change effects on the basin hydrology can be more significant than climate signals. Uncertainty in LULC change is portrayed by large uncertainty in quantity and location of change (Dalla-Nora et al., 2014). For the 3S basin magnitude of change (future land demands) was the major uncertainty source for the LULC change forecast (Shrestha et al., 2018a). The results suggest that uncertainty due to LULC should not be neglected and should be studied in more detail as

an important driver of watershed hydrology, as it can change the portrayal of hydrological implication under probable climate change scenarios at the river basin scale.

Uncertainties in sediment load projection

Both the peak and sediment load from the 3S basin is likely to increase in the future (2060s) as a result of changes in climate and LULC. For both LULC change scenarios and future climates (represented by GCMs and RCPs), the likelihood of increase in peak sediment load is more than 80% (Figure 4-8Figure 4-8). Increased sediment load can have adverse effects on reservoir storage, operation of hydraulic structures, and riverine ecology and morphology (Walling, 2008). Increased sediment load from watershed can accelerate the loss of reservoir storage affecting the energy generation from hydropower development (Arias et al., 2011), which can be a significant issue for the dam developers and operators.

The variability in future peak and annual sediment load changes for the 3S basin is largest under the LULC change scenarios as compared to other sources of uncertainties as presented in Figure 4-8 and Figure 4-9, respectively.

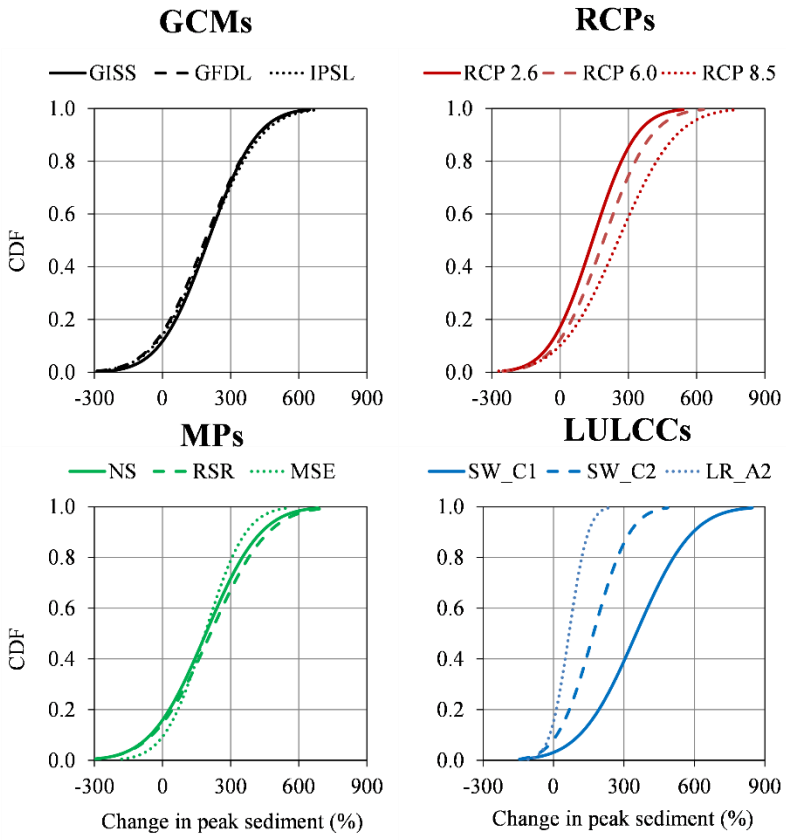

Figure 4-8. Plots of cumulative distribution function (CDF) to show the variability in annual peak sediment load changes at the outlet of 3S basin for 2060s period due to uncertainty in

global climate models (GCMs), representative concentration pathways (RCPs), model parameters (MPs) and land use/ land cover changes (LULCCs).

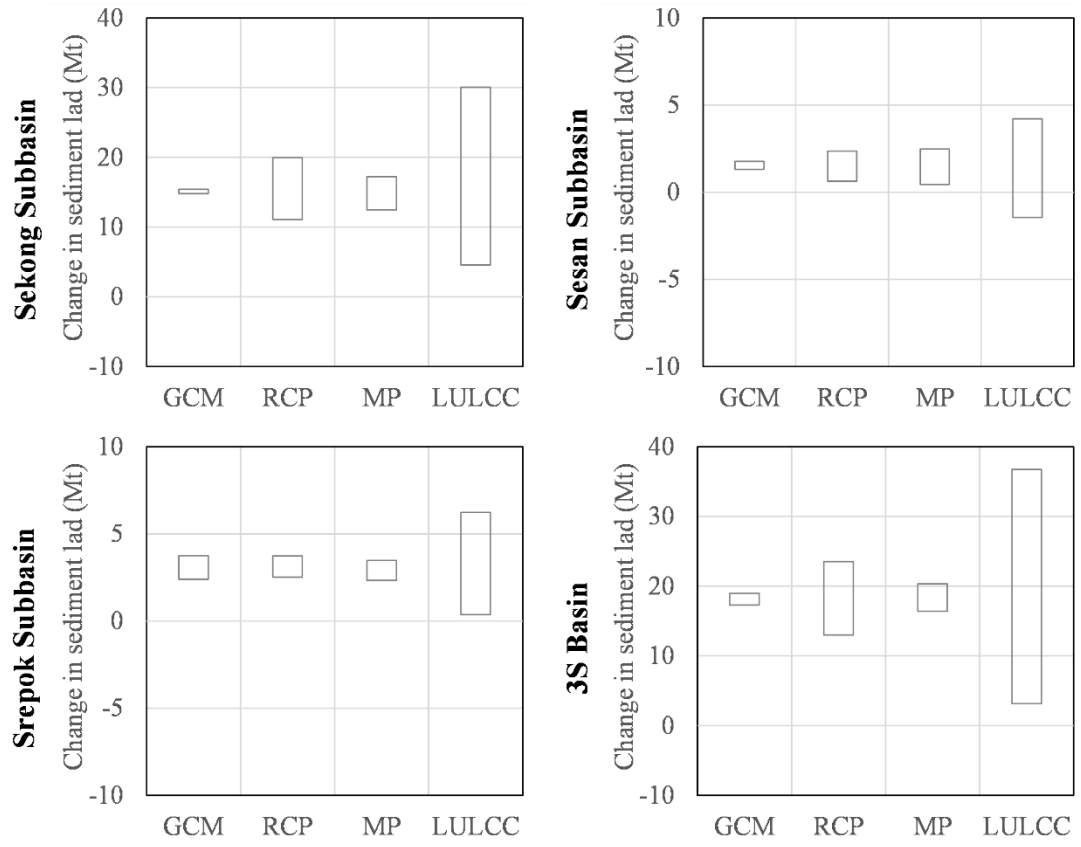

Figure 4-9. Plots of range of annual sediment load (Mt/yr) changes across subbasins and at the outlet of 3S basin 2060s period for four sources of uncertainty namely global climate model (GCM), representative concentration pathway (RCP), model parameter (MP) and land use/ land cover change (LULCC).

This suggests that the sediment load projection uncertainty is dominated by LULC changes for the 3S basin, which is also observed for all three subbasins (Figure 4-9). The GCM uncertainty is less important for the Sekong and Sesan subbains and the entire 3S basin. Sediment load projection uncertainty is large under LULC change scenarios primarily due to the large spread in changes of major LULC classes (forest, and agriculture). It is interesting to note that while the result shows that LUC is the greatest source of uncertainty in all three subbasins, a much larger uncertainty was observed in the Sekong than in the other two subbasins. This can be due to overall higher magnitude of sediment yields from the Sekong basin as compared to other two subbasins. The Sekong subasin has more high terrain with steep slopes which may have contributed to large increased sediment yields (Shrestha et al., 2018a).

Overall the future sediment load for the study basin is more sensitive to LULC changes as compared to temperature and precipitation (climate signals) changes, which is in agreement

with previous studies (for instance, Dai et al., 2009; Ma et al., 2014). Forest clearance for agricultural land expansion normally increases soil erosion from watershed resulting to high sediment yield (Walling, 1999). This study further highlights that for basin undergoing rapid hydropower development, such as the 3S, LULC planning needs to be carefully considered for mitigating the adverse effect of increased sediment. Well planned LULC practices can even counterweight the increases in sediment due to climate change (Rodriguez-Lloveras et al., 2016).

Conclusions

The study evaluated flow and sediment projection uncertainty combining 3 GCMs, 3 RCPs, 3 model parameters and 3 LULC change scenarios for the 3S basin. Based on the results, LULC change is found to dominate the uncertainties in future flow and sediment load. This is likely related to the larger spread of changes in LULC classes between the scenarios considered. The results for seasonal and annual flow and sediment projections suggest that for rapidly developing basins like the 3S where significant LULC change is anticipated, surface hydrology can be more influenced by processes related to LULC change than climate-driven processes. However, analyses at the subbasin-scale suggest that for flow extremes (peak and low flows) the most important uncertainty source vary with space. The choice of GCM and RCP is more important for flow extremes. This suggests that basin characteristics can have significant influence on the uncertainty of the peak discharge projections, hence for large basins uncertainty should be assessed at different/local scales.

In general, uncertainty in LULC changes can outweigh climate change uncertainty affecting future sediment projections and uncertainty; hence, uncertainty in LULC change should be included in understanding climate change impact on hydrology of basins undergoing rapid development.

A small, but representative number of GCMs and RCMs were used for this study and the sample size for each source of uncertainty may not be as inclusive as possible. Climate impact studies based on a few climate models may not totally capture the likely range of future climate change (McSweeney and Jones, 2016). It is debatable whether increasing sample size by adding more model sets would change the portrayal of the projection uncertainty, and although the sample size is small, the use of a wide and balanced set of combinations may better provide characterization of the projection uncertainty (Addor et al., 2014). Further, the sources of uncertainty cannot be equally represented as the results may bias the ones with the greatest

uncertainty and the most sensitive process. The conclusions are also based on simulations for the 2060s, which is considered a medium-term period for climate change impact studies. For farther future projections (e.g., 2090s), uncertainties due to the selection of future emission scenarios may become more important (Kundzewicz et al., 2018) and this may change the characterization of major sources of uncertainty for the far future. This analysis framework can be further extended to improve the understanding of future projection uncertainty for both flows and sediment.

Chapter 5

Sediment management for reservoir sustainability and cost implications under land use/land cover change uncertainty

Submitted as: Shrestha, B, Cochrane, TA, Caruso, BS, Arias, ME, Wild, TB, 2020. Sediment management for reservoir sustainability and cost implications under land use/land cover change uncertainty, Water Resources Research (Under Review).

Abstract

Addressing uncertainty in sediment predictions due to land use/land cover (LULC) change could better inform the selection of sediment management options for reservoir sustainability. We used the Nam Kong catchment of the Mekong River Basin in Southern Laos, with two hydropower dams in series, to understand the implications of LULC change uncertainty for catchment-level and reservoir-level sediment management options. The catchment-level sediment management options of terracing, vegetative filter strips and no tillage were evaluated applying the Soil and Water Assessment Tool (SWAT). The reservoir-level sediment management option of flushing was assessed using the Sediment Simulation Screening Python Model (*PySedSim*). Costs of sediment management options were assessed via the economic value of the loss in hydropower production and the avoided cost of dredging. Our results suggest that LULC projections resulted in high variability in loss of reservoir capacity and cost of sediment management. Terracing was found to be the best catchment-level management option at decreasing both the magnitude and variability in loss of reservoir storage for both dams, but it was also the most expensive option. Flushing was also effective in reducing sedimentation, but it was less economically beneficial compared to catchment-level sediment management options. Combinations of catchment-level and reservoir-level management strategies, however, can be effective in reducing the magnitude and variability in loss of reservoir storage and associated costs in response to LULC change uncertainty.

Introduction

Dams and reservoirs provide storage for reliable supply of water for irrigation and hydropower generation in addition to flood control, fishing and recreation. Recent statistics suggest that dam generates 16% of global electricity (IEA, 2018) and irrigate 40% of global irrigable land (FAO, 2016). Reservoir sedimentation results to loss of reservoir storage and hence affecting the benefits of dam (Smith et al., 2013). Over half of the world's large river systems are intercepted by dams and half of these have sediment trapping efficiency of 80% or more (Grill

et al., 2019; Nilsson et al., 2005; Vorosmarty et al., 2003) . Nearly 1% of global reservoir storage capacity is lost per year due to trapping of sediment (McCartney et al., 2000). Trapping of sediment by reservoirs can also significantly influence natural sediment fluxes, downstream river morphology, and ecosystem health and productivity (Wohl et al., 2015; Arias et al., 2014a; Kummu et al., 2010; Schmidt and Wilcock, 2008; Petts and Gurnell, 2005; Grant et al., 2003; Brandt, 2000; Kondolf, 1997) . Catchment erosion is important because it is one of the main sources of sediment to surface water bodies. Human alteration to a catchment accelerates erosion and sediment fluxes to lakes and artificial reservoirs (Yang et al., 2019; Walter and Merritts, 2008; Moehansyah et al., 2002). Climate change and land use/land cover (LULC) changes can also alter sediment yields (Shrestha et al., 2018b), which could substantially alter reservoir sediment trapping. Ultimately, excessive rates of erosion in catchments could significantly reduce energy generation (Kaura et al., 2019; Arias et al., 2011).

Reservoir storage capacity lost due to sedimentation can be mitigated, in general, by three strategies: minimizing sediment yield, routing sediment and removing sediment (Annandale, 2013; Sumi and Kantoush, 2011; Morris and Fan, 1998). The first strategy do not address the issue of sediment starvation downstream of the reservoir in contrast to the remaining strategies (Kondolf et al., 2014a). The cost and applicability of each strategy will vary from one site to another, as a function of sediment accumulation (Morris and Fan, 1998), as well as physical, hydrological and financial parameters (Palmieri et al., 2001).

Uncertainty in future catchment sediment load production due to factors such as LULC change and climate change need to be considered in implementation of any sediment management plans for reservoir sustainability. Sediment projections provided without addressing the associated range of potential future changes could mislead the selection of sediment management strategies and associated costs. Assessment of uncertainty in hydrological predictions is crucial for effective and efficient management of resources (Brown et al., 2012; Milly et al., 2008). While studies have analysed the cost of sediment management options (for example, Smith et al., 2013; Palmieri et al., 2001), studies assessing the implications of uncertainty in sediment projections on sediment management options and costs are limited. In basins where rapid conversion of forest to agricultural lands is expected, the sediment projection uncertainty due to LULC change is usually larger than the uncertainty due to global climate models (GCMs), representative concentration pathways (RCPs) and model parameters (as concluded in Chapter 4). This chapter presents logical follow on from the work presented in Chapter 4, in that here the implication of sediment management options for reservoir

sustainability and associated cost under the greatest source of uncertainty (i.e., uncertainty due to LULC changes) in sediment projections is assessed. In this chapter, the focus moves on from the more straightforward projections of river flow and sediment load (as presented in Chapter 2, 3 and 4) to explore management options for reservoir sustainability. The Nam Kong catchment of the Mekong River in Southern Laos was used as a case study.

Study Area

The Nam Kong catchment covers part of Laos and drains an area of 1281 km^2 (Figure 5-1). This particular study area was selected so that a pristine catchment can be explored to assess the effects of potential future LULC changes. Further, Nam Kong River is a tributary of the Sekong, which is the last unobstructed major tributary of the Mekong River and is incredibly important from a fishery perspective (Thomas et al., 2018). The fishery value of Sekong River is under threat by intensive hydropower development plans. In order to balance the hydropower and ecological concerns the government of Laos recently adopted a sustainable hydropower master plan that includes a careful dealing with sediment management. However, this plan does not address uncertainty in LULC change. Thus, this paper provides a timely and important input to the sustainable hydropower development, from a conceptual perspective.

The elevation of the Nam Kong catchment ranges between 298 and 1447 m above mean sea level. Based on 2003 LULC data, obtained from the Mekong River Commission (MRC), the catchment was dominated by forest (mostly dryland bush type forest), which covered almost 99% of the total area. Soil in this catchment is predominantly sandy clay loam. The proposed hydropower facilities (Nam Kong 1 and Nam Kong 3), with total combined active storage capacity of 804 million cubic meters, are expected to have an average electricity generation of 639 GWh/yr (Table 5-1). Both projects are expected to be commissioned by 2020.

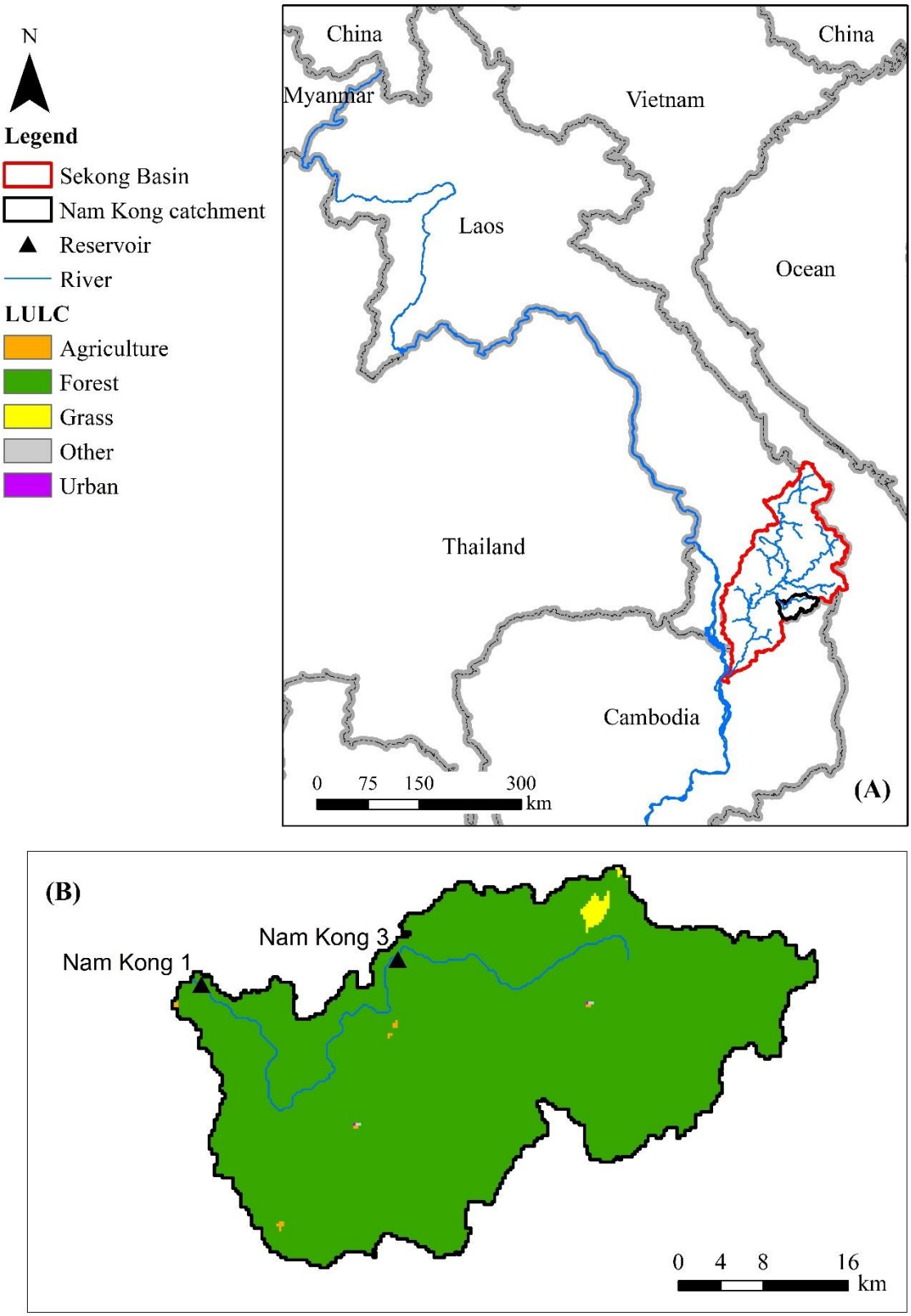

Figure 5-1. Nam Kong catchment location map (A), and LULC (2003) and hydropower dam sites (B)

Table 5-1. Characteristics of the Nam Kong 1 and Nam Kong 3 hydropower schemes.

Parameter	Nam Kong 1	Nam Kong 3
Installed capacity (MW)	150	75
Mean energy production (GWh/yr)	469	170
Active storage (10^6 m^3)	505	299
Catchment area (km^2)	1281	648
Dam height (m)	105	62
Mid or low level flushing outlets	Unknown	Unknown

Source: Mekong River Commission, 2008

Methodology

The conceptual framework used to evaluate the sediment management options and estimate the cost of sediment management in the Nam Kong catchment is presented in Figure 5-2**.** The framework includes the following stages: (1) LULC change projection; (2) catchment erosion modelling; (3) catchment-level management evaluation; (4) reservoir sedimentation estimation; (5) reservoir-level management evaluation; and (6) cost of sediment management. Each element of this conceptual framework is discussed in detail below.

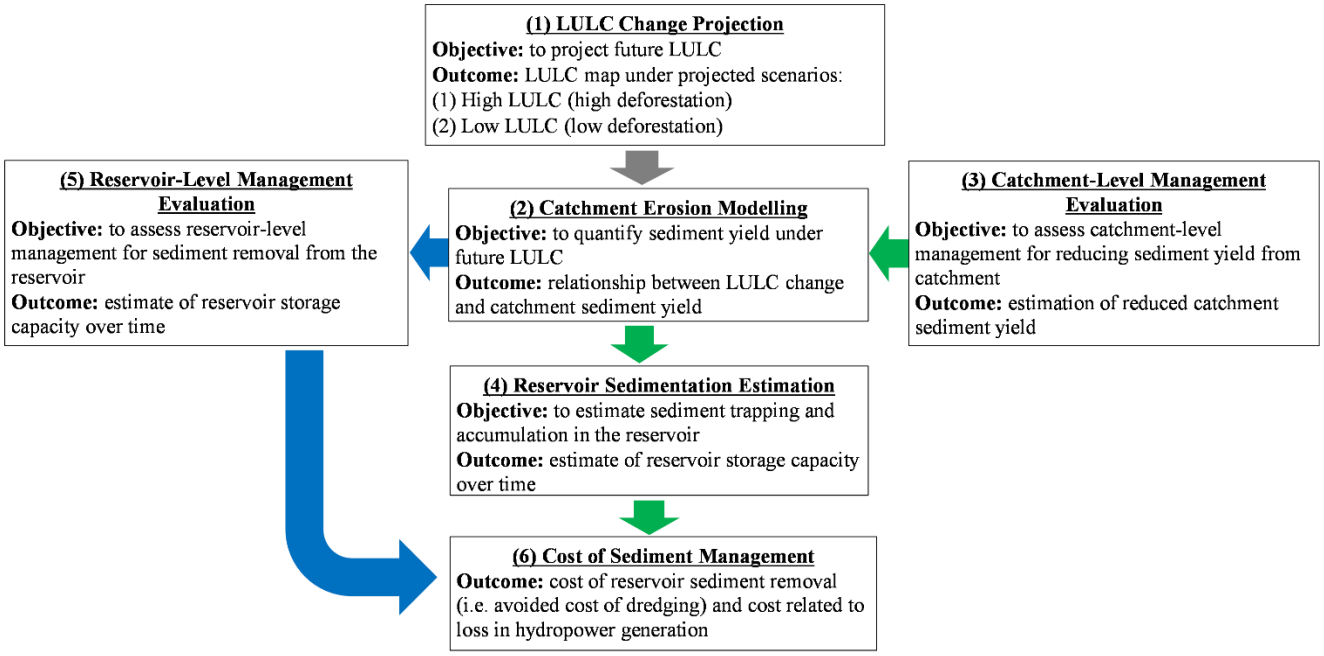

Figure 5-2. Conceptual framework for evaluation of the sediment management options and estimation of the cost of sediment management. Note: Green arrow refers to flow path for catchment-level management evaluation process and blue arrow refers to flow path for reservoir-level management evaluation process.

Land use/land cover change projection

LULC change projections were adopted from Chapter 3 (Shrestha et al., 2018a), which covered the broader Sekong, Srepok and Sesan River (3S) Basin. The Land Change Modeler (LCM;

(Eastman, 2009) was used to project future LULC change for 2030, 2060 and 2090. LCM uses Markov chain prediction method to predict the amount of LULC change and uses either logistic regression or machine learning methods to model the transition potential of land (Mas et al., 2014). LCM is used in this study because of its wider application in simulating LULC dynamics (Rodríguez Eraso et al., 2013; Sangermano et al., 2012; Fuller et al., 2011). For details on LCM readers are referred to Eastman (2009). Two future LULC scenarios were considered: (a) low LULC demand/change scenario and (b) high LULC demand/change scenario. The land demands for low- and high-LULC scenarios were estimated through simple extrapolations of past LULC trends in the 3S Basin for the 1993 – 1997 and 1997 – 2010 periods, respectively, when conversion of forest to agriculture (maize and cassava) was the primary land use transition. Based on past historical trends, the annual rate of change for the primary LULC for the 3S Basin was lowest for the period 1993–1997 (2.6% for agriculture and -0.2% for forest) and highest for the period 1997–2010 (6.2% for agriculture and -1.1% for forest). These rates of change were used to capture the maximum uncertainty in LULC projection as Shrestha et al. (2018a) found, in a study of future LULC scenarios for the 3S Basin, that LULC demand induces large uncertainties in future LULC forecasting. The transitions potential was modeled using Logistic Regression (LR), which generates change/transition potential using calculated relationships between LULC change and drivers. All the data sets used for LULC change modelling were obtained from the MRC.

Catchment erosion modelling

The Soil and Water Assessment Tool (SWAT) (Arnold et al., 1998; Srinivasan et al., 1998), was used for simulating catchment soil erosion and sediment yield under baseline and LULC change scenarios. This model was selected because it has been widely evaluated in the Mekong Basin (Mohammed et al., 2018; Trang et al., 2017; Oeurng et al., 2016), thus limiting the uncertainty associated with applying a new model to a basin for the first time. SWAT subdivides the catchment into several hydrological response units (HRUs). Each HRU consist of lumped area with unique LULC, slope, soil and management combination. SWAT calculates erosion from each HRU using the Modified Universal Soil Loss Equation (MUSLE), lumps them and routes the sediment loads in channels to the catchment outlet using a simplified version of the Bagnold (1977) stream power equation. Readers are referred to Neitsch et al. (2011) for details on SWAT model. All the meteorological and spatial input data (like digital elevation model, soil and LULC) for the SWAT models were obtained from the MRC. For this study a 20-year simulation period (1986 – 2005) was used for the SWAT model for the baseline

LULC and for each LULC change scenario. The mean annual sediment load at each dam location was estimated based on the average over the 1986-2005 series. The mean annual sediment load is estimated till 2120 to conduct a future 100-year simulation to represent the typical lifetime of a dam.

Evaluation of catchment-level management

Sediment load to the reservoirs can be reduced by catchment management practices. Three catchment management practices were evaluated: terracing (TERR), vegetative filter strips (VFS) and no tillage (NOTILL) (Table 5-2). These management practices were evaluated using built-in SWAT modules. The selected catchments have steep slopes and long slope lengths; hence, terracing was selected as one of the catchment management practices because terracing is generally effective for such terrain. Terracing decreases hillslope length, which prevents gully formation and hence erosion (Tuppad and Srinivasan, 2008). Terracing was simulated in SWAT by adjusting the MUSLE practice factor (TERR_P) and average slope length (TERR_SL). The average slope length was reduced by 50% to represent potential implementation of terracing in the region. Vegetative filter strips (VFS) are areas of vegetation that filter runoff and trap sediment. VFS were analyzed in this study because of their high efficiency in minimizing sediment transfer to rivers (e.g Hann et al., 1994). VFS is also one of the recommended methods for reducing soil erosion because it is less labor intensive compared to other soil conservation practices such as contour plowing (GoLPDR, 2012). SWAT-defined threshold values (Table 5-2) were used for simulating the effect of VFS on catchment sediment yield. The strategy of eliminating tillage practices (i.e., No tillage) was evaluated because it is a widely adopted management practice to control erosion, reduce input cost, and maintain crop yield for long-term (Pittelkow et al., 2015). No tillage reduces soil erosion by limiting soil disturbance activities, which increases the soil water permeability and encourages accumulation of soil organic matter (Li et al., 2019).

Table 5-2. Catchment management practices analyzed in this study.

Practices	Variable name	Definition	Value
TERR: Terracing	TERR_P[a]	USLE practice factor adjusted for terraces	Slope range 0-2% = 0.12 Slope range 2-10% = 0.10 Slope range >10% = 0.16
	TERR_SL	Average slope length (m)	Slope length 0-2% = 60m Slope length 2-10% = 30m Slope length >10% = 10m
VFS: Vegetative Filter Strips	FILTER_RATIO[b]	Ratio of field area to filter strip area.	50
	FILTER_CON[b]	Ratio of the HRU which drains to the most concentrated 10 percent of the filter strip area	0.5
	FILTER_CH[b]	Ratio of the flow within the most concentrated 10 percent of the filter strip which is fully channelized	0.0
NOTILL: No Tillage	$C_{tillage}$[c]	Tillage method factor	0.25

Source: [a] Hann et al. (1994), [b]Neitsch et al. (2011), [c]Stone and Hilborn (2011)

Reservoir sedimentation estimation

PySedSim was used in this study to evaluate sedimentation, as well as to evaluate reservoir sediment management potential. *PySedSim*, is an object-oriented, Python-based, one-dimensional model developed to simulate flow and sediment in river reaches and reservoir(s) and estimate hydropower production in reservoir(s) (Wild et al., 2019a). *PySedSim* can be used to model multiple reservoir sediment management techniques, and has been applied in case studies in the Mekong River Basin (Wild et al., 2019b; Wild et al., 2016). The model is open-source and available at https://github.com/FeralFlows/pysedsim. *PySedSim* has similar simulation functionality to the original SedSim model (Wild et al., 2019a; Wild and Loucks, 2015) with respect to sediment production, transport, reservoir trapping, and reservoir management.

PySedSim calculates the amount of sediment trapped by individual reservoirs by estimating trapping efficiency. The method developed in Brune (1953) is used to estimate the trapping efficiency for each reservoir for each day as a function of the reservoir's residence time. In *PySedSim* the residence time for each simulation day is determined as the ratio between the average total water storage in the reservoir divided by the outflow or release of water from the reservoir. The model computes the volume of deposited sediment by dividing the trapped sediment mass by the bulk density of deposited sediment. The model assumes that the bulk density of deposited sediment remains stable and does not change due to compaction. For this

study the bulk density value of 1.2 tons/m^3 was used which is based on the major soil type in the catchment. Further the bulk density value used for this study lies between the reasonable range (1.1-15 tons/m^3) for the sediment deposited in reservoir as suggested by Lara and Pemberton (1963). For this study, the total reservoir storage was used for the analysis, which means that dead storage was also included. The major hydrological inputs to *PySedSim* are flows and sediment loads, which were obtained from the SWAT model. Other major inputs include reservoir characteristics data, reservoir operation rules, reservoir volume, elevation curve and reservoir operation rules, and reservoir outflows. Most of these data were obtained from MRC or from (Piman et al., 2013). A simulation period of 100 years was used in order to capture the long-term impact of sedimentation processes on reservoir storage capacity and hydropower generation over the commonly assumed 100-year lifetime of a dam (Wild et al., 2016).

Reservoir-level sediment management

Overview

Reservoir-level sediment management techniques consist of two general categories: minimizing sediment deposition in the reservoir by sediment routing, and directly removing sediment from the reservoir (Annandale, 2013). Flood bypass, off-channel reservoirs, sluicing and turbid density current venting from reservoirs are four major sediment routing strategies (Morris and Fan, 1998). Bypassing was not evaluated because it requires expensive infrastructure such as tunnels and the technique is most practical for short reservoirs with adequate slope to transport the sediment through the bypass channel or tunnel (Kondolf et al., 2014a). Off-channel reservoir and density current venting techniques were not considered either; off-channel reservoirs are rarely used because they require particularly favorable conditions (topography, available space, technology) and are expensive (Batuca and Jordann, 2000). The sediment removal efficiency of density current venting is less than 50% even in ideal conditions (UDWR, 2010) and there is uncertainty in the flow path of density currents (Tiˇgrek and Aras, 2012). Sluicing was not considered for this study because it was hypothesized to be ineffective from the beginning of the study due to the large size of reservoirs considered for this study. Reservoirs with dam height more than 15 m and storage capacity more than 3 million cubic meters are considered to be large-size reservoirs (Asmal, 2000). Sluicing is most suitable for narrow, elongated-shaped and small to medium-sized reservoirs (Batuca and Jordann, 2000), where flood discharge exceeds reservoir capacity (Morris and Fan, 1998).

Deposited sediment can be removed using two basic processes; hydraulic and mechanical. Hydraulic removal includes sediment flushing, while mechanical removal (not considered in this study) includes dredging, hydrosuction removal systems (i.e., siphoning), and trucking (i.e., dry excavation). Flushing is done by creating river-like velocities in the reservoir which scour and transport deposited sediment through low-level outlets (Tiˇgrek and Aras, 2012). Flushing can be conducted in two ways: pressure flushing (partial drawdown) and empty (free-flow) flushing (full drawdown) (Annandale, 2013). Pressure flushing releases water through the bottom outlets by keeping the reservoir water level high. On the contrary, empty (free-flow) flushing releases water by emptying the reservoir and routing water inflow from upstream by providing riverine conditions. For this study empty flushing was evaluated because this technique has been widely and successfully implemented (Atkinson, 1996; Kondolf et al., 2014a; Morris and Fan, 1998; Palmieri et al., 2003). Pressure flushing was not considered because it is not commonly used and is less effective as compared to full drawdown flushing (Annandale, 2013; Morris and Fan, 1998). Mechanical removal like dredging and trucking were not considered viable options because of their high operation cost, and siphoning is ineffective for anything but very small reservoirs (Batuca and Jordann, 2000). The avoided cost of dredging, however, was considered for comparative purposes only.

Although reservoir sediment management techniques can be simulated with *PySedSim*, this model is not capable of determining the technical and economic viability of candidate reservoir sediment management techniques. Thus, the REServoir CONservation (RESCON) model (Efthymiou et al., 2017; Palmieri et al., 2003) was used to evaluate the technical and economic viability of multiple sediment management techniques, while *PySedSim* was used only to simulate the hydropower, hydrology, and sedimentation implications of those techniques deemed feasible by RESCON. Only sediment flushing emerged as a reasonable option as a result of the RESCON analysis. RESCON does not assess sluicing and bypassing, but can assess hydrosuction, traditional dredging and trucking.

Flushing simulation in PySedSim

The *PySedSim* model simulates flushing in a three-stage process, namely drawdown, flushing, and refill (Wild et al., 2019a). *PySedSim* initiates drawdown when two conditions are met: 1) the user-specified date for flushing has been met, and 2) the reservoir inflow exceeds the user-specified minimum inflow target. For this study, only a date was specified in the model to initiate the drawdown process (Table 5-3). The flow threshold was not considered for the initiation of drawdown. The target drawdown start date in May-June was selected because this

time of year is appropriate in the Mekong to avoid conducting flushing during the main portion of the wet or dry season (Wild et al., 2016). Flushing during the dry season is likely to see limited sediment removal due to limited natural discharge rates, and also creates the possibility that the reservoir cannot be refilled. Flushing during the wet season is difficult because safe drawdown may be difficult to achieve, and because low-level outlets are not sized to accommodate full pass-through of wet season discharge. After initiation of drawdown the model uses the reservoir's low-level outlets to drain the reservoir to the specified maximum flushing water level elevation. The targeted flushing water level elevation is the maximum reservoir water level that will still result in successful flushing. It is to be noted that low-level outlets are not currently proposed as design elements at Nam Kong 1 and Nam Kong 3 per the available feasibility studies for these dams. However, low-level outlets will be needed to manage sediment effectively at these dams. The national government of Laos has committed to a strategic hydropower development plan that includes sediment management at its core. So, the lack of proposed outlets does not necessarily mean that the dam will not ultimately be required to have these outlets. The model drawdown the reservoir water level based on user specified daily drawdown rate. For this is study, the drawdown rate was restricted to a maximum of 2–3 m/day (Table 5-3) to ensure that the water released during drawdown does not exceed the typical wet-season flow and avoids destabilizing bank soil in the reservoir.

After completion of the drawdown process, the model initiates flushing for a user-specified duration. For successful flushing to occur, two criteria must be satisfied: (1) the reservoir water level should not exceed the specified maximum flushing water level elevation, and (2) the discharge through the low-level outlets must equal or exceeds the minimum target flushing discharge. The target flushing discharge rate for Nam Kong 1 and Nam Kong 3 was 1.1 and 1.3 times the mean annual inflow to the dams, respectively. The flushing durations and frequency provided in Table 5-3 were obtained from the RESCON model. For this study the flushing frequency of every 5 years is used. The selection of flushing frequency (annual, every two years, etc.) creates a tradeoff between hydropower loss and magnitude of sediment load released downstream (which is ecologically important). During a flushing event, some fraction of the volume of sediment deposited since the previous flushing event is removed (Wild et al., 2019a). The fraction of sediment removal is empirically determined by the ratio of trapezoidal cross-sectional area of the incised channel formed by flushing to the cross-sectional area of the reservoir (Wild et al., 2016), which varies over time as the incised channel evolves. This method of estimating the amount of sediment removal is based on the approach suggested by

Atkinson (1996). Once the flushing is completed, the refilling of the reservoir initiates. Figure 5-3 demonstrates the flushing process as simulated in *PySedSim* for Nam Kong 1 dam in the study area. During flushing, operating policy diverges from a normal state to drawdown (emptying) policy, which takes some time and power generation declines during emptying. After the target level of drawdown is achieved, the reservoir stays empty during the flushing duration and sediment is removed. After the targeted flushing duration, the reservoir fills up and returns back to a normal operating policy. It is assumed the reservoirs are flushed in a coordinated fashion (simultaneously). The flushing operation of downstream dam (Nam Kong 1) is carried out is such a way that the flushed sediment from upstream dam (Nam Kong 3) pass through the Nam Kong 1 dam.

Table 5-3. Input data for flushing process.

Input data	Nam Kong 3	Nam Kong 1
Flushing discharge (m^3/s)	42	70
Duration of flushing after complete drawdown (days)	13/6*	13/4*
Frequency of flushing events (yrs)	5	5
Start date	1-Jun	26-May
Drawdown rate (m/day)	2	3
Duration of drawdown (days)	19	25

Note: *Different values used for the High/Low LULC change scenarios

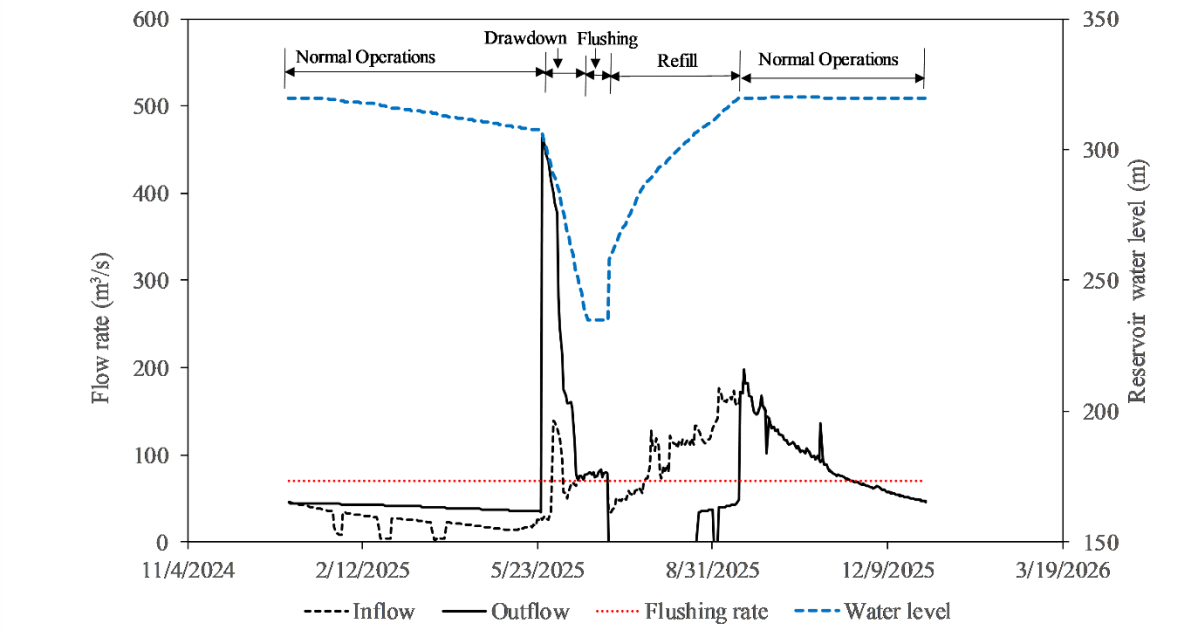

Figure 5-3. Flushing simulated by the *PySedSim* model for Nam Kong 1 dam under the high LULC change scenario.

Cost of sediment management

The cost of sediment management for both dams considered in this study was determined from the sum of two different costs: (1) the cost of reservoir sediment removal at the end of the dam's assumed lifetime of 100 years, and (2) the cost of loss in hydropower production that results from reservoir sedimentation and management. It is to be noted that the cost of sediment management does not include the implementation cost of sediment management options. Regarding the first cost component, it is assumed that all sediment that has accumulated in the reservoir by the end of each dam's lifetime will need to be removed to recover the site for use by future generations. Viable reservoir sites are limited in number and are thus a non-renewable resource. Forcing future generations to bear the cost of recovering this non-renewable resource, however, is unequivocally unsustainable because it does not promote intergenerational equity (Annandale, 2014). Thus, this recovery cost was accounted for as part of the cost associated with each dam. The cost of reservoir sediment removal (C_{sr}) was taken to be the avoided cost of dredging, which can be very expensive (Morris and Fan, 1998; Palmieri et al., 2003). The concept of relating cost of sediment retained in the landscape to the avoided cost of dredging has been successfully used in the InVEST model (Sharp et al., 2014). The C_{sr} at the end of 100 years of reservoir operation is estimated as:

$$C_{sr} = C_d \,.X \tag{5.1}$$

where X is the total amount of sediment removal at the end of 100 years of reservoir operation (m^3), and C_d is unit cost of dredging (US\$/m^3). A literature review was carried out for an appropriate unit cost of dredging. For this study a unit cost of dredging was assumed to be US\$ 3/m^3 as suggested by Annandale et al. (2016).

The second cost component accounts for the fact that hydropower generation is affected by sedimentation (via storage capacity loss and thus less effective reservoir operating policies), as well as by the process of emptying the reservoir for flushing. The flushing process, which is described in detail in the previous section, reduces both the turbine discharge and hydraulic head as a result of drawdown, flushing, and refill. The method of estimating the cost of loss in hydropower production is based on the framework suggested by Arias et al. (2011). The cost of loss in hydropower production for individual years ($C_{hp,t}$) is calculated as the difference in hydropower revenue between the baseline case and scenarios:

$$C_{hp,t} = (MHPG_{baseline} - HPG_{scenarios}\,).ELEC \tag{5.2}$$

where $MHPG_{baseline}$ is the maximum hydropower generated in the baseline case (kWh); $HPG_{scenarios}$ is the hydropower generated for scenarios (kWh); ELEC is the electricity selling price per kilowatt- hour (US$ kWh^{-1}); A fixed electricity rate of US $ 0.20 kWh^{-1}, which represents the highest electricity rate among the Lower Mekong countries, was used in this study. The total cost of loss in hydropower production for 100 years of reservoir operation (C_{hp}) was then estimated by adding up all individual $C_{hp,i}$.

The hydropower generated (HPG) was estimated using the *PySedSim* model. *PySedSim* calculates the hydropower production (MW) at reservoir j in period t as:

$$HPG = \frac{9.81}{1000} . e_{(j)} . h_{(j,t)} . Q_{(j,t)} \quad (5.3)$$

where $h_{(j,t)}$ is the hydraulic head above the turbines at reservoir j in time period t, $Q_{(j,t)}$ is the turbine discharge in units of m^3/s, and $e_{(j)}$ is the efficiency (fraction) of the turbines at reservoir j, assumed not to vary over time. For this study the $e_{(j)}$ was assumed to be 0.9. For this study the net present value (NPV) of the cost of reservoir sediment removal at the end of 100 years of reservoir operation is calculated as:

$$NPV\ of\ C_{sr} = \frac{C_{sr}}{(1+r)^{100}} \quad (5.4a)$$

It is to be noted that since C_{sr} from year 1 to 99 of reservoir operation will be zero, the present value during these periods will also be nil.

The net present value (NPV) of the cost of loss of hydropower over 100 years of reservoir operation is quantified as:

$$NPV\ of\ C_{hp} = \sum_{t=0}^{N} \frac{C_{hp,t}}{(1+r)^t} \quad (5.4b)$$

where r is the annual discount rate, which is assumed as 5% per year for this study, N is total number of years in the period and t is time (yr).

Each of the sediment management options considered for this study resulted in different time-patterns and magnitudes of sediment accumulation in the reservoir, and thus had different costs of reservoir sediment removal at the end of 100 years, and different costs associated with lost hydropower production over time. Note that the costs of sediment removal after 100 years, and the costs of lost hydropower production were first estimated for the baseline case (i.e., do-

nothing option). Each of the sediment management options considered for this study were then compared to the baseline cost.

Results and Discussion

Land use/ land cover (LULC) change and catchment sediment load

LULC change results presented here were adopted from Chapter 3 (Shrestha et al., 2018a), which cover the broader 3S Basin. Based on the predicted future LULC (Figure 5-4), forested land in the Nam Kong catchment is expected to decrease 18%, 33% and 39% by 2030, 2060 and 2090, respectively, under the low-LULC change scenario. Under the high LULC change scenario, forest is estimated to decrease 45%, 66% and 100% by 2030, 2060 and 2090, respectively, due to agricultural expansion.

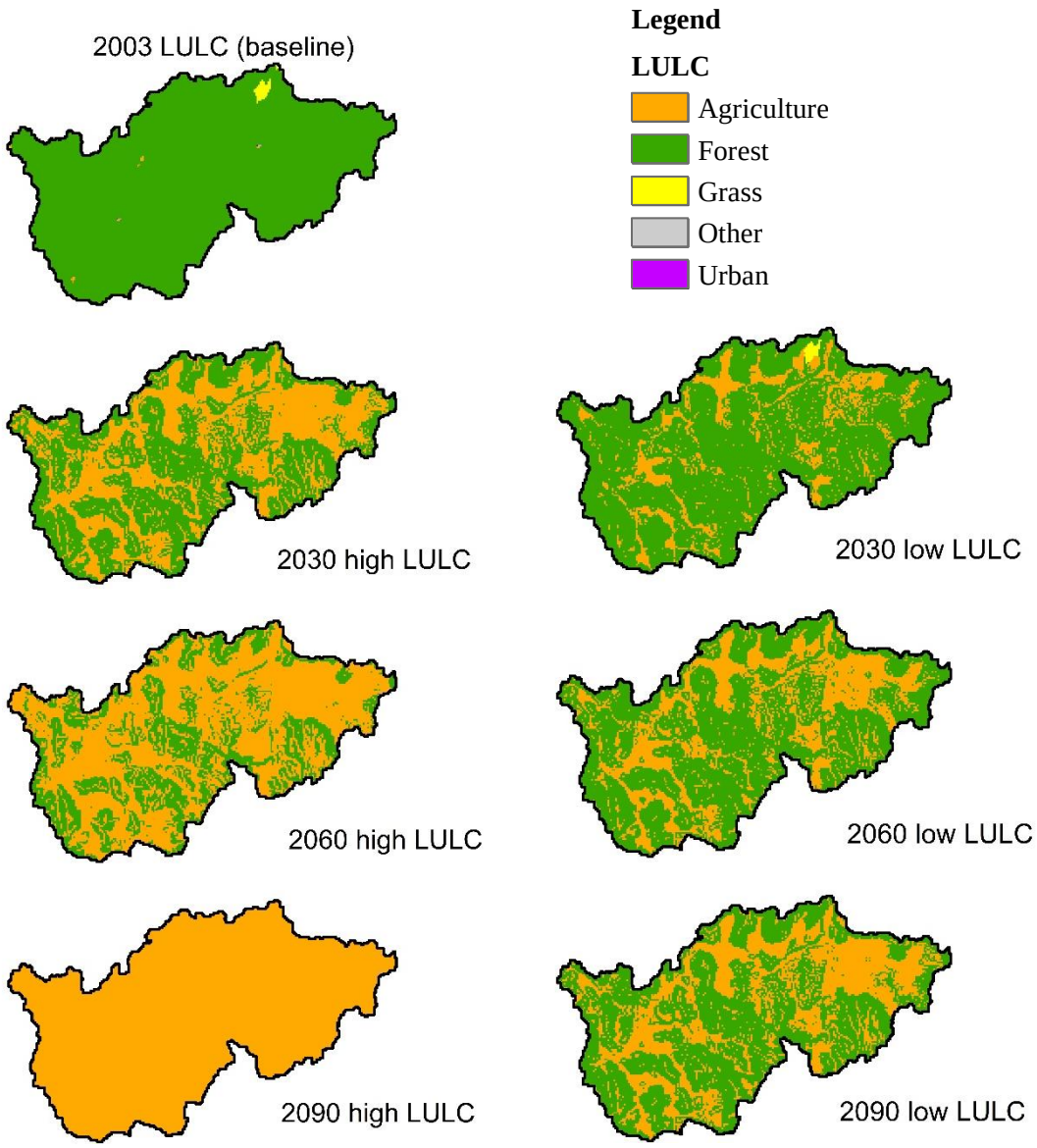

Figure 5-4. Baseline and projected LULC in the Nam Kong catchment.

The 2090 high LULC scenario is an extreme case where in the entire study catchment is converted to agriculture and also considers conversion of protected areas (Chapter 3). The elevation of catchment ranges from 250 to 1447 m above the mean sea level (amsl) and majority of area (nearly 93% of total area) is lowland (i.e., elevation less than 1000 m amsl). Further the catchment receives more than 2000 mm of average annual rainfall. In this study, it is assumed that maize and cassava will be the main agriculture crop farmed intensively in the 3S basin. Globally cassava is mainly cultivated in lowland area with gentle slopes (0-10%) and average rainfall of 1000-1500 mm, however it is also produced up to elevation of 1800 m amsl and also found on steep slopes of 15-50% in Asian nations like China, Vietnam and Indonesia (FAO and IFAD, 2000). Hence, there is possibility of large-scale conversion of forest area to agriculture in studied catchment. Nevertheless, it is acknowledged that converting very steep slopes and high land to agriculture will then also lead to very high erosion rates.

Under the baseline scenario with the 2003 LULC map, a mean sediment load of 0.02 million tons per year (Mt/yr) at the Nam Kong 3 dam location is estimated, while at the Nam Kong 1 dam location it was estimated at 0.29 Mt/yr. There is a stark difference in sediment load between the two dams. The catchment area of Nam Kong 1 is roughly twice the size of Nam Kong 3, but sediment load is an order of magnitude larger. The reason for this big difference is that area downstream of the Nam Kong 3 dam is the main source of sediment in the catchment as presented in Chapter 3 (Shrestha et al., 2018a). As expected, the sediment load increases over time as conversion of forest to agriculture occurs. By 2120, in year 100, the annual mean sediment load is estimated to range between 0.46 and 1.06 Mt at the Nam Kong 3 dam location and between 1.17 and 3.56 Mt at the Nam Kong 1 dam location in response to LULC changes (Figure 5-5). The sediment load for high-LULC change flattens out after 2090 because the catchment has reached full agriculture cover. The high variability in sediment loads due to LULC changes was observed, which is largely due to the higher sediment yield under the high LULC change scenario.

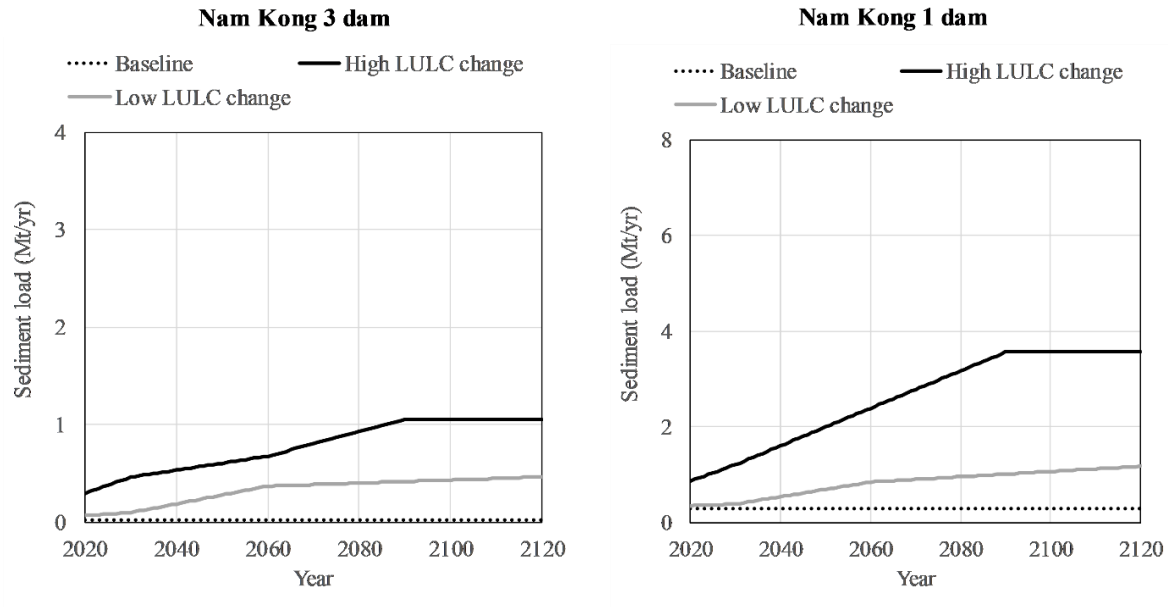

Figure 5-5. Mean annual sediment load over time for Nam Kong 3 dam location (left) and Nam Kong 1 dam location (right).

Reservoir sedimentation due to land use/land cover (LULC) change

Figure 5-6 presents the resultant decrease in the reservoir's capacity for the two dams operating in series under the two LULC change and the baseline (no LULC change) cases. Loss of storage capacity for the reservoirs due to reservoir sedimentation under baseline conditions is not significant. The initial reservoir volume is estimated to decrease by nearly 4% and 0% for Nam Kong 1 and Nam Kong 3 reservoirs, respectively, after 100 years. For Nam Kong 1 reservoir the reduction in reservoir storage capacity due to sedimentation ranges from 8 to 28% after 100 years across the LULC change scenarios. By 2120, the Nam Kong 3 reservoir volume is estimated to decrease by 11-26% due to LULC change.

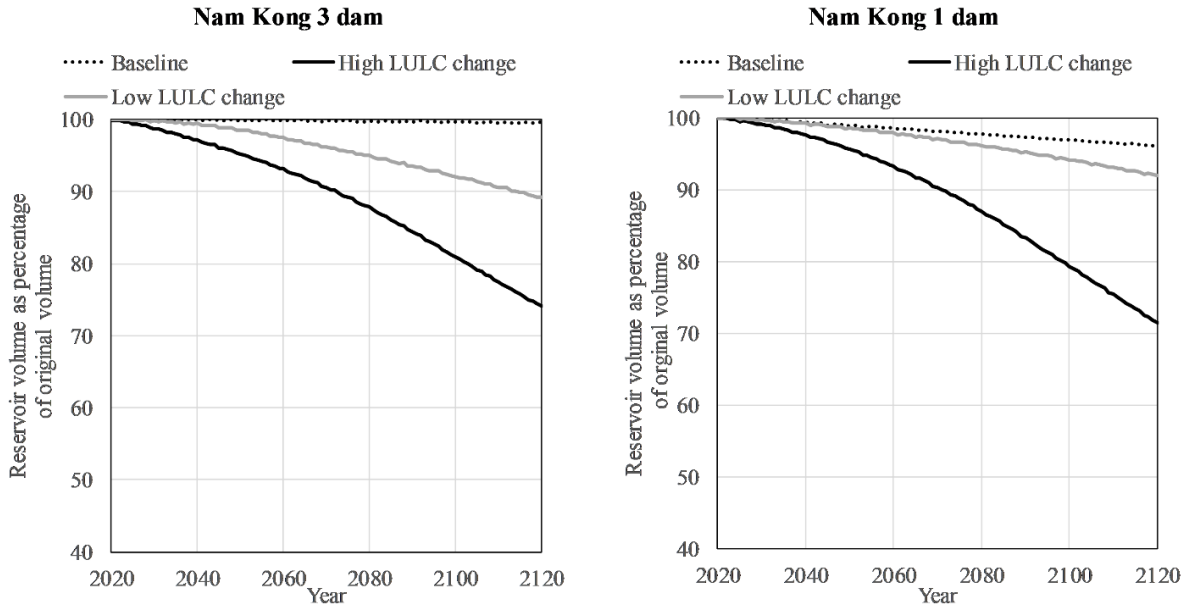

Figure 5-6. Reservoir total water storage capacity (volume) for Nam Kong 3 and Nam Kong 1 reservoirs over time, expressed as a percentage of initial reservoir total water storage capacity.

The results indicate that variability in projected future sediment yield results in large uncertainties in reduced reservoir capacity, which are due to differences between LULC change projections (Figure 5-5 and Figure 5-6). The results also indicate that variability in loss of reservoir capacity increases with time for both dams. This analysis is based on two dams operating in series; hence it is worth noting that the loss of reservoir volume for Nam Kong 1 is influenced by the magnitude of sediment trapped in Nam Kong 3. Increased sediment load due to LULC changes generally can result in significant reduction of reservoir storage capacity, which can affect power generation capacity. The reduction in storage capacity, considering LULC change, can be a significant factor in the cost-benefit ratio of hydropower projects. Hence, the dam designer and planner should take potential LULC change into account in the design and operation of dams.

Impact of catchment-level sediment management on reservoir storage

The loss of reservoir volume after testing three different catchment management options suggest that terracing is the most effective option to minimize reservoir storage capacity loss (Figure 5-7). For Nam Kong 1, implementation of terracing can reduce the loss of reservoir volume from 8-28% to 1-3%. Interestingly, terracing also reduced the wide variability in loss of reservoir volume due to the LULC scenario. In general, vegetative filter strips are the least effective catchment-level reservoir sedimentation management option evaluated in this case study. Terracing is likely more effective in reducing sediment/soil erosion because terracing

reduces hillslope length and gradient, which results in decreasing surface runoff and velocity, while vegetative filter strips were only implemented in agricultural land bordering the river reaches. The effectiveness of filter strips to minimize sediment transfer to rivers is a function of the location and amount of permanent vegetative cover (Zhou et al., 2009), and implementation in large areas (i.e., the filter strips themselves are large) can increase sediment load reduction (Woznicki et al., 2011).

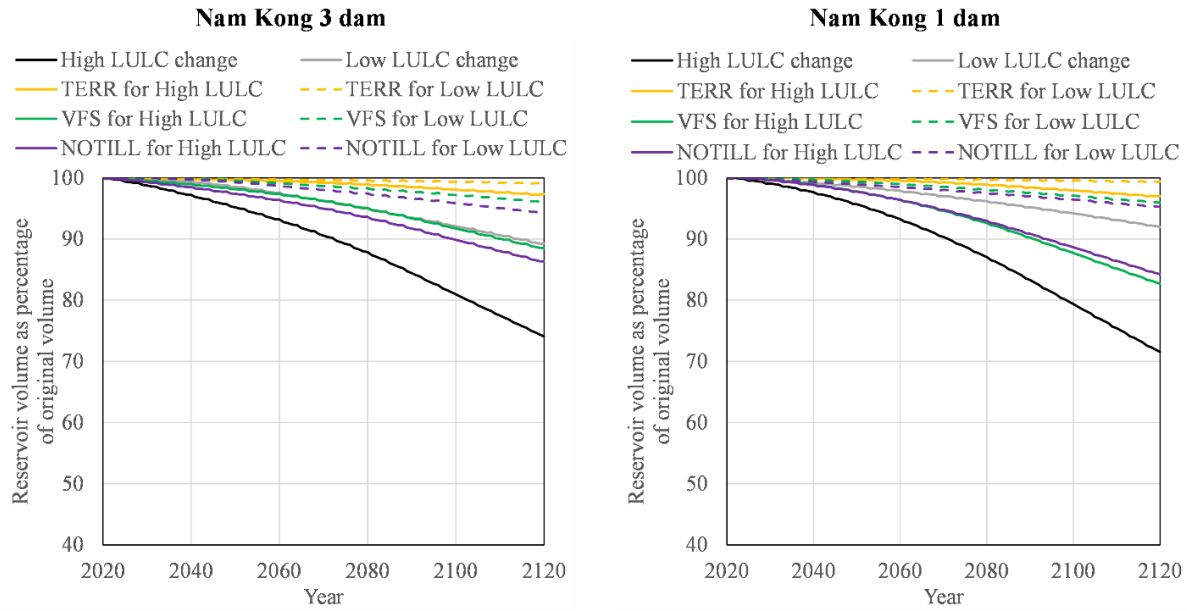

Figure 5-7. Reservoir total water storage capacity (i.e., volume) for Nam Kong 3 and Nam Kong 1 reservoirs over time for various catchment-level reservoir sediment management options under LULC change uncertainty. Storage capacity is expressed as a percentage of initial reservoir total water storage capacity. TERR = Terracing, VFS = Vegetative Filter Strips and NOTILL = No Tillage.

Impact of flushing on reservoir storage

Figure 5-8 shows the effect of flushing on the reservoir storage capacity of both dams operating in series. The results indicate that periodic flushing (i.e., every five years) can minimize the loss of reservoir storage capacity and significantly reduce variability in loss of reservoir capacity. The model simulation results show that over 100 years of reservoir flushing operations (4-13 days every 5 years) can remove more than 90% of the total sediment inflow to the reservoirs. For example, under the high LULC change case for Nam Kong 1, if flushing is not implemented the reservoir will trap 176.3 Million Tons (Mt) of sediment over 100 years, which is nearly 93% of the total sediment inflow to the reservoir. Implementation of flushing can remove 95% of total sediment inflow (246.5 Mt) to the Nam Kong 1 reservoir (Table 5-4). This high degree of flushing effectiveness is a function of both the magnitude of flushing

discharge available during the target flushing time period of May-June, as well as the extensive width of the incised channel created by flushing relative to the reservoir width.

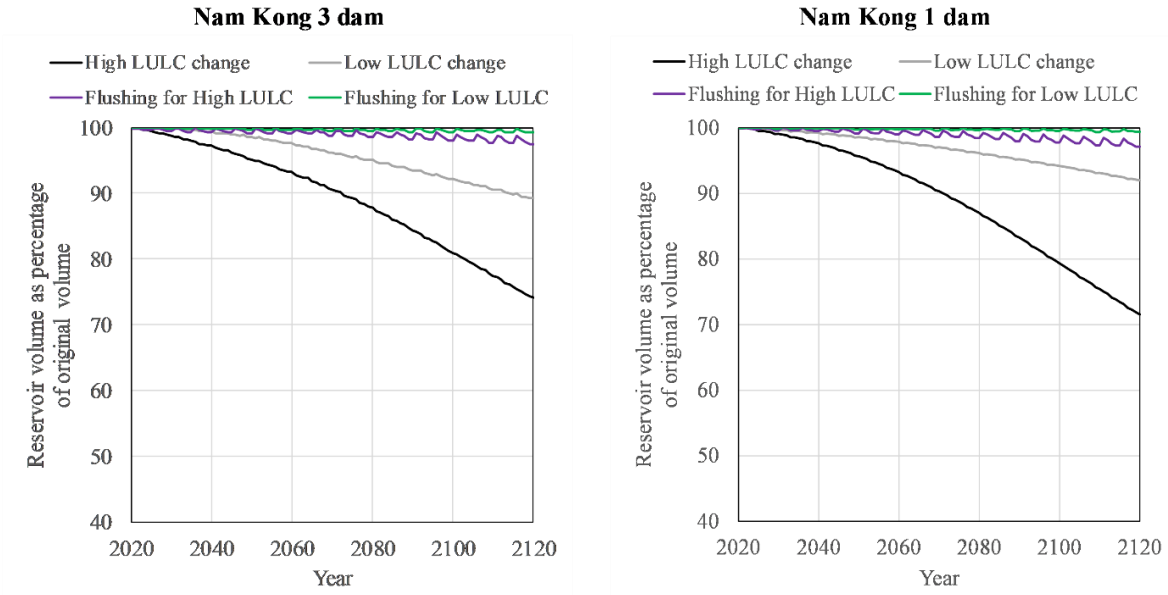

Figure 5-8. Reservoir volume for Nam Kong 3 and Nam Kong 1 reservoirs over time for flushing options under LULC change uncertainty.

Table 5-4. Reservoir sediment budget over 100 years of operation for the Nam Kong 3 and the downstream Nam Kong 1 reservoirs (flushed simultaneously).

Sediment Budget	Nam Kong 3		Nam Kong 1	
	No Flushing	Flushing	No Flushing	Flushing
High LULC change scenario				
Total sediment inflow (Mt)	79.2	79.2	189.6	258.3
Total sediment outflow (Mt)	6.6	75.3	13.3	246.5
Trapped Sediment (Mt)	72.6	3.9	176.3	11.8
Low LULC change scenario				
Total sediment inflow (Mt)	33.0	33.0	52.8	82.3
Total sediment outflow (Mt)	2.6	32.0	3.4	79.8
Trapped Sediment (Mt)	30.4	1.0	49.4	2.5

In general, flushing can be successfully implemented and is an effective reservoir-level management option to reduce the lost reservoir storage of both dams when efforts are coordinated. Unlike catchment-level management options, flushing also releases the trapped sediment back to the river crucial for the riverine ecosystem. However, flushing can significantly alter the sediment and flow pulse of the river which can have ecological (Grimardias et al., 2017; Espa et al., 2016) and geomorphological (Brandt and Swenning, 1999) implications. In this study, for flushing to be successful, its frequency was set at 5-year

intervals. This simply means that the sediment trapped for 5 years will be flushed in a short duration, ranging from 4 – 13 days depending upon the dam and LULC scenario (please refer to Table 5-3 for details). This can suddenly introduce large amounts of sediment to the river. Morris and Fan (1998) suggest that flushing, in general, can suddenly increase sediment concentration with magnitudes exceeding 100 g/L, which can last for several weeks. Hence, the amount, timing and frequency of sediment released during flushing should be carefully planned in order to minimize adverse effects to riverine ecosystems (Wild et al., 2016). Dams can be flushed more often to minimize the release of large amounts of sediment to the river, but the impacts on power generation can be even sharper.

Cost of sediment management

The annual estimated revenue from hydropower generation from the Nam Kong 1 and Nam Kong 3 reservoirs is US$ 119 million and US$ 34 million, respectively. For Nam Kong 1, the cost of reservoir sediment removal (taken as avoided cost of dredging), after 100 years of operation (i.e., at the end of the dam's lifetime), ranges from US$ 123.53 to 440.73 million without sediment management strategies. The net present value (NPV) of the cost of reservoir sediment removal ranges from US$ 0.94 to 3.35 million if no sediment management options are implemented (Table 5-5). The total cost of loss in hydropower production due to loss of reservoir volume is estimated to range from US$ 25.81-77.73 million, and the NPV for the cost of loss in hydropower ranges from US$ 1.46 – 4.50 million, for Nam Kong 1 without sediment management strategies. For Nam Kong 3, over 100 years of operation, the total cost of loss in hydropower generation ranges from US$ 7.80 to 20.14 million and the NPV ranges from US$ 0.42 – 1.25 million if no sediment management options are implemented. The total cost of loss in hydropower for both dams due to loss of reservoir capacity is not significant compared to total revenue generated by both dams operating over 100 years. This result suggests that for high dams, with large storage and loss in reservoir storage due to sedimentation, reduced power generation revenues may not be significant. This might not encourage dam developers or operators to take measures to reduce sedimentation in order to regain the lost reservoir storage. However, the lost revenue due to sedimentation could be used for catchment conservation practices and reservoir-level options which would offset sedimentation and thus reservoir volume loss. Further, trapping sediment for 100 years may ultimately adversely impact critical river ecosystems. Maintaining riverine ecosystems, rather than storage capacity and energy production, might be the reason to motivate the dam developer and operators to implement sediment management, which is likely the case for most reservoirs in the 3S basin (Wild and

Loucks, 2014). For dam developers and operators to view sediment management as an economic benefit, the cost of maintaining the critical riverine ecosystem must be accounted in the traditional paradigm of economic analysis (Wild et al., 2016). Nevertheless, for smaller storage dams, the reduced power generation revenues may be significant (Kaura et al., 2019) and hence, the financial benefits of sediment management options will be important.

Through this study the most economically feasible or most optimal catchment management strategies are not assessed, but present how the cost of sediment management changes when various interventions are made with the aim to reduce erosion from the catchment and hence increase the life span of the reservoirs (i.e., quantify the economic benefit of catchment management to hydropower and reservoir storage). Out of three catchment management practices used in the study, terracing is the most effective method, decreasing the magnitude and variability of the cost of sediment management significantly for both dams (Figure 5-9). Terracing provides greater economic benefit to dam developers and operators as compared to other options considered in this study. For instance, over 100 years of operation, terracing will provide a benefit of US$ 134.60 – 461.60 million (NPV of US$ 2.2 – 7.1 million) and US $76.40 – 179.8 million (NPV of US$ 0.9 -2.4 million) for Nam Kong 1 and Nam Kong 3 dams, respectively. Vegetative filter strips is the least effective method in reducing the cost of sediment management.

Table 5-5. Details on cost of sediment management over 100 years. The units of cost is in Million US$.

Sediment management options	Nam Kong 3				Nam Kong 1			
	Cost of reservoir sediment removal	Net present value of cost of reservoir sediment removal	Total cost of loss in hydropower production	Net present value of cost of loss in hydropower production	Cost of reservoir sediment removal	Net present value of cost of reservoir sediment removal	Total cost of loss in hydropower production	Net present value of cost of loss in hydropower production
High LULC change scenario								
Do nothing	181.50	1.38	20.14	1.25	440.73	3.35	77.73	4.50
Terracing (TERR)	19.88	0.15	1.96	0.11	49.58	0.38	7.25	0.37
Vegetative Filter Strips (VFS)	81.02	0.62	8.25	0.50	272.00	2.07	38.04	2.07
No Tillage (No Till)	96.36	0.73	10.42	0.68	245.60	1.87	40.72	2.39
Flushing	9.85	0.07	77.49	13.76	29.55	0.22	530.50	95.01
Low LULC change scenario								
Do nothing	76.01	0.58	7.80	0.42	123.53	0.94	25.81	1.46
Terracing (TERR)	6.65	0.05	0.78	0.06	12.37	0.09	2.41	0.14
Vegetative Filter Strips (VFS)	27.63	0.21	2.81	0.15	65.02	0.49	10.86	0.60
No Tillage (No Till)	40.21	0.31	4.10	0.22	75.13	0.57	14.85	0.90
Flushing	2.48	0.02	61.58	10.98	6.21	0.05	477.36	85.58

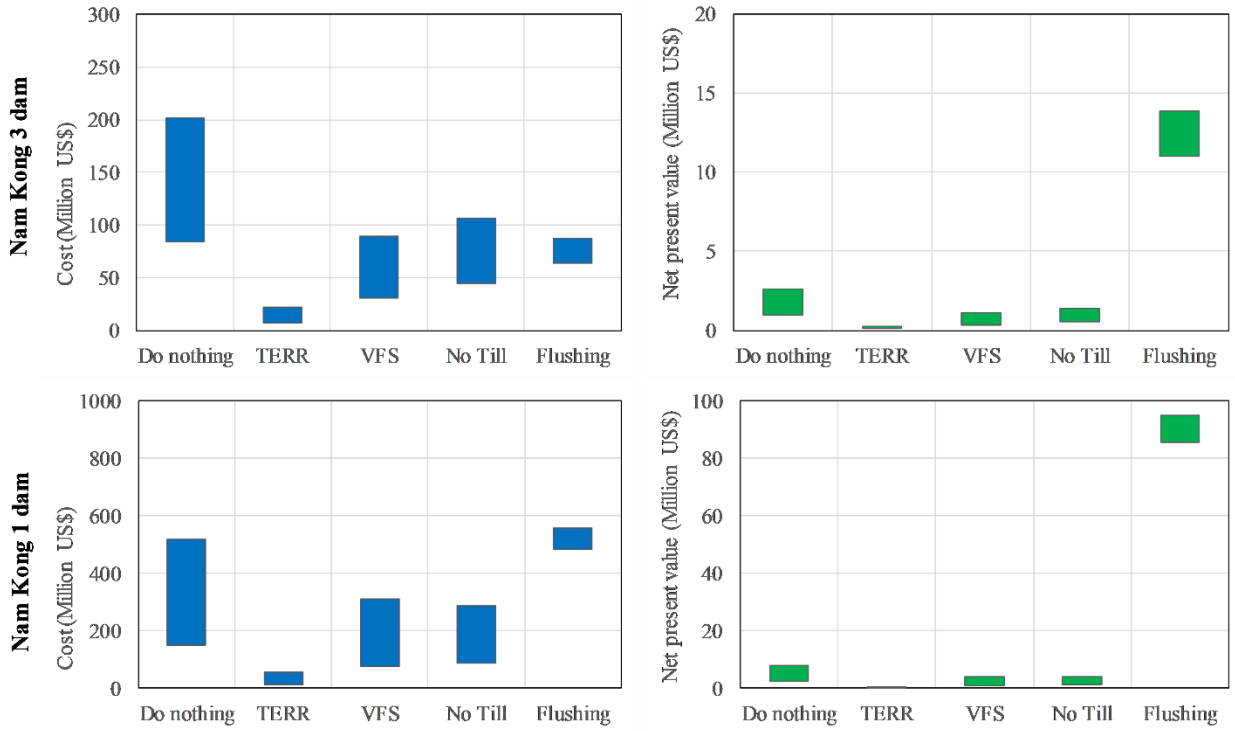

Figure 5-9. Costs and net present value of no sediment management and sediment management options over 100 years of reservoir operation. TERR = Terracing, VFS = Vegetative Filter Strips and No Till = No Tillage. Note: Cost presented in this figure refers to cost of reservoir sediment removal plus total cost of loss in hydropower production, and net present value is the sum of net present value of cost of reservoir sediment removal and net present value of cost of loss in hydropower production. There is a range for each bar which is due to the LULC change scenario differences.

The selection of management practices for reducing erosion from the catchment depends not only on the technical effectiveness, but also on the financial viability of the measures (Verstraeten et al., 2002). Hence, the estimation of actual cost and complete cost-benefit analysis for each option is required. The catchment management option which is most effective in reducing the loss of reservoir volume, and decreasing the costs of sediment removal and loss of hydropower generation may not be the most cost-effective option to implement. The large-scale implementation of terracing can be very expensive despite its high benefit as compared to other options. Terracing is labor intensive and does have high implementation and maintenance costs. Yang et al. (2014) suggested the cost per hectare of terracing in China ranges from US$ 1900 to US$ 4000 depending on slope gradient (the higher the slope gradient the higher the cost of terracing). Options such as no tillage and vegetative filter strips would be easier, less labor intensive and less costly to implement. For instance, a study conducted in an Iowa agricultural catchment found the annual

cost of implementation and maintenance to be lowest for vegetative filter strips (US$ 3.2 per hectare) and highest for terracing (US$ 126.4 per hectare) (Zhou et al. (2009). It is to be noted that the cost of terracing in Iowa is much less than in China as mentioned above due to differences in the type of terracing. In the Iowa case, terracing is on low slopes. Further, the integration of different catchment management practices may provide most cost-effective results. Management of increased sediment due to LULC changes in catchments with multiple dams often requires an integrated sediment management approach. Several studies (for example Bosch et al., 2013; Li et al., 2019) have suggested that integration of various catchment-level management practices can produce the most effective result.

The results suggest flushing, although effective in minimizing the loss in reservoir capacity, may provide the least economic benefit to dam developers and operators as compared to catchment-level management options in the case study dams in Southern Laos. For example, for Nam Kong 1 dam over 100 years of operation, while catchment-level management options will provide an economic benefit with NPV ranging from US$ 0.90 to 7.10 million, flushing provides none. The cost of loss in hydropower is higher with flushing as compared to catchment management options (Table 5-5), as there is lost opportunity to generate energy during the flushing process. Since the dams are high in the study area, the total duration of the flushing process, more specifically drawdown and refill, is quite significant (more than 19 days for Nam Kong 3 and more than 25 days for Nam Kong 1 dam). Hence, during the flushing period the dam operator will not be able to produce energy for a considerable period. Flushing with long duration is expensive mainly due to significant loss of hydropower generation (Espa et al., 2016). For high dams the drawdown and refill period will be similar for both cases (i.e, high LULC change and low LULC change) even though the flushing duration varies (Table 5-3). For more optimal reservoir sediment management solutions, a combination of reservoir-level management techniques may be required because the effectiveness of each technique can change over time (Annandale et al., 2016).

Conclusions

This study aimed to understand the effect of catchment sediment management options for reservoir sustainability and associated cost due to sediment projections variability caused by LULC changes. This critical issue is explored in the Nam Kong Catchment in Laos, which is situated in the ecologically critical Se Kong, Se San, and Sre Pok ("3S") river basins of the Mekong basin in

Southeast Asia. Due to planned intensive and pervasive hydropower development plans in the Mekong (many of which are planned in Laos), this region is facing critical challenges with respect to balancing hydropower and ecological concerns (Wild et al., 2019b; Moran et al., 2018; Zhong and Hao, 2017; Ziv et al., 2012; Grumbine et al., 2012). Thus, this study evaluates sediment management options (both catchment management and reservoir management), in the context of LULC change, in one of the world's most critical river basin development contexts. The national government of Laos recently adopted a sustainable hydropower master plan that includes a significant focus on sediment management. Thus, this paper provides timey input to an ongoing policy discussion in Laos regarding development of the ecologically rich Sekong river basin. The results of the study's simulations suggest that uncertainty in LULC changes can result in high variability in loss of reservoir capacity and cost. Increased sediment load due to LULC changes can generally result in significant reduction of reservoir storage. Hence, dam planners should consider future potential LULC changes in the design and operation of dams.

The results suggest that for high dams with large storage, loss in reservoir storage due to LULC change-induced sedimentation may not significantly reduce power generation revenues, because loss of reservoir storage is relatively low even in the worst-case scenario. This may not motivate dam developers to implement measures to manage sediment. However, for smaller storage dams, loss in power generation revenues due to sedimentation would be significant and the financial benefits of sediment management options (both catchment-level and reservoir-level) will be substantial as well. It is also important to address the issue of conservation of land as a way to reduce sedimentation of reservoirs. Establishing conservation areas will also help achieve the goal of reducing reservoir volume loss. Further, the benefit of maintaining riverine ecosystems may be the incentive which might encourage dam developers to implement sediment management options (Wild and Loucks, 2014). Hence, the economic value of maintaining the riverine ecosystem should also be included in estimating the cost of sediment management.

The result suggests catchment management can significantly reduce long-term reservoir volume loss. For the Nam Kong case study, terracing was the most effective method and vegetative filter strips the least effective in increasing the life span of the reservoirs and hence reducing the cost of sediment management. Terracing can also decrease the wide variability in lost reservoir capacity and the cost of sediment management. However, terracing would undoubtedly be the most

expensive measure to implement as compared to other options considered in the study. This suggests that the best erosion control measures that provide the most benefit may be too expensive to implement and thus other alternatives may be more feasible. Hence, the estimation of actual cost and complete cost benefit analysis for each catchment management options is critical for the selection of the best catchment management option(s) for minimizing the effects of uncertainty in LULC changes.

The assessment highlights that flushing is an effective reservoir-level management option to minimize loss of reservoir storage, but it may be less economically beneficial as compared to catchment management options. However, catchment-level management options do not address the issue of sediment starvation downstream which is crucial for downstream riverine ecosystem and morphology (Kondolf, 1997). Hence, a combination of both catchment-level and reservoir-level sediment management approaches is required to maintain reservoir capacity as well as meet the sediment demand downstream. This is especially true for the high LULC change case where excessive erosion from the catchment can have adverse effects for both reservoir storage and river morphology and ecology. Further, flushing can provide increasing economic benefits to dam developers and operators as the loss in reservoir storage increases.

The findings presented in this study may only be true for the site-specific Nam Kong case study because the cost and effectiveness of any sediment management option may vary depending upon reservoir size and location (Morris and Fan, 1998). The result also highlights that it is difficult to generalize what sediment management option will work at any particular dam, which creates a challenge for assessing sediment management potential at the basin scale. However, the method presented in this study can be used globally to assess sediment management options for reservoir sustainability considering uncertainty in LULC change.

Chapter 6 Conclusions, Recommendations, and Future Research

Conclusions and recommendations

This study aimed to assess the uncertainty in sediment predictions and the implication of sediment management options and cost under uncertainty in sediment projections for catchments with hydropower dams. Four important sources of uncertainty were evaluated: global climate models (GCMs), representative concentration pathways (RCPs), model parameterization and land use/land cover (LULC) changes (Chapters 2, 3 and 4) to better characterise and identify the dominant source of uncertainty for flow and sediment load projections for the 3S basin. Lastly, the focus was moved on from the more straightforward projections of flow and sediment load to explore management options for reservoir sustainability and cost implication under the greatest source of uncertainty (Chapter 5). Conclusions for the key thesis objectives are presented below.

Objective 1: How do future climate scenarios and model parameterization affect the uncertainty in flow and sediment projections?

Based on the evaluation of three sources of uncertainty: GCMs, RCPs and model parameterisation, it can be concluded that in large basins the major sources of uncertainty in flow and sediment can vary over time and in space. For example, in the 3S basin results indicate for both flow and sediment model parameterization is the major contributing source of uncertainty in shorter term (2030 time period), but the selection of GCMs and RCPs dominates in longer term (2060 time period). Since model parameter uncertainty can have significant implications on future flow and sediment projections, a careful calibration and validation should be considered in order to reduce the parameter uncertainty.

Objective 2: How do land use/land cover (LULC) change scenarios affect the uncertainty in flow and sediment projections?

Based on the evaluation of uncertainty in LULC change scenario alone, it can be concluded that uncertainty in future LULC change, primarily driven by LULC demand, can result in large flow and sediment variability. Hence, careful selection of LULC demand scenarios is vital in reducing uncertainty in future LULC changes. Further, interestingly the modelling results, specific to the 3S basin, showed contrasting result of deforestation effect on flow (decrease in flow), suggesting that model calibration process and parametrization (particularly of vegetation and cover factors)

needs to be carefully considered as this can have implications on the direction of streamflow changes.

Objective 3: How do combined future climate scenarios, model parameterization and LULC change scenarios affect the uncertainty in flow and sediment projections? What is the major source of uncertainty in flow and sediment projections?

Based on the assessment of uncertainty in future flow and sediment combining GCMs, RCPs, model parameters and LULC change scenarios, it can be concluded that for a rapidly developing basin (i.e. 3S basin) where significant LULC change is anticipated the selection of LULC change scenarios can dominate the uncertainties in future flow and sediment load. Our results suggest that the choice of LULC change scenario is more important that climate change uncertainty for seasonal and annual flow and sediment. In contrast the choice of GCM and RCP is more important for flow extremes. Our study results highlight that uncertainty in LULC change scenarios should not be neglected, but rather studied in more detail and included along with other important sources of uncertainties (i.e. GCMs, RCPs and model parameters) in climate change impact studies as this can have noticeable effect on portrayal of dominant source of uncertainty in prediction of flows and sediment which is critical for better water and sediment management. Despite the uncertainty in sediment projection, our results showed increase in future sediment load, which highlights hydropower reservoirs with rapidly developing basins can be under threat of excess sedimentation, leading to potential detrimental energy production losses over time. It is to be noted that our conclusions are based on simulations for the medium-term period (2060s) and the portrayal of major sources of uncertainty may change for the farther future projections (e.g., 2090s). Nevertheless, the analytical framework present in this study can be further extended to improve the understanding of uncertainty in future flows and sediment.

Objective 4: What is the implication of sediment management options and associated cost under the greatest source of uncertainty in sediment projections?

Based on the evaluation of the reservoir sustainability under uncertainty in sediment projections due to LULC change, it can be concluded that LULC change induced uncertainty in sediment loads can result in high variability in loss of reservoir capacity and cost of sediment management. Our results show that for larger storage dams the loss of reservoir storage may not significantly reduce

power generation revenue. For dams with a smaller storage to inflow ratio, loss of storage could have a significant impact on power generation revenue. The lost revenue value due to sedimentation predictions under business as usual could be used for catchment-level and reservoir-level sediment management options, which would offset sedimentation and thus increase the reservoir sustainability for future generations. The economic value of maintaining the riverine ecosystem should be included in estimating the cost of sediment management. The financial benefits of sediment management options are important, particularly for the smaller storage to inflow ratio reservoirs.

Further, it can be concluded that sediment management options can significantly reduce the magnitude and variability in loss of reservoir capacity and cost of sediment management. For the case study of sediment management of two hydropower dams (Nam Kong 1 and Nam Kong 3) and their catchments, terracing performed the best at decreasing both the magnitude and variability in loss of reservoir storage and thus the long-term cost of sediment management for both dams, but it is the most expensive option to implement. Flushing was the best reservoir-level option to reduce sedimentation, but it is not as effective as the catchment-level sediment management options. However, catchment-level management options do not address the issue of sediment starvation downstream of the reservoir and hence an integrated approach is recommended when considering overall benefits. The outcomes of the study show that it is difficult to generalize what sediment management option will work at any particular dam, which out a detailed study of the system. The methodology develop in this thesis can be readily applied and used globally to assess sediment management options for reservoir sustainability considering uncertainty in climate variables and LULC change.

Future areas of research

Integrated sediment management studies

The holistic and effective management of sediment in catchments with series of hydropower dams requires integration of various sediment management approaches. There is need to better understand the effect of integrated sediment management on reservoir sustainability for basins undergoing rapid development, considering uncertainty in climate and LULC change. Use of various modelling frameworks to study the effect of sediment management options on reservoir sustainability can introduce model error. Hence, there is a need to a develop a single tool (for

example under SWAT modelling framework) which can assess both catchment-level and reservoir-level sediment management options.

Social aspect of sediment management

For the sustainability of any sediment management option, it should not have any negative implication to the community. Hence, further study is needed to understand community vulnerability and risk to sediment management options.

Optimization of sediment management

Sediment management is more challenging in a large basin like 3S with numerous series of reservoirs. This also makes subscribing a single sediment management option nearly impossible. In order to identify the most effective and economically sound sediment management option there is a need for optimization study of sediment management.

Effect of reservoir size to inflow ratio on sediment impact

The reservoir size and sediment inflow influence both the rate and the magnitude of loss of reservoir capacity. Further, this will also have implication on cost-effectiveness/ financial benefit of sediment management options. Hence, a good understating on the effect of reservoir size to inflow ratio on sediment impact is required for better sediment management in basins with multiple reservoirs.

Cost implications of flushing sediment

The cost of emptying a reservoir for sediment management can go beyond just lost generation revenue and managing the associated sediment pulse. In particular, the wider electricity network would need to have sufficient spare capacity be able to cope with the disruption in supply for the period of days/weeks it takes to empty and refill the reservoir. Otherwise, the resultant reduction in industrial/commercial activity could add substantial additional costs. In the case of a cascade of hydroelectric dams (i.e., as in the case study here), synchronous flushing may be required which can cause even more substantial disruption. Hence the cost implication of emptying a reservoir needs to be further explored considering aspects as discussed above.

Calibration/ validation improvements

In general, hydrological model is calibrated against observed flow data series. This calibration process can produce an acceptable statistical relationship between simulated and observed flows, but bias other hydrological processes such as water balance and sediment balance. Hence, the model will generate erroneous results when simulating climate changes, LULC changes and management scenarios. There is a need for improvements in calibration/validation with evapotranspiration or other data sets to avoid misrepresentation of the impact of LULC change on runoff.

Ecological aspects of sediment management

Sediment management for reservoir sustainability should not undermine the riverine ecology. The quantification of ecological benefit of sediment management for reservoir substantiality can guide better selection of management options. Research is needed to better understand the ramifications of changes in flows and sediment on riverine habitats, food sources, migration, and reproduction.

Appendix

Appendix 2-1: Supplementary Material for Chapter 2

A. Supplementary Methods

Soil distribution and land use/ land cover (LULC) details of the 3S basin

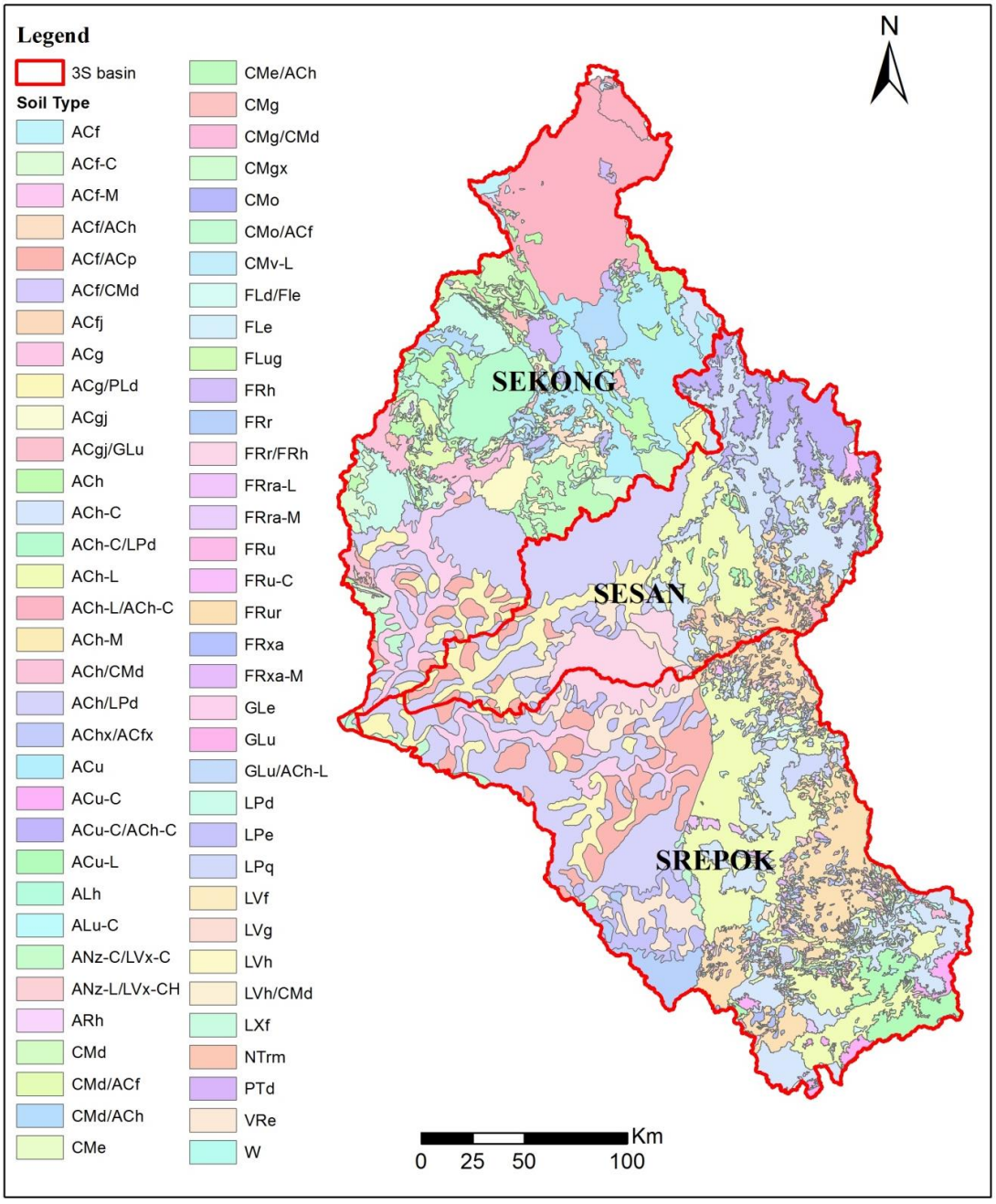

Figure S2-1. Soil type distribution map of the 3S basin (Source: MRC, 2010). For details of soil type, refer to Table S2-1.

Table S2-1. Major soil types of the 3S basin and their properties (values based on soil map used in the SWAT model of the 3S basin developed by Mekong River Commission)

Soil Name	Major soil	Depth of Soil Layer (mm)	Texture	Composition (%)			Bulk Density (g/cm^3)	Available Water Capacity (mm/mm)	Saturated Hydraulic Conductivity (mm/h)
				Sand	Silt	Clay			
ACh-L/ACh-C	Acrisol	0-300	Sandy Clay Loam	55	24	21	1.46	0.23	6.50
ACh	Acrisol	0-300	Sandy Clay Loam	55	24	21	1.46	0.23	6.50
		300-600	Sandy Clay Loam	50	23	28	1.46	0.22	3.49
		600-1000	Sandy Clay Loam	48	20	32	1.48	0.19	2.56
		1000-2000	Sandy Clay Loam	52	18	30	1.44	0.16	2.90
ACh-C	Acrisol	0-300	Sandy Clay Loam	55	24	21	1.46	0.23	6.50
		300-600	Sandy Clay Loam	50	23	28	1.46	0.22	3.49
		600-1000	Sandy Clay Loam	48	20	32	1.48	0.19	2.56
		1000-2000	Sandy Clay Loam	52	18	30	1.44	0.16	2.90
ACu	Acrisol	0-300	Clay Loam	37	24	39	1.27	0.22	1.95
		300-600	Clay	33	21	46	1.34	0.2	1.61
		600-1000	Clay	29	22	50	1.34	0.2	1.60
		1000-2000	Clay	28	20	53	1.36	0.15	1.57
LPd	Leptosol	0-300	Sandy Clay Loam	59	16	25	1.2	0.28	4.20
CMd/ACh	Cambisol	0-300	Clay Loam	37	33	31	1.23	0.24	3.39
		300-600	Clay Loam	44	27	30	1.23	0.22	3.36
		600-1000	Sandy Clay Loam	48	26	27	1.24	0.22	4.12
		1000-2000	Loam	46	28	26	1.28	0.1	4.47
ACh-C/LPd	Acrisol	0-300	Sandy Clay Loam	55	24	21	1.46	0.23	6.50
		300-600	Sandy Clay Loam	50	23	28	1.46	0.22	3.49
		600-1000	Sandy Clay Loam	48	20	32	1.48	0.19	2.56
		1000-2000	Sandy Clay Loam	52	18	30	1.44	0.16	2.90
ACu-C/ACh-C	Acrisol	0-300	Clay Loam	37	24	39	1.27	0.22	1.95
		300-600	Clay	33	21	46	1.34	0.2	1.61
		600-1000	Clay	29	22	50	1.34	0.2	1.60
		1000-2000	Clay	28	20	53	1.36	0.15	1.57
ACh/CMd	Acrisol	0-300	Sandy Clay Loam	55	24	21	1.46	0.23	6.50
		300-600	Sandy Clay Loam	50	23	28	1.46	0.22	3.49
		600-1000	Sandy Clay Loam	48	20	32	1.48	0.19	2.56
		1000-2000	Sandy Clay Loam	52	18	30	1.44	0.16	2.90
LVh	Luvisol	0-300	Loam	47	33	20	1.54	0.22	8.07
		300-600	Loam	42	31	27	1.59	0.21	4.23
		600-1000	Loam	45	31	25	1.66	0.19	5.16
		1000-2000	Loam	47	34	20	1.63	0.13	8.19

Table S2-1 continued…

Soil Name	Major soil	Depth of Soil Layer (mm)	Texture	Composition (%)			Bulk Density (g/cm^3)	Available Water Capacity (mm/mm)	Saturated Hydraulic Conductivity (mm/h)
				Sand	Silt	Clay			
ACf-C	Acrisol	0-300	Sandy Clay Loam	53	18	30	1.46	0.21	2.87
		300-600	Clay	43	17	41	1.45	0.2	1.64
		600-1000	Clay	40	17	43	1.45	0.2	1.56
		1000-2000	Clay	40	18	42	1.43	0.14	1.62
CMe/ACh	Cambisol	0-300	Loam	39	34	27	1.49	0.22	4.42
		300-600	Loam	42	32	26	1.53	0.2	4.65
		600-1000	Loam	45	29	26	1.55	0.19	4.48
		1000-2000	Loam	41	33	26	1.49	0.13	4.76
ACh-L	Acrisol	0-300	Sandy Clay Loam	55	24	21	1.46	0.23	6.50
ACh/LPd	Acrisol	0-300	Sandy Clay Loam	55	24	21	1.46	0.23	6.50
		300-600	Sandy Clay Loam	50	23	28	1.46	0.22	3.49
		600-1000	Sandy Clay Loam	48	20	32	1.48	0.19	2.56
		1000-2000	Sandy Clay Loam	52	18	30	1.44	0.16	2.90
GLe	Gleysol	0-300	Clay Loam	23	39	39	1.49	0.22	2.66
		300-600	Clay	25	35	41	1.53	0.21	2.34
		600-1000	Clay Loam	27	35	38	1.57	0.2	2.53
		1000-2000	Clay Loam	27	37	36	1.55	0.08	2.89
FRur	Ferralsol	0-300	Clay	28	20	52	1.2	0.23	1.59
		300-600	Clay	29	19	52	1.19	0.22	1.55
		600-1000	Clay	32	18	50	1.19	0.23	1.50
		1000-2000	Clay	33	20	47	1.22	0.22	1.54
ACg/PLd	Acrisol	0-300	Clay Loam	42	31	27	1.25	0.23	4.19
		300-600	Clay Loam	35	32	33	1.47	0.21	3.00
		600-1000	Clay Loam	37	29	34	1.55	0.19	2.64
		1000-2000	Clay Loam	43	26	31	1.59	0.11	2.95
ACf/ACp	Acrisol	0-300	Sandy Clay Loam	53	18	30	1.46	0.21	2.87
		300-600	Clay	43	17	41	1.45	0.2	1.64
		600-1000	Clay	40	17	43	1.45	0.2	1.56
		1000-2000	Clay	40	18	42	1.43	0.14	1.62
FRr/FRh	Ferralsol	0-300	Clay	37	17	47	1.28	0.2	1.47
		300-600	Clay	33	15	53	1.26	0.21	1.40
		600-1000	Clay	33	15	52	1.24	0.21	1.42
		1000-2000	Clay	33	17	50	1.24	0.16	1.44
LPe	Leptosol	0-300	Sandy Clay Loam	59	16	25	1.2	0.28	4.20
CMo/ACf	Cambisol	0-300	Clay Loam	36	25	39	1.2	0.23	2.02
		300-600	Clay	35	22	43	1.28	0.21	1.74
		600-1000	Clay	36	23	41	1.32	0.19	1.82
		1000-2000	Clay Loam	39	23	39	1.42	0.14	1.95
VRe	Vertisol	0-300	Clay	16	27	58	1.65	0.17	2.07
		300-600	Clay	15	24	61	1.68	0.16	2.16
		600-1000	Clay	16	24	60	1.69	0.16	2.10
		1000-2000	Clay	23	26	52	1.67	0.11	1.80

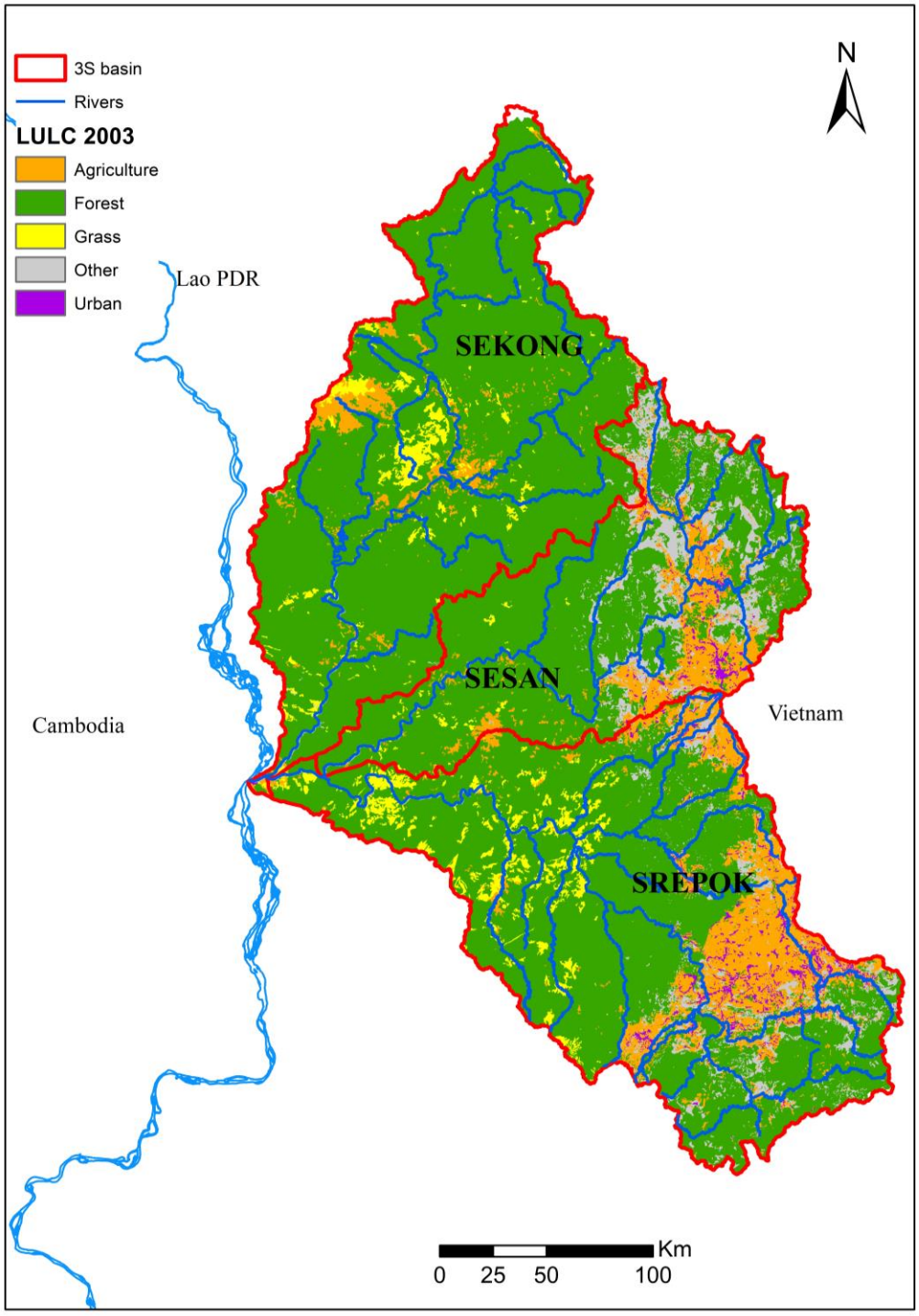

Figure S2-2. Land use/ land cover (LULC) for the study area (Source: MRC, 2010)

SWAT Model description

SWAT is a river basin or watershed scale, semi-distributed, process-based, and continuous hydrologic and water quality model initially developed by Arnold et al. (1993b). The model

evaluates the effect of LULC management on water, sedimentation, and agricultural chemical yields in large complex watersheds which are heterogeneous in LULC, soil and management conditions over a long period of time. SWAT subdivides a watershed into different sub basins connected by a stream network, and further into hydrological response units (HRUs). HRUs are the lumped land areas within the subbasin that comprise unique land cover, soil, slope and management combinations. The 3S SWAT model was discretized into 140 subbasins (Figure S2-3) and 2282 HRUs. Table S2-2 provides the details on number of HRU by subbasin. SWAT simulates the hydrology of the watershed in two phases. The land phase of the hydrologic cycle controls the amount of water, sediment, nutrient and pesticide loadings to the main channel in each subbasin. The water or routing phase of the hydrologic cycle controls the movement of water, sediment, nutrients and pesticide loadings through the channel network of the watershed into the outlet.

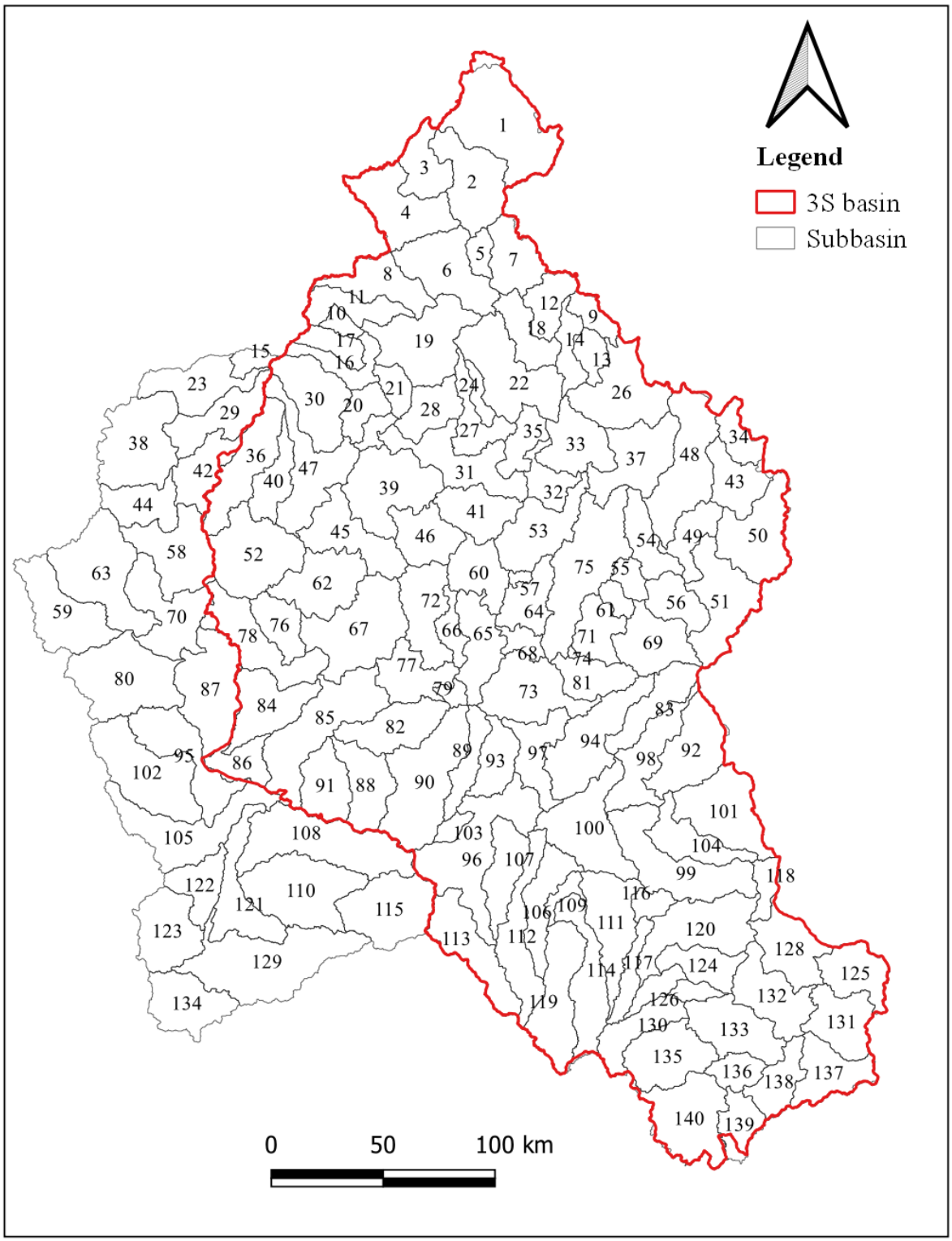

Figure S2-3. Subbasins for the 3S SWAT model

Table S2-2. Details on number of HRU by subbasin for the 3S SWAT model

Subbasin number	Number of HRU	Subbasin number	Number of HRU	Subbasin number	Number of HRU	Subbasin number	Number of HRU
1	10	36	17	71	25	106	10
2	10	37	28	72	10	107	10
3	10	38	13	73	22	108	14
4	14	39	15	74	13	109	17
5	10	40	15	75	26	110	17
6	10	41	16	76	13	111	14
7	11	42	8	77	19	112	11
8	12	43	29	78	18	113	16
9	19	44	15	79	16	114	34
10	10	45	9	80	12	115	8
11	13	46	13	81	25	116	17
12	14	47	12	82	13	117	24
13	12	48	29	83	21	118	12
14	13	49	20	84	10	119	12
15	19	50	40	85	22	120	25
16	16	51	23	86	15	121	11
17	13	52	22	87	13	122	12
18	8	53	11	88	15	123	16
19	8	54	22	89	14	124	16
20	9	55	14	90	14	125	23
21	11	56	28	91	13	126	25
22	14	57	8	92	22	127	20
23	12	58	14	93	10	128	16
24	11	59	15	94	24	129	10
25	11	60	8	95	11	130	30
26	23	61	9	96	22	131	34
27	13	62	13	97	11	132	30
28	12	63	15	98	20	133	19
29	9	64	11	99	20	134	12
30	12	65	16	100	12	135	39
31	13	66	15	101	27	136	34
32	10	67	19	102	22	137	20
33	11	68	18	103	3	138	26
34	16	69	17	104	21	139	21
35	11	70	8	105	14	140	24

Surface runoff computation and flood routing

SWAT estimates the surface runoff volume from HRUs using the Soil Conservation Service (SCS) curve number method (USDA-SCS, 1972) or the Green and Ampt infiltration method (Green and Ampt, 1911). In this study, the SCS curve number method has been used, which is a function of the soil's permeability, LULC and antecedent soil water conditions as defined in SWAT. SCS defines three antecedent moisture conditions: dryness (wilting point), average moisture, and wetness (field capacity). SWAT calculates the peak runoff rate with a modified rational method. The model offers three options for estimating potential evapotranspiration: the Hargreaves (Hargreaves et al., 1985), Pristley-Taylor (Priestley and Taylor, 1972), and Penman-Monteith (Monteith, 1965) methods. The Penman-Monteith method is used in this study. SWAT uses Manning's equation to define flow rate and velocity. Water is routed through the channel network using the variable storage routing method developed by Williams (1969) or the Muskingum routing methods, which are variations of the kinematic wave model. For this study, the variable storage routing method is used.

Sediment yield computation and transport

The model calculates the surface erosion within each HRU with the Modified Universal Soil Loss Equation (MUSLE) (Williams, 1975). The MUSLE equation used to calculate sediment yield is:

$$\text{sed} = 11.8 \text{ x } \left(Q_{\text{surf}} \text{ x } q_{\text{peak}} \text{ x area}_{\text{hru}}\right)^{0.56} \text{x } K_{\text{USLE}} \text{ x } C_{\text{USLE}} \text{ x } P_{\text{USLE}} \text{ x } LS_{\text{USLE}} \text{ x CFRG} \qquad (1.1)$$

where sed is the sediment yield (metric tons/day), Q_{surf} is the surface runoff volume (mm/ha/day), q_{peak} is the peak runoff rate (m^3/s), $area_{hru}$ is the area of the HRU (ha), K_{USLE} is the USLE soil erodibility factor, C_{USLE} is the USLE cover and management factor, P_{USLE} is the USLE support practice factor, LS_{USLE} is the USLE topographic factor and CFRG is the coarse fragment factor.

The sediment-routing model (Arnold et al., 1995) that simulates sediment transport in the channel network consists of two components operating simultaneously: deposition and degradation. SWAT uses a simplified version of the Bagnold (1977) stream power equation to estimate deposition/degradation in the channels. In this simplified method the maximum amount of sediment that can be transported from a reach segment is a function of the peak channel velocity. The peak channel velocity, $v_{ch,pk}$ is calculated as:

$$v_{ch,pk} = \frac{q_{ch,pk}}{A_{ch}} \qquad (1.2)$$

where $q_{ch,pk}$ is the peak flow rate (m^3/s) and A_{ch} is the cross-sectional area of flow in the channel (m^2). The peak flow rate is defined as:

$$q_{ch,pk} = prf.\, q_{ch} \tag{1.3}$$

where prf is the peak rate adjustment factor, and q_{ch} is the average rate of flow (m^3/s).

The maximum amount of sediment that can be transported from a reach segment is calculated as:

$$conc_{sed,ch,mx} = c_{sp}.\, v_{ch,pk}^{spexp} \tag{1.4}$$

where $conc_{sed,ch,mx}$ is the maximum concentration of sediment that can be transported by the water (ton/m^3 or kg/L), c_{sp} is a coefficient defined by the user, $v_{ch,pk}$ is the peak channel velocity (m/s), and spexp is an exponent defined by the user which normally varies between 1.0 and 2.0.

The amount of deposition and degradation is based on the maximum concentration of sediment in the reach and the concentration of sediment in the reach at the beginning of the time step. The maximum concentration of sediment calculated with equation 1.4 is compared to the concentration of sediment in the reach at the beginning of the time step, $conc_{sed,ch,i}$. If $conc_{sed,ch,i} > conc_{sed,ch,mx}$, deposition is the dominant process in the reach segment, otherwise, degradation is the dominant process in the reach segment.

The final amount of sediment in the reach is determined as:

$$sed_{ch} = sed_{ch,i} - sed_{dep} + sed_{deg} \tag{1.5}$$

where sed_{ch} is the amount of suspended sediment in the reach (metric tons/day), $sed_{ch,i}$ is the amount of suspended sediment in the reach at the beginning of the time period (metric tons/day), sed_{dep} is the amount of sediment deposited in the reach segment (metric tons/day), and sed_{deg} is the amount of sediment reentrained in the reach segment (metric tons/day).

The amount of sediment transported out of the reach is calculated as:

$$sed_{out} = sed_{ch}\, \frac{V_{out}}{V_{ch}} \tag{1.6}$$

where sed_{out} is the amount of sediment transported out of the reach (metric tons/day), sed_{ch} is the amount of suspended sediment in the reach (metric tons/day), V_{out} is the volume of outflow during the time step (m^3/day), and V_{ch} is the volume of water in the reach segment (m^3/day). Detailed descriptions of the different model components can be found in Neitsch et al. (2011).

GCMs and emission scenarios

Details of three RCPs used in the study are provided in Table S2-3.

Table S2-3. Description of Representative Concentration Pathways (RCPs) to consider in this study (adapted from Moss et al. (2010))

Name	Radiative forcing	Concentration (ppm)
RCP2.6	Peak at ~3 Wm^{-2} before 2100 and then declines	Peak at ~490 CO_2 –equivalent before 2100 and then declines
RCP6.0	~6 Wm^{-2} at stabilization after 2100	~850 CO_2 –equivalent (at stabilization after 2100)
RCP8.5	>8.5 Wm^{-2} in 2100	>1370 CO_2 –equivalent in 2100

B. Supplementary Results and Discussion

Calibration and Validation of the SWAT model

The ranges of selected parameters that are used for the model calibration are presented in Figure S2-4.

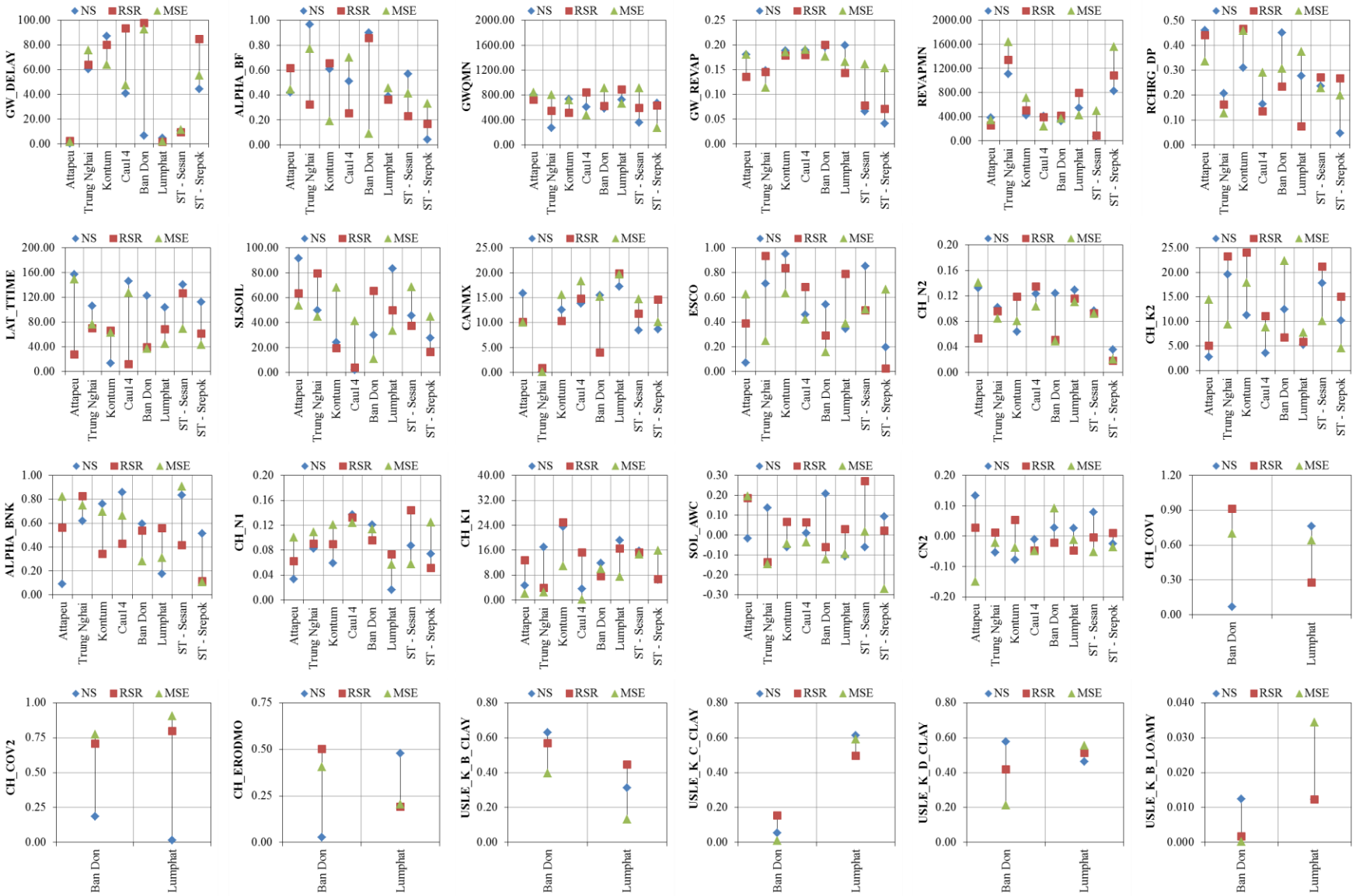

Figure S2-4. Resulting range of selected parameters used for the model calibration

Climate change projections

The changes in temperature and precipitation for the three subbasins (Sekong, Sesan and Srepok) are presented in Figure S2-5 to reflect the variability of climate change projections across the 3S basin.

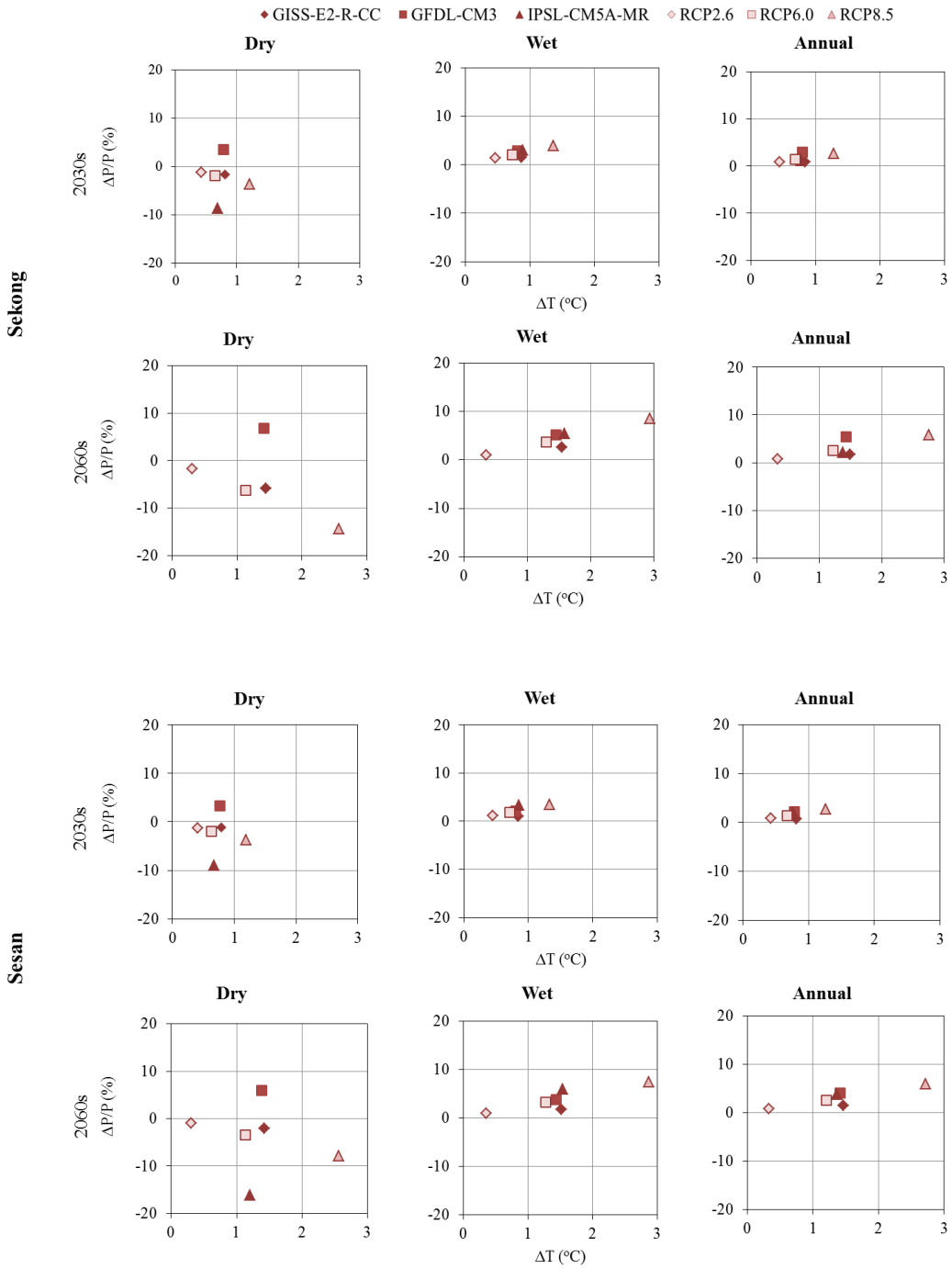

Figure S2-5 (continued)

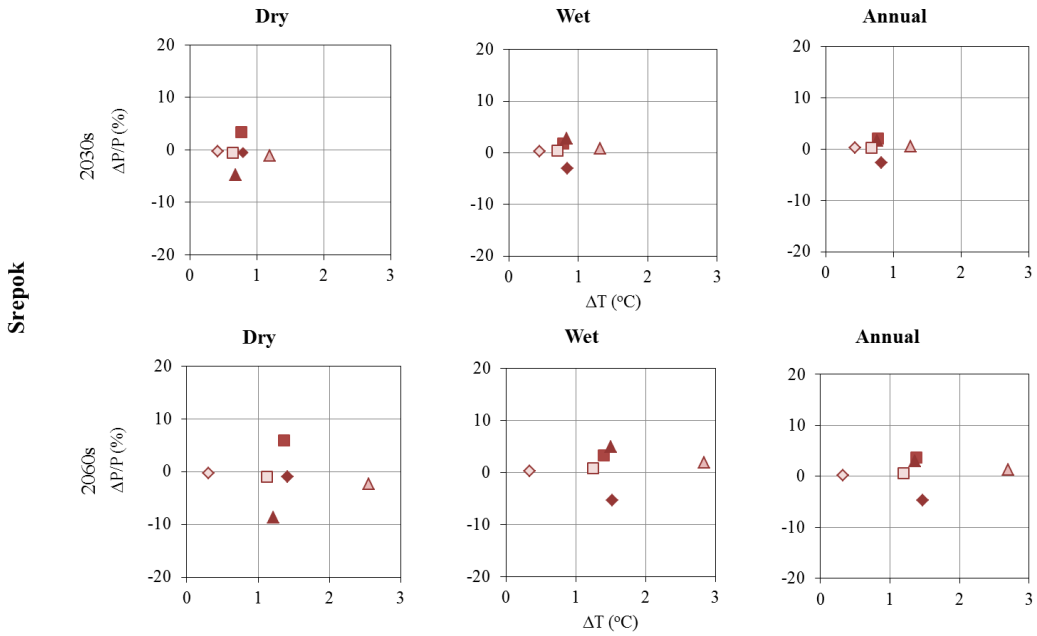

Figure S2-5. Scatterplots of changes in mean temperature (ΔT) and precipitation (ΔP) for GCMs and RCPs for 2030s (2021 – 2040) and 2060s (2051 – 2070) time horizons as compared to the base line period (1986 – 2005).

Appendix 3-1 Supplementary Material for Chapter 3

A. Supplementary Methods

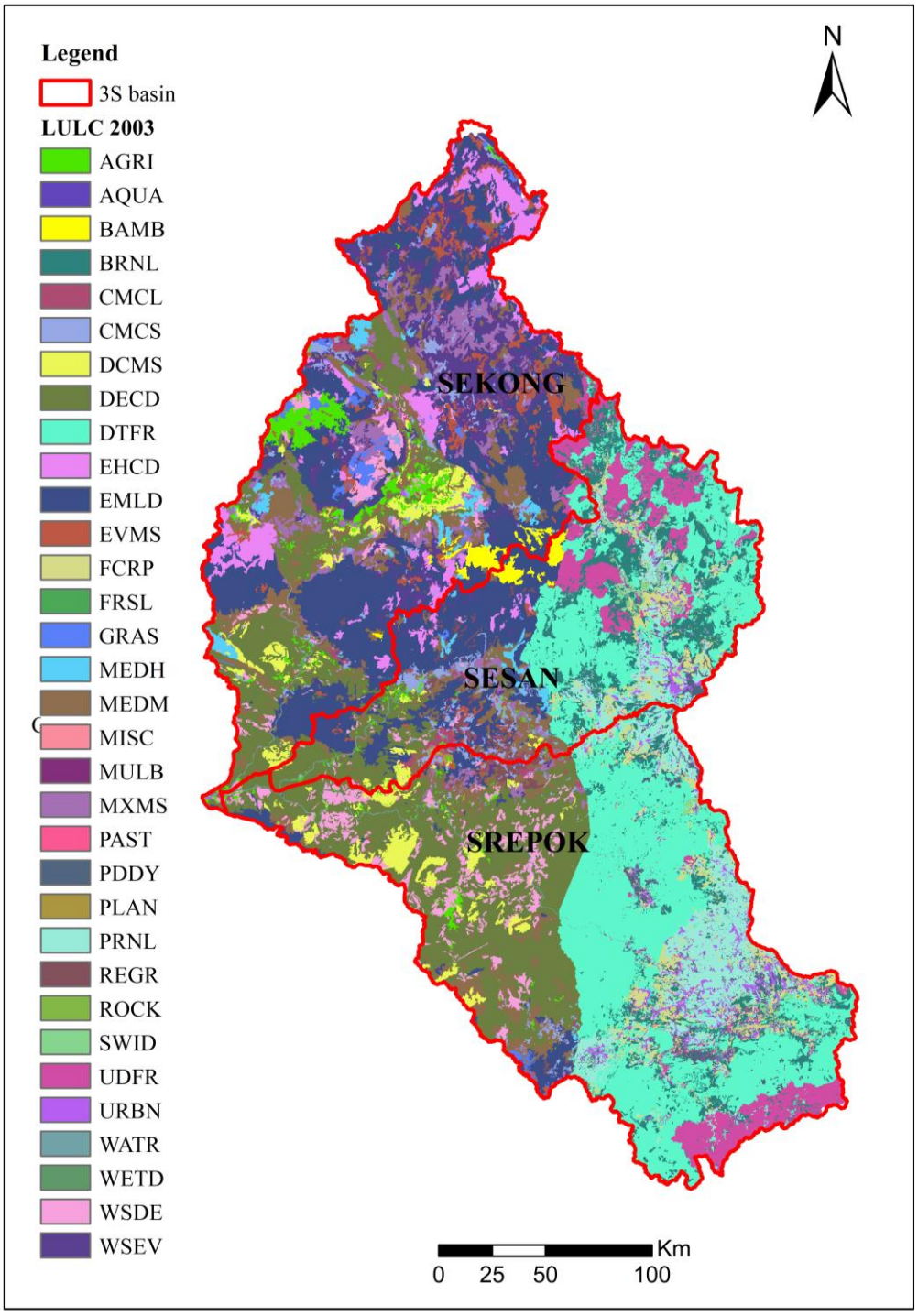

Figure S3-1. LULC map for 2003 of the 3S basin with original LULC class (Source: MRC, 2010). For details of original LULC class and simplified class, refer to Table S3-1.

Table S3-1. Original LULC class for 2003 of the 3S basin, their description and corresponding simplified LULC class

Original LULC class							Simplified class (Value)
Value	Code	Description	SWAT default Curve Number				
			A	B	C	D	
11	EHCD	Evergreen, high cover density	25	55	70	77	Forest (1)
12	EMLD	Evergreen,medium-low cover density	28	61	77	85	
13	EVMS	Evergreen mosaic	30	66	84	92	
17	MEDH	Mixed(evg&decid), high cov density	36	60	73	79	
18	MEDM	Mixed(evg&dec)med-low cover density	40	66	80	87	
19	MXMS	Mixed mosaic	43	72	88	95	
20	DECD	Deciduous	45	66	77	83	
22	DCMS	Deciduous mosaic	50	73	85	91	
40	REGR	Regrowth	49	69	79	84	
61	WSEV	Wood- and shrubland, evergreen	39	61	74	80	
63	BAMB	Bamboo	67	77	83	87	
81	CMCS	Crop mosaic, cropping area <30	42	49	54	56	
101	UDFR	LMB Undisturbed forest	25	55	70	77	
416	MULB	LMB Mulberry tree	65	76	84	87	
213	FRSL	LMB Forest land	36	60	73	79	
214	DTFR	LMB Disturbed forest land	36	60	73	79	
54	PLAN	Plaintains	67	77	83	87	Agriculture (2)
82	CMCL	Crop mosaic, cropping area >30	50	58	62	65	
91	AGRI	Agricultural land - intensive	31	59	72	79	
103	PDDY	LMB Paddy field	62	73	81	84	
104	FCRP	LMB Field crop	67	78	85	89	
107	PRNL	LMB Perennial land	67	77	83	87	
239	SWID	LMB Swidden cultivation	67	77	83	87	
62	GRAS	Grassland	49	69	79	84	Grass (3)
64	WSDR	Wood- and shrubland, dry	39	61	74	80	
224	PAST	Pasture	49	69	79	84	
95	WATR	Water	92	92	92	92	Others (4)
97	WETD	Wetland	49	69	79	84	
225	AQUA	LMB Aquacultural land	49	69	79	84	
102	MISC	LMB Miscellaneous land	45	66	77	83	
92	BRNL	Barren land	45	66	77	83	
93	ROCK	Rocks	45	66	77	83	
94	URBN	Urban or built-over area	45	66	77	83	Urban (5)

Theoretical description of Land Change Modeler

The Land Change Modeler (LCM) is a tool for the assessment and prediction of LULC change and modeling (Figure S3-2). LCM predicts LULC change through the following steps: (1) change analysis, (2) transition potential modeling, (3) estimation of the demand for land and (4) prediction of future LULC.

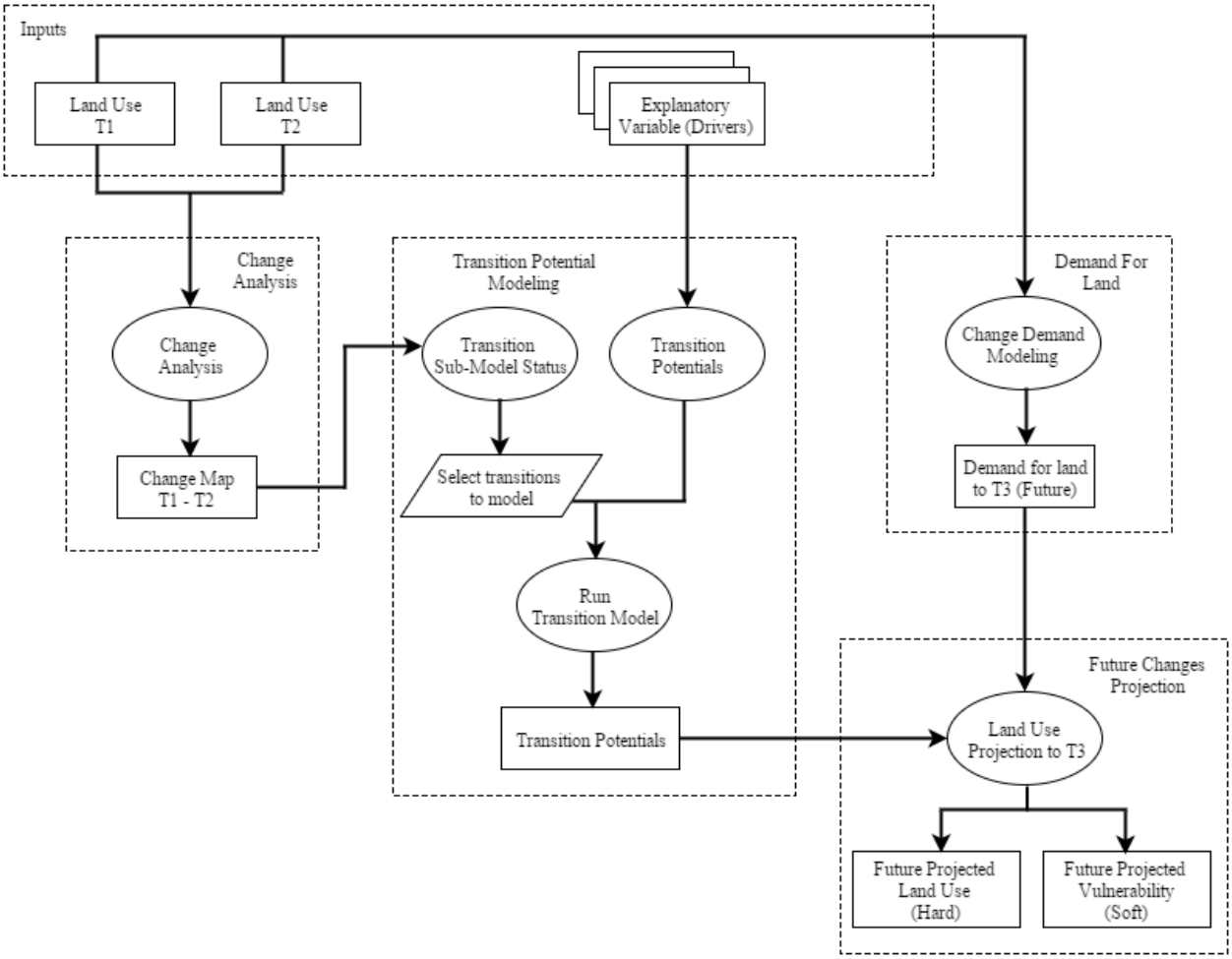

Figure S3-2. LULC prediction framework of Land Change Modeler (adapted from Sangermano et al. (2012))

Change Analysis

Change Analysis (Figure S3-2) is the first step in the modelling process. A change analysis is performed between two LULC maps (T1 and T2) to quantify and locate past LULC change. As part of change analysis, the spatial trend of change between two LULC maps can be generalized, which allows the separation of broad regional patterns of change from fine-scale patterns

(Eastman, 2009). Generalization of spatial trend allows the identification of focal areas of change which would be difficult to recognize through visual inspection of the LULC change map (Sangermano et al., 2012).

Transition Potential Modeling

Transition Potential Modeling (Figure S3-2) is the second step in the change prediction process which creates suitability maps of the likelihood for areas to transition from one LULC type to another. Transition potentials are the potential of the land to experience a particular transition in a specific time frame (Eastman et al., 2005; Paegelow and Olmedo, 2008). Transition potentials are derived from the relationship between LULC transitions and explanatory variables (drivers). In LCM, transitions are modeled using either a multi-layer perceptron (MLP) neural network, logistic regression (LR), or a similarity-weighted instance-based machine learning tool (SimWeight). Once calibrated, the model is used to predict future scenarios. For this study logistic regression and SimWeight were used. Both MLP and SimWeight can be perceived as black box approaches as they model transitions without the necessity of understanding the relationship between drives and change (Mas et al., 2014), however only SimWeight was used as it is capable of producing results that can rival or even exceed those of the MLP, it can give feedback on the relative importance of the independent variables, and the algorithm is simple to interpret (Sangermano et al., 2010).

Logistic regression is a type of generalized linear model that uses a logit function to relate presence/absence LULC data with data of any form of explanatory variable and yields a probability for the occurrence of the considered LULC type that can be interpreted as a transition potential (Eastman et al., 2005). The logistic regression supplies coefficients, also called maximum likelihood estimates, that explain the influence of selected drivers over the initial spatial arrangement of each LULC (Santini and Valentini, 2011).

Demand for land and future change projection

In LCM, the future demand for land (the quantity of change) can be modeled through a Markov Chain analysis (Burnham, 1973) or a user provided transition probability matrix from an external model. The Markov chain provides the model with the estimated areas of each LULC category for future dates and the amount of change for each transition (Mas et al., 2014). For this study, the estimated areas of each LULC category for future date was calculated through simple

extrapolations of past trends of the historic period. The amount of change for each transition (i.e. transition probability matrix) generated through a Markov Chain analysis was modified to model the desired future demand for land. After the evaluation of transition potential and estimation of quantity of changes, LCM then spatially allocates the changes using a multi-objective land allocation (MOLA) algorithm (Eastman et al., 1995) that assigns changes to the locations with high transition potential until the demand for land is satisfied.

Driving factors and model calibration

The driving factors used for this study (Table S3-2) were selected based on a review of the literature, past LULC studies in the 3S basin (Takamatsu et al., 2014; Ty et al., 2012) and data availability. All data sets were obtained from the MRC at a spatial resolution of 250 m x 250 m.

Table S3-2. Summary of the characteristics of the datasets for the driving factors considered in the study

Type	Name	Units
Climate	Mean annual precipitation	mm
Soil	Clay content	%
	Sand content	%
	Silt content	%
	Soil depth	mm
Topography	Slope	%
	Elevation	m amsl
Accessibility	Distance to road*	m
	Distance to stream	m
	Distance to hydropower dams*	m
Socio-economy	Population density*	Number of inhabitants /unit area

Source: Mekong River Commission
Note: * Drivers of dynamic nature

The model was calibrated using 1993 and 1997 LULC data for both transition potential approaches (i.e. Logistic Regression and SimWeight). Validation using the 2010 dataset was not done because despite the aggregation of classes, the 2010 dataset was remarkably different from the other two (1993 and 1997). Temporally resolved LULC datasets frequently include different classifications and scales which reduce the validation consistency despite harmonization efforts (Santini and Valentini, 2011). The historical changes between 1993 and 1997 LULC maps were analyzed by ignoring transitions less than 500 hectares, which generated nine major transitions, namely: forest

to agriculture, forest to grass, forest to others, agriculture to forest, agriculture to grass, agriculture to others, grass to forest, grass to agriculture and grass to others (Table S3-3). The major transitions were modeled in separate sub-models by means of LR using a 10% stratified random sampling. Before generating the transition potentials using LR, the importance of each driver to discriminate change was evaluated. A sensitivity analysis on the variables was performed using a Jackknife approach (Capen et al., 1986) where the model was first run with all drivers, and then run twice for each driver (once with the driver alone and once without the driver). For each transition potential the relative operating characteristic (ROC) was calculated. The ROC is a measure for the goodness of fit of a LR model (Pontius Jr and Schneider, 2001). A completely random model gives a ROC value of 0.5 and perfect fit results in a ROC value of 1. The ROC values obtained in the Jackknife analysis were used to identify the importance of each driver to the model. This information was used to select the final set of drivers (Table S3-3) used for the generation of final transition potentials. The goodness of fit of the calibration for the transition models by LR is indicated by ROC values (Table S3-3). High ROC values were found for Grass to others (0.95) and Forest to others (0.94) transitions, while relatively high-to-moderate values (0.82 – 0.74) were found for other transitions.

For the SW transition potential modelling approach, the set of drivers that was found sensitive to each transition by LR was used to ensure consistency in driving factors used for both transition potential modelling approaches. In addition, LR is the more useful approach to understand the effect of the explanatory variables on change and their interactions because during the regression model elaboration, a large number of methods and indices can be used to select the variables with more predictive power based on their relative contribution to the model (Mas et al., 2014). The SW model calculates the relevance weights of each driver, which were used to select the final set of drivers for the generation of final transition potentials. The relevance weight is an indication of that variable's importance in the model, which is determined by comparing the standard deviation of the variable inside areas that have changes, to the standard deviation of the variable for the study region (Sangermano et al., 2010). The only parameters that need to be specified to calculate the relevance weight is the K value and threshold for relevance weight. The K value is the number of nearest instances in variable space to consider. The K value governs the degree of generality of the solution and can be determined automatically by the model depending upon the sample size used for calibration. For this study, K values used were determined automatically by the model and the

default value of 0.01 was used as a threshold for relevance weight. The final set of drivers, their relevance weights and the K value are provided in Table S3-4.

Table S3-3. Final set of drivers used to generate transition potentials using the logistic regression model and summary of the results for the goodness of fit of the calibration for the transition models as indicated by relative operating characteristic (ROC) values

Transition Model	**Driving factors**	**ROC**
Forest to agriculture	Precipitation, Slope, Elevation, Soil depth, Distance to stream, Distance to hydropower dam, Distance to road, Population density	0.76
Forest to grass	Precipitation, Slope, Elevation, Sand content, Distance to hydropower dam, Distance to road, Population density	0.81
Forest to others	Precipitation, Slope, Elevation, Clay content, Soil depth, Distance to stream, Distance to hydropower dam, Distance to road, Population density	0.94
Agriculture to forest	Precipitation, Elevation, Clay content, Sand content, Silt content	0.80
Agriculture to grass	Precipitation, Elevation, Clay content, Sand content, Silt content	0.82
Agriculture to others	Precipitation, Clay content, Sand content, Silt content	0.74
Grass to forest	Precipitation, Slope, Elevation, Clay content, Soil depth, Distance to road, Population density	0.76
Grass to agriculture	Clay content, Sand content, Silt content, Distance to stream, Distance to hydropower dam, Distance to road, Population density	0.75
Grass to others	Precipitation, Slope, Elevation, Soil depth, Distance to stream, Distance to hydropower dam, Distance to road, Population density	0.95

Table S3-4. Final set of drivers used to generate transition potentials using the SimWeight model

Transition Model	Driving factors	Relevance Weight	Number of nearest instances in variable space to consider (K)
Forest to agriculture	Population density	1.00	100
	Distance to road	0.21	
	Distance to hydropower dam	0.07	
	Distance to stream	0.06	
	Soil depth	0.13	
	Elevation	0.18	
	Slope	0.37	
Forest to grass	Population density	1.00	100
	Elevation	0.31	
	Slope	0.36	
	Precipitation	0.07	
Forest to others	Population density	1.00	35
	Distance to road	0.12	
	Distance to hydropower dam	0.62	
	Distance to stream	0.33	
	Soil depth	0.63	
	Clay content	0.24	
	Elevation	0.38	
	Slope	0.49	
	Precipitation	0.68	
Agriculture to forest	Silt content	0.19	100
	Sand content	0.21	
	Clay content	0.21	
	Elevation	0.11	
	Precipitation	0.39	
Agriculture to grass	Silt content	0.64	20
	Elevation	0.90	
	Precipitation	0.71	
Agriculture to others	Silt content	0.70	11
	Precipitation	0.42	
Grass to forest	Population density	1.00	100
	Elevation	0.35	
	Slope	0.32	
Grass to agriculture	Population density	1.00	100
	Distance to road	0.14	
	Distance to stream	0.04	
Grass to others	Population density	1.00	13
	Distance to road	0.71	
	Distance to hydropower dam	0.38	
	Distance to stream	0.20	
	Soil depth	1.00	
	Elevation	0.95	
	Slope	0.96	
	Precipitation	0.69	

SWAT Model calibration, validation and performance evaluation

Table S3-5. Original agricultural LULC class for 2003 of the 3S basin, their management data and corresponding simplified LULC class

Original LULC class	Simplified class	Management Operations			
		Year		Operation	Heating Units
Crop mosaic, cropping area>30	Agriculture	1	1	Plant/begin. growing season	0.15
		1	11	Auto fertilization initialization	0.01
		1	5	Harvest and kill operation	1.20
Agricultural land - intensive	Agriculture	1	1	Plant/begin. growing season	0.15
		1	11	Auto fertilization initialization	0.01
		1	5	Harvest and kill operation	1.20
LMB Field crop	Agriculture	1	5	Harvest and kill operation	0.85
		1	6	Tillage operation	0.17
		1	1	Plant/begin. growing season	0.22
		1	5	Harvest and kill operation	1.20
		1	6	Tillage operation	0.21
		1	1	Plant/begin. growing season	0.32
		1	10	Auto irrigation initialization	0.02
		1	11	Auto fertilization initialization	0.05
		1	11	Auto fertilization initialization	0.05
LMB Paddy field	Agriculture	1	5	Harvest and kill operation	1.10
		1	6	Tillage operation	0.23
		1	1	Plant/begin. growing season	0.26
		1	10	Auto irrigation initialization	0.01
		1	11	Auto fertilization initialization	0.26
		1	5	Harvest and kill operation	1.20
		1	6	Tillage operation	0.20
		1	1	Plant/begin. growing season	0.25
		1	10	Auto irrigation initialization	0.01
		1	11	Auto fertilization initialization	0.02
LMB Perennial land	Agriculture	1	1	Plant/begin. growing season	0.15
		1	11	Auto fertilization initialization	0.01
		1	5	Harvest and kill operation	1.20

Details of the parameters calibrated and their fitted ranges used in the study are provided in Table S3-6.

Table S3-6. Calibrated parameters and their fitted range for the 3S SWAT model.

Parameter name	Description and units	Fitted range	
		Min	Max
Flow variables			
v__GW_DELAY.gw[a]	Groundwater delay time (days)	0.25	87.01
v__ALPHA_BF.gw	Baseflow alpha factor (1/days)	0.04	0.97
v__GWQMN.gw[b]	Threshold depth of water in the shallow aquifer required to return flow to occur (mm)	0.00	804.17
v__GW_REVAP.gw	Groundwater "revap" coefficient (-)	0.02	0.2
v__REVAPMN.gw	Threshold depth of water in the shallow aquifer for "revap" or percolation to the deep aquifer to occur (mm)	1.00	1107.33
v__RCHRG_DP.gw	Deep aquifer percolation fraction (-)	0.05	0.46
v__LAT_TTIME.hru	Lateral flow travel time (days)	0.00	157.25
v__SLSOIL.hru[b]	Slope length for lateral subsurface flow (m)	0.00	91.7
v__CANMX.hru	Maximum canopy storage (mm)	0.00	17.2
v__ESCO.hru	Soil evaporation compensation factor (-)	0.07	0.95
v__CH_N2.rte	Mannings "n" value for the main channel	0.01	0.13
v__CH_K2.rte	Effective hydraulic conductivity in main channel alluvium (mm/hr)	0.00	19.57
v__ALPHA_BNK.rte	Baseflow alpha factor for bank storage (days)	0.00	0.86
v__CH_N1.sub	Manning's "n" value for the tributary channels	0.01	0.14
v__CH_K1.sub	Effective hydraulic conductivity in tributary channel alluvium (mm/hr)	0.00	23.47
r__SOL_AWC(1).sol	Available water capacity in the soil layer (mm/mm soil)	-0.11	0.21
r__CN2.mgt[c]	Initial SCS runoff curve number for moisture condition II (-)	-0.08	0.13
Sediment variables			
v_SPCON.bsn	Linear parameter for calculating the maximum amount of sediment that can be re-entrained during channel sediment routing (-)	0.0089*	
v_SPEXP.bsn	Exponent parameter for calculating sediment re-entrained in channel sediment routing (-)	1.1554*	
v_PRF_BSN.bsn	Peak rate adjustment factor for sediment routing in the main channel (-)	0.6354*	
v_USLE_C (Forest).dat	Minimum value for the cover and management factor for the land cover (-)	0.0014	0.0162
v_USLE_C (Agriculture).dat		0.0126	0.3934
v_USLE_C (Grass land).dat		0.1114*	
v_USLE_C (Barren land).dat		0.5689*	
v_CH_COV1.rte	Channel erodibility factor (-)	0.0678	0.7610
v_CH_COV2.rte	Channel cover factor (-)	0.0150	0.1847
v_CH_ERODMO.rte	Channel erodability factor (-)	0.0268	0.4790
v_USLE_K .sol	USLE equation soil erodibility (K) factor (0.013 metric ton m^2 hr / (m^3-metric ton cm))	0.0110	0.6311

Note: [a] The extension (e.g., .gw) refers to the SWAT input file where the parameter occurs; [b] The qualifier (v) refers to the substitution of a parameter by a value from the given range; [c] The qualifier (r) refers to relative change in the parameter where the value from the SWAT database is multiplied by 1 plus a factor in the given range. * Only one value for the whole basin.

B. Supplementary Results and Discussion

Uncertainty in LULC projection

Details on the spatial variability of changes in LULC for the study basin are presented below:

Table S3-7. Percent cover of each LULC class for various LULC change scenarios for 2060.

Scenario	Class Name	Sekong		Sesan		Srepok		3S	
		LR	SW	LR	SW	LR	SW	LR	SW
A1	Forest	69.2	75.6	73.3	68.0	74.7	68.9	72.3	71.1
	Agriculture	29.8	23.2	24.3	29.7	20.5	27.6	24.8	26.5
	Grass	0.4	0.8	1.1	0.6	3.5	1.9	1.8	1.2
	Urban	0.0	0.0	0.1	0.1	0.0	0.0	0.1	0.1
	Others	0.6	0.4	1.2	1.6	1.3	1.6	1.0	1.1
A2	Forest	76.5	79.4	67.4	65.5	73.6	69.0	73.1	72.0
	Agriculture	22.6	19.3	30.1	32.1	21.9	27.5	24.1	25.5
	Grass	0.4	0.9	1.1	0.6	3.3	1.9	1.7	1.2
	Urban	0.0	0.0	0.1	0.1	0.0	0.0	0.1	0.1
	Others	0.5	0.4	1.3	1.7	1.2	1.6	1.0	1.2
B1	Forest	42.0	39.1	38.0	40.9	29.4	34.2	36.1	37.5
	Agriculture	53.0	53.7	50.6	40.5	48.1	53.6	50.5	50.5
	Grass	3.7	6.5	3.2	9.8	17.1	6.0	8.8	7.1
	Urban	0.0	0.0	0.1	0.1	0.0	0.0	0.1	0.1
	Others	1.3	0.7	8.1	8.7	5.4	6.2	4.5	4.8
B2	Forest	62.0	60.9	42.5	46.4	49.0	50.2	52.2	53.1
	Agriculture	32.4	32.8	44.6	32.5	33.2	37.0	35.6	34.4
	Grass	4.2	5.5	4.6	12.1	13.7	7.3	8.0	7.8
	Urban	0.0	0.0	0.1	0.1	0.0	0.0	0.1	0.1
	Others	1.4	0.8	8.2	8.9	4.1	5.5	4.1	4.6
C1	Forest	35.6	32.8	28.7	33.2	21.8	22.4	28.5	28.8
	Agriculture	57.8	57.6	55.1	44.1	53.1	61.9	55.2	56.0
	Grass	5.2	8.9	4.8	12.9	20.6	9.0	11.2	9.9
	Urban	0.0	0.0	0.1	0.1	0.0	0.0	0.1	0.1
	Others	1.4	0.7	11.3	9.7	4.5	6.7	5.0	5.2
C2	Forest	60.8	60.4	42.7	45.7	48.9	48.9	51.8	52.3
	Agriculture	34.1	33.3	46.1	35.1	33.9	39.1	36.8	36.0
	Grass	4.1	5.8	5.0	12.6	14.0	7.8	8.2	8.2
	Urban	0.0	0.0	0.1	0.1	0.0	0.0	0.1	0.1
	Others	1.0	0.5	6.1	6.5	3.2	4.2	3.1	3.4

References

Abbaspour, K. C., Johnson, C. A., and van Genuchten, M. T.: Estimating uncertain flow and transport parameters using a sequential uncertainty fitting procedure, Vadose Zone Journal, 3, 1340-1352, 2004.

Abbaspour, K. C., Yang, J., Maximov, I., Siber, R., Bogner, K., Mieleitner, J., Zobrist, J., and Srinivasan, R.: Modelling hydrology and water quality in the pre-alpine/alpine Thur watershed using SWAT, Journal of Hydrology, 333, 413-430, http://dx.doi.org/10.1016/j.jhydrol.2006.09.014, 2007.

Abbaspour, K. C.: SWAT-CUP2: SWAT calibration and uncertainty programs - A user manual. , Department of Systems Analysis, Integrated Assessment and Modelling (SIAM), Eawag, Swiss Federal Institute of Aquatic Science and Technology, Duebendorf, Switzerland, 95, 2008.

Adamson, P. T., Rutherfurd, I. D., Peel, M. C., and Conlan, I. A.: The hydrology of the Mekong River. The Mekong, Academic Press, San Diego, 53-76 pp., 2009.

Addor, N., Rössler, O., Köplin, N., Huss, M., Weingartner, R., and Seibert, J.: Robust changes and sources of uncertainty in the projected hydrological regimes of Swiss catchments, Water Resources Research, 50, 7541-7562, 10.1002/2014WR015549, 2014.

Agarwal, C., Green, G. M., Grove, J. M., Evans, T. P., and Schweik, C. M.: A Review and Assessment of Land-Use Change Models. Dynamics of Space, Time, and Human Choice. CIPEC Collaborative Report Series 1, Bloomington and South Burlington, Center for the Study of Institutions, Population, and Environmental Change, Indiana University and USDA Forest Service, 2001.

Annandale, G. W.: Quenching the thirst: Sustainable water supply and climate change, CreateSpace North Charleston, SC, 2013.

Annandale, G. W.: Reservoir sedimentation Sustainable water supply, climate change and reservoir sedimentation management: Technical and economic viability, in: Reservoir Sedimentation, edited by: Schleiss, A. J., Cesare, G., Franca, M. J., and Pfister, M., CRC Press, London, UK, 2014.

Annandale, G. W., Morris, G. L., and Karki, P.: Extending the life of reservoirs : sustainable sediment management for dams and run-of-river hydropower, World Bank Group. , Washington, D.C. , 2016.

Araújo, M. B., and New, M.: Ensemble forecasting of species distributions, Trends in Ecology and Evolution, 22, 42-47, 2007.

Arias, M. E., Cochrane, T. A., Lawrence, K. S., Killeen, T. J., and Farrell, T. A.: Paying the forest for electricity: a modelling framework to market forest conservation as payment for ecosystem services benefiting hydropower generation, Environmental Conservation, 38, 473-484, 10.1017/S0376892911000464, 2011.

Arias, M. E., Cochrane, T. A., Kummu, M., Lauri, H., Holtgrieve, G. W., Koponen, J., and Piman, T.: Impacts of hydropower and climate change on drivers of ecological productivity of Southeast Asia's most important wetland, Ecol. Model., 272, 252-263, https://doi.org/10.1016/j.ecolmodel.2013.10.015, 2014a.

Arias, M. E., Piman, T., Lauri, H., Cochrane, T. A., and Kummu, M.: Dams on Mekong tributaries as significant contributors of hydrological alterations to the Tonle Sap Floodplain in Cambodia, Hydrology and Earth System Sciences, 18, 5303-5315, 10.5194/hess-18-5303-2014, 2014b.

Arias, M. E., Lee, E., Farinosi, F., Pereira, F. F., and Moorcroft, P. R.: Decoupling the effects of deforestation and climate variability in the Tapajós river basin in the Brazilian Amazon, Hydrological Processes, 32, 1648-1663, 10.1002/hyp.11517, 2018.

Arnold, J. G., Allen, P. M., and Bernhardt, G.: A comprehensive surface-groundwater flow model, Journal of Hydrology, 142, 47-69, https://doi.org/10.1016/0022-1694(93)90004-S, 1993a.

Arnold, J. G., Allen, P. M., and Bernhardt, G.: A Comprehensive Surface-groundwater Flow Model, Journal of Hydrology, 142, 47-69, 10.1016/0022-1694(93)90004-s, 1993b.

Arnold, J. G., Williams, J. R., and Maidment, D. R.: Continuous-time Water and Sediment Routing Model for Large Basins, Journal of Hydraulic Engineering-Asce, 121, 171-183, 10.1061/(asce)0733-9429(1995)121:2(171), 1995.

Arnold, J. G., Srinivasan, R., Muttiah, R. S., and Williams, J. R.: Large area hydrologic modeling and assessment. Part I: Model development, Journal of American Water Resources Association, 34, 73-89, 1998.

Arnold, J. G., Moriasi, D. N., Gassman, P. W., Abbaspour, K. C., White, M. J., Srinivasan, R., Santhi, C., Harmel, R. D., van Griensven, A., Van Liew, M. W., Kannan, N., and Jha, M. K.: SWAT: Model Use, Calibration, and Validation, Transactions of the Asabe, 55, 1491-1508, 2012.

Asmal, K.: Dams and development: a new framework for decision-making. The report of the World Commission on dams, Earthscan Publications Ltd, London, xxxvii + 404 pp. pp., 2000.

Atkinson, E.: The feasibility of flushing sediments from Reservoirs, TDR Project R5839, Rep.0D 137, HR Wallingford, UK, 1996.

Bagnold, R. A.: Bedload transport in natural rivers, Water Resources Research 13, 303-312, 1977.

Batuca, D. G., and Jordann, J. M.: Silting and Desilting of Reservoirs, A.A. Balkema, Rotterdam, The Netherlands, 2000.

Benaman, J., Shoemaker, C. A., and Haith, D. A.: Calibration and validation of soil and water assessment tool on an agricultural watershed in upstate New York, Journal of Hydrologic Engineering, 10, 363-374, 10.1061/(asce)1084-0699(2005)10:5(363), 2005.

Bennett, K. E., Werner, A. T., and Schnorbus, M.: Uncertainties in Hydrologic and Climate Change Impact Analyses in Headwater Basins of British Columbia, Journal of Climate, 25, 5711-5730, 10.1175/jcli-d-11-00417.1, 2012.

Berc, J., Lawford, R., Bruce, J., Mearns, L., and Easterling, D.: Conservation Implications of Climate Change: Soil Erosion and Runoff from Croplands: A Report from the Soil and Water Conservation Society, Ankeny (IA): Soil and Water Conservation Society, 2003.

Beven, K.: Rainfall-Runoff Modelling: The Primer, John Wiley & Sons, Chichester, 2001.

Bieger, K., Hörmann, G., and Fohrer, N.: Simulation of streamflow and sediment with the soil and water assessment tool in a data scarce catchment in the three gorges region, China, J. Environ. Qual., 43, 37-45, 2014.

Bieger, K., Arnold, J. G., and Srinivasan, R.: Introduction to SWAT+ Soil and Water Assessment Tool SWAT+ WorkShop University of Canterbury, Christchurch, New Zealand 2019.

Bogaart, P. W., Van Balen, R. T., Kasse, C., and Vandenberghe, J.: Process-based modelling of fluvial system response to rapid climate change - I: model formulation and generic applications, Quaternary Science Reviews, 22, 2077-2095, 10.1016/s0277-3791(03)00143-4, 2003.

Bormann, H., Breuer, L., Graeff, T., Huisman, J. A., and Croke, B.: Assessing the impact of land use change on hydrology by ensemble modelling (LUCHEM) IV: Model sensitivity to data aggregation and spatial (re-)distribution, Advances in Water Resources, 32, 171-192, 10.1016/j.advwatres.2008.01.002, 2009.

Bosch, N. S., Allan, J. D., Selegean, J. P., and Scavia, D.: Scenario-testing of agricultural best management practices in Lake Erie watersheds, Journal of Great Lakes Research, 39, 429-436, 10.1016/j.jglr.2013.06.004, 2013.

Bosshard, T., Carambia, M., Goergen, K., Kotlarski, S., Krahe, P., Zappa, M., and Schär, C.: Quantifying uncertainty sources in an ensemble of hydrological climate-impact projections, Water Resources Research, 49, 1523-1536, doi:10.1029/2011WR011533, 2013.

Brandt, S. A., and Swenning, J.: Sedimentological and geomorphological effects of reservoir flushing: the cachí reservoir, costa rica, 1996, Geografiska Annaler: Series A, Physical Geography, 81, 391-407, 10.1111/j.0435-3676.1999.00069.x, 1999.

Brandt, S. A.: Classification of geomorphological effects downstream of dams, Catena, 40, 375-401, 10.1016/S0341-8162(00)00093-X, 2000.

Braud, I., Vich, A. I. J., Zuluaga, J., Fornero, L., and Pedrani, A.: Vegetation influence on runoff and sediment yield in the Andes region: observation and modelling, Journal of Hydrology, 254, 124-144, 10.1016/s0022-1694(01)00500-5, 2001.

Breuer, L., Huisman, J. A., Willems, P., Bormann, H., Bronstert, A., Croke, B. F. W., Frede, H. G., Graeff, T., Hubrechts, L., Jakeman, A. J., Kite, G., Lanini, J., Leavesley, G., Lettenmaier, D. P., Lindstroem, G., Seibert, J., Sivapalan, M., and Viney, N. R.: Assessing the impact of land use change on hydrology by ensemble modeling (LUCHEM). I: Model intercomparison with current land use, Advances in Water Resources, 32, 129-146, 10.1016/j.advwatres.2008.10.003, 2009.

Briassoulis, H.: Analysis of land use change: Theoretical and modeling approaches. In:Loveridge S. (ed.), The Web Book of Regional Science, West Virginia University Morgantown, 2000.

Brown, C., Ghile, Y., Laverty, M., and Li, K.: Decision scaling: Linking bottom-up vulnerability analysis with climate projections in the water sector, Water Resources Research, 48, 10.1029/2011wr011212, 2012.

Bruijnzeel, L. A.: Hydrology of moist tropical forests and effects of conversion: a state of knowledge review, Free University, Amsterdam, 1990.

Brune, G. M.: Trap Efficiency of Reservoirs, Transactions of the American Geophysical Union 34, 407-418, 1953.

Burnham, B. O.: Markov intertemporal land use simulation model, Southern Journal of Agricultural Economics, 5, 253-258, 1973.

Bussi, G., Dadson, S. J., Prudhomme, C., and Whitehead, P. G.: Modelling the future impacts of climate and land-use change on suspended sediment transport in the River Thames (UK), Journal of Hydrology, 542, 357-372, https://doi.org/10.1016/j.jhydrol.2016.09.010, 2016.

Calder, I. R.: Hydrologic effects of land-use change, in: Handbook of hydrology, edited by: Maidment, D. R., McGraw-Hill, New York, 13.11-13.50, 1993.

Cambien, N., Gobeyn, S., Nolivos, I., Eurie Forio, M. A., Arias-Hidalgo, M., Dominguez-Granda, L., Witing, F., Volk, M., and Goethals, P. L. M.: Using the soil and water assessment tool to simulate the pesticide dynamics in the data scarce guayas River Basin, Ecuador, Water (Switzerland), 12, 1-21, 10.3390/w12030696, 2020.

Capen, D. E., Fenwick, J. W., Inkley, D. B., and Boynton, A. C.: On the measurement of multivariate models of songbird habitat in New England forests., in: Wildlife 2000: modelling habitat relationships of terrestrial vertebrates., edited by: Verner, J. A., Morrison, M. L., and Ralph, C. J., University of Wisconsin Press, Madison, 171–175, 1986.

Chawla, I., and Mujumdar, P. P.: Partitioning uncertainty in streamflow projections under nonstationary model conditions, Advances in Water Resources, 112, 266-282, https://doi.org/10.1016/j.advwatres.2017.10.013, 2018.

Chen, J., Brissette, F. P., and Leconte, R.: Uncertainty of downscaling method in quantifying the impact of climate change on hydrology, Journal of hydrology, 401, 190-202, 2011a.

Chen, J., Brissette, F. P., Poulin, A., and Leconte, R.: Overall uncertainty study of the hydrological impacts of climate change for a Canadian watershed, Water Resources Research, 47, 10.1029/2011wr010602, 2011b.

Chen, L., Chang, J., Wang, Y., Peng, S., Li, Y., Long, R., and Wang, Y.: The regional asymmetric effect of increased daily extreme temperature on the streamflow from a multiscale perspective: A case study of the Yellow River Basin, China, Atmospheric Research, 228, 137-151, 10.1016/j.atmosres.2019.06.003, 2019.

Chen, X., Yang, T., Wang, X., Xu, C. Y., and Yu, Z.: Uncertainty Intercomparison of Different Hydrological Models in Simulating Extreme Flows, Water Resour Manage, 27, 1393-1409, 2013.

Clark, M. P., Kavetski, D., and Fenicia, F.: Pursuing the method of multiple working hypotheses for hydrological modeling, Water Resources Research, 47, 2011.

Cochrane, T. A., Arias, M. E., and Piman, T.: Historical impact of water infrastructure on water levels of the Mekong River and the Tonle Sap system, Hydrology and Earth System Sciences, 18, 4529-4541, 10.5194/hess-18-4529-2014, 2014.

Dahl, T. A., Kendall, A. D., and Hyndman, D. W.: Impacts of projected climate change on sediment yield and dredging costs, Hydrological Processes, 32, 1223-1234, 10.1002/hyp.11486, 2018.

Dai, S., Yang, S., and Li, M.: The sharp decrease in suspended sediment supply from China's rivers to the sea: anthropogenic and natural causes, Hydrological Sciences Journal, 54, 135-146, 2009.

Dalla-Nora, E. L., de Aguiar, A. P. D., Lapola, D. M., and Woltjer, G.: Why have land use change models for the Amazon failed to capture the amount of deforestation over the last decade?, Land Use Policy, 39, 403-411, 10.1016/j.landusepol.2014.02.004, 2014

DeFries, R., and Eshleman, K. N.: Land-use change and hydrologic processes: a major focus for the future, Hydrological Processes, 18, 2183-2186, doi:10.1002/hyp.5584, 2004.

Di Baldassarre, G., Elshamy, M., van Griensven, A., Soliman, E., Kigobe, M., Ndomba, P., Mutemi, J., Mutua, F., Moges, S., Xuan, Y., Solomatine, D., and Uhlenbrook, S.: Future hydrology and climate in the River Nile basin: a review, Hydrological Sciences Journal-Journal Des Sciences Hydrologiques, 56, 199-211, 10.1080/02626667.2011.557378, 2011.

Dierauer, J. R., Whitfield, P. H., and Allen, D. M.: Climate Controls on Runoff and Low Flows in Mountain Catchments of Western North America, Water Resources Research, 54, 7495-7510, 10.1029/2018WR023087, 2018.

Du, J., Rui, H., Zuo, T., Li, Q., Zheng, D., Chen, A., Xu, Y., and Xu, C.-Y.: Hydrological Simulation by SWAT Model with Fixed and Varied Parameterization Approaches Under Land Use Change, Water Resour Manage, 27, 2823-2838, 10.1007/s11269-013-0317-0, 2013.

Eastman, J. R., Jin, W., Kyem, P., and Toledano, J.: Raster procedures for multi-criteria/multi-objective decisions, Photogrammetric Engineering and Remote Sensing, 61, 539-547, 1995.

Eastman, J. R., Solorzano, L. A., and Van Fossen, M.: Transition potential modeling for land-cover change, in: GIS, spatial analysis and modeling, edited by: Maguire D.J., Batty M., and F., G. M., ESRI Press, Redlands, 357-385, 2005.

Eastman, J. R.: IDRISI Taiga guide to GIS and image processing Clark University, Clark Labs, IDRISI Productions, Worcester, 2009.

Eckhardt, K., Breuer, L., and Frede, H.-G.: Parameter uncertainty and the significance of simulated land use change effects, Journal of Hydrology, 273, 164-176, https://doi.org/10.1016/S0022-1694(02)00395-5, 2003.

Efthymiou, N. P., Palt, S., Annandale, G. W., and Karki, P.: Reservoir Conservation Model: RESCON 2 Beta, Economic and Engineering Evaluation of Alternative Sediment Management Strategies. , World Bank, Washington DC, 2017.

Ellison, D., Morris, C. E., Locatelli, B., Sheil, D., Cohen, J., Murdiyarso, D., Gutierrez, V., Noordwijk, M. v., Creed, I. F., Pokorny, J., Gaveau, D., Spracklen, D. V., Tobella, A. B., Ilstedt, U., Teuling, A. J., Gebrehiwot, S. G., Sands, D. C., Muys, B., Verbist, B., Springgay, E., Sugandi, Y., and Sullivan, C. A.: Trees, forests and water: Cool insights for a hot world, Global Environmental Change, 43, 51-61, https://doi.org/10.1016/j.gloenvcha.2017.01.002, 2017.

Elshamy, M., Di Baldassarre, G., and van Griensven, A.: Characterizing Climate Model Uncertainty Using an Informal Bayesian Framework: Application to the River Nile, Journal of Hydrologic Engineering, 18, 582-589, 10.1061/(asce)he.1943-5584.0000656, 2013.

Espa, P., Brignoli, M. L., Crosa, G., Gentili, G., and Quadroni, S.: Controlled sediment flushing at the Cancano Reservoir (Italian Alps): Management of the operation and downstream environmental impact, Journal of Environmental Management, 182, 1-12, https://doi.org/10.1016/j.jenvman.2016.07.021, 2016.

FAO, and IFAD: An assessment of the impact of cassava production and processing on the environment and biodiversity., Proceedings of the validation forum on the global cassava development strategy, Rome, 2000.

AQUASTAT website. , access: 8/21/2019, 2016.

Feddema, J. J., Oleson, K. W., Bonan, G. B., Mearns, L. O., Buja, L. E., Meehl, G. A., and Washington, W. M.: The importance of land-cover change in simulating future climates, Science, 310, 1674-1678, 2005.

Fiener, P., Auerswald, K., and Van Oost, K.: Spatio-temporal patterns in land use and management affecting surface runoff response of agricultural catchments-A review, Earth-Science Reviews, 106, 92-104, 10.1016/j.earscirev.2011.01.004, 2011.

Fuller, D. O., Hardiono, M., and Meijaard, E.: Deforestation Projections for Carbon-Rich Peat Swamp Forests of Central Kalimantan, Indonesia, Environmental Management, 48, 436-447, 10.1007/s00267-011-9643-2, 2011.

Gädeke, A., Hölzel, H., Koch, H., Pohle, I., and Grünewald, U.: Analysis of uncertainties in the hydrological response of a model-based climate change impact assessment in a subcatchment of the Spree River, Germany, Hydrological Processes, 28, 3978-3998, 10.1002/hyp.9933, 2014.

Gan, T. Y., Dlamini, E. M., and Biftu, G. F.: Effects of model complexity and structure, data quality, and objective functions on hydrologic modeling, Journal of Hydrology, 192, 81-103, 10.1016/S0022-1694(96)03114-9, 1997.

Gao, J., Sheshukov, A. Y., Yen, H., Douglas-Mankin, K. R., White, M. J., and Arnold, J. G.: Uncertainty of hydrologic processes caused by bias-corrected CMIP5 climate change projections with alternative historical data sources, Journal of Hydrology, 568, 551-561, https://doi.org/10.1016/j.jhydrol.2018.10.041, 2019.

Gassman, P. W., Sadeghi, A. M., and Srinivasan, R.: Applications of the SWAT Model Special Section: Overview and Insights, J. Environ. Qual., 43, 1-8, 10.2134/jeq2013.11.0466, 2014.

Girvetz, E. H., Zganjar, C., Raber, G. T., Maurer, E. P., Kareiva, P., and Lawler, J. J.: Applied Climate-Change Analysis: The Climate Wizard Tool, Plos One, 4, 10.1371/journal.pone.0008320, 2009.

Glavan, M., and Pintar, M.: Strengths, Weaknesses, Opportunities and Threats of Catchment Modelling with Soil and Water Assessment Tool (SWAT) Model,, in: Water Resources Management and Modeling, IntechOpen, Purna Nayak, 2012.

GoLPDR: Selected agriculture concepts, approaches, commodities for development of climate change training and adaptation modules for LAO PDR: 3. On-farm and community level water management, Government of Lao People’s Democratic Republic (GoLPDR), 2012.

Gong, Y. W., Shen, Z. Y., Liu, R. M., Hong, Q., and Wu, X.: A comparison of single- and multi-gauge based calibrations for hydrological modeling of the Upper Daning River Watershed in China's Three Gorges Reservoir Region, Hydrology Research, 43, 822-832, 10.2166/nh.2012.021, 2012.

Grant, G. E., Schmidt, J. C., and Lewis, S. L.: A Geological Framework for Interpreting Downstream Effects of Dams on Rivers, in: A Peculiar River, edited by: O'Connor, J. E., and Grant, G. E., 203-219, 2003.

Gray, J. R., Glysson, G. D., Turcios, L. M., and Schwarz, G. E.: Comparability of suspended-sediment concentration and total suspended solids data., US Department of the Interior, US Geological Survey. , 2000.

Green, W. H., and Ampt, G. A.: Studies on soil physics Part I - The flow of air and water through soils, Journal of Agricultural Science, 4, 1-24, 1911.

Grill, G., Lehner, B., Thieme, M., Geenen, B., Tickner, D., Antonelli, F., Babu, S., Borrelli, P., Cheng, L., Crochetiere, H., Ehalt Macedo, H., Filgueiras, R., Goichot, M., Higgins, J., Hogan, Z., Lip, B., McClain, M. E., Meng, J., Mulligan, M., Nilsson, C., Olden, J. D., Opperman, J. J., Petry, P., Reidy Liermann, C., Sáenz, L., Salinas-Rodríguez, S., Schelle, P., Schmitt, R. J. P., Snider, J., Tan, F., Tockner, K., Valdujo, P. H., van Soesbergen, A., and Zarfl, C.: Mapping the world's free-flowing rivers, Nature, 569, 215-221, 10.1038/s41586-019-1111-9, 2019.

Grimardias, D., Guillard, J., and Cattanéo, F.: Drawdown flushing of a hydroelectric reservoir on the Rhône River: Impacts on the fish community and implications for the sediment management, Journal of Environmental Management, 197, 239-249, https://doi.org/10.1016/j.jenvman.2017.03.096, 2017.

Grumbine, R. E., Dore, J., and Xu, J. C.: Mekong hydropower: drivers of change and governance challenges, Frontiers in Ecology and the Environment, 10, 91-98, 10.1890/110146, 2012.

Gupta, H. V., Kling, H., Yilmaz, K. K., and Martinez, G. F.: Decomposition of the mean squared error and NSE performance criteria: Implications for improving hydrological modelling, Journal of Hydrology, 377, 80-91, 10.1016/j.jhydrol.2009.08.003, 2009.

Guy, H. P., and Norman, V. W.: Field methods for measurement of fluvial sediment, US Govt. Print. Off., 1970.

Hann, C. T., Barfield, B. J., and Hayes, J. C.: Design hydrology and sedimentology for small catchments, Academic Press, San Diego, USA, 1994.

Hanratty, M. P., and Stefan, H. G.: Simulating climate change effects in a Minnesota agricultural watershed, J. Environ. Qual., 27, 1524-1532, 1998.

Hardy, R. L.: Multiquadric equations of topology and other irregular surface, Journal of Geophysical Research, 76, 1905 - 1915, 1971.

Hargreaves, G. L., Hargreaves, G. H., and Riley, J. P.: Agricultural Benefits for Senegal River Basin, Journal of Irrigation and Drainage Engineering-Asce, 111, 113-124, 1985.

Harrison, C.: What factors control mechanical erosion rates?, International Journal of Earth Sciences, 88, 752-763, 2000.

Hawkins, E., and Sutton, R.: The potential to narrow uncertainty in projections of regional precipitation change, Clim. Dyn., 37, 407-418, 10.1007/s00382-010-0810-6, 2011.

Huang, Y., Lin, W., Li, S., and Ning, Y.: Social impacts of dam-induced displacement and resettlement: A comparative case study in China, Sustainability (Switzerland), 10, 10.3390/su10114018, 2018.

Huisman, J. A., Breuer, L., Bormann, H., Bronstert, A., Croke, B. F. W., Frede, H. G., Graeff, T., Hubrechts, L., Jakeman, A. J., Kite, G., Lanini, J., Leavesley, G., Lettenmaier, D. P., Lindstroem, G.,

Seibert, J., Sivapalan, M., Viney, N. R., and Willems, P.: Assessing the impact of land use change on hydrology by ensemble modeling (LUCHEM) III: Scenario analysis, Advances in Water Resources, 32, 159-170, 10.1016/j.advwatres.2008.06.009, 2009.

ICEM: USAID Mekong ARCC Climate Change Impact and Adaptation Study for the Lower Mekong Basin: Main Report, ICEM – International Centre for Environmental Management, Bangkok, 2013.

World Register of Dams. General Synthesis https://www.icold-cigb.org/GB/world_register/general_synthesis.asp, access: 8/21/2019, 2018.

IEA: Renewables 2018. Analysis and Forecasts to 2023, International Energy Agency 2018.

Intralawan, A., Wood, D., Frankel, R., Costanza, R., and Kubiszewski, I.: Tradeoff analysis between electricity generation and ecosystem services in the Lower Mekong Basin, Ecosystem Services, 30, 27-35, https://doi.org/10.1016/j.ecoser.2018.01.007, 2018.

IPCC: Climate Change 2013: The Physical Science Basis. Contribution of Working Group I to the Fifth Assessment Report of the Intergovernmental Panel on Climate Change, Cambridge University Press, Cambridge, United Kingdom and New York, NY, USA,, 2013.

Jackson, W. L., Gebhardt, K., and Van Haveren, B. P.: Use of the modified universal soil loss equation for average annual sediment yield estimates on small rangeland drainage basins, Drainage basin sediment delivery. Proc. symposium, Albuquerque, 1986, 413-422, 1986.

Jiang, T., Chen, Y. D., Xu, C. y., Chen, X., Chen, X., and Singh, V. P.: Comparison of hydrological impacts of climate change simulated by six hydrological models in the Dongjiang Basin, South China, Journal of Hydrology, 336, 316-333, 10.1016/j.jhydrol.2007.01.010, 2007.

Johnson, C. W., Gordon, N. D., and Hanson, C. L.: North-west rangeland sediment yield analysis by the MUSLE, Transactions of the American Society of Agricultural and Biological Engineers, 26, 1889-1895, 1986.

Johnston, R., and Smakhtin, V.: Hydrological Modeling of Large river Basins: How Much is Enough?, Water Resour Manage, 28, 2695-2730, 10.1007/s11269-014-0637-8, 2014.

Joseph, J., Ghosh, S., Pathak, A., and Sahai, A. K.: Hydrologic impacts of climate change: Comparisons between hydrological parameter uncertainty and climate model uncertainty, Journal of Hydrology, 566, 1-22, https://doi.org/10.1016/j.jhydrol.2018.08.080, 2018.

Jung, I. W., Chang, H., and Moradkhani, H.: Quantifying uncertainty in urban flooding analysis considering hydro-climatic projection and urban development effects, Hydrol. Earth Syst. Sci., 15, 617-633, 10.5194/hess-15-617-2011, 2011.

Juston, J. M., Kauffeldt, A., Montano, B. Q., Seibert, J., Beven, K. J., and Westerberg, I. K.: Smiling in the rain: Seven reasons to be positive about uncertainty in hydrological modelling, Hydrological Processes, 27, 1117-1122, 10.1002/hyp.9625, 2013.

Karlsson, I. B., Sonnenborg, T. O., Refsgaard, J. C., Trolle, D., Børgesen, C. D., Olesen, J. E., Jeppesen, E., and Jensen, K. H.: Combined effects of climate models, hydrological model structures and land use scenarios on hydrological impacts of climate change, Journal of Hydrology, 535, 301-317, 10.1016/j.jhydrol.2016.01.069, 2016.

Kaura, M., Arias, M. E., Benjamin, J. A., Oeurng, C., and Cochrane, T. A.: Benefits of forest conservation on riverine sediment and hydropower in the Tonle Sap Basin, Cambodia, Ecosystem Services, 39, 101003, https://doi.org/10.1016/j.ecoser.2019.101003, 2019.

Kay, A. L., Davies, H. N., Bell, V. A., and Jones, R. G.: Comparison of uncertainty sources for climate change impacts: Flood frequency in England, Climatic Change, 92, 41-63, 2009.

Kenny, G. J., Warrick, R. A., Mitchell, N. D., Mullan, A. B., and Salinger, M. J.: CLIMPACTS: an integrated model for assessment of the effects of climate change on the New Zealand environment, Journal of Biogeography, 22, 883-895, 1995.

Khan, M. S., Coulibaly, P., and Dibike, Y.: Uncertainty analysis of statistical downscaling methods, Journal of Hydrology, 319, 357-382, 2006.

Khresat, S., Al-Bakri, J., and Al-Tahnan, R.: Impacts of land use/cover change on soil properties in the Mediterranean region of northwestern Jordan, Land Degradation and Development, 19, 397-407, 10.1002/ldr.847, 2008.

Kingston, D. G., Thompson, J. R., and Kite, G.: Uncertainty in climate change projections of discharge for the Mekong River Basin, Hydrology and Earth System Sciences, 15, 1459-1471, 10.5194/hess-15-1459-2011, 2011.

Koehnken, L.: IKMP Discharge and Sediment Monitoring Program Review, Recommendations and Data Analysis (No. Part 2: Data analysis of preliminary results). , Information and Knowledge Management Programme, Mekong River Comission, Vientaine, Lao PDR, 2012.

Koehnken, L.: Discharge sediment monitoring project (DSMP) 2009-2013 summary and analysis of results, Mekong River Commission/Gesellschaft für Internationale Zusammenarbeit, Phnom Penh, Cambodia, 2014.

Kondolf, G. M.: Hungry water: Effects of dams and gravel mining on river channels, Environmental Management, 21, 533-551, 10.1007/s002679900048, 1997.

Kondolf, G. M., Gao, Y., Annandale, G. W., Morris, G. L., Jiang, E., Zhang, J., Cao, Y., Carling, P., Fu, K., Guo, Q., Hotchkiss, R., Peteuil, C., Sumi, T., Wang, H.-W., Wang, Z., Wei, Z., Wu, B., Wu, C., and Yang, C. T.: Sustainable sediment management in reservoirs and regulated rivers: Experiences from five continents, Earth's Future, n/a-n/a, 10.1002/2013EF000184, 2014a.

Kondolf, G. M., Rubin, Z. K., and Minear, J. T.: Dams on the Mekong: Cumulative sediment starvation, Water Resources Research, 50, 5158-5169, 10.1002/2013WR014651, 2014b.

Koomen, E., Rietveld, P., and de Nijs, T.: Modelling land-use change for spatial planning support, Annals of Regional Science, 42, 1-10, 10.1007/s00168-007-0155-1, 2008.

Krause, P., Boyle, D. P., and Bäse, F.: Comparison of different efficiency criteria for hydrological model assessment, Advances in Geosciences, 5, 89-97, 2005.

Kummu, M., Lu, X. X., Wang, J. J., and Varis, O.: Basin-wide sediment trapping efficiency of emerging reservoirs along the Mekong, Geomorphology, 119, 181-197, 10.1016/j.geomorph.2010.03.018, 2010.

Kundzewicz, Z. W., Krysanova, V., Benestad, R. E., Hov, Ø., Piniewski, M., and Otto, I. M.: Uncertainty in climate change impacts on water resources, Environmental Science & Policy, 79, 1-8, https://doi.org/10.1016/j.envsci.2017.10.008, 2018.

Lacombe, G., Ribolzi, O., de Rouw, A., Pierret, A., Latsachak, K., Silvera, N., Pham Dinh, R., Orange, D., Janeau, J. L., Soulileuth, B., Robain, H., Taccoen, A., Sengphaathith, P., Mouche, E., Sengtaheuanghoung, O., Tran Duc, T., and Valentin, C.: Contradictory hydrological impacts of afforestation in the humid tropics evidenced by long-term field monitoring and simulation modelling, Hydrol. Earth Syst. Sci., 20, 2691-2704, 10.5194/hess-20-2691-2016, 2016.

Lara, J. M., and Pemberton, E. L.: Initial unit weight of deposited sediments, Federal Interagency Sedimentation Conference, 1963.

Li, P., Muenich, R. L., Chaubey, I., and Wei, X.: Evaluating Agricultural BMP Effectiveness in Improving Freshwater Provisioning Under Changing Climate, Water Resour Manage, 33, 453-473, 10.1007/s11269-018-2098-y, 2019.

Li, Y., Chen, B. M., Wang, Z. G., and Peng, S. L.: Effects of temperature change on water discharge, and sediment and nutrient loading in the lower Pearl River basin based on SWAT modelling, Hydrological Sciences Journal-Journal Des Sciences Hydrologiques, 56, 68-83, 10.1080/02626667.2010.538396, 2011.

Li, Z., and Fang, H.: Impacts of climate change on water erosion: A review, Earth-Science Reviews, 163, 94-117, https://doi.org/10.1016/j.earscirev.2016.10.004, 2016.

Lu, S., Kayastha, N., Thodsen, H., Van Griensven, A., and Andersen, H. E.: Multiobjective calibration for comparing channel sediment routing models in the soil and water assessment tool, J. Environ. Qual., 43, 110-120, 2014a.

Lu, X., Kummu, M., and Oeurng, C.: Reappraisal of sediment dynamics in the Lower Mekong River, Cambodia, Earth Surface Processes and Landforms, 39, 1855-1865, 10.1002/esp.3573, 2014b.

Lutz, A., Terink, W., Droogers, P., Immerzeel, W., and Piman, T.: Development of baseline climate data set and trend analysis in the Mekong Basin, Mekong River Commission: Vientiane, Laos, 1-127, 2014.

Ma, X., Lu, X. X., van Noordwijk, M., Li, J. T., and Xu, J. C.: Attribution of climate change, vegetation restoration, and engineering measures to the reduction of suspended sediment in the Kejie catchment, southwest China, Hydrol. Earth Syst. Sci., 18, 1979-1994, 10.5194/hess-18-1979-2014, 2014.

Mas, J. F., Kolb, M., Paegelow, M., Camacho Olmedo, M. T., and Houet, T.: Inductive pattern-based land use/cover change models: A comparison of four software packages, Environmental Modelling and Software, 51, 94-111, 10.1016/j.envsoft.2013.09.010, 2014.

Masih, I., Maskey, S., Uhlenbrook, S., and Smakhtin, V.: Assessing the Impact of Areal Precipitation Input on Streamflow Simulations Using the SWAT Model1, Journal of the American Water Resources Association, 47, 179-195, 10.1111/j.1752-1688.2010.00502.x, 2011.

Maurer, E. P.: Uncertainty in hydrologic impacts of climate change in the Sierra Nevada, California, under two emissions scenarios, Climatic Change, 82, 309-325, 2007.

McCartney, M. P., Sullivan, C., and Acreman, M. C.: Ecosystem impacts of large dams, United Nation Foundation, Washington, DC, 2000.

McSweeney, C. F., and Jones, R. G.: How representative is the spread of climate projections from the 5 CMIP5 GCMs used in ISI-MIP?, Climate Services, 1, 24-29, https://doi.org/10.1016/j.cliser.2016.02.001, 2016.

Mendoza, P. A., Clark, M. P., Mizukami, N., Newman, A. J., Barlage, M., Gutmann, E. D., Rasmussen, R. M., Rajagopalan, B., Brekke, L. D., and Arnold, J. R.: Effects of Hydrologic Model Choice and Calibration on the Portrayal of Climate Change Impacts, Journal of Hydrometeorology, 16, 762-780, 10.1175/JHM-D-14-0104.1, 2014.

Mendoza, P. A., Clark, M. P., Mizukami, N., Gutmann, E. D., Arnold, J. R., Brekke, L. D., and Rajagopalan, B.: How do the selection and configuration of hydrologic models affect the portrayal of climate change impacts?, Hydrological Processes, n/a-n/a, 10.1002/hyp.10684, 2015.

Michael, A., Schmidt, J., Enke, W., Deutschlander, T., and Malitz, G.: Impact of expected increase in precipitation intensities on soil loss - results of comparative model simulations, Catena, 61, 155-164, 10.1016/j.catena.2005.03.002, 2005.

Milly, P. C. D., Betancourt, J., Falkenmark, M., Hirsch, R. M., Kundzewicz, Z. W., Lettenmaier, D. P., and Stouffer, R. J.: Climate change - Stationarity is dead: Whither water management?, Science, 319, 573-574, 10.1126/science.1151915, 2008.

Minville, M., Brissette, F., and Leconte, R.: Uncertainty of the impact of climate change on the hydrology of a Nordic watershed, Journal of Hydrology, 358, 70-83, 2008.

Mockler, E. M., Chun, K. P., Sapriza-Azuri, G., Bruen, M., and Wheater, H. S.: Assessing the relative importance of parameter and forcing uncertainty and their interactions in conceptual hydrological model simulations, Advances in Water Resources, 97, 299-313, 10.1016/j.advwatres.2016.10.008, 2016.

Moehansyah, H., Maheshwari, B. L., and Armstrong, J.: Impact of land-use changes and sedimentation on the Muhammad Nur Reservoir, South Kalimantan, Indonesia, Journal of Soils and Sediments, 2, 9-18, 10.1007/BF02991245, 2002.

Mohammed, I. N., Bolten, J. D., Srinivasan, R., and Lakshmi, V.: Satellite observations and modeling to understand the Lower Mekong River Basin streamflow variability, Journal of Hydrology, 564, 559-573, 10.1016/j.jhydrol.2018.07.030, 2018.

Monteith, J. L.: Evaporation and the environment. In: The State and Movement of Water in Living Organisms, 19th Symposia of the Society for Experimental Biology., 1965.

Moran, E. F., Lopez, M. C., Moore, N., Müller, N., and Hyndman, D. W.: Sustainable hydropower in the 21st century, Proceedings of the National Academy of Sciences, 115, 11891-11898, 10.1073/pnas.1809426115, 2018.

Moriasi, D. N., Arnold, J. G., Van Liew, M. W., Bingner, R. L., Harmel, R. D., and Veith, T. L.: Model evaluation guidelines for systematic quantification of accuracy in watershed simulations, Transactions of the ASABE, 50, 885-900, 2007.

Morris, G. L., and Fan, J.: Reservoir sedimentation handbook: Design and management of dams, reservoirs, and watersheds for sustainable use, McGraw-Hill Professional, New York, 1998.

Moss, R. H., Edmonds, J. A., Hibbard, K. A., Manning, M. R., Rose, S. K., van Vuuren, D. P., Carter, T. R., Emori, S., Kainuma, M., Kram, T., Meehl, G. A., Mitchell, J. F. B., Nakicenovic, N., Riahi, K., Smith, S. J., Stouffer, R. J., Thomson, A. M., Weyant, J. P., and Wilbanks, T. J.: The next generation of scenarios for climate change research and assessment, Nature, 463, 747-756, 10.1038/nature08823, 2010.

MRC: Stage 2 development of MRC Toolbox: Final report (WP016), Information and Knowledge Management Programme, Mekong River Commission (MRC), Phnom Penh, Cambodia 2010.

MRC: Application of MRC modelling tools in the 3S basin, Mekong River Commission (MRC), Phnom Penh, Cambodia 2011.

MRC: 1st Draft Report on Defining basin-wide climate change scenarios for the Lower Mekong Basin (LMB), Mekong River Commission (MRC), Phnom Penh, Cambodia 2015.

Muleta, M. K., and Nicklow, J. W.: Sensitivity and uncertainty analysis coupled with automatic calibration for a distributed watershed model, Journal of Hydrology, 306, 127-145, http://dx.doi.org/10.1016/j.jhydrol.2004.09.005, 2005.

Murphy, J. M., Sexton, D. M. H., Barnett, D. N., Jones, G. S., Webb, M. J., and Stainforth, D. A.: Quantification of modelling uncertainties in a large ensemble of climate change simulations, Nature, 430, 768-772, 10.1038/nature02771, 2004.

Najafi, M. R., Moradkhani, H., and Jung, I. W.: Assessing the uncertainties of hydrologic model selection in climate change impact studies, Hydrological Processes, 25, 2814-2826, 2011.

Nash, J. E., and Sutcliffe, J. V.: River flow forecasting through conceptual models part I — A discussion of principles, Journal of Hydrology, 10, 282-290, http://dx.doi.org/10.1016/0022-1694(70)90255-6, 1970.

Ndomba, P. M., Mtalo, F. W., and Killingtveit, A.: A guided SWAT model application on sediment yield modeling in Pangani river basin: Lessons learnt, Journal of Urban and Environmental Engineering, 2, 53-62, 10.4090/juee.2008.v2n2.053062, 2008a.

Ndomba, P. M., Mtalo, F. W., and Killingtveit, A.: SWAT model application in a data scarce tropical complex catchment in Tanzania, Physics and Chemistry of the Earth, 33, 626-632, 10.1016/j.pce.2008.06.013, 2008b.

Neitsch, S. L., Arnold, J. G., Kiniry, J. R., and Williams, J. R.: Soil and Water Assessment Tool theoretical documentation, version 2009, Texas Water Resources Institute, College Station, Texas, USA, 2011.

Nguyen, T. H., Masih, I., Mohamed, Y. A., and Van der Zaag, P.: Validating rainfall-runoff modelling using satellite-based and reanalysis precipitation products in the Sre Pok catchment, the Mekong river basin, Geosciences, 8, 164, 2018.

Nilsson, C., Reidy, C. A., Dynesius, M., and Revenga, C.: Fragmentation and flow regulation of the world's large river systems, Science, 308, 405-408, 10.1126/science.1107887, 2005.

O'Neal, M. R., Nearing, M. A., Vining, R. C., Southworth, J., and Pfeifer, R. A.: Climate change impacts on soil erosion in Midwest United States with changes in crop management, Catena, 61, 165-184, 10.1016/j.catena.2005.03.003, 2005.

Oeurng, C., Cochrane, T. A., Arias, M. E., Shrestha, B., and Piman, T.: Assessment of changes in riverine nitrate in the Sesan, Srepok and Sekong tributaries of the Lower Mekong River Basin, Journal of Hydrology: Regional Studies, 8, 95-111, 10.1016/j.ejrh.2016.07.004, 2016.

Ogle, S. M., Breidt, F. J., Eve, M. D., and Paustian, K.: Uncertainty in estimating land use and management impacts on soil organic carbon storage for US agricultural lands between 1982 and 1997, Global Change Biology, 9, 1521-1542, 10.1046/j.1365-2486.2003.00683.x, 2003.

Ono, K., Kazama, S., Gunawardhana, L. N., and Kuraji, K.: An investigation of extreme daily rainfall in the Mekong River Basin using a gridded precipitation dataset, Hydrological Research Letters, 7, 66-72, 2013.

Paegelow, M., and Olmedo, M. T. C.: Advances in geomatic simulations for environmental dynamics, in: Modelling environmental dynamics, advances in geomatic solutions, edited by: Paegelow M., and C., O. M. T., Springer, Berlin, 3-54, 2008.

Palmieri, A., Shah, F., and Dinar, A.: Economics of reservoir sedimentation and sustainable management of dams, Journal of Environmental Management, 61, 149-163, 10.1006/jema.2000.0392, 2001.

Palmieri, A., Shah, F., Annandale, G. W., and Dinar, A.: Reservoir Conservation, Volume-I: The RESCON Approach, The World Bank, 2003.

Partheniades, E.: Unified view of wash load and bed material load, Journal of the Hydraulics Division, 103, 1037-1057, 1977.

Petts, G. E., and Gurnell, A. M.: Dams and geomorphology: Research progress and future directions, Geomorphology, 71, 27-47, 10.1016/j.geomorph.2004.02.015, 2005.

Piman, T., Cochrane, T. A., Arias, M. E., Green, A., and Dat, N. D.: Assessment of Flow Changes from Hydropower Development and Operations in Sekong, Sesan, and Srepok Rivers of the Mekong Basin, Journal of Water Resources Planning and Management, 139, 723-732, 10.1061/(asce)wr.1943-5452.0000286, 2013.

Pittelkow, C. M., Linquist, B. A., Lundy, M. E., Liang, X., van Groenigen, K. J., Lee, J., van Gestel, N., Six, J., Venterea, R. T., and van Kessel, C.: When does no-till yield more? A global meta-analysis, Field Crops Research, 183, 156-168, http://dx.doi.org/10.1016/j.fcr.2015.07.020, 2015.

Pontius Jr, R. G., and Schneider, L. C.: Land-cover change model validation by an ROC method for the Ipswich watershed, Massachusetts, USA, Agriculture, Ecosystems & Environment, 85, 239-248, 10.1016/S0167-8809(01)00187-6, 2001.

Poulin, A., Brissette, F., Leconte, R., Arsenault, R., and Malo, J.-S.: Uncertainty of hydrological modelling in climate change impact studies in a Canadian, snow-dominated river basin, Journal of Hydrology, 409, 626-636, http://dx.doi.org/10.1016/j.jhydrol.2011.08.057, 2011.

Prestele, R., Alexander, P., Rounsevell, M. D. A., Arneth, A., Calvin, K., Doelman, J., Eitelberg, D. A., Engström, K., Fujimori, S., Hasegawa, T., Havlik, P., Humpenöder, F., Jain, A. K., Krisztin, T., Kyle, P., Meiyappan, P., Popp, A., Sands, R. D., Schaldach, R., Schüngel, J., Stehfest, E., Tabeau, A., Van Meijl, H., Van Vliet, J., and Verburg, P. H.: Hotspots of uncertainty in land-use and land-cover change projections: a global-scale model comparison, Global Change Biology, n/a-n/a, 10.1111/gcb.13337, 2016.

Priestley, C. H. B., and Taylor, R. J.: On the Assessment of Surface Heat Flux and Evaporation Using Large-Scale Parameters, Monthly Weather Review, 100, 81-92, 10.1175/1520-0493(1972)100<0081:OTAOSH>2.3.CO;2, 1972.

Prudhomme, C., and Davies, H.: Assessing uncertainties in climate change impact analyses on the river flow regimes in the UK. Part 2: future climate, Climate Change, 93, 197-222, 10.1007/s10584-008-9461-6, 2009.

Pruski, F. F., and Nearing, M. A.: Climate-induced changes in erosion during the 21st century for eight U.S. locations, Water Resources Research, 38, 1298, 10.1029/2001WR000493, 2002.

Refsgaard, J. C., and Storm, B.: Construction, Calibration And Validation of Hydrological Models, in: Distributed Hydrological Modelling, edited by: Abbott, M., and Refsgaard, J., Water Science and Technology Library, Springer Netherlands, 41-54, 1996.

Rey, F.: Influence of vegetation distribution on sediment yield in forested marly gullies, Catena, 50, 549-562, 10.1016/s0341-8162(02)00121-2, 2003.

Rodriguez-Lloveras, X., Buytaert, W., and Benito, G.: Land use can offset climate change induced increases in erosion in Mediterranean watersheds, CATENA, 143, 244-255, 10.1016/j.catena.2016.04.012, 2016.

Rodríguez Eraso, N., Armenteras-Pascual, D., and Alumbreros, J. R.: Land use and land cover change in the Colombian Andes: Dynamics and future scenarios, Journal of Land Use Science, 8, 154-174, 10.1080/1747423X.2011.650228, 2013.

Rossi, C. G., Srinivasan, R., Jirayoot, K., Le Duc, T., Souvannabouth, P., Binh, N., and Gassman, P. W.: Hydrologic evaluation of the lower mekong river basin with the soil and water assessment tool model, International Agricultural Engineering Journal, 18, 1-13, 2009.

Rostamian, R., Jaleh, A., Afyuni, M., Mousavi, S. F., Heidarpour, M., Jalalian, A., and Abbaspour, K. C.: Application of a SWAT model for estimating runoff and sediment in two mountainous basins in central Iran, Hydrological Sciences Journal, 53, 977-988, 10.1623/hysj.53.5.977, 2008.

Runkel, R. L., Crawfored, C. G., and Cohn, T. A.: Load Estimator (LOADEST): A FORTAN program for estimating constituent loads in streams and rivers. U.S. Geological Survey, Reston, Virginia (USA). , 2004.

Samaras, A. G., and Koutitas, C. G.: Modeling the impact of climate change on sediment transport and morphology in coupled watershed-coast systems: A case study using an integrated approach, International Journal of Sediment Research, 29, 304-315, https://doi.org/10.1016/S1001-6279(14)60046-9, 2014.

Sangermano, F., Eastman, J. R., and Zhu, H.: Similarity Weighted Instance-based Learning for the Generation of Transition Potentials in Land Use Change Modeling, Transactions in GIS, 14, 569-580, 10.1111/j.1467-9671.2010.01226.x, 2010.

Sangermano, F., Toledano, J., and Eastman, J. R.: Land cover change in the Bolivian Amazon and its implications for REDD+ and endemic biodiversity, Landscape Ecology, 27, 571-584, 10.1007/s10980-012-9710-y, 2012.

Santhi, C., Arnold, J. G., Williams, J. R., Dugas, W. A., Srinivasan, R., and Hauck, L. M.: Validation of the swat model on a large river basin with point and nonpoint sources, Journal of the American Water Resources Association, 37, 1169-1188, 10.1111/j.1752-1688.2001.tb03630.x, 2001.

Santini, M., and Valentini, R.: Predicting hot-spots of land use changes in Italy by ensemble forecasting, Regional Environmental Change, 11, 483-502, 2011.

Schmidt, J. C., and Wilcock, P. R.: Metrics for assessing the downstream effects of dams, Water Resources Research, 44, 10.1029/2006wr005092, 2008.

Servat, E., and Dezetter, A.: Selection of calibration objective functions in the context of rainfall-runoff modelling in a Sudanese savannah area, Hydrological Sciences Journal/Journal des Sciences Hydrologiques, 36, 307-330, 1991.

Setegn, S. G., Srinivasan, R., Melesse, A. M., and Dargahi, B.: SWAT model application and prediction uncertainty analysis in the Lake Tana Basin, Ethiopia, Hydrological Processes, 24, 357-367, 10.1002/hyp.7457, 2010.

Sharp, R., Tallis, H. T., Ricketts, T., Guerry, A. D., Wood, S. A., Chaplin-Kramer, R., Nelson, E., Ennaanay, D., Wolny, S., Olwero, N., Vigerstol, K., Pennington, D., Mendoza, G., Aukema, J., Foster, J., Forrest, J., Cameron, D., Arkema, K., Lonsdorf, E., Kennedy, C., Verutes, G., Kim, C. K., Guannel, G., Papenfus, M., Toft, J., Marsik, M., Bernhardt, J., Griffin, R., Glowinski, K., Chaumont, N., Perelman, A., Lacayo, M., Mandle, L., and Hamel, P.: InVEST User's Guide. , The Natural Capital Project, Stanford., 2014.

Shaw, E. H., and Lynn, P. P.: Areal rainfall using two surface fitting techniques, Bulletin of the International Association and Hydrological Science, XVII,, 4-2, 1972.

Shi, H., Chen, J., Liu, S., and Sivakumar, B.: The role of large dams in promoting economic development under the pressure of population growth, Sustainability (Switzerland), 11, 10.3390/su11102965, 2019.

Shrestha, B., Babel, M. S., Maskey, S., van Griensven, A., Uhlenbrook, S., Green, A., and Akkharath, I.: Impact of climate change on sediment yield in the Mekong River basin: a case study of the Nam Ou basin, Lao PDR, Hydrology and Earth System Sciences, 17, 1-20, 10.5194/hess-17-1-2013, 2013.

Shrestha, B., Cochrane, T. A., Caruso, B. S., Arias, M. E., and Piman, T.: Uncertainty in flow and sediment projections due to future climate scenarios for the 3S Rivers in the Mekong Basin, Journal of Hydrology, 540, 1088-1104, 10.1016/j.jhydrol.2016.07.019, 2016.

Shrestha, B., Cochrane, T. A., Caruso, B. S., and Arias, M. E.: Land use change uncertainty impacts on streamflow and sediment projections in areas undergoing rapid development: A case study in the Mekong Basin, Land Degradation and Development, 29, 835-848, 10.1002/ldr.2831, 2018a.

Shrestha, B., Maskey, S., Babel, M. S., van Griensven, A., and Uhlenbrook, S.: Sediment related impacts of climate change and reservoir development in the Lower Mekong River Basin: a case study of the Nam Ou Basin, Lao PDR, Climatic Change, 149, 13-27, 10.1007/s10584-016-1874-z, 2018b.

Smith, C., Williams, J., Nejadhashemi, A. P., Woznicki, S., and Leatherman, J.: Cropland management versus dredging: An economic analysis of reservoir sediment management, Lake and Reservoir Management, 29, 151-164, 10.1080/10402381.2013.814184, 2013.

Smith, J. E., and Heath, L. S.: Identifying influences on model uncertainty: An application using a forest carbon budget model, Environmental Management, 27, 253-267, 10.1007/s002670010147, 2001.

Sperber, K., Annamalai, H., Kang, I. S., Kitoh, A., Moise, A., Turner, A., Wang, B., and Zhou, T.: The Asian summer monsoon: an intercomparison of CMIP5 vs. CMIP3 simulations of the late 20th century, Clim. Dyn., 41, 2711-2744, 10.1007/s00382-012-1607-6, 2013.

Srinivasan, R., Ramanarayanan, T. S., Arnold, J. G., and Bednarz, S. T.: Large area hydrologic modeling and assessment. Part II: Model application, Journal of American Water Resources Association, 34, 91-101, 1998.

Stibig, H. J.: Interpretation and Delineation from Satellite Images, Technical Notes 2 of the Forest Cover Monitoring Project, a Co-operation project between the Mekong River Commission (MRC) and the Gesellschaft fuer Technische Zusammenarbeit (GTZ). , Mekong River Commission, Vientiane, Laos, 1997.

Stone, R. P., and Hilborn, D.: Universal Soil Loss Equation (USLE) Factsheet Order No. 12-051, Ministry of Agriculture, Food and Rural Affairs, Ontario, Canada, 2011.

Sumi, T., and Kantoush, S. A.: Sediment management strategies for sustainable reservoir, 2011.

Surfleet, C. G., and Tullos, D.: Uncertainty in hydrologic modelling for estimating hydrologic response due to climate change (Santiam River, Oregon), Hydrological Processes, 27, 3560-3576, 10.1002/hyp.9485, 2013.

Syvitski, J. P. M., Peckham, S. D., Hilberman, R., and Mulder, T.: Predicting the terrestrial flux of sediment to the global ocean: a planetary perspective, Sedimentary Geology, 162, 5-24, 10.1016/s0037-0738(03)00232-x, 2003.

Syvitski, J. P. M., Kettner, A. J., Peckham, S. D., and Kao, S. J.: Predicting the flux of sediment to the coastal zone: Application to the Lanyang Watershed, Northern Taiwan, Journal of Coastal Research, 21, 580-587, 10.2112/04-702a.1, 2005.

Takamatsu, M., Kawasaki, A., Rogers, P. P., and Malakie, J. L.: Development of a land-use forecast tool for future water resources assessment: Case study for the Mekong River 3S Sub-basins, Sustainability Science, 9, 157-172, 2014.

Tebaldi, C., and Arblaster, J. M.: Pattern scaling: Its strengths and limitations, and an update on the latest model simulations, Climatic Change, 122, 459-471, 2014.

Teuling, A. J., Uijlenhoet, R., van den Hurk, B., and Seneviratne, S. I.: Parameter sensitivity in LSMs: An analysis using stochastic soil moisture models and ELDAS soil parameters, Journal of Hydrometeorology, 10, 751-765, 2009.

Teutschbein, C., Wetterhall, F., and Seibert, J.: Evaluation of different downscaling techniques for hydrological climate-change impact studies at the catchment scale, Clim. Dyn., 37, 2087-2105, 10.1007/s00382-010-0979-8, 2011.

Thomas, G., Annandale, G. W., Bouapao, L., Hortle, K., Jensen, E., Kaini, P., Kondolf, G. M., Cooper, M. M., Meier, P., Meynell, P., Knight, P., and Wild, T.: Sustainable Hydropower Master Plan for the Xe Kong Basin in Lao PDR, National Heritage Institute California, USA, 2018.

Thompson, J. R., Green, A. J., Kingston, D. G., and Gosling, S. N.: Assessment of uncertainty in river flow projections for the Mekong River using multiple GCMs and hydrological models, Journal of Hydrology, 486, 1-30, 10.1016/j.jhydrol.2013.01.029, 2013.

Tiˇgrek, S., and Aras, T.: Reservoir sediment management, CRC Press/Balkema, Leiden,The Netherlands, 2012.

Trang, N. T. T., Shrestha, S., Shrestha, M., Datta, A., and Kawasaki, A.: Evaluating the impacts of climate and land-use change on the hydrology and nutrient yield in a transboundary river basin: A case study in the 3S River Basin (Sekong, Sesan, and Srepok), Science of The Total Environment, 576, 586-598, https://doi.org/10.1016/j.scitotenv.2016.10.138, 2017.

Troin, M., Arsenault, R., Martel, J. L., and Brissette, F.: Uncertainty of hydrological model components in climate change studies over two nordic quebec catchments, Journal of Hydrometeorology, 19, 27-46, 10.1175/JHM-D-17-0002.1, 2018.

Tuppad, P., and Srinivasan, R.: Bosque River environmental infrastructure improvement plan: Phase II BMP modeling report., College Station, Tex.: Texas A&M University, Texas AgriLife Research, 2008.

Turner, B. L., Lambin, E. F., and Reenberg, A.: The emergence of land change science for global environmental change and sustainability, Proceedings of the National Academy of Sciences, 104, 20666-20671, 10.1073/pnas.0704119104, 2007.

Ty, T., Sunada, K., Ichikawa, Y., and Oishi, S.: Scenario-based Impact Assessment of Land Use/Cover and Climate Changes on Water Resources and Demand: A Case Study in the Srepok River Basin, Vietnam—Cambodia, Water Resour Manage, 26, 1387-1407, 10.1007/s11269-011-9964-1, 2012.

UDWR: Managing Sediment in Utah's Reservoirs, Utah Division of Water Resources (UDWR), Utah, 2010.

USACE: The potential impact of increased corn production for ethanol in the Great Lakes-St. Lawrence river region. , US Army Corps of Engineers (USACE) Great lakes and Ohio River divison, 2007.

USDA-SCS: National engineering handbook, Section 4 Hydrology, Chapter 4-10, United States Department of Agriculture – Soil Conservation Service(USDA-SCS), Washington, USA, 1972.

Van Liew, M. W., Veith, T. L., Bosch, D. D., and Arnold, J. G.: Suitability of SWAT for the conservation effects assessment project: Comparison on USDA Agricultural Research Service watersheds, Journal of Hydrologic Engineering, 12, 173-189, 10.1061/(asce)1084-0699(2007)12:2(173), 2007.

Verburg, P. H., Schot, P. P., Dijst, M. J., and Veldkamp, A.: Land use change modelling: Current practice and research priorities, GeoJournal, 61, 309-324, 2004.

Verstraeten, G., Van Oost, K., Van Rompaey, A., Poesen, J., and Govers, G.: Evaluating an integrated approach to catchment management to reduce soil loss and sediment pollution through modelling, Soil Use and Management, 18, 386-394, 10.1079/sum2002150, 2002.

Vetter, T., Huang, S., Aich, V., Yang, T., Wang, X., Krysanova, V., and Hattermann, F.: Multi-model climate impact assessment and intercomparison for three large-scale river basins on three continents, Earth System Dynamics, 6, 17-43, 10.5194/esd-6-17-2015, 2015.

Vorosmarty, C. J., Meybeck, M., Fekete, B., Sharma, K., Green, P., and Syvitski, J. P. M.: Anthropogenic sediment retention: major global impact from registered river impoundments, Global and Planetary Change, 39, 169-190, 10.1016/s0921-8181(03)00023-7, 2003.

Walling, D.: Evaluation and analysis of sediment data from the Lower Mekong River, Report prepared for the Mekong River Commission, 2005.

Walling, D. E.: Linking land use, erosion and sediment yields in river basins, Hydrobiologia 410, 223–240, 1999.

Walling, D. E.: The changing sediment load of the Mekong River, Ambio, 37, 150-157, 10.1579/0044-7447(2008)37[150:TCSLOT]2.0.CO;2, 2008.

Walter, R. C., and Merritts, D. J.: Natural Streams and the Legacy of Water-Powered Mills, Science, 319, 299, 10.1126/science.1151716, 2008.

Wang, Q., Liu, R., Men, C., Guo, L., and Miao, Y.: Effects of dynamic land use inputs on improvement of SWAT model performance and uncertainty analysis of outputs, Journal of hydrology, 563, 874-886, 2018.

Wang, W., Lu, H., Yang, D., Sothea, K., Jiao, Y., Gao, B., Peng, X., and Pang, Z.: Modelling hydrologic processes in the Mekong River basin using a distributed model driven by satellite precipitation and rain gauge observations, PLoS ONE, 11, 10.1371/journal.pone.0152229, 2016.

Watson, B. M., and Putz, G.: Comparison of temperature-index snowmelt models for use within an operational water quality model, J. Environ. Qual., 43, 199-207, 2014.

Wei, W., Chen, L., Fu, B., Lue, Y., and Gong, J.: Responses of water erosion to rainfall extremes and vegetation types in a loess semiarid hilly area, NW China, Hydrological Processes, 23, 1780-1791, 10.1002/hyp.7294, 2009.

Wilby, R. L., and Harris, I.: A framework for assessing uncertainties in climate change impacts: Low-flow scenarios for the River Thames, UK, Water Resources Research, 42, 10.1029/2005wr004065, 2006.

Wilby, R. L., and Dessai, S.: Robust adaptation to climate change, Weather, 65, 180-185, doi:10.1002/wea.543, 2010.

Wild, T. B., and Loucks, D. P.: Managing flow, sediment, and hydropower regimes in the Sre Pok, Se San, and Se Kong Rivers of the Mekong basin, Water Resources Research, 50, 5141-5157, 10.1002/2014WR015457, 2014.

Wild, T. B., and Loucks, D. P.: An Approach to Simulating Sediment Management in the Mekong River Basin, in: Sediment Matters, edited by: Heininger, P., and Cullmann, J., Springer International Publishing, Cham, 187-199, 2015.

Wild, T. B., Loucks, D. P., Annandale, G. W., and Kaini, P.: Maintaining Sediment Flows through Hydropower Dams in the Mekong River Basin, Journal of Water Resources Planning and Management, 142, 10.1061/(ASCE)WR.1943-5452.0000560, 2016.

Wild, T. B., Loucks, D. P., and Annandale, G. W.: SedSim: A River Basin Simulation Screening Model for Reservoir Management of Sediment, Water, and Hydropower., Journal of Open Research Software, 7, https://doi.org/10.5334/jors.261, 2019a.

Wild, T. B., Reed, P. M., Loucks, D. P., Mallen-Cooper, M., and Jensen, E. D.: Balancing Hydropower Development and Ecological Impacts in the Mekong: Tradeoffs for Sambor Mega Dam, Journal of Water Resources Planning and Management, 145, 05018019, doi:10.1061/(ASCE)WR.1943-5452.0001036, 2019b.

Wilk, J., Andersson, L., and Plermkamon, V.: Hydrological impacts of forest conversion to agriculture in a large river basin in northeast Thailand, Hydrological Processes, 15, 2729-2748, 10.1002/hyp.229, 2001.

Williams, J. R.: Flood routing with variable travel time or variable storage coefficients., Transactions of the ASAE 12, 100-103, 1969.

Williams, J. R.: Sediment-yield prediction with universal equation using runoff energy factor. Present and Prospective Technology for Predicting Sediment Yield and Sources: Proceedings of the Sediment Yield Workshop,, USDA Sedimentation Lab., Oxford, Mississippi, 1975.

Winemiller, K. O., McIntyre, P. B., Castello, L., Fluet-Chouinard, E., Giarrizzo, T., Nam, S., Baird, I. G., Darwall, W., Lujan, N. K., Harrison, I., Stiassny, M. L. J., Silvano, R. A. M., Fitzgerald, D. B., Pelicice, F. M., Agostinho, A. A., Gomes, L. C., Albert, J. S., Baran, E., Petrere, M., Zarfl, C., Mulligan, M., Sullivan, J. P., Arantes, C. C., Sousa, L. M., Koning, A. A., Hoeinghaus, D. J., Sabaj, M., Lundberg, J. G., Armbruster, J., Thieme, M. L., Petry, P., Zuanon, J., Vilara, G. T., Snoeks, J., Ou, C., Rainboth, W., Pavanelli, C. S., Akama, A., Soesbergen, A. v., and Sáenz, L.: Balancing hydropower and biodiversity in the Amazon, Congo, and Mekong, Science, 351, 128, 10.1126/science.aac7082, 2016.

WLE–Mekong: Mekong Hydropower Map and Portal. Available here: https://wle-mekong.cgiar.org/maps/. 2017.

Wohl, E., Barros, A., Brunsell, N., Chappell, N. A., Coe, M., Giambelluca, T., Goldsmith, S., Harmon, R., Hendrickx, J. M. H., Juvik, J., McDonnell, J., and Ogden, F.: The hydrology of the humid tropics, Nature Climate Change, 2, 655, 10.1038/nclimate1556, 2012.

Wohl, E., Bledsoe, B. P., Jacobson, R. B., Poff, N. L., Rathburn, S. L., Walters, D. M., and Wilcox, A. C.: The natural sediment regime in rivers: Broadening the foundation for ecosystem management, BioScience, 65, 358-371, 10.1093/biosci/biv002, 2015.

Woznicki, S. A., Nejadhashemi, A. P., and Smith, C. M.: Assessing best management practice implementation strategies under climate change scenarios, Transactions of the ASABE, 54, 171-190, 2011.

Xu, H., Xu, C.-Y., Chen, H., Zhang, Z., and Li, L.: Assessing the influence of rain gauge density and distribution on hydrological model performance in a humid region of China, Journal of Hydrology, 505, 1-12, 2013.

Xu, J. X.: Sediment flux to the sea as influenced by changing human activities and precipitation: Example of the Yellow River, China, Environmental Management, 31, 328-341, 10.1007/s00267-002-2828-y, 2003.

Xue, Z., Liu, J. P., and Ge, Q. A.: Changes in hydrology and sediment delivery of the Mekong River in the last 50 years: connection to damming, monsoon, and ENSO, Earth Surface Processes and Landforms, 36, 296-308, 10.1002/esp.2036, 2011.

Yang, J., Reichert, P., Abbaspour, K. C., Xia, J., and Yang, H.: Comparing uncertainty analysis techniques for a SWAT application to the Chaohe Basin in China, Journal of Hydrology, 358, 1-23, 10.1016/j.jhydrol.2008.05.012, 2008.

Yang, T. B., Wang, S. L., and Yang, W. H.: Construction design and cost estimation on the machine building terraces, Soil Water Conserv. China, 1, 25-27, 2014.

Yang, W., Long, D., and Bai, P.: Impacts of future land cover and climate changes on runoff in the mostly afforested river basin in North China, Journal of Hydrology, 570, 201-219, https://doi.org/10.1016/j.jhydrol.2018.12.055, 2019.

Yip, S., Ferro, C. A. T., Stephenson, D. B., and Hawkins, E.: A Simple, Coherent Framework for Partitioning Uncertainty in Climate Predictions, Journal of Climate, 24, 4634-4643, 10.1175/2011JCLI4085.1, 2011.

Yu, P., Wang, Y., Coles, N., Xiong, W., and Xu, L.: Simulation of Runoff Changes Caused by Cropland to Forest Conversion in the Upper Yangtze River Region, SW China, PloS one, 10, e0132395, 2015.

Zabaleta, A., Meaurio, M., Ruiz, E., and Antigüedad, I.: Simulation climate change impact on runoff and sediment yield in a small watershed in the Basque Country, northern Spain, J. Environ. Qual., 43, 235-245, 2014.

Zhang, C., Chu, J. G., and Fu, G. T.: Sobol"s sensitivity analysis for a distributed hydrological model of Yichun River Basin, China, Journal of Hydrology, 480, 58-68, 10.1016/j.jhydrol.2012.12.005, 2013.

Zhang, X., and Nearing, M.: Impact of climate change on soil erosion, runoff, and wheat productivity in central Oklahoma, Catena, 61, 185-195, 2005.

Zhang, X., Xu, Y. P., and Fu, G.: Uncertainties in SWAT extreme flow simulation under climate change, Journal of Hydrology, 515, 205-222, http://dx.doi.org/10.1016/j.jhydrol.2014.04.064, 2014.

Zhong, C., and Hao, L.: Dilemmas of hydropower development in Laos, Energy Sources, Part B: Economics, Planning, and Policy, 12, 570-575, 10.1080/15567249.2016.1244579, 2017.

Zhou, X., Helmers, M., Al-Kaisi, M., and Hanna, M.: Cost-effectiveness and cost-benefit analysis of conservation management practices for sediment reduction in an Iowa agricultural watershed, Journal of Soil and Water Conservation, 64, 314-323, 10.2489/jswc.64.5.314, 2009.

Zhu, Y.-M., Lu, X. X., and Zhou, Y.: Sediment flux sensitivity to climate change: A case study in the Longchuanjiang catchment of the upper Yangtze River, China, Global and Planetary Change, 60, 429-442, 10.1016/j.gloplacha.2007.05.001, 2008.

Ziv, G., Baran, E., Nam, S., Rodriguez-Iturbe, I., and Levin, S. A.: Trading-off fish biodiversity, food security, and hydropower in the Mekong River Basin, Proceedings of the National Academy of Sciences of the United States of America, 109, 5609-5614, 10.1073/pnas.1201423109, 2012.